RNA recognition in immune cells

Dissertation

for

the degree of

Doctor of Natural Sciences

(Dr. rer. nat.)

submitted to the

Faculties of Pharmacy

of the Philipps-University Marburg

presented by

Tina von Thülen

born in Wilhelmshaven

Marburg/Lahn 2010

Accepted from the Faculties of Pharmacy
of the Philipps-University Marburg: _____

Referees: Prof. Dr. Stefan Bauer
Prof. Dr. Roland Hartmann

Oral examination: _____

Dedicated to my parents

Human subtlety will never devise an invention more beautiful, more simple, or more direct than does Nature - because in her inventions, nothing is lacking - and nothing is superfluous…

Leonardo da Vinci

Table of contents

1. Introduction

1.1. Immunity- an overview

Host defense against invading microbial pathogens is elicted by two different types of immune responses: innate and adaptive immunity. There is a synergistic interplay between these two divisions. The innate immune system is an evolutionarily conserved form of host defense found in most multicellular organisms, which provides the first line of defense against infections. Innate defense mechanisms, then, initiate and provide time for the development of adaptive immune responses, which are characterized by high diversity, specificity and memory. Adaptive immunity is only found in vertebrates and is based on the activation of B and T lymphocytes. The enormous diversity of mature lymphocytes is generated by the rearrangement of different gene segments in individual lymphocytes.

1.1.1. Innate immunity

The main components of innate immunity are as follows: (1) The epithelium, which serves as a physical barrier to invading microbial pathogens and also secretes cytokines and antimicrobial peptides (see 1.2). (2) The cellular fraction, which is composed of circulating cells like phagocytic cells (neutrophils, macrophages), natural killer (NK) cells and dendritic cells. These cells combat infections by phagocytic destruction. Moreover, macrophages and dendritic cells are able to present detected microbial pathogens on their surface, thereby activating the adaptive immune system. They serve an important interface function, linking the innate and adaptive immune responses. (3) Blood proteins, including members of the complement system and other mediators of inflammation; and (4) Proteins called cytokines and chemokines, which lead to the recruitment of further immune cells.

The innate immune system uses a limited number of germline-encoded pattern recognition receptors (PRRs) to recognize conserved structures originally called pathogen-associated molecular patterns (PAMPs). PAMPs are generated by microbes and are not present on mammalian cells, suggesting that PAMPs are good targets for innate immunity to discriminate between self and non-self (Janeway and Medzhitov 2002; Janeway 2005; Abbas 2007; Uematsu and Akira 2008).

1.1.2. Pattern recognition receptors (PRRs)

PRRs are either located on the cell membrane, localized in intracellular compartments like the endosome or present in the cytosol. Due to their molecular structure, they can be subdivided into Toll-like receptors (TLRs), Retinoic acid-inducible gene I (RIG-I)-like receptors (RLRs) and Nucleotide-binding and oligomerization domain (NOD)-like receptors (NLRs), the latter of which are described in the discussion section below. These receptors show modular domain architecture with ligand-binding and signaling domains, the latter being regulated either through dimerization and oligomerization or through conformational changes by enzymatic activities. Subsequently, signaling domains recruit adaptor proteins that initiate intracellular signaling (Lee and Kim 2007).

1.1.2.1. Toll-like receptors (TLRs)

Toll was originally identified as a Drosophila gene involved in establishing the dorsal-ventral axis during the embryogenesis of the fly, but then it was discovered that the Toll protein was required to explain the resistance of flies to fungal infection (Lemaitre et al. 1996). The TLRs represent the human homolog to the Toll protein. TLRs are able to recognize microbes in different cellular locations. They are either expressed on the cell surface (TLR 1, 2, 3, 4, 5, and 6) or in intracellular compartments, namely endosomes (TLRs 3, 7, 8, and 9) (Ahmad-Nejad et al. 2002). Based on their primary sequences, TLRs can be divided into several subfamilies, each of which recognizes related PAMPs: the subfamily of TLR1, TLR2, and TLR6 recognizes lipids, whereas the closely-related TLR7, TLR8, and TLR9 recognize nucleic acids and nucleoside analogs (Akira et al. 2006). The major ligands for TLRs are shown in Table 1.

TLRs consist of a leucine-rich-repeat-containing extracellular domain (LRRs), which mediates ligand binding and a cytoplasmic signaling domain homologous to that of the interleukin 1 receptor (IL-1R), termed the Toll/IL-1R homology (TIR) (Akira et al. 2006). Ligand-induced TLR dimerization permits the binding of TIR-domain-containing adaptor molecules. Four of these adaptors are MyD88 (myeloid differentiation protein 88), TIRAP (TIR domain-containing adaptor protein), TRIF (TIR domain-containing adaptor inducing IFN-ß), and TRAM (TRIF-related adaptor molecule) (Akira et al. 2006). The TLR signaling pathways are shown in Figure 1. MyD88 is utilized by all TLRs except TLR3 and leads to the activation of the IKK complex (inhibitor of nuclear factor-κB (IKB)-kinase complex), so that NF-κB is realesed from its inhibitor and translocates to the nucleus, where it induces the expression of inflammatory cytokines (Akira et al. 2006).

Table 1: Mammalian pattern recognition receptors: their major ligands and cell types (modified after (Lee and Kim 2007)).

TLRs	Major ligands (or activators)
TLR1	Triacyl lipopeptides from bacteria and mycobacteria
TLR2	LTA from gram-positive bacteria, yeast zymosan, lipopeptides (Pam_3CSK_4, MALP2), lipoarabinomannan from mycobacteria
TLR3	Viral dsRNA, Poly (I:C)
TLR4	LPS from gram-negative bacteria, mannan from Candida albicans, GIPLs from Trypanosoma, viral envelope proteins from RSV and MMTV
TLR5	Bacterial flagellin
TLR6	Diacyl lipopeptides from Mycoplasma, LTA from gram-positive bacteria, yeast zymosan
TLR7	ssRNA from RNA viruses, imiquimod, resiquimod (R848), synthetic poly U RNA, certain siRNAs
TLR8	Resiquimod (R848), viral ssRNA
TLR9	Bacterial and viral CpG DNA, Hemozoin from Plasmodium
TLR10	Unknown
TLR11	Profilin-like molecule from Toxoplasma gondii, unknown ligand(s) from uropathogenic bacteria

TLR3 does not bind MyD88 but rather utilizes the TRIF adaptor protein and mediates the activation of the transcription factor IRF-3 (interferon response factor-3) (Akira et al. 2006). TLR4 engages two different signaling pathways. MyD88 and TIRAP lead to NF-κB activation, while TRAM and TRIF lead to activation of IRF-3. The main role of the MyD88-dependent pathway downstream of TLR4 is to induce the expression of inflammatory cytokines such as IL-6, IL-12, and TNF-α, whereas the main role of the TRIF-dependent pathway is to induce the expression of type-I IFNs (Akira et al. 2006).

TLRs within the endosomes recruit MyD88, leading to the activation of IRF-7, a transcription factor that, like IRF-3, induces type-I interferon gene expression. Plasmacytoid dendritic cells (pDCs) represent a subset of immune cells that specializes in the detection of viruses. These cells express TLR7 and TLR9 and produce large amounts of type-I interferons upon the detection of viruses (Akira et al. 2006; Fitzgerald-Bocarsly et al. 2008).

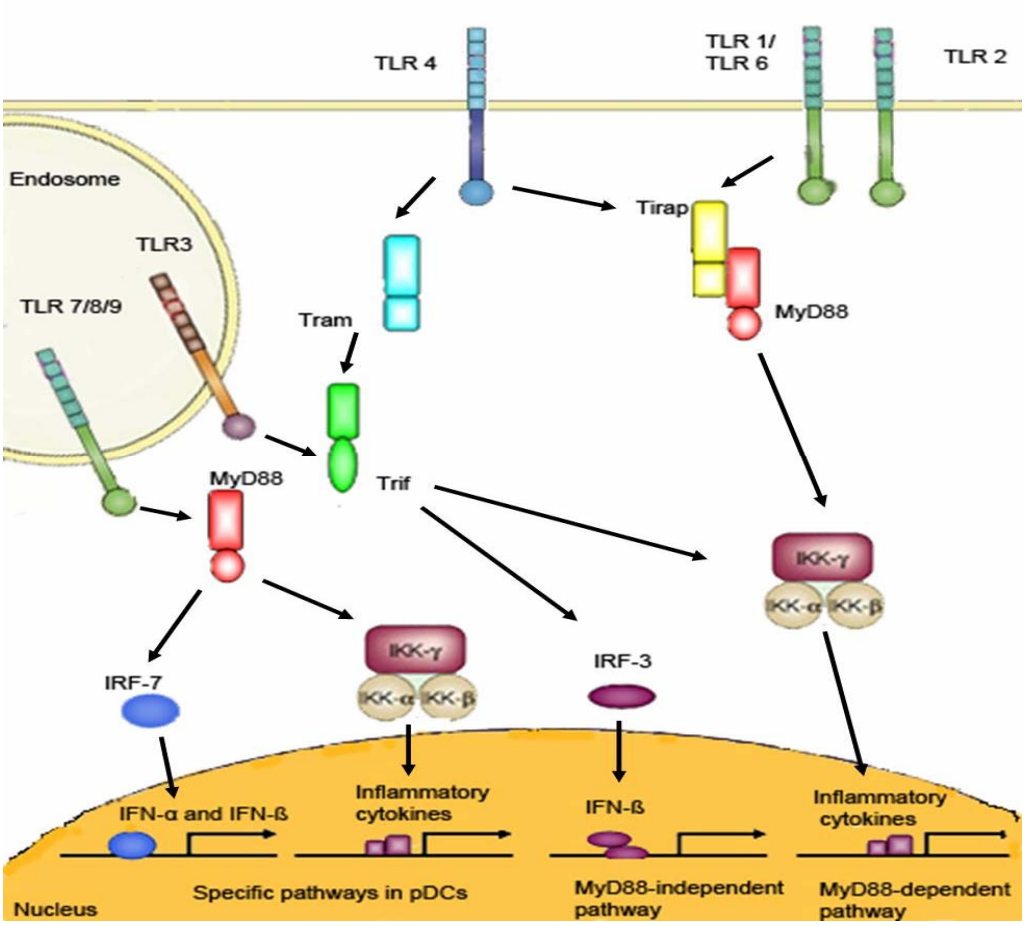

Figure 1: TLR signaling pathway (modified after (Akira and Takeda 2004; Saito and Gale 2008)). Simplified representation of the major pathways leading to the expression of cytokines and type-I interferons. All TLRs apart from TLR3 share a common pathway called the MyD88-dependent pathway that induces inflammatory cytokine production. The TIR domain-containing adaptor, MyD88, associates with the cytoplasmic TIR domain of TLRs, leading to the activation of the IKK complex (inhibitor of nuclear factor-KB (IKB)-kinase complex), which consists of IKK-α, IKK-ß and IKK-γ, so that NF-κB is realesed from its inhibitor and translocates to the nucleus. TIRAP, a second TIR domain-containing adaptor, specifically mediates the MyD88-dependent pathway via TLR2 and TLR4. In the TLR4- and TLR3-mediated signaling pathways, a MyD88-independent pathway exists that leads to activation of IRF-3. A third TIR domain-containing adaptor, TRIF, mediates this MyD88-independent pathway. A fourth TIR-domain containing adaptor, TRAM, is specific to the TLR4-mediated MyD88-independent/TRIF-dependent pathway. TLR7/8/9 act in pDCs cells via a unique pathway to induce IFN-α. TLR2 is shown to form a heterophilic dimer with TLR1 or TLR6, but the other TLRs are believed to form homodimers.

1.1.2.2. Cytoplasmic PRRs

The RLR family is composed of three members RIG-I (retinoic acid-inducible gene I), MDA-5 (melanoma-differentiation-associated gene 5) and LPG2 (laboratory of physiology and genetics 2) which were originally described as RNA helicases (Yoneyama et al. 2004). These cytosolic RNA receptors are also expressed ubiquitously in non-immune

cells. The amino termini of RIG-I and MDA-5 contain two CARDs (caspase activation and recruitment domains), that interact with downstream adaptor molecules. LPG2 does not harbor this amino-terminal domain and has therefore been reported to be a negative regulator for RIG-I/MDA-5 signaling (Rothenfusser et al. 2005; Yoneyama et al. 2005; Pippig et al. 2009). However, recent studies observed that LPG2 act as a positive regulator of RIG-I- and MDA-5-mediated viral recognition, except for the influenza virus (Satoh et al. 2010). The central portion of all three family members shows homologies with the DexD/H box RNA helicase family and is implicated in dsRNA binding and ATP-dependent unwinding (Cordin et al. 2006). The carboxy-terminus harbors a regulatory or repression domain (RD) that interacts with the helicase domain and inhibits signaling by the amino-terminal CARDs (Saito et al. 2007). The C-terminal regulatory domain (RD) of RIG-I acts as a sensor for 5`-triphosphates in RNA and dsRNA, and the binding of these structures induce an ATP-dependent conformational change (Cui et al. 2008; Takahasi et al. 2008; Takahasi et al. 2009; Yoneyama and Fujita 2010) that damasks the N-terminal CARDs for interaction with the CARD-containing adaptor IPS-1 (IFN-ß promoter stimulator 1) also termed CARDIF (CARD-adaptor inducing IFN-ß), MAVS (mitochondrial antiviral signaling), and VISA (virus-induced signaling adaptor), which is localized within the mitochondrial membrane, for NF-κB and IRF-3 activation and subsequent production of IFN-ß (Kawai et al. 2005; Meylan et al. 2005; Seth et al. 2005; Xu et al. 2005; Kumar et al. 2006; Sun et al. 2006). Recently it was discovered that MITA, also termed STING (stimulator of interferon genes), functions downstream of RIG-I and IPS-1 (Ishikawa and Barber 2008; Zhong et al. 2008). Besides its immunostimulatory activity, RIG-I and MDA-5 ligands also initiate a proapoptotic signaling and have therapeutic potential for virus infection or tumor therapy (Besch et al. 2009). For enteroviral infection, it was shown that the RIG-I pathway is active in beta cells and could contribute to the induction of insulitis (Garcia et al. 2009).

1.1.2.3. Cooperative recognition in innate immunity

PAMP recognition is rendered additionally complex by cell-type-specific expression of different sets of PRRs. In conventional dendritic cells (cDCs) and fibroblasts virus protection is mediated by the cytosolic residing RLRs, whereas in plasmacytoid dendritic cells (pDCs) virus recognition is mediated by TLRs (Kato et al. 2005; Koyama et al. 2007; McCartney and Colonna 2009): Therefore, TLRs and RLRs function cooperatively to provide ubiquitous immune protection. Kumagai et al. showed that alveolar macrophages and cDCs act as the first-line sensor for invading viruses, producing IFN-α at the site of

infection. In contrast, pDCs are not activated until the initial defense line is broken by the viruses. Given that several viruses (e.g., the influenza virus) suppress the RLR-mediated signaling pathway, it is tempting to speculate that hosts have evolved two different type-I production systems to make it more difficult for viruses to escape the antiviral response (Kumagai et al. 2007; Kumagai et al. 2009).

1.1.3. Nucleic acids recognition

1.1.3.1. Recognition of DNA

Unmethylated CpG motifs present in bacterial DNA (Hemmi et al. 2000; Bauer et al. 2001) have been shown to trigger the endosomally-located TLR9. The low frequency and high rate of methylation of CpG motifs prevent recognition of mammalian DNA by TLR9 under physiological circumstances.

Further, non-self DNA is also capable of triggering cytosolic receptors (Hochrein et al. 2004; Krug et al. 2004; Hornung and Latz 2010), as is evidenced in the recently discovered DNA sensors, DAI (DNA-dependent activator of IRFs) (Ishii et al. 2006; Stetson and Medzhitov 2006; Takaoka et al. 2007), the inflammasome (Muruve et al. 2008) and AIM2 (absent in melanoma 2) (Hornung et al. 2009). A role in detecting DNA was also ascribed to STING (Ishikawa et al. 2009). Moreover, it was shown that the DNA-dependent RNA polymerase III converts microbial DNA in the cytosol to 5`-triphosphates RNA to induce IFN-β through the RIG-I pathway (Ablasser et al. 2009; Cao 2009; Chiu et al. 2009; Choi et al. 2009).

1.1.3.2. Recognition of RNA

RNA recognition by TLR3

TLR3 recognizes long dsRNAs, as was demonstrated by a high sensitivity for Poly I:C (Polyinosine-deoxycytidylic acid), a synthetic analogue to dsRNA (Alexopoulou et al. 2001). Long dsRNAs are naturally absent in eukaryotic cells, but viral RNA has been observed to form long dsRNA intermediates during the process of replication. Eukaryotic messenger RNA, which tends to form intermolecular duplex-structures, has been characterized as a further target structure for TLR3 when entering the endosomal compartments as described for messenger RNA of necrotic or apoptotic cells (Kariko et al. 2004). Cellular localization of TLR3 differs depending on cell type. TLR3 localizes to endosomal compartments in cDCs, whereas it is expressed on the cell surface of

fibroblasts (Matsumoto et al. 2003). Additionally, instances of TLR3-independent recognition of viral dsRNA via RNA-helicases exist (compare 1.1.2.2).

RNA recognition by TLR7 & 8

Mouse TLR7 and human TLR7 & 8 recognize synthetic antiviral imidazoquinoline components (R848 and imiquimod) which are structurally related to nucleic acids, as well as uridine-rich or uridine/guanosine-rich ssRNA of both viral and host origins (Jurk et al. 2002; Heil et al. 2003; Lee et al. 2003; Diebold et al. 2004; Heil et al. 2004; Lund et al. 2004; Diebold et al. 2006). Although both TLR7 & 8 are expressed in mice, mouse TLR8 appears to be non-functional (Heil et al. 2004). IFN-α production by pDCs from TLR7-deficient mice is impaired after infection with the influenza virus or vesicular stomatitis virus (VSV) (Diebold et al. 2004; Lund et al. 2004). TLR7 & 8 are exclusively expressed in endosomal compartments. Therefore, the differentiation between endogenous and non-self-RNA molecules has been linked to the localization of the ligands within the cell. Unlike virus particles whose genomes are sheltered in the capsid, self-RNAs are degraded by extracellular RNases when they are released from the cell, and are not delivered to the endosome (Akira et al. 2006). Furthermore, mammalian RNA contains many modified nucleosides making them significantly less stimulatory via TLR7 & 8 (Ishii and Akira 2005; Kariko et al. 2005; Kariko and Weissman 2007). Studying various modification patterns, it has been shown that the 2`-position of the ribose is relevant for immunorecognition principles. Methylation led to an abrogation of cytokine secretion. Bacterial RNA is also recognized by TLR7 due to its lower content of nucleotide modifications (Eberle et al. 2009). In addition, TLR7 detects short dsRNA such as small interfering RNA (siRNA) in a sequence-dependent manner (Hornung et al. 2005). The expression of TLR7 & 8 is restricted to pDCs, which are known to produce vast amounts of type-I interferons upon viral infections (Liu 2005; Fitzgerald-Bocarsly et al. 2008).

Discrimination between self (host) and viral nucleic acids occurs on the basis of modifications and structural features, as well as on cellular compartments where viral but not host-derived nucleic acids are normally found. Endogenous RNA molecules (e.g. messenger RNA) reside either in the cytosol or in the nucleus and do not enter endosomal locations that participate in the uptake of exogenous substances. A failure of this discrimination results in the development of autoimmune diseases (Rifkin et al. 2005).

RNA recognition by RLRs

Whereas TLRs detect viral components in specific cells such as dendritic cells and macrophages, RLRs sense viral infections in the cytoplasm of most cell-types. RIG-I and MDA-5 recognize different types of viral RNA (Kato et al. 2006; Loo et al. 2008). RIG-I detects negative-strand viruses (e.g., paramyxovirus, influenza virus), ssRNA containing 5`-triphosphate (Hornung et al. 2006; Pichlmair et al. 2006) and short dsRNA (Hausmann et al. 2008; Kato et al. 2008), whereas MDA-5 senses positive-strand RNA viruses (e.g., encephalomyocarditis virus) and the dsRNA-mimic Poly I:C (Gitlin et al. 2006). However, viruses have developed the ability to circumvent these innate antiviral defenses. For example, it was shown that RIG-I is degraded during encephalomyocarditis virus infection (Barral et al. 2009; Papon et al. 2009) or inhibited by the Ebola viral protein 35 (VP35) (Leung et al. 2010). Even Poly I:C was reported to promote RIG-I degradation (Kim et al. 2008). Furthermore, the V proteins of many paramyxoviruses inhibit the function of MDA-5. However, it was shown that V protein-deficient viruses are in addition to RIG-I recognized by MDA-5 (Ikegame et al. 2010). This ligand-induced inhibition or degradation of the receptor makes it difficult to find a relation between nucleic acid structure and the dependent sensor. A specific RNA-sequence or structure activating MDA-5 has not yet been identified. Pichelmair et al. have found that MDA-5 activation requires a RNA web rather than merely long molecules of dsRNA (Pichlmair et al. 2009). Interestingly, the length of dsRNA is important for differential recognition by RIG-I and MDA-5. The MDA-5 ligand can be converted to a RIG-I ligand by shortening its length (Kato et al. 2008). However, the aforementioned structural features are absent from self-RNA. 5`-triphosphate and dsRNA are two molecular patterns that enable RIG-I to discriminate pathogenic from self-RNA. The dsRNA translocation activity on RNA that contains 5`-triphosphate serves as a signal verification mechanism by activating the ATPase only when the RNA features both PAMPs, the 5`-triphosphate and dsRNA. Integration of more than one PAMP in a single activation mechanism could be important for the selective discrimination of host- from viral-RNA (Myong et al. 2009). However, the exact structure of RNA detected by RIG-I remains controversial (Schlee et al. 2009). One study on activating ligands for RIG-I demonstrated that 5`-triphosphate with homopulyuridine or homopolyriboadenine motifs present in the genomes of hepatitis C virus (HCV) is a key feature for RIG-I-mediated RNA recognition (Saito et al. 2008; Uzri and Gehrke 2009). Cellular RNAs also contain poly-U and poly-A motifs, but self-RNAs are typically capped and bound by proteins (Afonina et al. 1998; Yusupov et al. 2001). In the past, most studies demonstrated that single-stranded 5`-triphosphate RNA is sufficient to bind to and

activate RIG-I (Pichlmair et al. 2006). These studies used *in vitro* transcription for generation of 5`-triphosphate RNAs without analyzing the purity of those RNA molecules. In fact, an unintended formation of dsRNA was the cause of RIG-I activity of the *in vitro* transcribed RNA (Schlee et al. 2009; Schmidt et al. 2009). Even for negative-strand RNA viruses known to activate RIG-I, it was shown by Schlee et al. that they contain 5`- and 3`-sequences that form a short double-strand with a perfectly blunt end ("panhandle") (Schlee et al. 2009). Furthermore, products of host RNA cleavage by RNase L, which bear 5`-hydroxyl- and 3`-monophosphate ends, were suggested to contribute to RIG-I activation (Malathi et al. 2007; Rehwinkel and Reis e Sousa 2010). Figure 2 presents an overview of the important nucleic acid sensor molecules described above, their respective ligands and the responsible target structures.

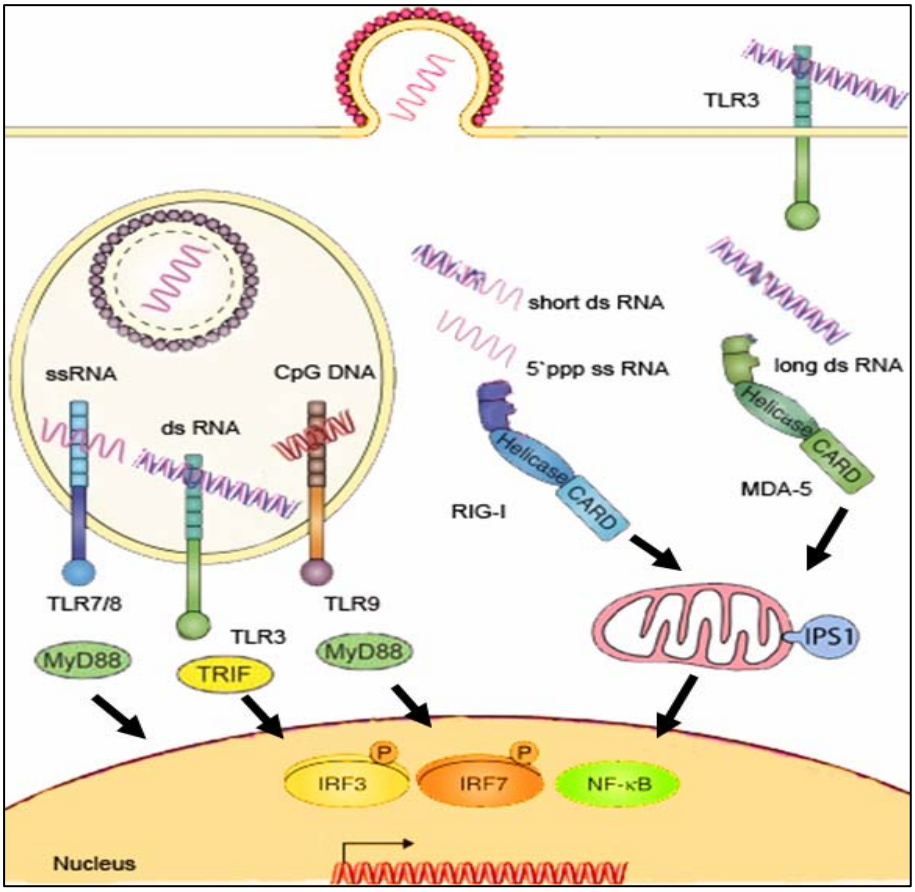

Figure 2: Sensors for nucleic acids (modified after (Seth et al. 2006; Saito and Gale 2008; Barral et al. 2009; McCartney and Colonna 2009)). Toll-like receptors are expressed in cellular membranes at the cell surface or intracellular. Besides Toll-like receptors, there are helicases in the cytosol. MDA-5 and RIG-I distinguish their ligands by size; MDA-5 binds to long dsRNA, whereas RIG-I binds short dsRNA and ssRNA bearing a 5`-triphosphate end. Among the TLRs, TLR3 recognizes dsRNA, TLR7 & 8 recognize ssRNA, and TLR9 binds to CpG DNA. Upon binding of nucleic acids, intracellular adaptor molecules are recruited and initiate the activation of NF-κB and IRF-dependent target genes. IPS is a mitochondrial protein that participates in the signaling pathway downstream of RIG-I and MDA-5. Not mentioned in this figure is the negative regulator of RIG-I/MDA-5: LGP2 and the cytosolic DNA receptor DAI.

1.2. Antimicrobial peptides (AMPs)

Antimicrobial peptides are important effector molecules of innate immunity. They are ubiquitous defense biomolecules found in virtually all forms of life (Jenssen et al. 2006). Currently, about 900 different AMPs and proteins have been described (Brogden 2005). Although AMPs are diverse in their amino-acid sequence, structure and size, they are mostly amphipathic, containing both cationic and hydrophobic faces (Molhoek et al. 2009). In mammals, there are two main families of AMPs, the defensins and the cathelicidins (Zasloff 2002; Yang et al. 2004). This work will concentrate on cathelicidins. Cathelicidins consist of an N-terminal anionic signal peptide (preregion), a highly conserved cathelin-like domain (proregion) and a structurally variable cationic antimicrobial peptide at the C-terminus (hence the name "cathelicidin") as shown in Figure 3 (Zanetti et al. 1995). The anionic prosegment neutralizes the cationic peptide and maintains an inactive propetide during intracellular transport and storage to avoid intracellular toxicity (Ramanathan et al. 2002).

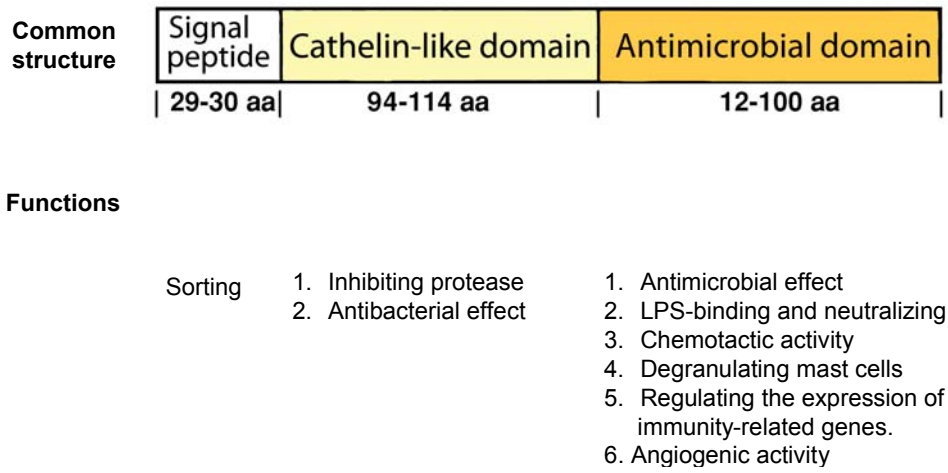

Figure 3: Cathelicidins and their activities (modified after (Yang et al. 2004)). All cathelicidins have a common primary structure that contains an N-terminal signal peptide, a highly conserved cathelin-like domain in the middle, and a highly variable C-terminal antimicrobial domain. For the C-terminal antimicrobial domain of cathelicidins, several activities have been identified.

The only known human cathelicidin LL-37 or hCAP-18 (cationic antimicrobial peptide of 18 kDa), was isolated from bone marrow (Larrick et al. 1995; Gudmundsson et al. 1996). Cathelicidins are usually stored in the granules of neutrophils. They are also produced by various epithelial cells and keratinocytes (Agerberth et al. 2000; Dorschner et al. 2001)

and by mononuclear cells (monocytes, NK cells, B cells, and γ-, δ- T cells) (Frohm et al. 1997; Bals et al. 1998; Durr et al. 2006), as an inactive proform. They undergo processing to the mature peptides during or after secretion by proteases. The 18 kD human cationic antimicrobial protein (hCAP18) can be cleaved by either elastase (Gudmundsson et al. 1996) or proteinase 3 (Sorensen et al. 2001) to liberate its C-terminal antimicrobial domain (Zanetti 2004). This peptide is called "LL-37" because it begins with two leucine residues and has 37 amino acid residues (Gudmundsson et al. 1996; Yang et al. 2004).

The cathelicidins in mouse and rat have also been characterized and named CRAMP (cathelin-related antimicrobial peptide) (Gallo et al. 1997) and rCRAMP (Termen et al. 2003).

The gene encoding LL-37 consists of 4 exons of which the first three encode the signal peptide and the cathelin region. The cathelin domain is similar to members of the cystatin superfamily of protease inhibitors (Zaiou and Gallo 2002; Zaiou et al. 2003). The fourth exon encodes the processing site and the antimicrobial domain (Gudmundsson et al. 1996) and is located on chromosome 3 (Gudmundsson et al. 1995), which is homologous to mouse chromosome 9, where the gene encoding CRAMP is located (Gallo et al. 1997).

The C-terminal AMPs of cathelicidins are microbicidal against a broad spectrum of microorganisms (Zasloff 2002), including bacteria (Turner et al. 1998), fungi (Dorschner et al. 2004), parasites (Johansson et al. 1998) and viruses (Howell et al. 2004). The mechanism of cathelicidin-mediated microbial killing depends on the formation of ion channels or pores in the microbial cell membrane. AMPs preferentially interact with prokaryotic cells, although at high concentrations eukaryotic cells are also ruptured. The reason for this preference may be the presence of negatively-charged molecules in prokaryotic membranes, such as phospholipids, lipotechoic acid, and LPS. Eukaryotic membranes, on the other hand, are dominated by neutral zwitterions and cholesterol, resulting in a more neutral charge (Zasloff 2002).

LL-37 also possesses a potent endotoxin-neutralizing activity due to interaction with a negatively-charged lipid A portion of the LPS molecule (Larrick et al. 1995; Nagaoka et al. 2001; Kandler et al. 2006; Mookherjee et al. 2006). LL-37 was shown to protect mice and rats from LPS-mediated lethality in septic shock (Kirikae et al. 1998; Scott et al. 2002; Cirioni et al. 2006; Alalwani et al. 2010). LL-37 suppressed proinflammatory cytokine production induced by agonists of TLR4 and TLR2/1, while leaving TLR2/6, TLR5, TLR7 and TLR8 responses unchanged (Molhoek et al. 2009).

In addition to the antimicrobial effects, LL-37 exhibits a number of other host-defense and immunoregulatory functions. LL-37 has chemotactic activities on neutrophils, monocytes

and T cells. This activity was shown to be mediated via the formyl-peptide receptor-like 1 (FPRL-1) (De et al. 2000). Mouse CRAMP (1-39) also exhibits a direct effect on the migration and function of leukocytes (Kurosaka et al. 2005). Furthermore, LL-37 has been shown to mediate release of IL-1ß from monocytes via an additional receptor, P2X(7) (Elssner et al. 2004). LL-37 additionally exhibited effects on the maturation of dendritic cells (Davidson et al. 2004). This shows a role for LL-37 as a potent immunomodulatory molecule, which acts as a link between the innate and adaptive immune systems. Furthermore, LL-37 exerts wound-healing functions (Heilborn et al. 2003) and induces angiogenesis by a direct effect on endothelial cells mediated by FPRL-1 (Koczulla et al. 2003).

1.3. TLR ligands as adjuvants

The idea behind vaccines is to create a long-lasting immune reaction against a pathogen. Innate immunity does not provide long-lasting or protective immunity to the host (Pulendran and Ahmed 2006). In contrast, adaptive immunity relies on the clonal selection of lymphocytes with recombined highly affine receptors. This second immune response is more specific and leads to an increase in defense capabilities with every further exposure to the same antigen. Receptors of T cells recognize their antigens only in the form of peptides presented by specialized proteins that are encoded by genes in a locus called the major histocompatibility complex (MHC) (Janeway 2005; Abbas 2007). Thus, immunity must be associated with memory. This is achieved by introducing small amounts of non-infectious antigen to the host; an event we call vaccination. However, the antigen alone is not sufficient to create an immunological memory. There is a need for an adjuvant. Alum has a good safety record but is only a weak adjuvant (O'Hagan et al. 2001). CpG-DNA has been proven to be one of the strongest Th1-immune-response-inducing adjuvants known *in vivo* (Lipford et al. 2000; Krieg 2002). But the utilization of DNA as an adjuvant might raise certain safety concerns, like the risk of DNA integration into the genome or overstimulation of the immune system. For this reason, RNA has been tested as an adjuvant. Since RNA is very prone to hydrolysis, the RNA molecules have to be protected from immediate degradation either through interaction with cationic proteins or through chemical modification of the phosphodiester backbone. With regard to RNA, it has been reported that mRNA molecules (Scheel et al. 2004) induce immune stimulation and specific antibody production (Westwood et al. 2006). Vaccination with mRNA combines two aspects of an immunization: Firstly, RNA induces immune stimulation; secondly, the

protein coding from the mRNA serves as an antigen. Hoerr at al. proposed that the application of mRNA coding for the model antigen ß-galactosidose leads to induction of cytotoxic T cells and antigen-specific antibodies (Hoerr et al. 2000). As adjuvant, RNA induces a Th2-type humoral response that means the antibody response was primarily of the IgG1 isotype. Recently, it was shown that the injection of single-stranded synthetic RNA, when complexed to the cationic transfection reagent DOTAP and OVA, works as adjuvant. In comparison with CpG-DNA, immunostimulatory RNA induced lower frequencies of cytotoxic T cells, but RNA did not induce splenomegaly, which is in contrast to the effect of CpG-DNA. RNA is a weaker but safer adjuvant than CpG-DNA (Hamm et al. 2007). Interestingly, some novel studies have confirmed that eukaryotic RNA can be a potent adjuvant for immune responses (Riedl et al. 2002; Scheel et al. 2004).

1.4. Hydrolysis of RNA

RNA represents a ligand for various immunorecognition principles. RNA degradation is catalyzed by enzymes, called ribonucleases. These enzymes are ubiquitous and are crucial for processing RNA into mature forms. They are not only important for RNA metabolism, cell maturation, physiological cell death, and promotion of blood vessel formation, but also for host defense against RNA viruses (Arnold and Ulbrich-Hofmann 2006; Probst et al. 2006). Ribonucleases activate the phosphodiester group through basic amino acids, metal ions or a combination of both. Water is often used as an external nucleophile (Kurz 1998). Ribonucleases that preferentially degrade ssRNA are the following: RNase A, RNase T1, RNase T2, RNase I, and RNase L (Meador et al. 1990; Raines 1998; Deshpande and Shankar 2002; Czaja et al. 2004; Malathi et al. 2007; Luhtala and Parker 2010). These endoribonucleases hydrolyze RNA to 3`-phosphomonoester via 2`,3`-cyclic nucleosides (Deshpande and Shankar 2002). RNase I cleaves every phosphodiester bond, unlike other ribonucleases, which cleave only after specific residues. For example, RNase A is a pyrimidine-specific (C and U) endoribonuclease (Raines 1998). RNase A is the founding member of a family of proteins, called the RNase A superfamily. Initially isolated from bovine pancreatic tissue, RNase A is a classic model system for protein studies, as a result of its thermostability and the relative abundance of its source tissue (Dyer and Rosenberg 2006; Rosenberg 2008). RNase A is a relatively small protein (124 residues, ~13.7 kDa) and it is a cationic protein at physiological pH, explaining its binding to RNA (poly-anion). RNase A has eight

cysteines that form four disulfide bonds, and the catalytic triade (Figure 4) consists of two histidines and one lysine.

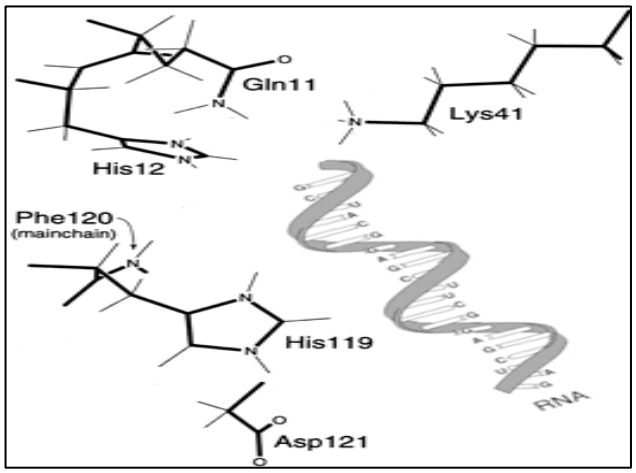

Figure 4: Active site of RNase A (modified after (Raines 1998)). The catalytic triade consist of two histidines and one lysine. Further site chains like phenylalanine stabilize the transition state during RNA cleavage.

The RNase A catalyzes the cleavage of the P-O 5`-bond of RNA, thereby catalyzing both the transphosphorylation of RNA to form a 2`,3`-cyclic phosphodiester intermediate and the hydrolysis of this cyclic intermediate to form a 3´-phosphomonoester. Figure 5 shows the mechanism of catalysis. The side chain of His12 acts as a base that abstracts a proton from the 2`-oxygen of a substrate molecule, and thereby facilitates its attack on the phosphorus atom. The side chain of His119 acts as an acid that protonates the 5`-oxygen to facilitate its displacement. The side chain of Lys41 and the main chain of Phe120 enhance catalysis by stabilizing this transition state. RNase A primarily catalyses transphosphorylation of RNA rather than hydrolysis of the cyclic intermediate. The 2`,3`-cyclic phosphodiester intermediate accumulates during catalysis by RNase A. It can be concluded that the 2`,3`-cyclic phosphodiester are true products of the transphosphorylation reaction and not intermediates as generally thought (Cuchillo et al. 1993; Thompson et al. 1994; Raines 1998).

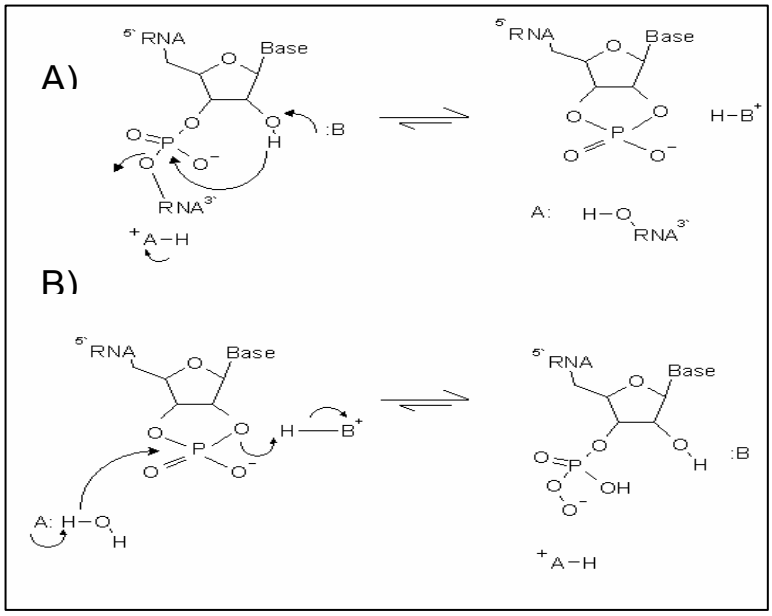

**Figure 5: Hydrolysis of the P-O 5`-bond in RNA (modified after (Raines 1998)).** This reaction occurs in two steps: (A) transphosphorylation of RNA to a 2`,3`-cyclic phosphodiester intermediate and (B) hydrolysis of this cyclic intermediate to a 3`-phosphomonoester. In both mechanisms, "B" is His12 and "A" is His119.

The endoribonuclease L (RNase L) is a latent enzyme expressed in nearly every mammalian cell type. Its activation requires it to bind to a small oligonucleotide, 2-5A. By regulating viral and cellular RNA expression, RNase L plays an important role in the antiviral and antiproliferative activities of IFN. RNase L cleaves RNAs at UpN (usually UpU and UpA) sequences in single-stranded regions of RNA. The products generated contain 5`-hydroxyl- and 3`-monophosphate ends (Bisbal and Silverman 2007; Silverman 2007; Silverman 2007).

Besides these nucleases, there are further single-stranded specific endoribonucleases, like the S1 nuclease from Aspergillus oryzae (Desai and Shankar 2003) and the P1 nuclease from Penicillium citrinum (Volbeda et al. 1991; Desai and Shankar 2003), which hydrolyze RNA to 5`-phosphomonoester.

Finally, a particular ds-specific endoribonuclease RNase III cannot be neglected. RNase III family members are divided into three structural classes. The first class is represented by Escheria coli RNase III, the second by Drosha, and the third by Dicer (Carmell and Hannon 2004). The bacterial RNase III, discovered in 1968 (Robertson et al. 1968), is the most studied member of this family (Gan et al. 2008). E. coli RNase III promotes maturation of ribosomal RNA (rRNA), tRNAs and mRNA, and can also initiate mRNA degradation (Nicholson 1999; Carmell and Hannon 2004). The products generated contain 5`-monophosphate and 3`-OH groups with two nucleotide 3`-overhangs (Conrad and Rauhut 2002; Carmell and Hannon 2004). Complete digestion of dsRNA results in ssRNA fragments of 12-15 bp. Class 2 and Class 3 RNases are essential for the biogenesis of miRNAs and siRNAs which are assembled into effector complexes to guide specific antiviral defenses via the RNA silencing pathway (Carmell and Hannon 2004;

Aliyari and Ding 2009). Dicer belongs to the same helicase family as do the RIG-I-like receptors (Deddouche et al. 2008).

Metal-ion-induced hydrolysis of RNA

Metal ions are an essential factor for the phosphodiester hydrolysis of nucleic acids by nucleases and ribozyms. For example, the aforementioned enzymes S1 nuclease and P1 nuclease are zinc metalloproteins and contain three Zn^{2+} atoms per molecule of the enzyme (McCall et al. 2000).

Pb^{2+}-induced cleavage patterns have been used in the analysis of RNA structures. Pb^{2+}-induced cleavage occurs preferentially in bulges, loops and other ssRNA regions. DsRNA segments are essentially resistant to breakage, but cleavages are also observed in paired regions destabilized by the presence of non-canonical interactions, bulges or other structural distortions (Hartmann et al. 2005).

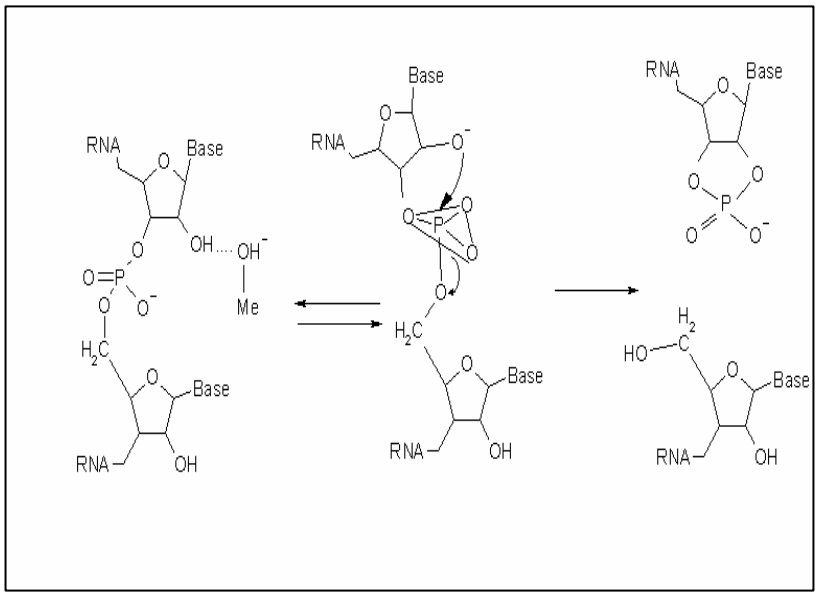

Figure 6: Mechanism of metal-ion-induced cleavage of RNA (modified after (Hartmann et al. 2005)). The metal ion facilitates deprotonation of the 2`-OH, resulting in a nucleophilic attack on the phosphorus atom and subsequent cleavage of the phosphodiester bond.

The simplified mechanism shown in Figure 6 might account for all types of cleavage induced by metal ions. First, the ionized metal ion hydrate acts as a Brönsted base by accepting a proton from the 2`-OH group of the ribose. Then, the activated anionic 2`-O attacks the phosphorus atom, and a penta-coordinated intermediate is formed. The phosphodiester bond is cleaved generating 2`,3`-cyclic phosphate and 5`-hydroxyl groups as cleavage products (Matsuo et al. 1995; Yashiro et al. 2002; Hartmann et al. 2005; Wang et al. 2007).

2. Goal of the project

RNA is present in abundance in host cells, but host cellular RNA fails to stimulate innate immune responses, unlike virus-derived RNA. TLRs as well as cytoplasmic receptors have been described to be triggered by non-self-RNA molecules. The immune system must possess mechanisms to discriminate molecular features between host and virus RNA species. Although some receptor ligand interactions could be identified already, essential parts of RNA immunorecognition remain unclear. This study intended to characterize the interaction of different RNA ligands with the respective immunoreceptors.

The first part of the work analyzed the influence of nucleotide modifications of RNA for inducing an immune response. Self-RNA is not immunostimulatory due to RNA modifications such as base-methylation, pseudouridine and 2`-O-methyl ribose. The immunostimulatory potentials of purified ribosomal 18S rRNA and *in vitro* transcribed 18S rRNA, which lack modifications, are beeing compared on human PBMCs and murine Flt3-derived immune cells. RNA oligonucleotides derived from the 18S rRNA with different modifications have been synthesized and should be tested for their behaviour concerning the induction of cytokines on immune cells.

In the second part of the work, the ability of LL-37, a human antimicrobial peptide and its murine homolog cathelicidin-related antimicrobial peptide (CRAMP) to function as carrier for immunostimulatory RNA and to induce innate immune activation should be analyzed. Since naturally occurring cathelicidin is produced at mucosal sites, it should function as immune activator by targeting RNA from virus-infected cells to immune cells. The central issue was to find out, if cathelicidins/RNA complexes are potent vaccine formulations, if cathelicidins are crucial for antiviral immune response against influenza infections and if viral immune recognition can be manipulated by synthetic LL-37/CRAMP. Since DOTAP is toxic at higher concentrations, non-toxic or natural carriers for immunostimulatory RNA are desirable.

Moreover, we set out to investigate the characteristics of RNA extracted from influenza-infected cells that are recognized as non-self structures. RNA of the influenza virus, which contains a 5`-triphosphate, directly interacts with RIG-I and is responsible for the induction of type-I IFN. The immunostimulatory potential of influenza-infected RNA was to be assessed by measuring the induction of IFN-α in human PBMCs and in cells from various knockout mice. In parallel, influenza-infected RNA should be used for transfection of HEK293 cells overexpressing RIG-I. The influence of the terminal 5`-triphosphate as well

as the confirmation of the influenza-infected RNA (ssRNA or dsRNA) on RIG-I-mediated signaling should be investigated.

Finally, immunorecogition of small self-RNAs should be analyzed. During viral infection cellular RNA serves as a ligand that stimulates the immune response. Viral RNA stimulates 2`-5` oligoadenylate synthetase (2`-5` OAS) to promote activation of an endonuclease, RNase L, which subsequently cleaves self-RNA to make small RNA species. The cleaved RNA, which contains a 3`-monophosphate group, serves as the ligand for RIG-I and MDA-5 to initiate signaling leading to type-I IFN production. This is surprising, since self-RNA is not stimulatory due to natural occurring RNA modifications. The aim of this study is to analyze the immunostimulatory nature of RNase treated self-RNAs. Therefore, responsiveness to small self-RNAs should be examined in different immune cells. Furthermore, self-RNAs were degraded by using different methods, like ultrasonic treatment, metal-ion induced hydrolysis or treatment with different RNase types and the generated fragments were compared for their immunostimulatory abilities. It was intended to identify structures and sequences that presumably have interesting properties as therapeutics in vaccination protocols.

Overall, the goal of the project is to discover novel basic viral and host immune mechanisms. Influenza viruses are a major concern for global public health. Therefore, new and efficient antiviral therapeutics and effective vaccine formulations are of major interest. Regarding autoimmune diseases, principle mechanism for recognizing self-RNAs have to be investigated.

3. Material

3.1. Machines and technical devices

Equipment	Manufacturer
Agarose gel chamber	OWL, Weilheim
Apotome	Zeiss, Jena
CASY-1 TT	Schärfe System, Reutlingen
Centrifuges	Pico Fuge-Stratagene, La Jolla USA Mikro 200R Centrifuge-Hettich, Tuttlingen Multifuge 1L-R Heraeus, Hanau
Diavert Microscope	Leitz, Bielefeld
Elutriation	Beckman J2-21M/E Centrifuge
FACS Calibur	Becton Dickinson, Basel
Fine scale	Sartorius, Göttingen
Gel imaging system	Fröbel, Lindau
Gene Pulser x-cell	Biorad, Hercules, USA
Heating blocks	PeqLab Biotechnologie GMbH TS-100 Thermo Shaker, Peqlab Erlangen
HPLC "BioCAD Sprint"	Applied Biosystems, USA
Incubator	HERA cell 240® (37°C / 5% CO_2) HERA cell 240 ® (37°C / 7.5% CO_2), Heraeus, Hanau Heraeus Lamin Air® (37°C / 7.5% CO_2)
MACS Midi-Separator	Miltenyi Biotec, Bergisch Gladbach
MACS Multistand	Miltenyi Biotec, Bergisch Gladbach
Microplate	Nunc Denmark Poly Sorte
Microplate Spectrophotometer	Molecular Devices, Ismaning
Microplate Washer	Molecular Devices, Ismaning
Mini Opticon	Bio-Rad, Hercules, USA
Neubauer	W. Schreck, Hofheim
Normal scale	Mettler, P1000
Orion II Microplate Luminometer	Berthold Detection System, Pforzheim
PAA-gel chamber	PeqLab, Erlangen
pH-Meter	WTW, Weilheim

Equipment	Manufacturer
Pipetus	Hirschmann Laborgeräte, IBS Integra Biosciences
Spectrophotometer	NanoDrop® Spectrophotometer peQLab, Wilmington, USA
Steril bench	HERA Safe®, Heraeus Lamin Air®
Thermocycler Elite	Helena, Sunderland, UK
Thermocycler Eppendorf	Eppendorf, Hamburg
TS–100 Thermoshaker	Peqlab, Erlangen
Ultrasonic Homogenizer	Bandelin
Vortexer, REAX 2000	Heidolph, Schwabach
Water bad	WTW, Weilheim Kottermann Labortechnik, Haake D8

3.2. Software

Software	Manufacturer
Microsoft Office	Microsoft Corporation, Redmond, USA
Sigma Plot	Systat Software Inc., Chicago, USA
CellQuest Pro	BD Biosciences, San Jose, USA
EndNote	The Thomson Corporation, Stamford, USA
Flowjo for Macintosh	Tree Star, Inc., Ashland, USA
AxioVision LE	Carl Zeiss MicroImaging GmbH

3.3. Equipment

Equipment	Manufacturer
4 mm Electroporation cuvette	Bio-Rad, Hercules, USA
Flat Cap Strips	Bio-Rad, Hercules, USA
Low Tube Strip, WHT	Bio-Rad, Hercules, USA
Membrane Filter, pore size 25 mm	Millipore
Cell strainer	BD Falcon, Franklin Lakes NY USA

3.4. Chemicals

Chemicals	Manufacturer
$(MgCO_3)4Mg(OH)_2 \times 5H_2O$	Roth, Karlsruhe
Acrylamide M-Bis	Roth, Karlsruhe
Agar Agar	Roth, Karlsruhe
Agarose	Invitrogen, Karlsruhe
Ammonium acetate	Roth, Karlsruhe
Ammoniumpersulfate	Sigma Aldrich, Taufkirchen
Bacto-Agar	Becton Dickinson
Bovine serum albumin (BSA)	Roth, Karlsruhe
CaCl	Roth, Karlsruhe
Chloroform	Sigma Aldrich, Taufkirchen
Citric acid	Roth, Karlsruhe
Crystal violet	Serva, Heidelberg
DAPI (4,6 Diamidin-2-phenylindol-dihydrochlorid)	Roche, Mannheim
Diethylpyrocarbonat (DEPC)	Roth, Karlsruhe
Dithiothreitol (DTT)	AmpliScribe™ T7, SP6 Transcription Kit Epicentre, Biozym, Hess. Oldendorf
DMSO	Merck, Ismaning
EDTA (Etylendiamintetraacetacid)	Roth, Karlsruhe
Eosin	Merk, Ismaning Roth, Karlsruhe
Ethanol p.a. 99.8%	Roth, Karlsruhe
Ethidiumbromide	Roth, Karlsruhe
Glycerol	ICN Biomedicals, Inc, Aurora, Ohio
HEPES	Roth, Karlsruhe
Hydrogen peroxide	Roth, Karlsruhe
Isopropanol	Roth, Karlsruhe
Kaliumchlorid	Roth, Karlsruhe
Kaliumdihydrogenphosphate	Roth, Karlsruhe
Lead (II) acetate trihydrate (316512-5G)	Sigma-Aldrich, Taufkirchen
Methanol	Roth, Karlsruhe

Chemicals	Manufacturer
$MgSO_4$	Roth, Karlsruhe
MOPS (3-(N-Morpholino)-Propansulfonacid)	Roth, Karlsruhe
Mowiol	Sigma Aldrich, Taufkirchen
N,N,N`,N`-Tetraethylmethylenediamin (TEMED)	Sigma Aldrich, Taufkirchen
Na_2HPO_4 anhydrate	Roth, Karlsruhe
NaCl	Roth, Karlsruhe
Natriumacetat	Roth, Karlsruhe
Natriumazide	Merk, Ismaning
Natriumchlorid solution	Merk, Ismaning
Natriumhydroxid	Merck, Darmstadt
Phenol	Roth, Karlsruhe
Phenol:Chloroform:Isoamylalcohol (25:24:1)	Roth, Karlsruhe
Polyvinylalkohol-88	Sigma Aldrich, Taufkirchen
HCl	Merck, Darmstadt
SDS (Natriumdodecylsulfate)	Roth, Karlsruhe
Sulphuric acid	Roth, Karlsruhe
Tetraethylammoniumchloride (TEACL)	SIGMA, Spruce Street, Saint Louis, Missouir, USA
TMB Microwell Peroxidase Substrate System	KPL, Clopper Road, Gaithersburg, Maryland, USA
Tris-(hydroxymethyl)-aminomethane	Roth, Karlsruhe
Tris-HCL	Roth, Karlsruhe
Trizol®	Sigma-Aldrich, Munich
Tween 20	Roth, Karlsruhe
Ultra-pure water	Biochrom AG, Berlin
UltraLink® Immobilized Streptavidin	PIERCE, Meridian Road, Rockford, USA

3.5. Biochemicals, kits and enzymes

Biochemicals	Manufacturer
5 x Lysing Solution	Promega, Mannheim
Alkaline Phosphatase	Sigma Aldrich, Munich
Alkaline Phosphatase, Calf Intestinal (CIAP) [1 U/µl] (M1821)	Promega, Mannheim
AmpliScribe™ T7, SP6 Transcription Kit	Epicentre, Biozym, Hess. Oldendorf
ATP	Roth, Karlsruhe
Benzonase 25 U/µl (M00047398)	Novagen, Darmstadt
Biotin (powder)	Sigma, Munich
Chicken egg albumin (OVA)	Profos AG, Regensburg, Germany
Coenzyme A	PJL, Kleinblittersdorf
D-Luciferin	PJL, Kleinblittersdorf
DNase I recombinant, RNase-free [10 U/µl] (10776785001)	Roche, Mannheim
dNTPs	Invitrogen, Karlsruhe
Donkey-α-rabbit-IgG-HRP	Dianova GmbH, Hamburg
DTP	PJL, Kleinblittersdorf
Ficoll	PAA Laboratories, Pasching
FMS-like tyrosine kinase 3 Ligand (Flt3-L)	From own cell line purified: TU Munich
RNA Fragmentation Reagent	Ambion
Granulocyte macrophage colony stimulating factor (GM-CSF) (315-03)	Peprotech
Heparin "Liquemin N 25000"	Roche, Mannheim
human AB Serum	Sigma
Klenow Fragment	New England Biolabs, Frankfurt a.M.
Macrophage colony stimulating factor (M-CSF) (416 ML)	Tebu
Micro Bio-Spin 30 Columns in RNase-Free Tris	Bio-Rad, Hercules, USA
Mini Elute DNA PCR Purification Kit	PeqLab, Erlangen
Mycoplasma Detection Kit	Lonza, Switzerland
Nuclease P1 [0.3 U/µl] (N8630)	Sigma Aldrich, Taufkirchen
o-Phenylenediaminedihydrochloride (OPD), 20 mg tablet (P7288)	Sigma-Aldrich, Munich

Biochemicals	Manufacturer
Optimen (31985047)	GIBCO, Invitrogen Corporation
PeqGold Plasmid Mini Praep Kit	PeqLab, Erlangen
Proteinase K [10 mg/ml]	Roche, Mannheim
Pvu II	New England Biolabs, Frankfurt a.M.
Recombinant human IFN-α (300-02A)	Peprotech
Recombinant human IL-6 (200-06)	R&D Biosystems, Wiesbaden
Recombinant human TNF-α (300-01A)	Peprotech
Recombinant murine IFN-α (HC1040a)	Hycult biotechnology b. v.
Recombinant murine IL-6 (406-ML)	R&D Biosystems, Wiesbaden
Recombinant murine IFN-ß (12400-1) [100,000 U/ml] (12400-1)	PBL Interferon Source, Piscataway, NJ
Red blood cell lysing solution (RBL)	Sigma, Munich
RNase [500 µg/ml] [15 U/ml] (11119915001) called RNase A in the figures	Roche, Mannheim
RNase A [100 mg/ml] [7000 U/ml] (19101) not used for the figures	Quiagen
RNase I [10 U/µl] (N6901K)	Epicentre
RNase III [1 U/µl] (RN029050)	Epicentre
RNase III [1.3 U/µl]	BioLabs
RNase T1 from Aspergillus oryzae [1,46 mg protein/ml, 300,000–600,000 U/mg protein] [657 U/µl]	Sigma
RNase T2 [34,000 U/ml] (R-6398)	Sigma
SvP (snake venom protease) [50ng/µl] [0,01 U/mg] (P3134)	Sigma Aldrich, Munich
Silencer® siRNA Construction Kit	Ambion
Streptavidin-beads	Pierce
Streptavidin-POD (11 089 153 001)	Roche, Mannheim
SuperScript III CellsDirect cDNA Synthesis System	Invitrogen, Karlsruhe
T4 Polynucleotide Kinase 10 U/µl (#EK0031)	Fermentas
Taq PCR Master Mix Kit	Quiagen, Hilden
Tricin	Roth, Karlsruhe
Waters C18 SepPak columns	Waters Corporation, Milford/Massachusets
XBRIDGE^{TM} OST C_{18} columns	Waters Corporation, Milford/Massachusets

3.6. Antibodies

Antibody	Manufacturer
ELISA	
Coating Antibody Human IFN-α (BMS216MST)	Bender MedSystems, Vienna, Austria
HRP-conjugate (23010-11)	Bender MedSystems,Vienna, Austria
Purified Rat Anti-Human IL-6 Monoclonal Antibody (554543)	BD Pharmingen, Heidelberg
Biotinylated Rat Anti-Human IL-6 (554546)	BD Pharmingen, Heidelberg
Purified Mouse Anti-Human TNF Monoclonal Antibody (551220)	BD Pharmingen, Heidelberg
Biotinylated Mouse Anti-Human TNF Monoclonal Antibody (554511)	BD Pharmingen, Heidelberg
Rat Monoclonal Antibody against Mouse Interferon Alpha (RMMA-1) (22100-1)	PBL, New Brunswick,USA
Rabbit Polyclonal Antibody against Mouse Interferon Alpha (32100-1)	PBL, New Brunswick,USA
Polyclonal rabbit anti-mouse IFN-ß (32 400-1)	PBL, New Brunswick,USA
Monoclonal rat anti-mouse IFN-ß (22 400-1)	PBL, New Brunswick,USA
Monoclonal Anti-mouse IL-6 Antibody (MAB 406)	R&D, Biosystems, Wiesbaden
Biotinylated Anti-mouse IL-6 Antibody (BAF406)	R&D, Biosystems, Wiesbaden
anti-rat IgG antibody H&L POD-conjugated (ab6734)	Abcam, UK
POD-conjuagated goat anti-rabbit IgG (111-035-045)	Immuno Research
ELISA Immunization	
biotin-SP-conjugated AffiniPure goat anti-mouse IgG	Jackson ImmunoResearch, Hamburg
FACS	
Mouse anti-human BDCA-2-PE	Miltenyi Biotec, Bergisch Gladbach
Mouse anti-human CD11b-APC	BD Pharmingen, Heidelberg
Mouse anti-human CD14-FITC	BD Pharmingen, Heidelberg
Rat Anti murine B220-FITC	BD Pharmingen, Heidelberg
Rat Anti murine CD11c-APC Rat	BD Pharmingen, Heidelberg
Anti murine CD11b-FITC	BD Pharmingen, Heidelberg
Rat IgG, Fc Blocking	Jackson ImmunoResearch, Hamburg

Antibody	Manufacturer
Mouse IgG, Fc Blocking	Jackson ImmunoResearch, Hamburg
TO-PRO® iodide solution in DMSO [SKU#T3605]	Invitrogen
Apotome	
Lamp-1 (Purified Mouse Anti-Human CD107a) (555798)	BD Pharmingen, Heidelberg
Transferrin Conjugates (T2872)	Invitrogen, Karlsruhe
Lysotracker (L7528)	Invitrogen, Karlsruhe
Purified Mouse Anti-EEA-1 (610456)	BD Biosciences
Rhodamine (TRITC)-conjugated AffiniPure F (ab`)2 Fragment Goat Anti-Mouse IgG (H+L) (115-026-003)	Dianova
DAPI	Roche, Mannheim

3.7. Size markers

Markers	Manufacturers
6 x DNA Marker	Fermentas, St. Leon Rot
6 x Loading Dye Solution	Fermentas, St. Leon Rot
2 x RNA Loading Dye Solution	Fermentas, St. Leon Rot
Gene Ruler 100 bp DNA-Marker (SM0321)	Fermentas, St. Leon Rot
Gene Ruler 1 kbp DNA-Marker (SM0313)	Fermentas, St. Leon Rot
RiboRulerTM RNA Ladder (SM1821)	Fermentas, St. Leon Rot

3.8. Buffers and media

Name	Compounds
0.1% DEPC (Diethyl-Pyrocarbonat) solution	Milli-Q-H_20 1/1000 Volume DEPC 3 h stir 2 x autoclave
6 x loading dye solution (Fermentas)	30% (v/v) Glycerin 0.25% (w/v) Bromphenol blue 0.25% (w/v) Xylenblau dissolved in water

Name	Compounds
Blocking buffer 1%	10 g BSA 1 x; 0.5 ml Tween 20; ad 1 l with PBS-deficient
EDTA 0.5 M	18.612 g EDTA; 50 ml H_20, neutralize with NaOH pellets; ad 100 ml with ddH_20
ELISA substrate buffer	7.3 g $C_6H_8O_7$; 11.87 g Na_2HPO_4 x $2H_2O$; ad at 1 l with ddH_2O
ELISA wash buffer	500 ml 10 x PBS; 2.5 ml Tween 20; ad 5 l with ddH_2O
Eosin solution	2 g Eosin, 250 mg Natriumazid, 450 ml 0.9% Natriumchlorid, 50 ml FCS Mix well and filter through an paper filter storage: unsterile, 4°C
FACS-Puffer	PBS def., 3% FCS, 0.01% Azide
Freezing medium	90% FCS 10% DMSO sterile
Kristallviolett solution	2% stock solution: 2 g Kristallviolett 20 ml Ethanol 96% 10 ml Formaldehyde at least 35% 70 ml Aqua distilled 0.2% working solution: 10 ml stock solution 10 ml Formaldehyde 80 ml Aqua distilled.
Liposomal buffer	20 mM HEPES, 150 mM NaCl adjust ad pH 7.4 1/1000 Volume DEPC 3 h stir 2 x autoclave
Luciferase-Assay buffer 1 l	132 mg D-Luciferin; 210 mg Coenzyme A; 5140 mg DTT; 292 mg ATP; 520 mg $(MgCO_3)_4Mg(OH)_2$ x 5 H_2O; 322mg $MgSO_4$; 3584 mg Tricin; 37.2 mg EDTA
MACS-buffer	PBS def.; 3% FCS; 2 mM EDTA
MOPS	0.2 M MOPS (Morpholinopropansulfonsäure), 50 mM Natriumacetat (trihydrate), 10 mM EDTA adjust pH ad 7.0 ad H_20 ad 1 l

Name	Compounds
Mowiol	2 g Polyvinylalcohol 4-88 (Mowiol), 6 g Glycerin, 6 ml H_20 shake over night at room temperature 12 ml Tris pH 8.5 2 g DABCO heat for 10 min at 50°C and shake centrifugation for 15 min at 5,000 g froze supernatant at -20°C
NEB Restrictionsendonuclease buffer 10 x	Acquired from New England Biolabs, Frankfurt a.M.
PBS-deficient 10 x	2 g KCl; 2 g KH_2PO4; 80 g NaCl; 11.5 g Na_2HPO_4 x $2H_2O$; ad 1 l with ddH_2O
Red blood cell lysis buffer (Sigma-Aldrich, Taufkirchen)	8.3 g/l NH_4Cl in 0.01 M Tris pH 7.5
RNase III reaction buffer	20 mM Hepes 66 mM K-Acetate 10 mM Mg-Acetate 0.5 mM DTT DEPC 1:1000 adjust pH ad 6.5
Substrate solution	7.3 g citric acid x H_20 ($C_6H_8O_7$), 11.87 g Na_2HPO_4 x $2H_20$, ad 1 l H_20
TAE buffer for PAE Gel	4 mM Tris- Acetate, 1 mM EDTA
TAE DNA-Gel Running buffer 50 x	242 g Tris Base; 57.1 ml acetic acid (100%); 100 ml 0.5 M EDTA (pH 8) ad 1 l with H_20
TAECL 3.6 M	14,9 g ad 25 ml (Mr = 165,7 g)
TBE	0.089 M Tris OH, 0.089 M boric acid, 0.002 M EDTA
Trypsine solution (10 x) PAA	0.5% Trypsine 0.2% EDTA in PBS

3.9. Mice

Mice	Source
C57/BL6 wild-type mice	Animal Facility BMFZ, Marburg
TLR7-deficient mice on a C57/BL6 background	Prof. Dr. Shizo Akira; Osaka; Japan
TLR3-deficient mice on a C57/BL6 background	Prof. Dr. Shizo Akira; Osaka; Japan
TLR3 & 7-deficient mice on a C57/BL6 background	Animal Facility BMFZ, Marburg

Mice	Source
MyD88-deficient mice on a C57/BL6 background	Prof. Dr. Shizo Akira; Osaka; Japan
IPS-deficient mice on a C57/BL6 background	Prof. Jürg Tschopp, Lausanne, Schweiz
Unc-deficient mice on a C57/BL6 background	Prof. Bruce Beutler, La Jolla, USA

3.10. Embryonated chicken eggs

Specific-pathogen-free (SPF) chicken eggs were purchased from Lohmann, Tierzucht Cuxhaven.

3.11. Transfection reagents

Transfection reagent	Manufacturer	Stimulation of
DOTAP (11811177001)	Roche, Mannheim	PBMCs, Mouse culture
DOTAP	Roth, Karlsruhe	HEKs
Lipofectamine 2000 (11668-019)	Invitrogen UK	PBMCs, Mouse culture

3.12. Peptides

Peptide	Sequence	Manufacturer
LL-37 (SP-LL-37)	LLGDFFRKSKEKIGKEFKRIVQRIKDFLRNLVPRTES	Innovagen, Lund, SWEDEN
sLL-37 (SP-LL-37SCR)	GLKLRFEFSKIKGEFLKTPEVRFRDIKLKDNRISVQR	Innovagen, Lund, SWEDEN
Biotinylated LL-37 (SP-LL-37BT-1)	Biotin-Ahx-LLGDFFRKSKEKIGKEFKRIVQRIKDFLRNLVPRTES	Innovagen, Lund, SWEDEN
CRAMP (1-39) (SP-CRPL-1)	ISRLAGLLRKGGEKIGEKLKKIGQKIKNFFQKLVPQPEQ	Innovagen, Lund, SWEDEN
CRAMP	GLLRKGGEKI GEKLKKIGQK IKNFFQKLVP QPEQ	Innovagen, Lund, SWEDEN

3.13. Plasmids

Plasmid Vector	Source
Luciferase Reporter Plasmid p-125 Luc	Prof. Takashi Fujita, Kyoto University, Japan
pEFflag RIG-I (full)	Prof. Takashi Fujita, Kyoto University, Japan
pEFflag MDA-5 (full)	Prof. Takashi Fujita, Kyoto University, Japan
pES BOS	Prof. Takashi Fujita, Kyoto University, Japan
Renilla reporter plasmids	TU Munich
Trif	TU Munich
pGEM-T Easy	Promega, Madison, USA

3.14. Oligonucleotides

Stimulative Oligo	Sequence	Manufacturer
18S rRNA anti bio	5`-(BIO) TAA TGA TCC TTC CGC AGG TTC ACC TAC GGA AAC -3`	MWG
RIG-I ligand 3`-P RNA template	5`-GGG ACC CTG AAG TTC ATC CCC TAT AGT GAG TCG TAC CTG TCT C-3`	Metabion, Martinsried

3.15. Ligands for stimulation

S = Phosphothioate (PTO)

Stimuli	Sequence	Source
RNA 40	5`-GCC CGU CUG UUG UGU GAC UsC-3`	IBA, Göttingen
RNA 63	5`-CAG GUC UGU GAU-3`	IBA, Göttingen
RNA 63-2`-O-methyl	5`-CAZ GUC UGU GAU-3` "Z" = 2`-O-Me guanosine	IBA, Göttingen
RNA 63-2`-deoxy	5`-CAZ GUC UGU GAU-3` "Z" = 2` dG	IBA, Göttingen
RNA 63-2`-F	5`-CAZ GUC UGU GAU-3`	IBA, Göttingen

Stimuli	Sequence	Source
	"Z" = 2`Fluoro dG	
R848	Resiquimod	Coley Pharmaceuticals, Langenfeld
Poly I:C (tlrl-pic)	Polyinosinic-polycytidylic acid; synthetic analog of dsRNA	InvivoGen, San Diego, USA
ODN 2216	5` GsGsGGGACGATCGTCsGsGsGsGsG sG-3`	TIB Molbiol, Berlin
LPS	Lipopolysaccharide from E. coli	Difco Laboratories, Detroit, USA

3.16. Primer

Primer for Cloning	Sequence	Manufacturer
Random Hexamers	NNNNNN	Metabion, Martinsried
RIG-I L	GAGCATGCACGAATGAAAGA	Metabion, Martinsried
RIG-I R	CTTCCTCTGCCTCTGGTTTG	Metabion, Martinsried

4. Methods

4.1. Cell culture

All work was done under a sterile bench, security grade two. All substances used in cell cultures were tested for mycoplasma and contaminations with endotoxin because such contaminations would lead to a mediator release. All media and buffers were sterilized for 20 min at 121°C and 1 bar. Solutions that were unstable or sensitive to heat were filtered.

4.1.1. Cell culture material

Material	Manufacturer
24 G cannula	BD Microlance™, BD, Heidelberg
96-well flat bottom plates	Greiner, Frickenhausen
96-well round bottom plates	Greiner, Frickenhausen
8 chamber culture slides	BD Falcon, Franklin Lakes NY USA
Cell scrapers	Greiner bio-one, Frickenhausen
Cell lysis buffer	Sigma-Aldrich, Taufkirchen
Combitipps	Eppendorf, Hamburg
Cryovials	Nunc, Wiesbaden
Eppendorf tubes (0.5 ml, 1.5 ml, 2 ml)	Eppendorf, Hamburg
Falcon (15 ml, 50 ml)	Greiner bio-one, Frickenhausen
Needle 24 G	Becton Dickinson, Heidelberg
Pasteur pipettes	Roth, Karlsruhe
Pipette tips	Avant Guard, USA
Plastic pipettes (2 ml, 5 ml, 10 ml, 25 ml)	Greiner, Frickenhausen
Syringe	Braun Omnifix 10 ml
Tissue culture dish	BD Falcon, Heidelberg
Tissue culture flash (175 cm^2, 75 cm^2, 25 cm^2)	Greiner, Frickenhausen
Tube 15 ml	Greiner, Frickenhausen

4.1.2. Cell lines

Cell line	Source
Madin-Darby canine Kidney (MDCK)	Institute for Immunology; BMFZ; Marburg
Human embryonic kidney cells (HEK293)	Institute for medical Microbiology; TU Munich; Munich

MDCK (Madin-Darby Canine Kidney)

The MDCK cell line was derived from the kidney of a normal female cocker spaniel in 1958 (Gaush et al. 1966). Some continuous cell lines of epithelial origin support the growth of influenza viruses, in the presence of added trypsine. The addition of trypsine improves the yield in cell lines that lack specific host proteases necessary for the proteolytic cleavage of HA to produce infectious particles (Klenk et al. 1975). MDCK cells have a polarized morphology, forming two-sided asymmetrical sheets with distinct apical and basolateral surfaces (Cereijido et al. 1978). When grown on non-permeable supports, such as plastic cell culture plates, MDCK cells are not fully polarized, since only the apical surface is exposed to the culture medium. However, this does not affect influenza virus growth in anchorage-dependent cell culture as budding and release only takes place from the apical plasma membrane (Matlin and Simons 1984). MDCK cells were maintained in RPMI complete medium at 37°C in a 5% humidified CO_2 environment.

Human embryonic kidney cells (HEK293)

HEK293 cells are adherent growing human cells from an embryonic kidney. HEK293 cells were maintained in DMEM complete medium at 37°C in a 7.5% humidified CO_2 environment.

Virus

A/PR/8:

The utilized Influenza-A-Virus Puerto Rico (A/PR/8) from the eight isolation was made available from Dr. Marianne Nain, Institute for Immunology in Marburg (Nain et al. 1990). The original virus, isolated in 1934 in Puerto Rico, can be regarded as adapted because of the many passages. Individual strains of influenza are named according to their antigenic group, geographic origin, strain number, year of isolation and mostly the antigenic classification of hemagglutinin and neuraminidase mentioned in the parenthesis [e.g. A/Puerto Rico/8/34 (H1N1) (De Jong et al. 2000).

4.1.3. Culture media

The employed media were from PAA (PAA Laboratories GmbH, Pasching, Austria), FCS (heat-inactivated fetal calf serum) from Biochrom (Biochrom Ag, Berlin), ß-Mercaptoethanol from Gibco (Invitrogen, UK) and L-glutamine/ penicillin/ streptomycin from PAA (Cölbe).

Media	Manufacturer
RPMI 1640	PAA, Cölbe
DMEM	PAA, Cölbe
Fetal Calf Serum (FCS)	Biochrom, Berlin
LSM 1077 Lymphocyte Separation Medium	PAA, Cölbe
ß-Mercaptoethanol	Gibco Invitrogen, UK
L-glutamine 200 mM (100 x)	PAA, Cölbe
Penicillin/Streptomycin (100 x)	PAA, Cölbe
Trypsine-EDTA (10 x)	PAA, Cölbe
human AB-Serum	Sigma Aldrich, St. Louis USA
Natriumpyruvate	PAA, Cölbe
non-essential amino acids	PAA, Cölbe
Dulbecco`s PBS^{++} (with Ca^{2+}, Mg^{2+})	PAA, Cölbe
Dulbecco`s PBS ^{def} (1 x)	PAA, Cölbe

Cell line	Media	Compounds
Flt3	RPMI 1640	10% FCS 1% Penicillin/Streptomycin 1% L-Glutamine 500 µl Mercaptoethanol
PBMCs	RPMI 1640	2% human AB Serum 1% Penicillin/Streptomycin 1% L-Glutamine 1% Natriumpyruvate 1% Amino acids
MDCKs	RPMI 1640	10% FCS 1% Penicillin/Streptomycin 1% L-Glutamine 1% Natriumpyruvate

Cell line	Media	Compounds
		1% Amino acids
HEKs	DMEM	10% FCS 1% Penicillin/Streptomycin 1% L-Glutamine 500 µl Mercaptoethanol

In the following the media with supplements are called DMEM complete and RPMI complete medium.

4.1.4. Passage of eukaryotic cells

Passage of MDCK cells and HEK293 cells

Cells were grown to near-confluence either in 75 cm^2 or 175 cm^2 tissue culture flasks. They were passaged after being washed twice with PBS^{def} and being dispersed with sufficient trypsine to cover the cells. Flasks with MDCK cells were then returned to the 37°C incubator until the cells had detached from the surface (7 min). HEK293 cells were incubated with trypsine at room temperature for a short while. After removing the trypsine solution, the cells were again incubated for 5 min in the 37°C incubator (MDCK cells) or for 3 min at room temperature (HEK293 cells) before being resuspended either in RPMI complete medium (MDCK cells) or in DMEM complete medium (HEK293 cells). HEK293 cells were then centrifuged for 6 min at room temperature and 1,300 rpm. Then the cell pellet was resuspended in 10 ml DMEM complete medium. For further cultivation, cells were split 1:10, usually two times per week.

4.1.5. A/PR/8 infection of MDCK cells

The influenza virus was grown in MDCK cell cultures (Garcia-Sastre et al. 1998). Cells were grown to 70-80% confluence, washed with PBS^{++} and inoculated with virus in 15 ml RPMI complete medium without FCS. For the infection 10 MOIs / cell were used. After adsorption for 1 hour at 37°C, the medium was replaced by 30 ml RPMI complete medium with 10% FCS. After an incubation time of 7 hours, the RNA was isolated from the infected cells through Trizol-treatment (4.3.1). Cells were harvested if cytopathogenic effect occurred. The cytopathogenic effect was manifested by cell rounding, cell shrinkage and foci of cell destruction.

4.1.6. Viable cell counts

For determination of cell number, an aliquot of cell suspension was diluted with eosin. The cells were then transferred to a neubauer hemocytometer, and viable cells were counted in 4 squares, each of 10^{-4} ml, and averaged. Vital cells remained unstained, while pink cytoplasm served as an indicator for a loss of cellular functionality due to the increased permeability of the membranes. Thus, dead cells could be distinguished from living cells, which appear yellow under the microscope. The following formula was used to calculate the viable cell number:

Cell number/ml = average cell number x 10^4 x dilution factor

The CASY cell counter was used as another method to determine cell number. Cells were suspended in an electrolyte buffer and aspirated through a precision-measuring capillary with a defined size. While passing through the measuring capillary, they were scanned in a low voltage field between two platinum electrodes. The resulting electrical signals generated by a cell passing the measuring capillary were analyzed by amplitude, pulse width, course of time and resulting pulse area. The analyzed pulse areas of cell signals were cumulated and assigned in a calibrated multi-channel analyzer (Handbook Schaerfe).

4.1.7. Freezing and thawing of cells

For long-term storage, cells were suspended in Cell Freezing Medium at a concentration of 3-5 x 10^6 cells/ml, and aliquots were added to cryovials, which were frozen slowly in foam racks. On the following day, the vials were transferred to liquid nitrogen for long-term storage. Cells were recovered from liquid nitrogen storage by quickly thawing a vial at 37°C, transferring the contents to 10 ml medium following by centrifugation in order to minimize the toxic effects of DMSO in the cell freezing medium. Then cells were transferred to a 25 cm^2 tissue culture flask containing fresh medium.

4.1.8. Mycoplasma test

Mycoplasma are one of the most common cell culture contaminations. Mycoplasma belong to the smallest known self-replicating microorganisms. Mycoplasma is a genus of bacteria largely characterized by the lack of a cell wall and a small genome with low GC content.

Cells were plated on a coverslip and rinsed with PBS. Then cells were subsequently stained with a DNA-binding fluorochrome stain (DAPI). Therefore, the DAPI stock solution in PBS was diluted 1:50 in methanol, and the cells were rinsed with this DAPI/Methanol solution (100 ng DAPI/ml). In the next step, the cells were stained and fixed with this solution for 15 min in an incubator. Again the cells were rinsed with methanol and were covered with glycerine. Then the cells were evaluated microscopically for the presence of the characteristic particulate or filamentous pattern of fluorescence on the cell surface, which is indicative of a mycoplasma infection.

4.1.9. Generation of primary cells

4.1.9.1. Generation of dendritic cells from bone marrow

Bone marrow cells are pluripotent cells, from which each hämatopoetic cell can be generated. Mice were sacrificed by cervical dislocation and femurs were prepared by flushing with a syringe with a 24 G cannula until the bone was completely white. Marrow clumps were disintegrated by pipetting up and down with a 5 ml serological pipette. The resulting suspension was transferred to 50 ml tubes. To separate cells from other bone marrow components, suspensions were spun down at 1,300 rpm for 6 min at room temperature. Red blood cell contaminations were removed with 5 ml blood cell lysis buffer. After an incubation time of 5 min, the reaction was stopped with 10 ml RPMI complete medium followed by centrifugation for 6 min at room temperature and 1,300 rpm. Then the marrow cells were resuspended in 5 ml RPMI complete medium and the cell number was determined in a Neubauer hemocytometer (4.1.6).

Cultivation and differentiation of bone marrow derived Flt3 cultures

The bone marrow cells were initially seeded at a density of 1.5 x 10^6/ml in RPMI complete medium in a cell culture bottle. Under the influence of a Flt3 ligand (FMS-like tyrosine kinase 3 ligand) with a concentration of 35 ng/ml, they differentiated into pDCs and cDCs. The cultures were maintained under an atmosphere of 37°C, 100% humidity and 7.5% CO_2. Cells were harvested on day 7 and seeded at a density of 2 x 10^6/ml (4.1.6) for experiments. The phenotype of the generated dendritic cells was analyzed by FACS (4.7). These cultures typically contained 30-50% CD45RA+CD11c+ pDCs, 30-50% CD45RA-CD11c+ cDCs and 15% CD11c-cells.

Cultivation and differentiation of bone marrow derived macrophages

Cells were seeded at a density of 0.5 * 10^6/ml in RPMI complete medium in a 10 cm petri dish. Under the influence of a M-CSF ligand (Macrophage Colony Stimulating Factor) with a final end concentration of 20 ng/ml, they differentiated into macrophages. The cultures were maintained under an atmosphere of 37°C, 100% humidity and 7.5% CO_2. After three days, 20 ng/ml M-CSF was additionally added. After 5 days, the non-adherent cells were first collected and then incubated for 10 min at 37°C with 5 ml PBS^{def}/3% FCS/ 2 mM EDTA to detach the adherent cells. Cells were seeded at a density of 1 x 10^6/ml (4.1.6) for experiments. The purity of the cells was analyzed by FACS analysis (4.7).

Cultivation and differentiation of bone marrow derived GM-CSF cultures

Cells were seeded at a density of 0.3 * 10^6/ml with RPMI complete medium in a cell culture bottle. Under the influence of a GM-CSF ligand (Granulocyte macrophage colony-stimulating factor) with a final end concentration of 10 ng/ml, they differentiated into cDCs. After three days, 5 ng/ml GM-CSF was additionally added. The cultures were maintained under an atmosphere of 37°C, 100% humidity and 7.5% CO_2. Cells were harvested on day 7 and seeded at a density of 2 x 10^6/ml (4.1.6) for experiments. These cultures typically contained more than 90% cDCs (CD11c+, CD11b+, B220-) (4.1.6).

4.1.9.2. Isolation of PBMCs

PBMC (peripheral blood mononuclear cells) (from the Department for transfusion medicine from the clinical centre at the Philipps University Marburg) were generated from heparinized blood of healthy donors by density centrifugation over the carbohydrate polymer Ficoll (LSM 1077, PAA). This yielded a population of mononuclear cells at the interface that was depleted of red blood cells and most polymorphonuclear leukocytes or granulocytes. The resulting PBMC population consisted mainly of lymphocytes and monocytes. The cells were layered over Ficoll and centrifuged over 30 min at 2,000 rpm without brake. Red blood cells and polymorphonuclear leukocytes or granulocytes are denser and were thus centrifuged through the Ficoll-Hypaque TM, while mononuclear cells consisting of lymphocytes together with some monocytes banded over it and could be recovered at the interface.

PBMCs were harvested, washed two times with PBS^{def} and resuspended in 20 ml RPMI complete medium without FCS. Finally, cell numbers were determined in a Neubauer

hemocytometer (4.1.6), and cells were seeded with 4% human AB Serum (after stimulation the final end concentration is 2%) onto a 96 well plate at a density of 3 x 10^6/well. Cells were maintained at 37°C in a 5% humidified CO_2 environment.

4.1.9.3. Isolation of monocytes from human blood

Human monocytes were isolated from buffy coats of healthy blood donors (Pauligk et al. 2004). The term 'centrifugal elutriation' describes a technique which involves the balance between a centrifugal force generated by the spinning rotor and a centripetal flow of liquid within a separation chamber. Cells present in the separation chamber are found in a position at which the two forces acting on them are at equilibrium. The position of each cell is determined by its size, shape and density. Because the chamber's geometry produces a gradient of flow rates from one end to the other, cells with a wide range of different sedimentation rates can be held in suspension. By increasing the flow rate of the elutriating fluid in steps, or by increasing the rotor speed, successive populations of relatively homogeneous cell sizes are washed from the chamber. Each population contains cells which are larger or more dense (i.e., faster sedimenting) than those of the previous fraction (Figdor et al. 1983). The following correlation exists between the flow rate and the rotor speed (Beckman, Instruction Manual):

$$F = X \times D^2 \times (RPM \times 10^{-3})^{-2}$$

F = flow rate at the pump in ml/min

X = 0, 0511 (Standard chamber)

D = cell diameter in µm

RPM = rotor speed pro minute

By using a constant rotor speed, some guidance is given from this expression in order to calculate the cell size elutriated at any flow rate. For the experiments, the JE-6B elutriation system with appropriated rotor and standard chamber was used. The standard chamber has a volume of 4.2 ml. Human peripheral blood mononuclear cells were isolated from blood on Ficoll-Paque gradients. The mononuclear cells (300–500 x 10^6), suspended in 35 ml RPMI complete medium, were loaded into a Beckman elutriation centrifuge. Separation by counterflow centrifugal elutriation was performed at a constant rotor speed from (3,000 rpm) and a variable flow rate (6-36 ml/min) at 4°C. Phosphate-buffered saline (PBS^{def}) supplemented with 0.1% bovine serum albumin and 0.01% EDTA was used as an elutriation medium. Cells were drawn in the separation chamber at flow rates of 7 ml/min, following flushing at 15 ml/min in order to remove trombozytes and erythrocytes. The

lymphocyte and NK-cell population was eluted at flow rates of 28.5 ml/min, whereas the monocytes population was eluted at flow rates of 36 ml/min.
The purified cell population was centrifuged at 1,400 rpm for 10 min at 4°C and resuspended in culture medium.

4.1.9.4. Isolation of untouched monocytes

After elutriation, the monocytes population had a purity of 60-80%. Therefore, the cells had to be further purified to get a homogenous monocyte population by using a magnetic activated cell sorting (MACS) kit, "Monocyte Isolation Kit II (human)". All non-monocytes were indirectly magnetically labeled by using a cocktail of biotin-conjugated antibodies as the primary label reagent, followed by anti-biotin monoclonal antibodies conjugated to microbeads as a secondary labeling reagent. The cell suspension was loaded onto a MACS LS column that was placed in the magnetic field of a MidiMACS separator. The magnetically-labeled non-monocytes were retained on the column, whereas all cells that were not labeled passed through and could be collected as the purified and untouched monocyte population. The separation was performed as described in the manufacturer's manual. The purity of the cultures was analyzed via FACS analysis (4.7) using antibodies against CD14, CD11b and BDCA2 and usually achieved 86-96% purity.
The cell number was counted (4.1.6), and monocytes were seeded in medium with 4% AB at 3 x 10^6/ml in 96-well flat-bottom plates and could be used for further experiments (4.6/4.8). As a control, PBMC were also used for stimulation (0.3x10^6 cells/well).

4.2. General nucleic acids techniques

4.2.1. Nucleic acid gel electrophoresis

Electrophoresis is the separation of charged particles within an electric field. Separation efficiency of macromolecules correlates with differences in size and charge. Electrophoretic mobility is proportional to the field strength and the net charge of the molecule.

Agarose gel electrophoresis

Agarose is a polysaccharide (composed of galactose and galactose derivatives); different pore size of the gel matrix are adjusted by varying the concentration of agarose. The pores in agarose gels are larger than in polyacrylamide gels. For RNA agarose gel

electrophoresis, it had to be ensured that no contaminating RNases were present. Therefore, the electrophoresis chamber and other accessories were incubated with 3% H_2O_2 for 30 minutes.

For gel preparation, agarose was dissolved in 1 x MOPS buffer by heating (e.g., in a microwave). Once the gel solution had cooled down to about 50-60°C, the solution was poured into a prepared gel tray with a comb. The solid gel was placed in an electrophoresis chamber containing 1 x MOPS. The nucleic acid samples (diluted to a concentration of approximately 1 µg) mixed with 6 x loading dye solution (to 1 x final concentration) were loaded into the gel pockets. The loading dye solution contained two dyes, bromphenol blue and xylene cyanol FF, for easy visual tracking of DNA migration during electrophoresis. (In 1% agarose gels bromphenol blue comigrates with ~300 bp fragments and xylene cyanol FF- with ~ 4000 bp fragment). Gels were run at 70-100 volts (7.5 mA/cm^2). Agarose concentrations were chosen according to the size of the expected fragments (Table 2).

In these experiments, RNA was analyzed with the help of agarose gel electrophoresis. RNA forms because of intramolecular base-pairing secondary structures, changing their course behavior in the gel. For this reason, an exact analysis of RNA was only possible in a denatured gel. Because in this work gel electrophoresis was only used in order to check RNA preparations, non-denatured gels as described above were sufficient.

Table 2: Separation range of DNA fragments in agarose gels of different concentrations.

% agarose (w/v)	Nucleic acid fragment size (kbp)
0.5	1.0 – 30
0.7	0.8 – 12
1.0	0.5 – 7
1.2	0.4 – 6.0
1.5	0.2 - 3.0
2.0	0.1 – 2.0

Polyacrylamide gel electrophoresis (PAGE)

Polyacrylamide (PAA) gels were generated by crosslinking polymers of acrylamide with the co-monomer bis-acrylamide. Unpolymerized polyacrylamide is a neurotoxin and therefore must be handled extremely carefully. Polymerization of polyacrylamide was initiated by addition of APS (ammonium persulfate, $(NH_4)_2S_2O_8$) and TEMED (N,N,N,N,-

Tetramethylethylendiamine). In an aqueous solution, APS forms radicals that react with PAA. TEMED also serves as a catalyst. Different concentrations of acrylamide used for gel electrophoresis correlate with different pore sizes.

Denaturing PAGE

Denaturing sample buffer	
6 x Loading Dye	500 µl
8 M Urea	240 µg
PAA gel solution	**15%**
10 x TBE	4 ml
Acrylamide/Bisacrylamide 30%	20 ml
Urea	19.22 g
H_20	ad 40 ml

In denaturing gels, the native structure of macromolecules that run within the gel is disrupted. PAA gels are usually supplemented with 8 M urea or another denaturing substance (e.g., formamide) before polymerization.

Table 3 indicates the fragment sizes of ssDNA that comigrate with the BPB and XCB dyes of the sample buffer in denaturing polyacrylamide gels of different percentages.

Table 3: Size of ss nucleic acids fragments (given in nucleotides) comigrating with the dyes of the sample buffer in denaturing polyacrylamide gels.

% Polyacrylamide	Bromphenol blue	Xylencyanol
5	35	130
6	26	106
8	19	70 – 80
10	12	55
20	8	25

For preparation of a PAA gel solution, urea was dissolved in the appropriate volume of 10 x TBE and the required volume of acrylamide/bisacrylamide stock solution was added. For gel preparation, glass plates were cleaned with 70% ethanol and assembled with spacers. Polymerization was initiated by adding 1/100 volume 10% (w/v) APS and 1/1000 volume

TEMED to the PAA gel solution. The gel solution was poured between the clamped glass plates, and a comb was inserted between the glass plates at the top to create pockets for later sample loading. After polymerization (approximately 1 h), the comb was removed, and the pockets were immediately rinsed using a syringe with 1 x TBE buffer to remove urea that had diffused from the gel matrix (which tended to accumulate in the pockets) and to avoid later polymerization of unpolymerized acrylamide within the pockets. The glass plates containing the gel were fixed in the electrophoresis equipment to bridge the buffer reservoirs filled with 1 x TBE buffer (supplemented with 8 M urea), and electrophoresis was performed at 5–30 mA (depending on gel size and PAA concentration).

4.2.2. Detection of nucleic acids from gels

Ethidium bromide staining

Ethidium bromide intercalates between the stacked bases of DNA and RNA. When excited by UV light between 254 nm (short wave) and 366 nm (long wave), it emits fluorescent light at 590 nm (orange).

For staining nucleic acids in agarose or PAA gels, the gels were carefully inserted into ethidium bromide staining solution (0.5 µg/ml in H_2O) and incubated while shaking for 10 min at room temperature. Staining solution was carefully removed, and gels were analyzed using an UV transluminator, where a photo was taken.

4.2.3. Photometric concentration determination of nucleic acids

The concentration of nucleic acids was determined by measuring the absorbance at 260 nm. Concentration could be calculated according to the Lambert-Beer law:

$A = \varepsilon * c * d$

(A: Absorbance; c: molar concentration of DNA/RNA [mol/l]; ε: molar extinction coefficient [1/(M*cm)]; d: path length of the cuvette [cm])

Samples were diluted in water (depending on the expected concentration), and the absorbance at 260 nm was measured against water using a UV spectrophotometer. The concentration was calculated using the known values c(1 A260) that represent the concentration corresponding to one absorbance unit at 260 nm (1 A260):

1 A260 ds DNA	corresponds to a c(1 A260) of ~ 50 µg / ml
1 A260 ss DNA	corresponds to a c(1 A260) of ~ 33 µg / ml
1 A260 RNA	corresponds to c(1 A260) of ~ 40 µg / ml

This results in a general formula for RNA/DNA concentration calculation:

$$c\left[\mu g/\mu l\right] = \frac{A_{260} \cdot c(1\,A_{260}) \cdot D_f}{1000}$$

(where c is concentration in µg/µl, Df is the dilution factor)

The purity of the preparation can be determined by forming the quotient E260nm/E280nm. The absorption maximum of nucleic acids is 260 nm, while amino acids or proteins respectively absorb best at 280 nm. Thus, the quotient of the absorption measured at these two wave length determines the degree of purity. An adequate purity is given for RNA by a proportion of > 2.0 and for DNA by a proportion of > 1.7.

4.2.4. Alcohol precipitation

Ethanol precipitation

Ethanol precipitation is a very common method of concentrating nucleic acids from aqueous solutions and removing salts. The precipitate of DNA/RNA, which was formed at a low temperature in the presence of moderate concentrations of monovalant cations, was recovered by centrifugation. Salts remained predominantly in the ethanol supernatant. For precipitation, 1/10 volume of 3 M NAOAc ph 5.0 was added to one volume of DNA/RNA solution, followed by mixing with 2.5 volumes of absolute ethanol. Samples were kept for at least 1 h at -80°C or overnight at -20°C and were then centrifuged for at least 30 min at 4°C, 13,000 rpm. For a more efficient removal of salts, the pellet was washed with 70% (v/v) ethanol and centrifuged for another 15 min at 13,000 rpm. The supernatant was discarded, the pellet was dried at room temperature and finally dissolved in an appropriate volume of ultra-pure water.

4.2.5. Phenol/chloroform extraction

Phenol/chloroform extraction is a common technique used to purify DNA or RNA samples. Such extractions are used whenever it is necessary to inactivate or remove enzymes. The procedure takes advantage of the fact that deproteinisation is more efficient when two

different organic solvents are used instead of one. The final extraction with chloroform also removes residual phenol.
An equal volume of phenol/chloroform was added to an aqueous DNA/RNA sample, vigorously vortexed (30 s) and then centrifuged (5 min, 13,000 rpm at room temperature) to achieve phase separation. The upper aqueous layer was removed carefully, avoiding the protein-containing interface, and transferred into a new tube. The lower organic layer and interface were discarded. The aqueous phase was extracted a second time using chloroform. The aqueous layer was also the upper layer in chloroform extractions. Afterwards DNA/RNA was concentrated by ethanol precipitation (4.2.4).

4.2.6. Micro Bio-Spin® 30 Columns

Micro Bio-Spin columns are designed for the rapid cleanup and purification of riboprobes, including the removal of unincorporated nucleotides or templates used for *in vitro* transcription. The columns are packed with a special grade of Bio-Gel P-30 polyacrylamide gel matrix suspended in 10 mM Tris buffer (pH 7.4). This unique gel produces very efficient, noninteractive separation by size. The columns are used to purify nucleic acids larger than 20 bases. The cleanup was performed according to the protocol provided by the manufacturer. First, the column was inverted several times to resuspend the settled gel. The cap was removed, so that the excess packing buffer began to flow. After discarding the buffer, the column was centrifuged for 2 min at 1,000 x g to remove the remaining packing buffer. The speed was important to ensure proper performance of the columns. Then the sample (10 – 75 µl) was carefully applied onto the top center of the gel bed, and the column was centrifuged again for 4 min at 1,000 x g. The collected purified sample was received in 10 mM Tris buffer.

4.2.7. XBRIDGE™ OST C_{18} columns

XBridge™ OST C_{18} columns, used for separations of detritylated synthetic oligonucleotides, are based on ion-pair, reversed-phase chromatographic principles. An efficient charge-based (length-based) oligonucleotide separation was achieved according to the protocol provided by the manufacturer.

4.3. RNA techniques

Water used for RNA-related work was ultra-pure water or water treated with DEPC (Diethyl-Pyrocarbonat) (0,1%) to eliminate contaminations with RNases. Briefly, DEPC was added to water and stirred for 12 hours. For RNase inactivation, water was autoclaved by the standard procedure.

4.3.1. Trizol RNA preparation from eukaryotic cells

Total cellular RNAs from MDCK, HEK, PBMCs and murine liver cells were isolated by the Trizol method according to the protocol provided by the manufacturer. One ml of Trizol is sufficient to isolate RNA from 5 - 10 x 10^6 cells or 10 cm^2 of culture dish surface for cells grown in monolayer. Trizol contains a mixture of phenol and guanidine thiocynate (GITC) in a mono-phase solution, which effectively dissolves DNA, RNA, and protein on homogenization or lysis of tissue sample. After addition of the reagent, the cell lysate should be passed several times through a pipette to form a homogenous lysate. We incubated the cell suspension for 5 min at room temperature. 0.2 ml chloroform were added per 1 ml Trizol and shaken for 15 s. After another 2 min of incubation at room temperature, the suspension was centrifuged for 30 min at 4°C and 4,000 rpm. The mixture separated into three phases: a colorless upper aqueous phase containing RNA, an interphase containing DNA and a red organic phase containing proteins. The aqueous phase was transferred into a new reaction tube, and RNA was precipitated by adding 0,5 ml isopropanol per ml Trizol and, after incubation for 10 min at room temperature, centrifuged for at least 30 min at 4°C and 4,000 rpm. The pellet was washed once with 70 % ethanol (at least 1 ml 70% ethanol per ml Trizol), centrifuged for another 15 min and air-dried. RNA was dissolved in ultra-pure water, and remaining residual DNA was removed by DNase I digest. After digestion, the RNA was phenol/chloroform (4.2.5) extracted and ethanol precipitated (4.2.4). Finally, the RNA was dissolved in water and the concentration was determined (4.2.3). DNase I digestion was performed as follows:

Component	Amount
RNA	50 µg
Buffer	5 µl
DNase I	10 Units (1 µl)
H_20	up to 50 µl

4.3.2. Isolation of the 18S rRNA from eukaryotic total RNA

18S rRNA was purified from total eukaryotic RNA using a biotinylated DNA-oligonucleotide complementary to the 3`-end of ribosomal RNA combined with streptavidin-beads (Tsurui et al. 1994). Since avidin bind preferentially to biotin, biotin-tagged molecules can be extracted from a sample by mixing them with beads which are covalently-attached to avidin, and washing away anything unbound to the beads. For preparation of the 18S rRNA, 500 µg total RNA (in a final volume of 75 µl) were incubated with 25 µl biotinylated DNA-Oligo in 100 µl TAECL (3.6 M) for 5 min at 70°C, in order to melt the secondary structure from the rRNA. Then the sample was incubated for 30 min in a water bath at 30°C. During this time, the biotinylated DNA-Oligo and the 18S rRNA hybridised through complementary base-pairing. Then 50 µl streptavidin-beads in 2,4 M TAECL were added and incubated for another 30 min. The hybrid of the biotinylated DNA-Oligo and the 18S rRNA binded to the streptavidin beads due to the high affinity between biotin and streptavidin. After 3 washes with 300 µl 2,4 M TAECL to remove unbound RNA, rRNA was eluted with 50 µl 2.4 M TAECl. Then the RNA/DNA-hybrid was melted for 5 min at 70°C. Finally, the eluate was dialysed for 2 hours against DEPC water on 25 nm filter, in order to purify the RNA from the high molar salt.
Precipitation was achieved according to the protocol described in section 4.2.4. The concentration of the RNA was determined (4.2.3), and the purity of the RNA was analysed using agarose elektrophoresis (4.2.1).

4.3.3. Virus isolation by inoculation in embryonated eggs

Candling and inoculation of eggs

Influenza virus strain A/Puerto Rico/8 (A/PR/8) was propagated in the allantoic fluid of 11-day-old specific pathogen free embryonated eggs (SPF) as described by Nain et al. (Nain et al. 1990). Embryonated eggs were incubated for 11 days at 37°C in a relative humidity of 40 – 60% and automatically rotated every six hours.
Eggs were examined with an egg candler and placed blunt-end up into egg trays. Infertile eggs and those with cracks were discarded. Then eggs were candled for identification of the air sac and vessels and marked for a clear area. Eggs were wiped with an iodine solution, and a small hole was drilled into the shell over the air sac without scarifying the membrane. Infectious A/PR/8 (A/PR/8 N.Y. Allantois 02.12.96) stock was diluted in sterile PBS (1:1000), and 200 µl were inoculated in the allantoic sac with a tuberculin syringe

and capillary needle (24 G x 1; 0.55 x 25 mm). The holes punched in the eggs were sealed with a drop of glue. Eggs were placed into a humidified incubator at 37°C for 2 days. The inoculated eggs were observed; deaths were regarded as non-specific, and those embryos were discarded.

Harvesting of inoculated chicken eggs

The next steps were performed at 4°C under sterile conditions.

Eggs were chilled at +4°C overnight before harvesting. This led to vessel constriction and death of the embryos. The top of each egg was cleaned with 70% ethanol before the shell over the air sac was broken and the allantoic membrane pushed away with sterile forceps. Allantoic fluid was obtained using a 10 ml syringe and needle (20G x 1,5; 0,9 x 40 mm) and was pooled from several eggs. Only clear fluid was collected, cloudy fluids were discarded. 7 – 12 ml allantoic fluid was harvested from each egg.

Purification of influenza A-virus

To pellet debris, fluid was centrifuged at 6,000 rpm for 30 min at 4°C without break. To purify the virus, allantoic fluid was pelleted in an ultracentrifuge in Ultra-ClearTM-Tubes at 18,000 rpm for 55 min at 4°C without break (Sorvall-Rotor JA-19 in Sorvall-Centrifuge or Beckman-Rotor 16250 in Beckman-Centrifuge). Supernatant was discarded, and pellet was covered with 500 µl PBS^{def}, swelled for one hour on ice and resuspended using a tuberculin syringe with a capillary needle. A 30-55% gradient from sucrose was made from a 60% sucrose parent solution in Ultra-ClearTM-Tubes (treated with 3% H_2O_2 for 90 min in the dark). Resuspended virus-pellet was placed on top of the sucrose gradient and centrifuged at 24,000 rpm for 16 hours at 4°C without break. The virus was located in a white and cloudy coat (near 45% sucrose) and was harvested and filled up with PBS^{def} in order to remove the sucrose. The virus was then pelleted at 24,000 rpm for 45-60 min at 4°C without break. Finally, the concentrated, purified virus was swelled in 500 µl PBS^{def} on ice for 1 hour and stored at –80 °C.

Extraction of viral RNA from allantoic fluid

RNA was extracted from infected allantoic fluid using the Trizol method (4.3.1).

Measurement of infectious units

One of the most important procedures in virology is measuring the concentration of a virus in a sample, or the virus titer. This parameter is determined by inoculating serial dilutions of virus into host cell cultures.

Hemagglutination assay

This assay uses the ability of the influenza virus to cause red blood cell-agglutination as a read-out. Members of the family Orthomyxoviridae (among other viruses) contain proteins that can bind to erythrocytes (red blood cells); these viruses can link multiple cells, resulting in a lattice. This property is called hemagglutination. Influenza viruses contain an envelope glycoprotein called hemagglutinin, which binds to N-acetylneuraminic acid-containing glycoproteins on erythrocytes. This test detects not only infectious but also defective virus particles. In practice, 25 µl of the virus suspension was plated in a serial 1:2 dilution in 96 well round bottom plates and mixed with 25 µl 1% chicken red blood cells. After incubation for 30 min at room temperature, the presence of the virus in wells was determined by agglutination. The endpoint for this assay was the reciprocal of the highest virus dilution at which complete haemagglutination could be detected. Titers were calculated as hemagglutinating units (HAU/ml).

Plaque-Assay

This test detects infectious virus particles. Therefore, MDCK monolayers were prepared in 6-well cell culture plates. Once confluent, the cells were washed with PBS^{++} and inoculated with 500 µl of virus dilutions. After adsorption at 37°C for one hour, 3 ml nutrient overlay (1.8% Bacto-Agar) were added to each well. Plates were then incubated for 4 days at 37°C. When the orginal infected cells release new progeny viruses, the spread to neighboring uninfected cells is restricted by the gel. As a result, each infectious particle produces a circular zone of infected cells, or plaque. To enhance the contrast between the plaque and the surrounding monolayer, the cells were stained with a vital dye. Living cells absorbed the stain, and plaque appeared clear against a purple background of healthy cells. The titer of a virus stock could thus be calculated in plaque-forming units (PFU) per milliliter from the dilution of the sample and the amount of plaque observed.

4.3.4. *In vitro* transcription

Human 18S rRNA was amplified from genomic DNA and cloned into pGEM (a kind gift from Andreas Kaufmann). pGEM plasmid containing human 18S rRNA was linearized with PvuII for 2 hours at 37°C.

Component	Amount
10 µg DNA	x µL
H_20	x µl
10 x NB Buffer	5 µl
Enzym Pvu II	2 µl
	Σ 50 µl

The linearized plasmid was purified according to the MinElute PCR Purification Kit Protocol (Peqlab, Erlangen). To confirm that the plasmid was fully linearized, the DNA was examined on an ethidiumbromide-stained agarose gel (4.2.1).

T7 transcription reaction

The linearized and purified RNA was used as the matrice for the T7 transcription reaction. RNA can be transcribed *in vitro* using DNA-dependent phage RNA polymerases (e.g., T7 RNA polymerase). T7 RNA polymerase recognises the specific T7 phage promotor sequence (5`-TAA TAC GAC TCA CTA TA-3`; sense strand) and starts polymerisation immediately downstream in the 5`-3` direction. The *in vitro* transcription was done according to the protocol specified in the AmpliScribeTM T7 Transcription Kit (Epicentre, Biozym, Hess. Oldendorf).

T7 transcription reaction

All components in the following table were mixed in a 1.5 ml reaction tube, and T7 RNA polymerase was added at the end, followed by incubation at 37°C for 3 hours. The remaining residual DNA was removed by DNase I digest. For the desalting and removal of mononucleotides, samples were purified according to the RNeasy Mini Protocol for RNA Cleanup. Transcription efficiency was analysed by agarose gel (4.2.1), and the concentration was determined (4.2.3). To obtain large amounts of RNA, preparative scale transcriptions were performed.

Component	Final concentration
x µl RNase-Free water	-
1 µg linearized template with appropriate promoter	50 ng/µl
2 µl 10 X AmpliScribe T7 Reaction Buffer	1 x
1.5 µl 100 mM ATP	7.5 mM
1.5 µl 100 mM CTP	7.5 mM
1.5 µl 100 mM GTP	7.5 mM
1.5 µl 100 mM UTP	7.5 mM
2 µl 100 mM DTT	10 mM
2 µl AmpliScribe T7 Enzyme Solution	-
Σ 20 µl	

4.3.5. Design of the RIG-I ligand 5`-3P RNA

Synthesis of the RIG-I ligand 5`-3P RNA was performed as described in the Silencer® siRNA Construction Kit from Ambion. The Silencer® siRNA Construction Kit overcomes the sequence requirements of traditional *in vitro* transcription strategies by using siRNA template oligonucleotides containing a "leader" sequence complementary to the T7 Promoter Primer included in the kit. The template oligonucleotide should have 21 nt encoding the siRNA at the 5`-end and 8 nt at the 3`-end complementary to the T7 Promoter Primer. The 8 nt at the 3`-end should be the following sequence: 5`-CCTGTCTC-3`. First, the template oligonucleotide was hybridized to a T7 Promoter Primer. Therefore, the components listed below were mixed and heated to 70°C for 5 min. Then the mixture was left at room temperature for 5 min.

Component	Amount
T7 Promoter Primer	2 µl
DNA Hyb buffer	6 µl
Sense template: oligonucleotide for RIG-I-ligand 5`-3P RNA	2 µl

Templates for RIG-I-ligand 5`-3P RNA
Sense Template 5`-GGG ACC CTG AAG TTC ATC CCC TAT AGT GAG TCG T**AC CTG TCT C**-3`
Antisense Template 5`-TAC GAC TCA CTA TAG GGG ATG AAC TTC AGG GTC C**CC CTG TCT C**-3`

The 3`-end of the hybridized DNA oligonucleotide was extended by the Klenow fragment of DNA polymerase to create ds siRNA transcription templates. The following components were added to the hybridized oligonucleotides and incubated for 30 min at 37°C

Component	**Amount**
10 x Klenow Reaction buffer	2 µl
10 x dNTP Mix	2 µl
Nuclease-free Water	4 µl
Exo-Klenow	2 µl

Then the siRNA templates were transcribed by T7 RNA polymerase. The following components were mixed and incubated for 2 h at 37°C

Component	**Amount**
si RNA template	2 µl
Nuclease-free water	4 µl
2 x NTP Mix	10 µl
10 x T7 Reaction Buffer	2 µl
T7 Enzyme Mix	2 µl

To design the siRNA, the resulting RNA transcripts of sense and antisense templates were hybridized to create dsRNA. But for the design of the RIG-I Ligand 5`-3P RNA, this step was not necessary. For purification of the RIG-I Ligand 5`-3P RNA, the DNA template was removed by digestion with DNase. Therefore, the following reagents were added to the last step above and incubated for 2 h at 37°C

Component	Amount
Digestion Buffer	6 µl
Nuclease-free Water	51,5 µl
DNase	2,5 µl

The resulting RIG-I ligand 5`-3P RNA was purified by glass fiber filter-binding and elution to remove excess nucleotides, short oligomers, proteins, and salts in the reaction.

4.3.6. Hydrolysis of RNAs with different RNase types

The treatment of RNA with different RNase types was performed as follows:

Component	Amount
RNA	50 µg
RNase Dilution in 2 x liposomal buffer	250 µl
H_20	ad 500 µl

The reaction mix was incubated for 1 h at 37°C. Then the solution was subjected to phenol/chloroform extraction (4.2.5) followed by ethanol precipitation (4.2.4). The pellet was dissolved in RNase-free water and the concentration was determined (4.2.3). Alternatively, the RNase-derived fragments were purified by using a Micro Bio-Spin column (4.2.6). The RNase-treated RNAs were analyzed either by PAGE (4.2.1) or agarose gel electrophoresis (4.2.1). Then immune cells were stimulated with the RNase-derived fragments by using liposomes (4.5).

4.3.7. Removing the 2`,3`-cyclic phosphate at the 3`-end of RNA

The enzyme that catalyses the removal of a 2`,3`-cyclic phosphate (e.g., that generated by RNase A cleavage) is the T4 polynucleotide kinase (T4 PNK), which has a 3`-phosphatase activity.

Component	Amount
RNA	10 pmol
Buffer (500 mM Tris-HCl pH 7.6 at 25°C, 100 mM $MgCl_2$, 50 mM DTT, 1 mM spermidine and 1 mM EDTA)	2 µl
T4 polynucleotide kinase	1 µl
H_20	ad 19 µl

The reaction mix was incubated for 30 min at 37°C. Then the solution was subjected to phenol/chloroform extraction (4.2.5) followed by ethanol precipitation (4.2.4). The pellet was dissolved in RNase-free water and the concentration was determined (4.2.3). The removal of the phosphate group led to a reduced net charge of the transcript, which, for small RNAs (less than 100 nt), could be monitored by a lower electrophoretic mobility of the RNA in comparison to the untreated RNA (4.2.1).

4.3.8. Fragmentation of RNA with Zn^{2+} or Pb^{2+}

Ambion® RNA Fragmentation Reagents contain a buffered zinc solution and are designed to fragment RNA to sizes of between 60-200 nucleotides.

Component	Amount concerning the Kit	Our procedure
RNA	20 – 50 µg	10 µg
Nuclease-free Water	to 18 µl	to 18 µl
10 x Fragmentation Buffer	2 µl	2 µl
Mix, spin briefly, and incubate at 70°C in a heating block	for 15 min	for 80 min
Stop Solution (200 mM EDTA pH 8.0)	2 µl	no

Pb^{2+} hydrolysis reactions were started by adding 1 µl of lead acetate solution (100 mM) followed by incubation for 60 min at 37°C.

Component	Amount
RNA	10 pmol RNA
PbAc 100 mM	1 µl
Liposomal buffer	4 µl

The fragmentized RNAs were subjected to phenol/chloroform extraction (4.2.5) and concentrated by ethanol precipitation (4.2.4). The pellet was dissolved in RNase-free water and the concentration was determined (4.2.3). Alternatively, the fragmentized RNA was cleaned up by using a Micro Bio-Spin column (4.2.6). Fragmentation was controlled by agarose gel electrophoresis (4.2.1). Then immune cells were stimulated with the fragmentized RNAs by using liposomes (4.5).

4.3.9. Ultrasonic treatment

RNAs were exposed to ultrasound waves for different lengths of time (0 s, 5 s, 10 s, 15 s, 20 s, 1 min). For this treatment, 40 µg RNA were aliquoted to an end volume with ultra-pure water of 100 µl in an Eppendorf tube and vortexed. Then the RNA solution was exposed to ultrasound waves. The degraded RNAs were analyzed by agarose gel electrophoresis (4.2.1), after which immune cells were stimulated with the degraded RNAs by using liposomes (4.5).

4.3.10. RNase III treatment of RNA

RNase III converts long dsRNA into a heterogeneous mix of short (18-25 bp) interfering RNAs (siRNA). We tested two different types of RNase III, one from Epicentre and one from BioLabs, in order to exclude an unspecific effect.

Component	Amount
RNA	50 µg
RNase III Dilution in 2 x RNase III buffer (3.8)	250 µl
H_20	ad 500 µl

RNase III treatment was controlled by agarose gel electrophoresis (4.2.1). Then immune cells were stimulated with the RNase III treated RNAs by using liposomes (4.5).

4.3.11. CIP treatment

Calf Intestinal Phosphatase (CIP) catalyses the hydrolysis of terminal 5`-phosphate groups from DNA and RNA.

Component	Amount
RNA	10 µg
CIP	2,5 µl
Liposomal buffer	ad 100 µl

The reaction components listed above were mixed and incubated for 1 h at 37°C. Then the solution was subjected to phenol/chloroform extraction (4.2.5) followed by ethanol precipitation (4.2.4). The pellet was dissolved in RNase-free water and the concentration was determined (4.2.3). CIP treatment was controlled by agarose gel electrophoresis (4.2.1). Then immune cells were stimulated with the CIP-treated RNAs by using liposomes (4.5).

4.4. DNA techniques

The polymerase chain reaction (PCR) is a method for the amplification of very small amounts of DNA. The following components are required: a thermostable DNA polymerase (Pfu polymerase or Taq polymerase); single- or double-stranded DNA (as a template); a forward and a reverse DNA primer, a buffer containing Mg^{2+} and dNTPs. The reaction is performed in three basic steps: denaturation of the double-stranded DNA at 95°C, annealing of primers to the DNA template at a temperature specific for the primers used, and elongation at 68 - 72°C for 5' 3' elongation of the annealed primer. The components listed below were mixed in a PCR reaction tube.

PCR reaction

template	x µl
Taq Mix	15 µl
Primer A	1 µl
Primer B	1 µl
H_20	x µl
	Σ 20 µl

PCR program

Initial denaturation	94°C	4 min
denaturation	94°C	30 s
annealing	58°C	60 s
elongation	72°C	60 s 34 cycles
final elongation	72°C	5 min
hold temperature	4°C	

An 5 - 10 µl aliquot of each reaction was checked on an agarose gel (4.2.1).

4.5. Transfection with DOTAP or Lipofectamine 2000 for "*in vitro*" stimulation

For stimulation, immune cells (e.g., human PBMCs (4.1.9.2), human HEKs (4.1.2) and murine immune cells (4.1.9.1)) were seeded in a range between 2 x 10^6/ml and 3 x 10^6/ml in 96-well flat bottom plates (100 µl/well). Each stimulation was performed in duplicate.

Stimulation with RNA or DNA

Exogenous RNA needs to cross the cell membrane in order to reach the cytoplasm or the endosomes. Cationic lipids in the form of liposomes or micelles are an efficient carrier for oligonucleotide (ODN) delivery into cells in culture. Cationic lipids are amphiphilic molecules, implying that they consist of a hydrophilic and a hydrophobic region, i.e., a (charged) cationic (amine) headgroup, attached via a linker (for example glycerol) to

usually double hydrocarbon chain. The cationic liposomes form a polyelectrolyte complex with the ODN (negatively charged molecules) (Xu and Szoka 1996; Zelphati and Szoka 1996).

Stimulation

Stimulation with RNA oligonucleotides was performed using transfection reagents. RNAs were encapsulated with DOTAP (Roche) in a 1:10 ratio for the stimulation of human PBMCs and murine immune cells. RNAs were complexed with DOTAP (Roth) in a 1:12,5 ratio for stimulation of HEKs. RNAs were formulated with Lipofectamine 2000 in a 1:250 ratio for stimulation of PBMCs and murine immune cells and in a 1:50 ratio for the stimulation of HEKs.

For a repeat determination, the corresponding amount of RNA was dissolved in 50 µl optimen in an Eppendorf tube and combined with 50 µl liposomal-mastermix. The mix was incubated for 15 min at room temperature before adding 110 µl medium. 100 µl were used in the stimulation of a 96-well that contained primary cells in 100 µl complete medium. For the stimulation without liposome, the corresponding amount of RNA was dissolved directly in 100 µl optimen. As a negative control for the liposomal transfection reagent, the cells were stimulated with liposome without adding RNA.

In order to achieve the desired end concentration, a double-concentrated RNA solution was prepared, due to the dilutionary effect from the cells being in 100 µl medium.

Incubation was performed for 16–20 h in a CO_2 incubator at 37°C. Then the cell supernatants were harvested (190 µl per well) and stored at -20°C. The supernatants were used to detect cytokines by ELISA (4.9).

Control-stimulation

Table 4 shows TLR ligands, which were employed as positive controls. 100 µl from double-concentrated ligands diluted in medium were added to the cells. As a negative control 100 µl medium was added to the cells.

Table 4 TLR ligands employed as positive controls

Stimulus	End concentration
CpG ODN 2216	1 µM
LPS	100 ng/ml
R848	200 ng/ml
RNA 40 or RNA 63	10 µg/ml
Poly (I:C)	10 µg/ml

4.6. Transfection with LL-37

For the stimulation of human PBMCs (4.1.9.2), human monocytes (4.1.9.3), human HEKs (4.1.2) and murine cultures (4.1.9.1), immune cells were seeded in a range between 2 x 10^6/ml and 3 x 10^6/ml in 96-well flat bottom plates (100 µl/well). Each stimulation was performed in duplicate.

LL-37 (10 µg) was either given directly into cell cultures (50 µg ml^{-1} = 10 µM) or first premixed with 2 µg RNA (peptide:RNA mass ratio of 5:1) in 10 µl of complete medium.

Non-infected MDCK-RNA or A/PR/8/MDCK-RNA were chosen as RNAs. After 30-minutes incubation at room temperature, the mix was added to the cell cultures. (The final concentration was 50 µg ml^{-1} of LL-37 and 10 µg ml^{-1} of RNA.)

Supernatants of stimulated cells were collected after overnight culture. Cytokine levels in the supernatants were determined by using ELISA kits (4.9).

4.7. FACS

To determine the purity of cells, characteristics of surface molecules were stained with fluorescence-labelled antibodies and analyzed by flow cytometry or FACS (fluorescence activated cell sorter). The most common fluorescent dyes are fluoresceinisothiocyanat (FITC), phycoerythrin (PE) and allophycocyanin (APC). Within the flow cytometer, the cell suspension is forced through a nozzle. As each cell passes through a laser beam, it scatters the laser light, and any dye molecules bound to the cell become excited and fluoresce. Sensitive photomultiplier tubes detect the scattered light (forward and side light-scattering properties), which provides information regarding the size and granularity of the cell. This information is used to distinguish different cell types. The result is visualized as

dot plots, coordinate systems that depict distinct cell populations. By using gates, the expression analysis is limited to certain cell populations. In addition to detecting scattering light, fluorescent signals are measured which give information on the binding of the labeled monoclonal antibodies and hence on the expression of cell-surface proteins by each cell.

For extracellular staining against the surface markers of immune cells, 5 x 10^5 cells were transferred into a FACS tube and washed with FACS buffer. After centrifugation for 6 min at 4°C and 1,400 rpm, the supernatant was removed, and the cells were incubated with a Fc-Block (Antibody against CD16/CD32) and the corresponding antibodies. After a short vortexing and an incubation time of 30 min in the dark at 4°C, cells were washed twice with 2 ml FACS buffer in order to remove non-binding antibodies. To maintain the cell structures for appropriate analysis; 300 µl of a 1% PFA solution in PBS was added, and the samples were vortexed. As a control, unstained cells were also analyzed by FACS.

All probes were measured with a BD FACSCalibur and analyzed with BD CellQuest.

Table 5: Fluorophore table of absorbance and emission wavelength.

Fluorescence canal	Fluorochrome	Absorption	Emission
FL1	FITC	495 nm	519 nm
FL2	PE	480/565 nm	578 nm
FL3	PI	536 nm	617 nm
FL4	APC	650 nm	660 nm

4.8. Immunofluorescence staining of LL-37/RNA complexes

The localization of cathelicidin/RNA complexes was analyzed by fluorescence microscopy on fixed cells as described in similar analysis (Ahmad-Nejad et al. 2002; Yasuda et al. 2006). Human monocytes (4.1.9.3) (0.5 x $10^6/cm^2$) were plated on 8-well chamber slides (1 cm^2/well) and rinsed after one hour with 1 x PBS^{++}. They were then stimulated with biotinylated LL-37 complexed to A/PR/8/MDCK-RNA as described above (4.6).

To visualize endosomes the cells were incubated with Transferrin and EEA-1, and to visualize lysosomes the cells were incubated with Lysotracker and Lamp. Transferrin (50 µg/ml) or Lysotracker (1000 nm) were added to the peptide solutions and incubated on the

cells for 30 min at room temperature. After washing three times with PBS, the cells were fixed with 4% (w/v) paraformaldehyde in PBS for 10 min at room temperature. Further stainings were performed with EEA-1 (1:100) or Lamp (1:100) in PBS containing 0,5% BSA and 0,5% saponine for 1 h at room temperature. The cathelicin is tracked in its biotinylated form by streptavidin-FITC. The streptavidin-FITC antibody is added in a 1:1000 dilution and incubated for 1 h at room temperature. In order to see the nucleus of the cells 4'-6-Diamidino-2-phenylindole (DAPI known to form fluorescent complexes with natural ds DNA) is added in a 1:1000 dilution.
Then cells are washed thrice with PBS/BSA/Saponine and once with ultra-pure water. Cells were covered with Mowiol (3.8), and a coverslip was added. The object slides could be stored up to two weeks in the dark at 4°C. Cells were analyzed using a Zeiss fluorescent microscope. Images were captured by digital image analysis equipment and processed with analysis software (AxionVision LE).

4.9. Cytokine detection by ELISA

Principle

A modification of ELISA known as a “capture” or “sandwich” ELISA can be used to determine the quantities of secreted cytokines or interferons from cell-free supernatants. The sandwich assay uses two different antibodies that are reactive with different epitopes on the antigen whose concentration needs to be determined. A fixed amount of one immobilized antibody is used to capture an antigen. Test solutions containing antigen at an unknown concentration, or a series of standard solutions with known concentrations of antigen, are added to the wells and allowed to bind. Unbound antigen is removed by washing. The binding of a second, enzyme-linked antibody that recognizes a nonoverlapping determinant on the antigen increases as the concentration of antigen increases and thus allows quantification of the antigen. A standard curve is constructed by adding varying amounts of a known standard preparation; the assay can then measure the amount of antigen in unknown samples by comparison with the standard.

Procedure

Supernatants from overnight cell cultures (4.5/4.6) were collected and stored at –20°C. Microtiter plates (Maxi Sorb Nunc Plate) were coated overnight at 4°C with a monoclonal

antibody. The purified capture antibodies were diluted in PBS^{def}, and 50 µl of this solution was dispensed into every well.

To block unspecific binding, 250 µl of a blocking buffer (10% BSA in PBS/Tween20) was transferred into every well and incubated at room temperature for 1 h. After 3 washing steps with PBS/Tween20, a 50 µl standard sample of the cytokine in question, with a defined concentration, was added to the plate, and a serial 1:2 dilution in medium was set up for a standard curve.

The samples to be measured were added to the plate in indicated solutions and incubated for 1-2 hours at room temperature. The plates were again washed three times with PBS/Tween20. To detect antibody-cytokine complexes, a detection antibody directed against the cytokine was diluted in blocking solution, and 50 µl of this solution was transferred into each well. The antibody was incubated for 1-2 hours at room temperature and washed with PBS/Tween20.

The detection antibody was either conjugated to an enzyme or was detected indirectly. The detection of biotinylated antibodies was performed through incubation with 50 µl of an enzyme-conjugated streptavidin dilution, called horseradish peroxidase (HRP). The horseradish peroxidase oxidized the substrate diaminobenzidine to produce a brown precipitate. For visualization, 100 µl of a colorless substrate (o-Phenylenediamine Dihydrochloride Tablet Sets) dissolved in substrate buffer was added and incubated at room temperature. The enzyme changes the colorless substrate into a colored reaction product. Reaction was stopped with 25 µl 4 N H_2S0_4 and absorbance was measured 490 nm (reference: 650 nm) using a Microplate ELISA reader and the SOFT Max® program. The cytokine concentrations were calculated by comparing the absorbance values of the samples to the standard curve obtained by linear regression. Analysis was performed in duplicate.

Used ELISA-Systems

The used systems are shown in the following table:

Detectable Protein	Name	Manufacturer	Original concentration	Used final concentration
Human-IFN-α				
Capture	Coating Antibody	Bender MedSystems, Vienna, Austria	100 µg/ml	10 µg/ml
Detection (HRP-conjugate)	HRP-conjugate	Bender MedSystems, Vienna, Austria	unspecified	1:1000
Standard	Recombinant Human Interferon-α	Peprotech	20 µg/ml	4 ng/ml
Human-IL-6				
Capture	Purified Rat Anti-Human IL-6 Monoclonal Antibody	BD Pharmingen, Heidelberg	500 µg/ml	0.5 µg/ml
Detection	Biotinylated Rat Anti-Human IL-6 monoclonal Antibody	BD Pharmingen, Heidelberg	500 µg/ml	0.5 µg/ml
Enzyme	Streptavidin-POD conjugate	Roche, Mannheim	500 U/ml	0.1 U/ml
Standard	Recombinant Human IL-6	Peprotech	10 ng/µl	10 ng/ml
Human-TNF-α				
Capture	Purified Mouse Anti-Human TNF Monoclonal Antibody	BD Pharmingen, Heidelberg	500 µg/ml	2 µg/ml
Detection	Biotinylated Mouse Anti-Human TNF Monoclonal Antibody	BD Pharmingen, Heidelberg	500 µg/ml	1 µg/ml
Standard	Recombinant Human TNF-α	R & D	10 µg/ml	5 ng/ml
Enzyme	Streptavidin-POD conjugate	Roche, Mannheim	500 U/ml	0.1 U/ml
Mouse-IFN-α				
Capture	Rat Monoclonal Antibody against Mouse Interferon Alpha (RMMA-1)	PBL, New Brunswick, USA	2000 µg/ml	1 µg/ml
Detection	Rabbit Polyclonal Antibody against Mouse Interferon Alpha	PBL, New Brunswick, USA	994 µg/ml	0,994 µg/ml

Detectable Protein	Name	Manufacturer	Original concentration	Used final concentration
Enzyme	POD-conjugated goat anti-rabbit IgG	Immuno Research	800 µg/ml	0,16 µg/ml
Standard	Recombinant mouse-IFN-α	PBL, Piscataway, NJ, USA	1 x 10^5 U/ml	500 U/ml
Mouse-IL-6				
Capture	Monoclonal Anti-mouse IL-6 Antibody	R&D Biosystems, Wiesbaden	500 µg/ml	1 µg/ml
Detection	Biotinylated Anti-mouse IL-6 Antibody	R&D Biosystems, Wiesbaden	500 µg/ml	100 ng/ml
Enzyme	Streptavidin-POD conjugate	Roche, Mannheim	500 U/ml	0.1 U/ml
Standard	Recombinant mouse-IL-6	R&D Biosystems, Wiesbaden	10 µg/ml	10 ng/ml
Mouse-IFN-ß				
Capture	Polyclonal rabbit anti-mouse IFN-ß)	PBL, New Brunswick, USA	1 mg/ml	2 µg/ml
Detection	Monoclonal rat anti-mouse IFN-ß	PBL, New Brunswick, USA	2.5 mg/ml	2.5 µg/ml
Enzyme	anti-rat IgG antibody H&L POD-conjugated	Abcam, UK	2 mg/ml	0.5 µg/ml
Standard	Recombinant Mouse Interferon Beta	R&D Biosystems, Wiesbaden	1 x 10^5 U/ml	500 U/ml

4.10. HPLC (high performance liquid chromatography)

Principle of HPLC

High-performance liquid chromatography is used in analytical chemistry to separate, identify and quantify compounds. HPLC utilizes a column that holds the stationary phase, a pump that moves the mobile phase through the column and a detector (UV or fluorescent) showing the retention times of the molecules. Retention time varies depending on the interactions between the stationary phase, the analysis of the molecules, and the solvent used. The retention time is considered a reasonably unique identifying characteristic of a given analyte. Reversed-phase HPLC has a non-polar stationary phase and an aqueous polar mobile phase. With these stationary phases,

retention time is longer for molecules which are more non-polar, while polar molecules elute more readily. A further refinement to HPLC has been to vary the mobile phase composition during the analysis, which is known as gradient elution. The retention can be decreased by adding a less polar solvent (methanol, acetonitrile) into the mobile phase to reduce the surface tension of water.

HPLC run

For the separation of the nucleosides, a RP-HPLC with a gradient from 5 mM NH_4OAc pH 6 (Buffer A), 40% Acetonitrile (Buffer B) and 66% Methanol (Buffer C) was performed. For the stationary phase a LC18-column from SUPERCOSIL (250 x 4.6 mm, 5 µm) was used. The run time was 60 min, and the detection was performed via UV-Detector.

4.11. Immunization

All animals were kept under specific pathogen-free conditions, and only female mice from 8-12 weeks of age were used for the experiments. Chicken egg albumin (OVA) was used as an antigen. ODN1668 PTO served as a positive control.

Preparation of the Injection

Animals were divided into groups of 2-3 mice, and 100 µl of the following vaccine formulations were injected:

Controls:

- liposomal buffer (20 mM HEPES, 150 mM NaCL, pH 7.4), 100 µl/mouse
- 100 µg OVA in liposomal buffer, 100 µl/mouse
- 100 µg OVA and 50 µg ODN 1668 PTO in liposomal buffer, 100 µl/mouse

with DOTAP:

- 30 µg DOTAP in liposomal buffer, 100 µl/mouse
- 100 µg OVA and 30 µg DOTAP in liposomal buffer, 100 µl/mouse

- 100 µg OVA and 30 µg DOTAP and 100 µg MDCK-RNA, 100 µl/mouse
- 100 µg OVA and 30 µg DOTAP and 100 µg A/PR/8-MDCK-RNA, 100 µl/mouse

with CRAMP:

- 200 µg CRAMP in liposomal buffer, 100 µl/mouse
- 100 µg OVA and 200 µg CRAMP in liposomal buffer, 100 µl/mouse
- 100 µg OVA and 200 µg CRAMP and 40 µg MDCK-RNA, 100 µl/mouse
- 100 µg OVA and 200 µg CRAMP and 40 µg A/PR/8-MDCK-RNA, 100 µl/mouse

Solutions:

Ova: 5 mg/ml in liposomal buffer

ODN 1668 PTO: 500 µM - 3,191 µg/µl ⇨ 50 µg/15,67 µl

4.11.1.1. Injection of mice

Mice were injected subcutaneously into the tail base with 100 µl of the vaccine formulations.

4.11.1.2. Antibody ELISA

The principle of ELISA is presented in section 4.9. Incubation times were chosen as described there. For antibody detection, serum was obtained from the blood of immunized mice 1 week after the second injection. ELISA plates were coated over night with 0.1 mg/ml OVA. Sera were diluted 1:3,000,000 and for detection the following antibody was used: biotin-SP-conjugated AffiniPure goat anti-mouse IgG (1:2,500). A streptavidin-HRP (1:5,000) was employed according to the manufacturer's instructions.

4.12. Electroporation

The regulation of gene expression is examined by reporter gene assays. For this purpose, DNA sequences carrying putative regulatory elements were cloned in front of a reporter gene. Here IFN-ß activity was measured using a reporter gene assay, which utilizes a

reporter plasmid containing the IFN-ß promoter cloned in front of the firefly luciferase gene. The protein encoded by the luciferase gene fluoresces in the presence of certain stimuli, making it easy to determine the level of its expression based on the level of luminescence. Firefly luciferase (Photinus pyralis) catalyzes the oxidation of luciferin to oxyluciferin. During this reaction photons are released at a wavelength of 562 nm. By employing a luminometer, the emitted light is measured and quantified. The average emitted light is given in Relative Light Units (RLU).

Polar molecules are allowed to pass membranes by electroporation. For this purpose, cells were adjusted to a final concentration of 3 x 10^6/400 µl in RPMI medium with 25% FCS. This suspension was transferred into a sterile 4 mm electroporation cuvette (Biorad) and mixed with 700 ng DNA of different types (Luciferase Reporter Plasmid, Plasmid with gene of interest, empty vector). The cuvette was placed into the electroporator, and a pulse of 220 V, 975 µF and ∞ Φ was carried out. The cells were transferred immediately into 10 ml DMEM with 10% FCS and seeded on a 96-well flat bottom plates. Then cells were stimulated and incubated for another 20 hours before adding 50 µl 1 x reporter lysis buffer. Lysates were shaken for 15 min and then stored at –80°C for 30 min. They were then analyzed for luciferase activity. 20 µl of cell-extract were transferred to each well of a 96-well polystyrene plate. Subsequently, the reaction was started in the luminometer by automatic injection of 25 µl Firefly Luciferin, and the emitted light was measured.

5. Results

5.1. Influence of RNA modifications at the 2`-position of ribose on immune stimulation

Recently, GU-rich ssRNA could be identified as a natural ligand for murine TLR7 and human TLR7/8 (Heil et al. 2004). In addition, it was shown that not only viral genomic ssRNA but also ssRNA-molecules of non-viral origin activate murine immune cells via TLR7 (Diebold et al. 2004). Self-RNA, such as ribosomal RNA (rRNA), is not stimulatory, due to natural occurring RNA modifications such as base-methylation, pseudouridine and 2`-O-methyl ribose (Maden 1990). This observation may explain the discrimination of self and non-self RNA by TLR7. Ribosomal RNA, which comprises 80% of total RNA, is the central part of the ribosome that is composed of two subunits. In eukaryotes, there are 40S and 60S subunits. The small subunit contains 18S rRNA (approx. 1874 bases), while the large subunit contains 28S rRNA (approx. 4718 bases) and two smaller subunits 5,8S rRNA (approx. 160 bases) and 5S rRNA (approx. 120 bases). In this study, we compared the immunostimulatory potential of ribosomal 18S rRNA with *in vitro* transcribed 18S rRNA and synthesized RNA oligonucleotides with different modifications. The 2`-position of ribose was considered critical for immunorecognition, as it is the position at which DNA and RNA structurally differ. The aim of this study was to analyse in more detail the recognition of ssRNA by TLR7 and TLR8.

5.1.1. Purified “natural” 18S rRNA in contrast to *in vitro* transcribed 18S rRNA

To investigate the stimulatory potential of eukaryotic ribosomal RNA, we purified 18S rRNA from total HEK293-RNA utilizing a 3`-complementary biotinylated DNA-oligonucleotide combined with streptavidin-coated beads (4.3.2.). Furthermore, we isolated *in vitro* transcribed 18S rRNA (4.3.4), which is not modified and does not contain 2`-O-ribose methyl groups.

Before transfecting cells with RNA, the RNA was purified (4.3.1/4.2.5) and its quality was confirmed by agarose gel electrophoresis (4.2.1/4.2.2). In all experiments, only RNA with an optical density quotient 260/280 nm of 2.0 or higher (4.2.3) and with high integrity was used. The RNAs used for stimulation are shown in Figure 7 A. The agarose gel shows for

total HEK293-RNA two bands, the 28S rRNA (4,7 kb) and the 18S rRNA (1,9 kb). 18S rRNA was purified from the total HEK293-RNA. As a comparison, we see the band for 18S rRNA generated by *in vitro* transcription.

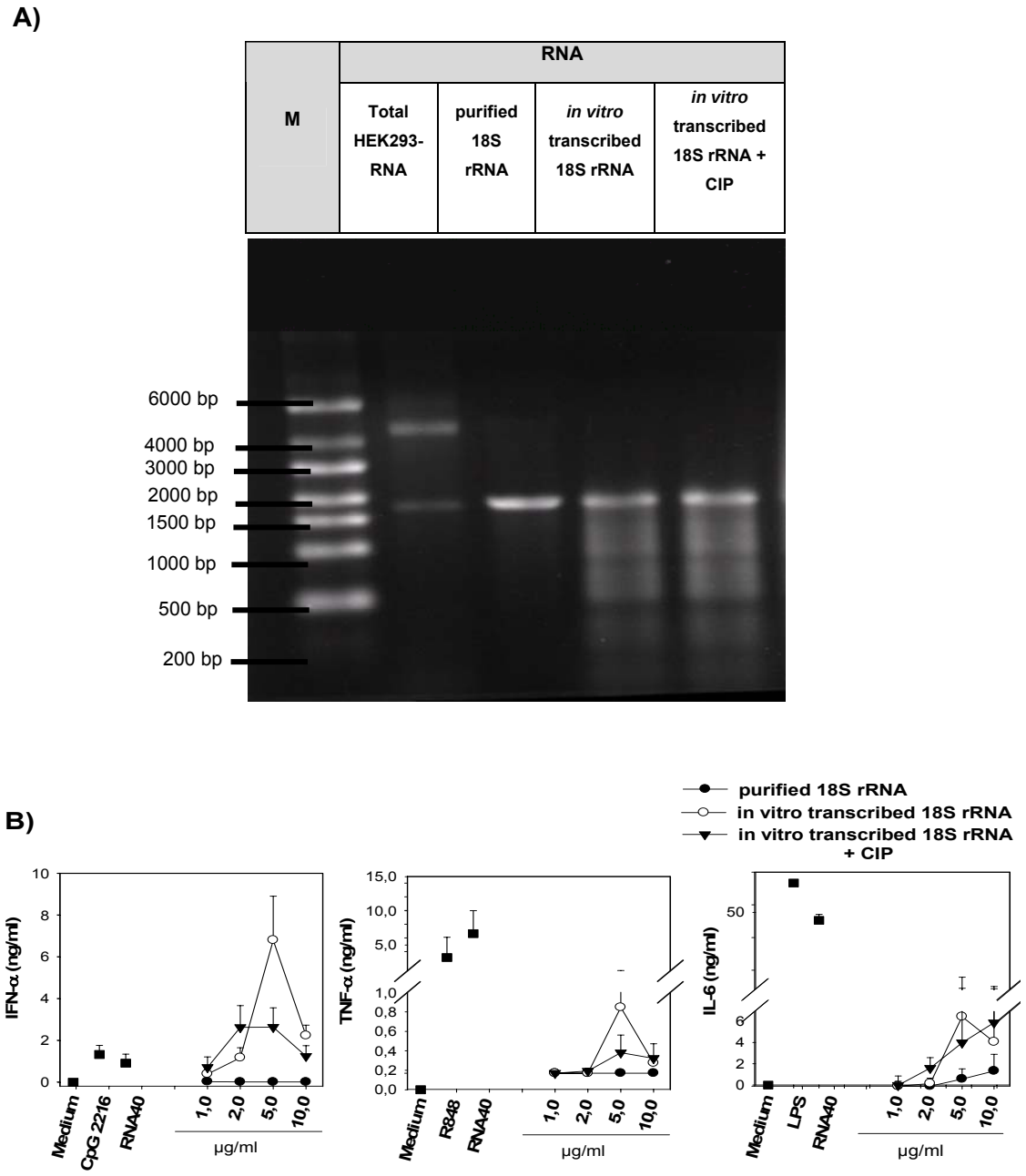

Figure 7: Analysis of *in vitro* transcribed 18S rRNA and purified 18S rRNA. A) Samples were analyzed by 1, 2 % agarose electrophoresis. Marker lane contains an RNA marker. B) Human PBMCs were stimulated with purified or *in vitro* transcribed 18S rRNA complexed to DOTAP. Cytokines were measured 24 hours post stimulation by ELISA. CpG 2216 (1 µM) and RNA 40 served as positive controls for IFN-α secretion. R848, RNA 40, and LPS served as positive controls for proinflammatory cytokine secretion. Mean values of 2 donors are shown.

For stimulating immune cells with RNA, the transfection reagent DOTAP was used as described in 4.5. The cationic transfection reagent DOTAP (N-[1-(2,3-Dioleoyloxy)propyl]-N,N,N-trimethyl-ammoniummethylsulfate) protects RNA from RNases and facilitates RNA uptake. The aforementioned RNAs were formulated with DOTAP and tested for type-I interferon secretion and proinflammatory cytokine induction like IL-6 and TNF-α in human PBMC cells (4.1.9.2) by ELISA (4.9). Positive controls for IFN-α secretion were the TLR ligands RNA 40 and CpG 2216. RNA 40, R848 and LPS were used as positive controls for proinflammatory cytokine secretion. Upon transfection of purified 18S rRNA complexed to DOTAP, there was no IFN-α secretion detectable in human PBMC cells, whereas *in vitro* transcribed 18S rRNA strongly induced type-I interferon (Figure 7 B). However, other cytokines such as IL-6 and TNF-α were induced by *in vitro* synthesized as well as by 18S rRNA purified from cells.

In parallel, murine Flt3-derived dendritic cells (4.1.9.1) were stimulated with the described RNAs. Flt3-derived dendritic cells were generated from wild-type and TLR7-deficient mice, in order to analyze a TLR dependency of the employed RNAs. The differentiation of the Flt3-derived dendritic cells was controlled by FACS analysis (4.7). Flt3-derived dendritic cells contain two cell types: pDCs and cDCs. Both cell types show characteristic cell markers; cDCs can be recognized by the expression of high levels of CD11c, whereas pDCs have a combination of B220 and CD11c. As an example, Figure 8 shows a FACS analysis of Flt3-derived cells. This Flt3-culture contained 25% pDCs and 33% cDCs.

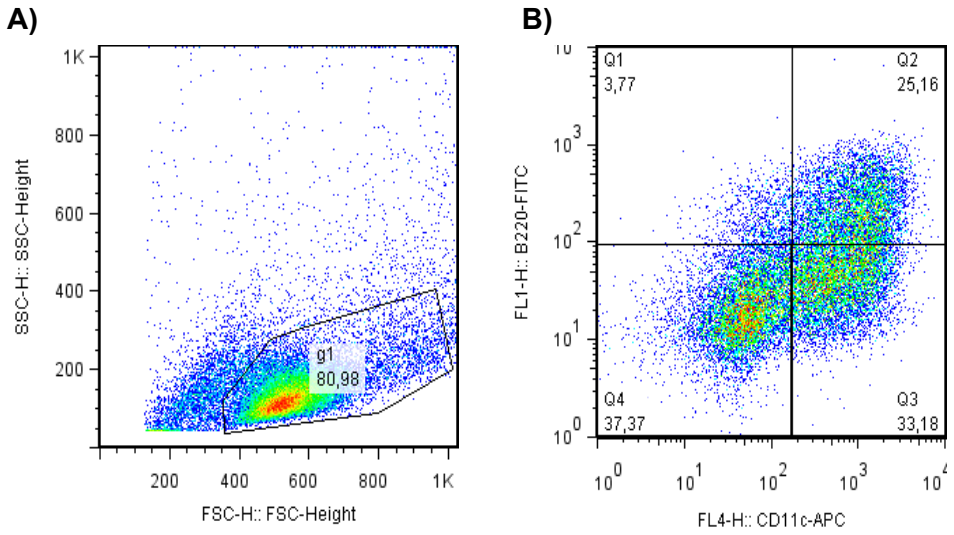

Figure 8: Characterisation of Flt3-derived dendritic cells. A representative flow cytometric analysis of Flt3-derived dendritic cells with anti-CD11c-APC and anti-B220-FITC is shown. A) Gate of living cells with FSC/SSC. B) Cells concerning the gate described in A. pDCs are shown in the upper right quadrant, whereas cDCs are shown in the lower left quadrant.

The Flt3-derived DCs were stimulated in the same way as described for PBMC cells. The supernatants were used for detection of IFN-α and IL-6 (4.9). Figure 9 shows that upon transfection of purified 18S rRNA complexed to DOTAP, there was no IFN-α secretion detectable in murine Flt3-derived dendritic cells, whereas *in vitro* transcribed 18S rRNA strongly induced type-I interferon in a TLR7-dependent manner. The proinflammatory cytokine IL-6 was not induced by purified 18S rRNA complexed to DOTAP. But for stimulation with *in vitro* transcribed 18S rRNA complexed to DOTAP, an IL-6 response was detectable in a TLR7-dependent manner. The TLR7-specific control RNA 40 showed only a weak IFN-α secretion in TLR7 $^{-/-}$ cells and R848 induced no IL-6 secretion in TLR7 $^{-/-}$ cells.

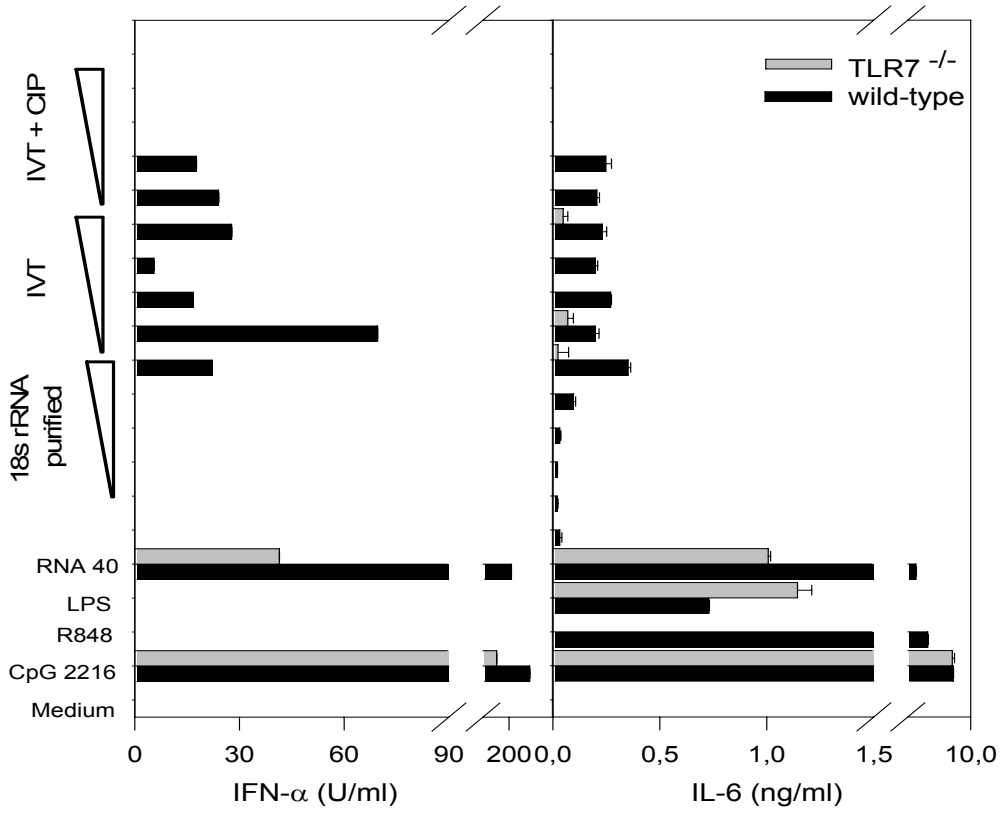

Figure 9: Analysis of the receptor responsible for recognizing purified or *in vitro* transcribed 18S rRNA. Murine Flt3-derived dendritic cells generated from a wild-type or a TLR7-deficient mouse were stimulated with purified or *in vitro* transcribed 18S rRNA complexed to DOTAP. RNA 40 and R848 served as specificity controls for the respective knockout cells. Cytokines were measured 24 hours post stimulation by ELISA (n = 2, one representative experiment is shown).

5.1.2. 2`-O-ribose methylated synthetic RNA sequences from 18S rRNA do not stimulate TLR7, but still stimulate TLR8

The presence of naturally occuring nucleotide modifications has been proposed to be important for RNA-mediated immunorecognition. To further investigate the influence of 2`-O-ribose methylation on the immunostimulatory activity of rRNA, we synthesized two RNA oligonucleotides derived from the 18S rRNA from nucleotides 1488-1499, both with and without the naturally occurring 2`-O-ribose methylation. At position 1490, the natural rRNA contains a 2`-O-ribose methylated guanosine (5`-CAG$_{2`\text{-O-methyl}}$GUCUGUGAU, RNA 63-2`-O-methyl, 5`-CAGGUCUGUGAU, RNA 63) (Maden 1990; Bachellerie and Cavaille 1997). Moreover, we designed RNA oligonucleotides that lack the 2`-oxygen (deoxy derivates) and those that feature a fluoro-group at this position (F-derivates). The different modifications of the RNA 63 oligonucleotides are shown in Figure 10.

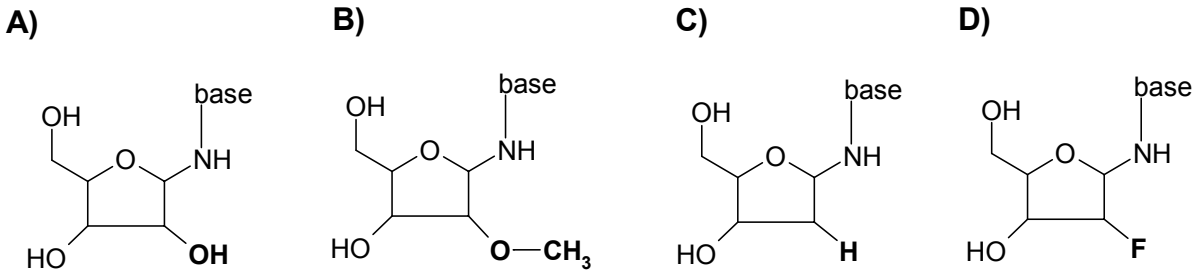

Figure 10: Structures of modified oligonucleotides used in this study. Synthetic RNA sequences from 18S rRNA. A) Guanosine without 2`-O-methyl-derivates. B) 2`-O-ribose methylated guanosine. C) 2`-deoxy derivates of guanosine. D) 2`-F derivates of guanosine. RNA 63M (as shown in B) contains a 2`-O-ribose methylated guanosine at position 3 and reflects the modification occurring in natural 18S rRNA. RNA 63 (as shown in A) has the same sequence but contains no modifications. RNA 63 deoxy (shown in C) shows a deoxy group at positon 3 of guanosine. RNA 63 F (shown in D) contains a fluoro group at position 3 of guanosine. Sequence of RNA 63: 5`CAGGUCUGUGAU- at position three represent the different modifications of guanosine. Modifications are depicted in bold letters.

RNA oligonucleotides were formulated with DOTAP and tested for type-I interferon secretion and proinflammatory cytokine induction like IL-6 and TNF-α from human PBMC cells over a concentration range from 0.2 µg/ml to 10 µg/ml (4.1.9.2), as shown in Figure 11 A. As controls, the same samples were used as described in section 5.1.1. A dose-

dependent IFN-α secretion was observed which varied between 1 and 4 ng/ml. RNA 63-2`-O-methyl showed a significantly decreased IFN-α response. Residual IFN-α was only detectable at the concentration of 1 µg/ml of RNA. Interestingly, none of the other modifications at position 3 of RNA 63, such as 2`-deoxy (RNA 63-2`-deoxy) and 2`-F (RNA 63-2`-F), influenced IFN-α production. And surprisingly, RNA 63-2`-O-methyl induced IL-6 and TNF-α in human PBMC cells similar to the other tested RNA oligonucleotides.

Next, we tested the RNA oligonucleotides complexed to DOTAP for cytokine induction on murine Flt3-derived dendritic cells (wild-type and TLR7-deficient) (4.1.9.1) as shown in Figure 11 B. In order to prove TLR7 dependency for the tested RNA oligonucleotides, Flt3-derived DCs from a TLR7-deficient mouse were generated. The Flt3-derived DCs were stimulated in the same way as described for PBMC cells, and a FACS analysis (as described for the Flt3-derived DCs in section 5.1.1) was performed. The supernatants of the stimulated cells were used for detection of IFN-α and IL-6 by ELISA (4.9). Interestingly, RNA 63 induced IFN-α and proinflammatory cytokine production (TNF-α, IL-6) in a TLR7-dependent manner. In contrast, RNA 63-2`-O-methyl was not immunostimulatory. The proinflammatory cytokine-induced production by RNA 63-2`-O-methyl which was observed in the human system was not found in murine immune cells. Since murine TLR8 itself is non-functional, this may explain the different proinflammatory cytokine response for the RNA 63-2`-O-methyl RNA in the human and murine immune systems. Indeed, genetic complementation assays in HEK293 cells with human TLR8 revealed that RNA 63 and RNA 63-2`-O-methyl activated NF-κB (unpublished data).

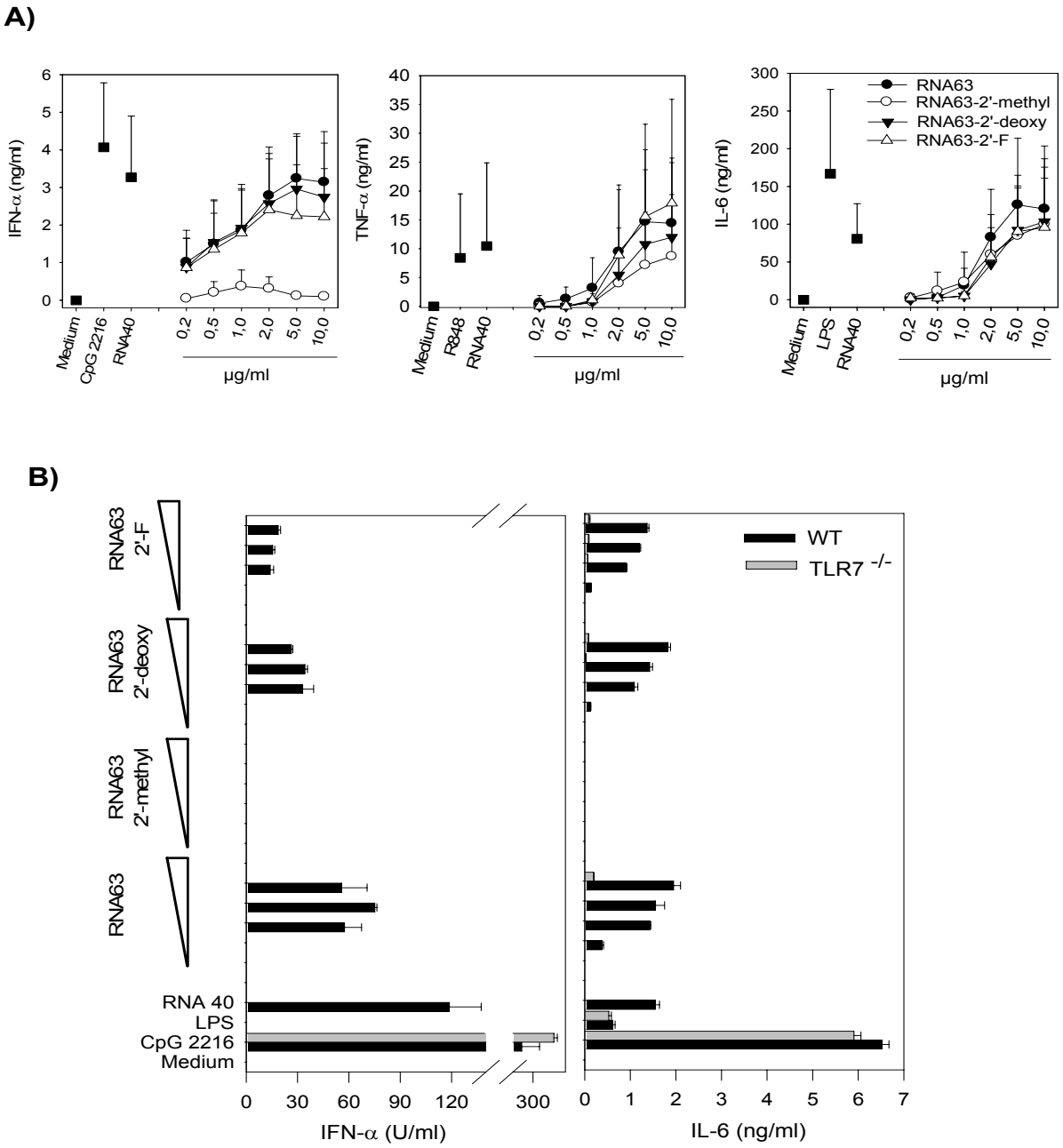

Figure 11: Influence of nucleotide modifications on RNA-mediated immunostimulation. Stimulation of human PBMCs (A) and murine Flt3-derived dendritic cells (B) with different modified RNA 63 oligonucleotides complexed to DOTAP in the indicated concentrations. RNA 63 was transfected with either unmodified (RNA 63), 2`-O-methyl (RNA 63 M), 2`-deoxy (RNA 63 deoxy) or with 2`-O-F (RNA 63 F). CpG 2216, RNA 40 and LPS served as positive controls. Cytokines were measured by ELISA 24 hours after stimulation. In (A) mean values of 6 different donors are shown. In (B) mean values of 2 experiments are shown.

5.1.3. Summary

TLR7 and TLR8 recognize RNA from pathogens and lead to subsequent immune stimulation. Self-RNA is either not at all or less immunostimulatory, due to RNA modifications such as 2`-O-ribose- or base methylations. Here, we showed that purified ribosomal 18S rRNA was not immunostimulatory, whereas *in vitro* transcribed 18S rRNA induced cytokines. A single 2`-O-ribose methylation within a natural fragment of 18S rRNA prevented IFN-α production. However, secretion of TNF-α and IL-6 was not impaired in human PBMCs. But the induction of the proinflammatory cytokines was not observed in murine immune cells. Since murine immune cells do not express a TLR8 receptor, we can conclude that a 2`-O-ribose methylation converts a TLR7/TLR8 ligand to a TLR8-specific ligand. Interestingly, other modifications at this position such as 2`-deoxy or 2`-F had no negative influence on TLR activation.

5.2. Analysis of the immunostimulatory capacity of RNA from virus-infected cells complexed to cationic lipids or natural carriers

One disadvantage of using RNA as an adjuvant may be the necessity of complexation to cationic lipids such as DOTAP for efficient immune stimulation. Since DOTAP is toxic at higher concentrations (Romoren et al. 2004), non-toxic or natural carriers for immunostimulatory RNA are desirable. Recently, LL-37 has been found as a key factor in mediating plasmacytoid dendritic cell (pDC) activation in psoriasis, a common autoimmune disease of the skin (Lande et al. 2007; Gilliet and Lande 2008). Accordingly, LL-37 forms aggregates with the self-DNA of dying cells, protects it against nuclease degradation and converts it into an inducer of type-I interferon production. The binding of LL-37 to DNA is driven by both the cationic charges of LL-37 (which interact with the negative charges of DNA) and the unique alpha-helical structure of LL-37 (which stabilizes these interactions with DNA) (Gilliet and Lande 2008). We investigated whether LL-37 or the mouse homolog CRAMP could function as such a carrier for RNA, especially for RNA from virus-infected cells as depicted in Figure 12 (4.6).

Previous studies have indicated that the ssRNA genome of the influenza virus is recognized by RIG-I in monocytes (Hornung et al. 2006; Pichlmair et al. 2006). The exact structure of RNA detected by RIG-I is currently controversial (Schlee et al. 2009). Several authors have reported that RIG-I detects ssRNA containing a 5`-triphosphate (Hornung et al. 2006; Pichlmair et al. 2006) as well as short dsRNA (Kato et al. 2008). Dephosphorylation of the influenza genome results in a loss of its ability to induce IFN-α, suggesting that the recognition of influenza virus RNA by RIG-I is mediated through 5`-triphosphate ssRNA (Hornung et al. 2006). On the other hand, earlier studies have postulated that dsRNA intermediates produced during influenza virus replication induce IFN-α (Jacobs and Langland 1996; Majde et al. 1998; Majde 2000). In contrast to these earlier findings, Weber et al. found that the recognition of negative ssRNA viruses is not accompanied by the formation of immunodetectable dsRNA, as determined using dsRNA-binding antibodies (Weber et al. 2006; Pichlmair and Reis e Sousa 2007). To address the question of which conformation of the influenza genome is responsible for inducing IFN-α, we isolated MDCK-RNA (MDCK = Madin-Darby canine Kidney) from non-infected and A/PR/8-infected cells (A/PR/8 = Influenza-A-Virus Puerto Rico) (4.1.5/4.3.1) and analyzed their immunostimulatory abilities.

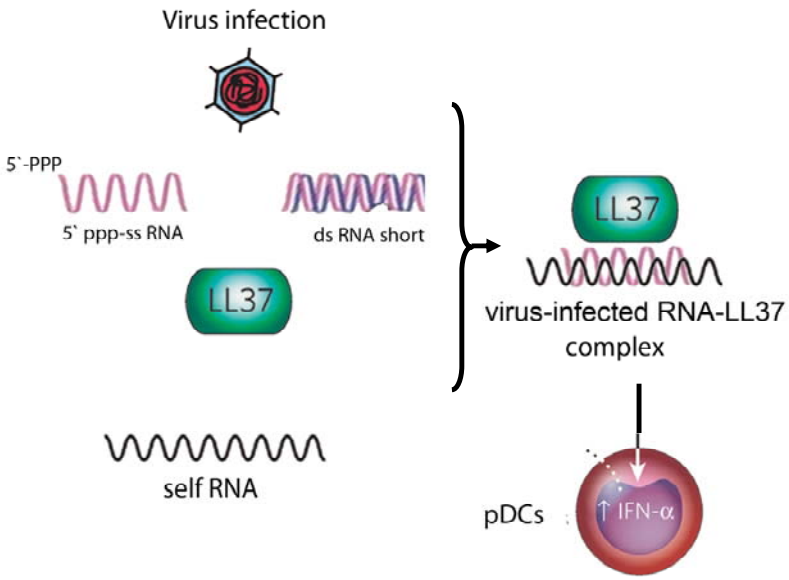

Figure 12: Role of LL-37 in a viral infection (modified after (Baumgarth and Bevins 2007)). Upon viral infection, LL-37 forms complexes with self-RNA and viral RNA. These complexes trigger a strong interferon production in immune cells.

5.2.1. Stimulation with RNA from virus-infected cells

Interestingly, RNAs from A/PR/8-infected cells (8h) and from non-infected cells were indistinguishable when visualized on an agarose gel by ethidium bromide staining (Figure 13). The eight gene segments for A/PR/8-RNA were not visible in RNA preparations from A/PR/8-infected cells as depicted in Figure 13 B.

For the stimulation of immune cells with RNA, the cationic transfection reagents DOTAP and Lipofectamine 2000 were used. The transfection reagent DOTAP (N-[1-(2,3-Dioleoyloxy)propyl]-N,N,N-trimethyl-ammoniummethylsulfate) enhances the cellular uptake of nucleic acids and increases their concentration within the endosomal/lysosomal vesicles (Yasuda et al. 2005). On the other hand, the transfection reagent Lipofectamine 2000 delivers nucleic acids to the cytoplasm (Astriab-Fisher et al. 2004; Dalby et al. 2004; Langlois et al. 2005). Moreover, we used natural carriers (cathelicidins) for complexation of RNA and analyzed where these natural carriers deliver nucleic acids.

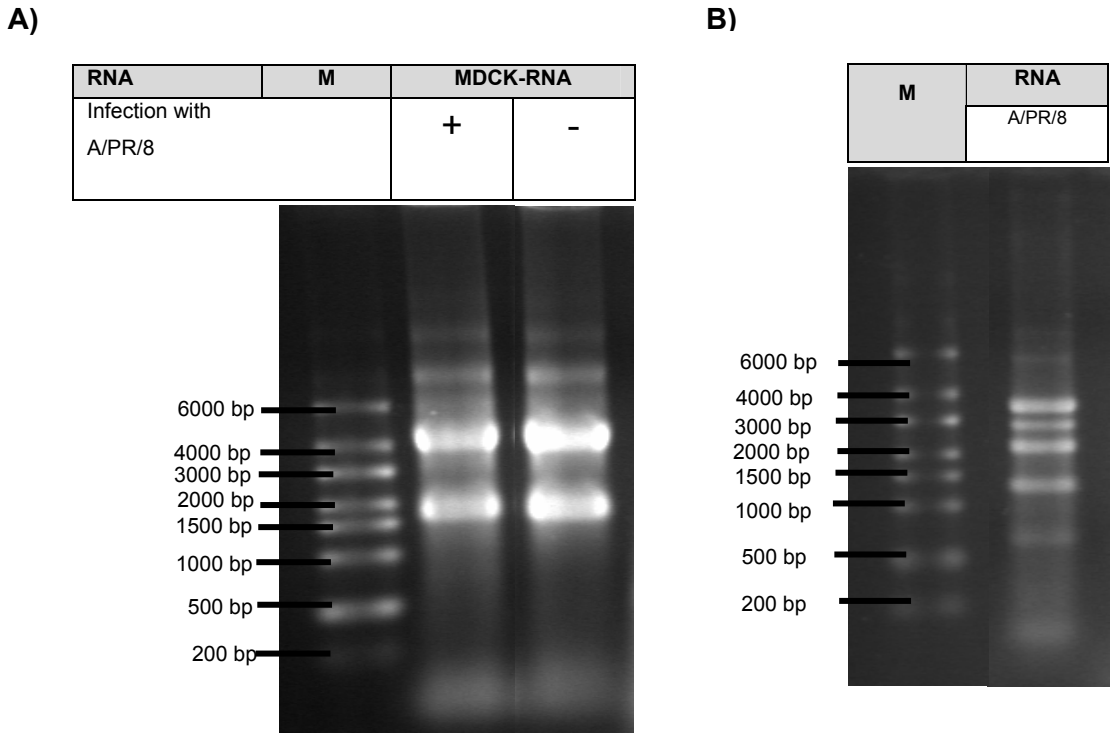

Figure 13: RNA preparations used for immune stimulation. A) Total RNA from uninfected or A/PR/8-infected MDCK cells was isolated and samples were analyzed by 1, 2 % agarose electrophoresis followed by ethidium bromide staining. The marker lane contains an RNA marker. B) Viral A/PR/8-RNA was visualized by ethidium bromide staining after separation on an 1, 2 % agarose gel with an RNA marker.

5.2.2. The immunostimulatory ability of RNA complexed to cathelicidins in human immune cells

A/PR/8/MDCK-RNA complexed to the cathelicidins LL-37 or CRAMP was tested for its ability to induce IFN-α in human PBMC cells (4.1.9.2). PBMC cells were stimulated as described in section 5.1 and the supernatants were used for detection of cytokines by ELISA (4.9). For PBMCs, the IFN-α secretion was confirmed with the positive controls RNA 40 and CpG 2216. Figure 14 depicts the IFN-α response to A/PR/8/MDCK-RNA complexed to LL-37, sLL-37 (a scrambled version of LL-37) and CRAMP (murine homolog of LL-37) in comparison to A/PR/8/MDCK-RNA encapsulated with DOTAP. For A/PR/8/MDCK-RNA complexed to a natural carrier, there was an IFN-α response detectable, although the levels of IFN-α were almost 4-fold lower compared to the IFN-α response for A/PR/8/MDCK-RNA complexed to DOTAP. Upon transfection of self-RNA complexed to cathelicidins, there was no IFN-α response detectable. However, we observed for self-RNA in a concentration range of 2 µg/ml complexed to DOTAP a

background IFN-α response in human PBMC cells, which, as we will later see, was not observed in Flt3-derived dendritic cells (Figure 14/Figure 17). It is remarkable that self-RNA complexed to LL-37 induced an IL-6 response, whereas the IL-6 response for self-RNA complexed to DOTAP (and in this experiment also to CRAMP) was variable on human PBMC cells (Figure 14).

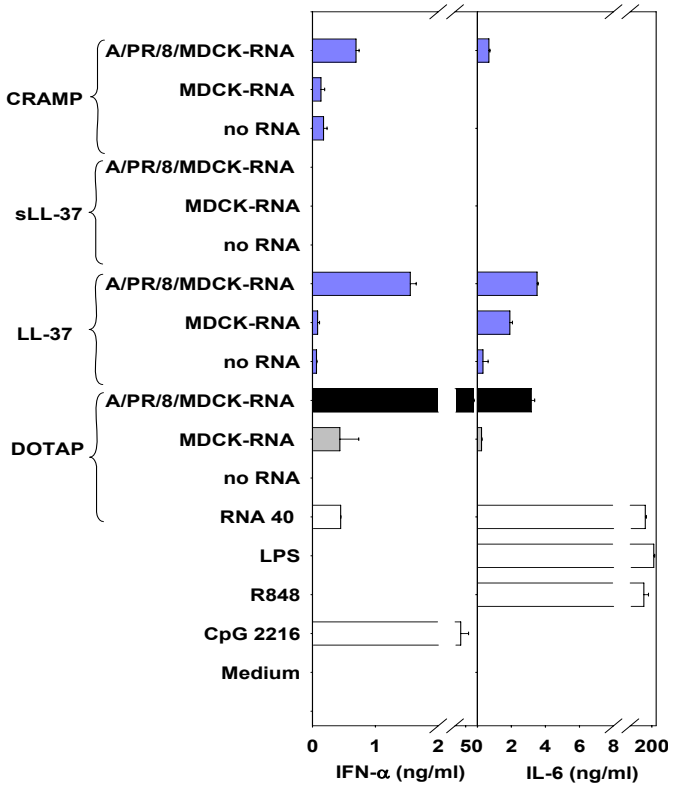

Figure 14: Complexation of RNA from A/PR/8-infected MDCK cells to LL-37 induced type I interferon in human PBMC cells. 10 µg of total RNA from uninfected or A/PR/8-infected MDCK cells was complexed to 50 µg LL-37, scrambled LL-37 or CRAMP and used for stimulation of human PBMCs at a final RNA concentration of 10 µg/ml. As a comparison, uninfected and A/PR/8/MDCK-RNA (2 µg/ml) was complexed to DOTAP. Cytokines were measured 24 hours post stimulation by ELISA (for A/PR/8/MDCK-RNA complexed to LL-37 or sLL-37 n = 30, for A/PR/8/MDCK-RNA complexed to CRAMP n = 8, one representative experiment is shown).

5.2.3. Monocytes are the main source of IFN-α upon recognition of RNA from A/PR/8-infected cells.

To address the question of which cell types of the human PBMC cells are responsible for recognizing the A/PR/8/MDCK-RNA complexed to cationic transfection reagents or to cathelicidins, we analyzed the immune activation of monocytes (4.1.9.3) in comparison to PBMC cells (4.1.9.2) as shown in Figure 16. Human monocytes were isolated from PBMC cells, purified via elutriation followed by MACS separation and stimulated. The purity of the monocytes was controlled by FACS analysis (4.7). Monocytes can be recognized by

the expression of high levels of CD14 and CD11b. As shown in Figure 15, the isolated monocytes showed a purity of about 90%, whereas PBMCs contained only 28% monocytes.

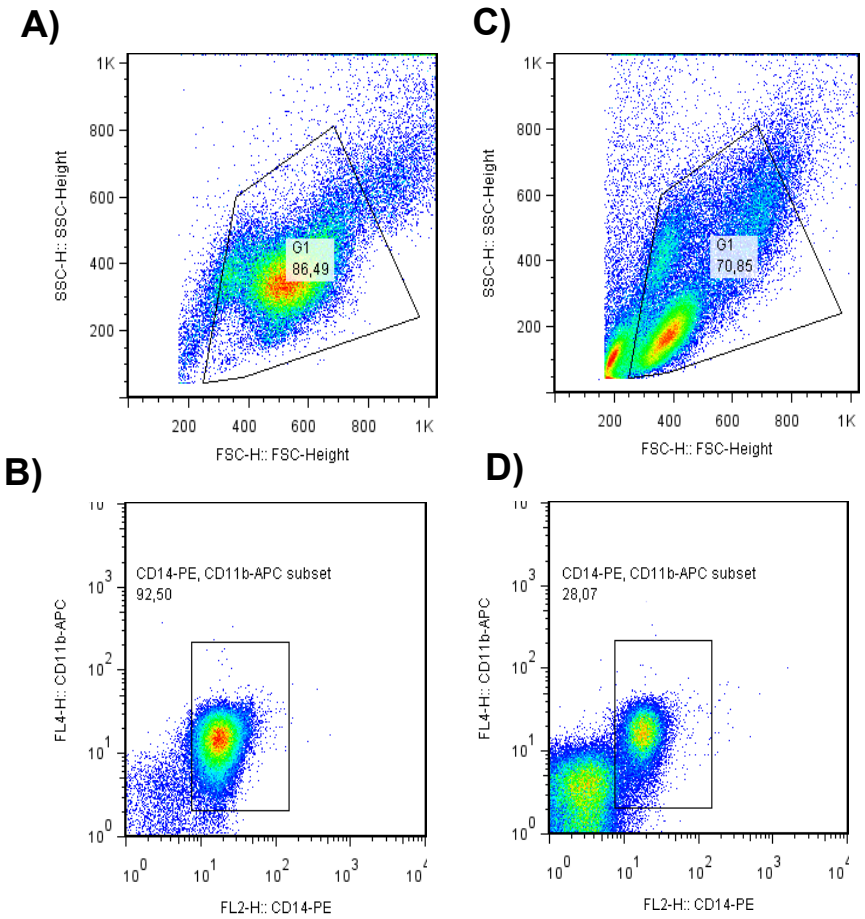

Figure 15: Characterization of human monocytes. A representative flow cytometric analysis of human monocytes with anti-CD14-PE and anti-CD11b-APC is shown. A) Gate of living monocytes with FCS/SSC. B) Cells concerning the gate described in A were stained with anti-CD14-PE and anti-CD11b-APC. C) Gate of living PBMC cells with FCS/SSC. D) Cells concerning the gate described in C were stained with anti-CD14-PE and anti-CD11b-APC.

The monocytes were stimulated in the same way as described for PBMC cells. The supernatants were used for detection of IFN-α (4.9). Upon transfection of CpG 2216 and RNA 40, there was no IFN-α secretion detectable in human monocytes (only a weak secretion for RNA 40), whereas these ligands induced type-I interferon in human PBMC cells. Stimulation with A/PR/8/MDCK-RNA complexed to LL-37 induced a type-I interferon response in human PBMC cells and monocytes. Here, the induced IFN-α response seemed to be higher for monocytes than for PBMC cells. Upon transfection with self-RNA,

there was no IFN-α response detectable. It is remarkable that self-RNA complexed to LL-37 induced an IL-6 response in PBMC cells and monocytes.

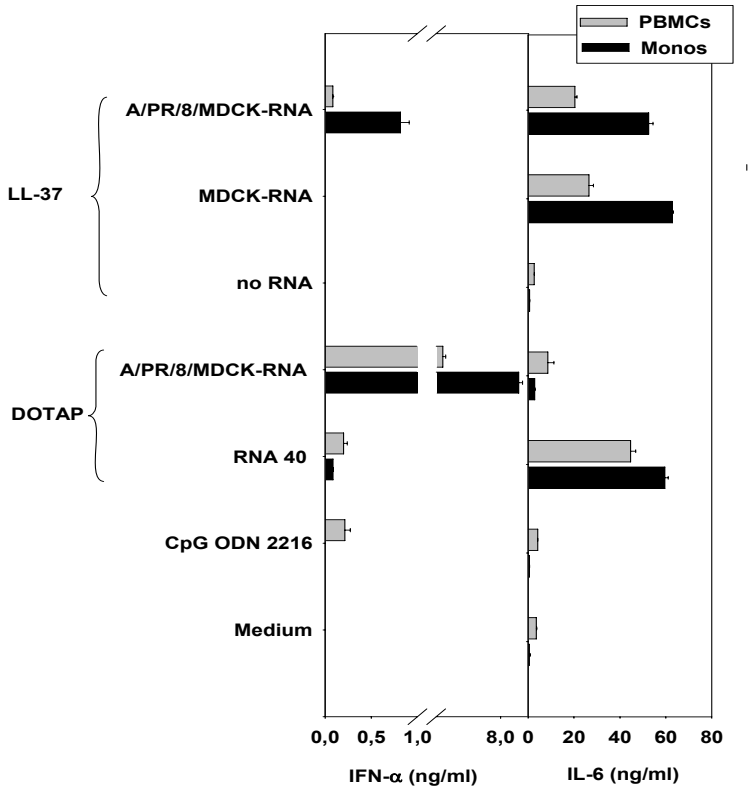

Figure 16: Analysis of the cell type of human PBMC cells responsible for recognizing A/PR/8/MDCK-RNA complexed to LL-37. A/PR/8/MDCK-RNA complexed to Dotap or LL-37 was used for stimulation of human PBMC cells and monocytes. Cytokines were measured 24 hours post stimulation by ELISA. CpG 2216 (1 µM) and RNA 40 served as positive controls (for ca. 90 % purity monocytes n = 2, for ca. 70 % purity monocytes n = 5; one representative experiment is shown).

5.2.4. Analysis of important RNA features for recognizing the A/PR/8/MDCK-RNA

Role of the 5`-triphosphate group for recognizing the A/PR/8/MDCK-RNA

To determine if the 5`-triphosphate group is involved in the recognition of A/PR/8/MDCK-RNA, we dephosphorylated the A/PR/8/MDCK-RNA with calf-intestine phosphatase (CIP) (4.3.11) and examined its immunostimulatory activity in murine Flt3-derived dendritic cells from a wild-type mouse (4.1.9.1). The differentiation of the cells to pDCs and cDCs was controlled by FACS analysis (4.7). The TLR ligands RNA 40 and CpG 2216 were used as positive controls for IFN-α secretion. The measured IFN-α induction, as presented in Figure 17, shows that dephosphorylation of the A/PR/8/MDCK-RNA complexed to DOTAP or Lipofectamine 2000 resulted in significant signal abrogation, indicating that its 5`-

triphosphate modification was quite efficiently removed. Dephosphorylation of the RIG-I ligand 5`-3P RNA complexed to Lipofectamine 2000 also abolished the IFN-α response, suggesting that RIG-I signaling in murine immune cells is mediated through the 5`-triphosphate ssRNA.

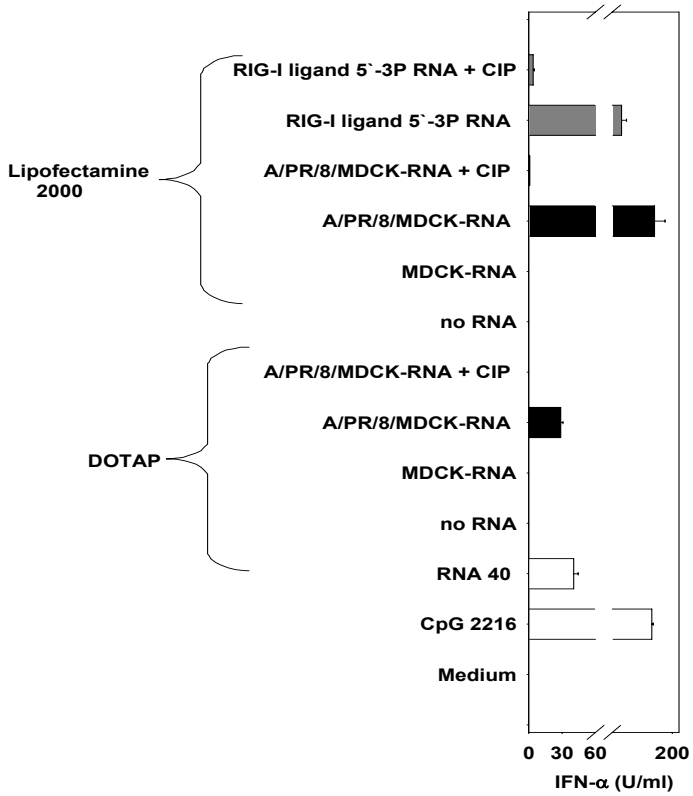

**Figure 17: Influence of the 5`-triphosphate end for recognizing RNA in murine immune cells.** RNA from uninfected and A/PR/8-infected MDCK cells (2 µg/ml) and RIG-I ligand 5`-3P RNA (0.2 µg/ml) were complexed to DOTAP or Lipofectamine 2000 that had been either mock treated or treated with CIP and used for stimulation of Flt3-derived dendritic cells. CpG 2216 and RNA 40 served as positive controls. IFN-α secretion was measured 24 hours post stimulation by ELISA (n = 8, one representative experiment is shown).

The same set of RNA ligands was assayed for their ability to induce IFN-α in human immune cells (PBMCs) isolated from healthy donors (4.1.9.2). For PBMCs the IFN-α secretion was also confirmed with the positive controls RNA 40 and CpG 2216. Figure 18 shows that, in contrast to murine Flt3-derived dendritic cells, the IFN-α response to A/PR/8/MDCK-RNA complexed either to DOTAP or Lipofectamine 2000 was not abrogated after dephosphorylation in human PBMCs, whereas for the RIG-I ligand 5`-3P RNA complexed either to DOTAP or Lipofectamine 2000, the IFN-α response was reduced after CIP-treatment. The question arises as to whether there are different features of RNA responsible for detection of A/PR/8/MDCK-RNA in murine and human immune cells. Moreover, we observed for MDCK-RNA in a concentration range of 2 µg/ml complexed to DOTAP or Lipofectamine 2000 a background IFN-α response in human PBMC cells that was not observed in Flt3-derived dendritic cells (Figure 17/Figure 18).

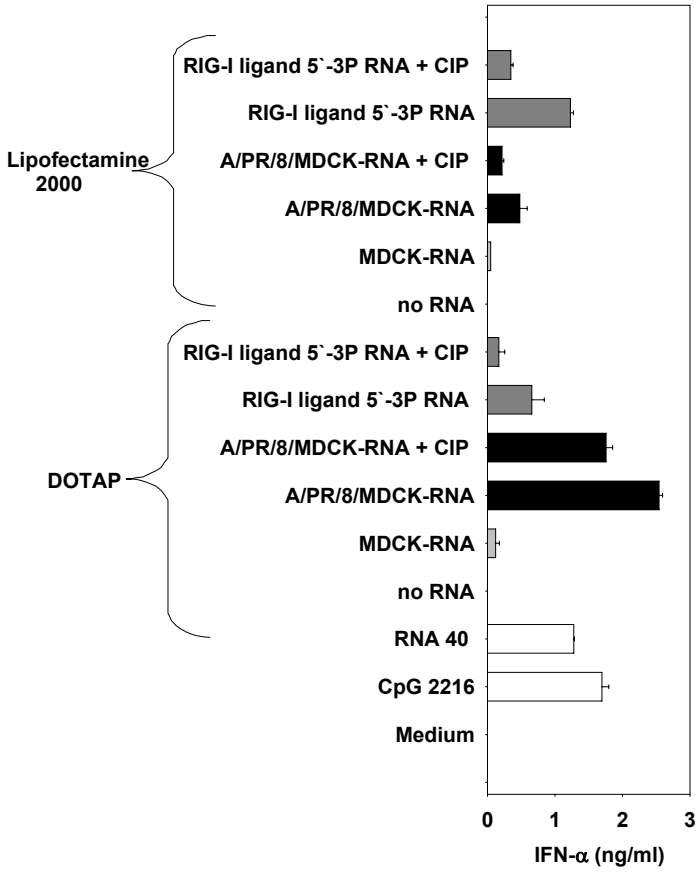

**Figure 18: Influence of the 5`-triphosphate end for recognizing RNA in human immune cells.** RNA from uninfected and A/PR/8-infected MDCK cells (2 µg/ml) and RIG-I ligand 5`-3P RNA (0.2 µg/ml) were complexed to DOTAP or Lipofectamine 2000 that was either mock treated or treated with CIP and used for stimulation of PBMCs. CpG 2216 and RNA 40 served as positive controls. IFN-α secretion was measured 24 hours post stimulation by ELISA (n = 6, one representative experiment is shown).

Conformation of the genome of negative-strand viruses

In order to analyze the conformation of the RNA prepared from A/PR/8-infected cells, we treated total A/PR/8/MDCK-RNA with the ds-specific RNase III (4.3.10) and compared their immunostimulatory capacity before and after treatment in human and murine immune cells (4.1.9). RNase III cleaves dsRNA or hairpin dsRNA regions of ssRNAs (Aliyari and Ding 2009). Upon treatment of A/PR/8/MDCK-RNA with RNase III, the RNA was complexed to DOTAP and used for stimulation of human PBMC cells. IFN-α induction was measured by ELISA and the already described positive controls CpG 2216 and RNA 40 were used. A/PR/8-infected MDCK-RNA remained immunostimulatory when treated with the ss-specific RNase A (data not shown), but signaling was abolished upon treatment with the ds-specific RNase III (Figure 19 A). The observed background IFN-α response for MDCK-RNA in a concentration range of 2 µg/ml complexed to DOTAP in human PBMC cells was also abrogated upon treatment with the ds-specific RNase III.

For A/PR/8/MDCK-RNA complexed to DOTAP, the same data were obtained in murine Flt3-derived dendritic cells (data not shown). Visualization of the virus-infected RNA that was either mock-treated or treated with RNase III by ethidium bromide staining did not

show any differences (Figure 19 B). These results indicate that besides the terminal 5`-triphosphate, the ds character of the virus-infected RNA is an important feature for immune signaling.

A)

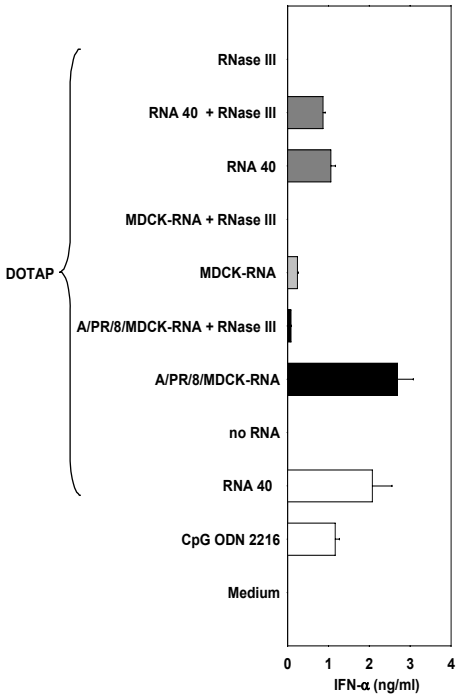

B)

RNA	M	MDCK-RNA						ssRNA 40		
Infection A/PR/8		+			-					
RNase III [U/ml]		-	0.1	0.5	-	0.1	0.5	-	0.1	0.5

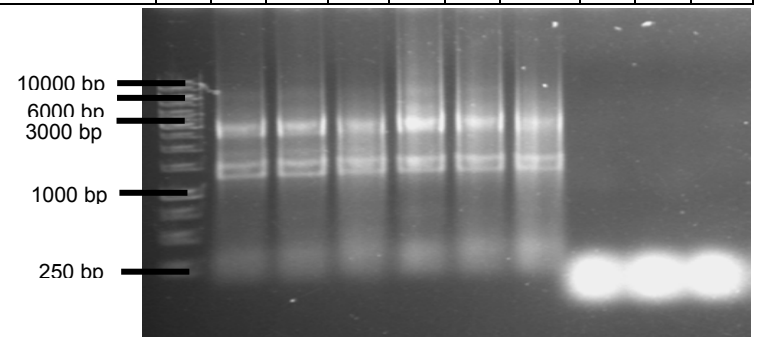

Figure 19: The ds character is an important feature for the A/PR/8/MDCK-RNA induced IFN-α production. A) RNA derived from MDCK cells either uninfected or infected with A/PR/8 (2 µg/ml) and ssRNA 40 (10 µg/ml) as a control were partially treated with RNase III (0.5 U/ml) complexed to DOTAP and used for stimulation of PBMC cells. IFN-α production was measured 24 hours post stimulation by ELISA. CpG 2216 (1 µM) and RNA 40 served as positive controls (n = 9, one representative experiment is shown). B) Different RNAs were incubated with varying amounts of RNase III. Samples were analyzed by 1, 2 % agarose electrophoresis with a 1 kbp DNA marker.

The specificity of RNase III was confirmed by using RNA 40 (a ssRNA). Since RNA 40 contains 20 bp, it shows the right size for cleavage through RNase III. The minimal substrate for RNase III contains 11 base pairs (bp) (Drider et al. 1999; Pertzev and Nicholson 2006; Gan et al. 2008). The ethidium bromide staining (Figure 19 B) for the

either mock- or RNase III-treated ssRNA 40 shows no differences. Furthermore, the IFN-α-inducing activity of RNA 40 was not abolished upon RNase III treatment (Figure 19 A), showing that RNase III had no toxic effect on the immune cells.

The importance of different features of RNA for IFN-α secretion

Comparing the immunostimulatory capacity of the RNA prepared from virus-infected cells with the RIG-I ligand 5`-3P RNA in PBMC cells shows that both require different features for IFN-α secretion. After treatment of A/PR/8/MDCK-RNA and the RIG-I ligand 5`-3P RNA with either RNase III or CIP, the RNAs were complexed to DOTAP or Lipofectamine 2000 and used for stimulation of PBMC cells. In Figure 20, IFN-α induction was measured by ELISA, and the already described controls were used. For A/PR/8/MDCK-RNA complexed to DOTAP or Lipofectamine 2000, phosphatase treatment had no influence on the IFN-α inducing ability, but cleavage with the ds-specific RNase III abrogated IFN-α secretion in PBMC cells.

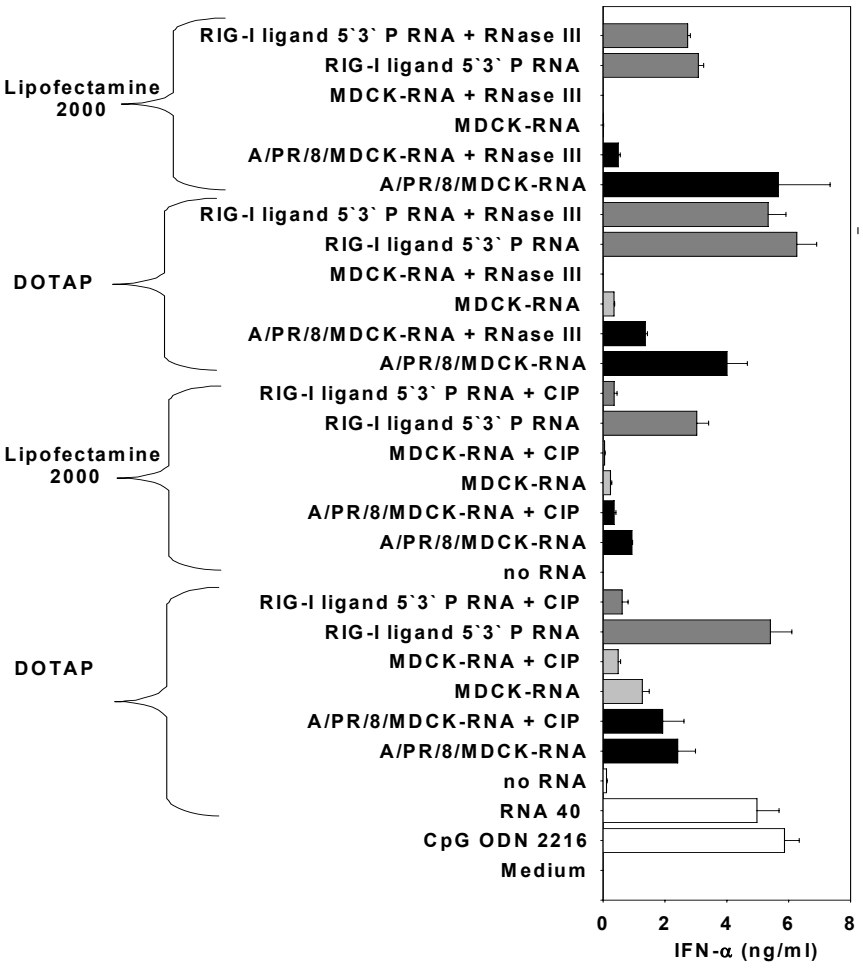

Figure 20: For the RIG-I ligand 5`-3P RNA the 5`-triphosphate end is important for recognition and the ds character has no influence. RNA from uninfected and A/PR/8-infected MDCK cells (2 µg/ml) and RIG-I ligand 5`-3P RNA (0.2 µg/ml) were partially treated with CIP or RNase III, then complexed to DOTAP or Lipofectamine 2000 and used for stimulation of PBMC cells. IFN-α production was measured 24 hours post stimulation by ELISA (n = 2, one representative experiment is shown). CpG 2216 (1µM) and RNA 40 served as positive controls.

In summary, for recognition of the virus-infected RNA the ds character is important. In contrast, for the RIG-I ligand 5`-3P RNA complexed to DOTAP or Lipofectamine 2000, only the 5`-triphosphate seems to be important, whereas treatment with the ds-specific RNase III has no influence for IFN-α secretion.

5.2.5. Analysis of the receptor recognizing the A/PR/8/MDCK-RNA

A previous study demonstrated the requirement of TLR7/MyD88 for the recognition of ssRNA viruses like the influenza virus in pDCs (Diebold et al. 2004; Lund et al. 2004). On the other hand, it was shown that genomic RNA prepared from a negative-strand RNA virus and RNA prepared from virus-infected cells triggered a potent IFN-α response in a phosphatase-sensitive manner in monocytes. 5`-triphosphate RNA directly binds to RIG-I (Hornung et al. 2006). To address the question of whether there is a TLR dependency for the recognition of A/PR/8/MDCK-RNA, we analyzed the immune activation of Flt3-derived dendritic cells and GM-CSF-derived dendritic cells from corresponding gene-deficient mice (TLR7 $^{-/-}$, Myd88 $^{-/-}$) (4.1.9.1). Flt3-derived dendritic cells can be regarded as analogs to human plasmacytoid dendritic cells. TLR7 and TLR9 expressed in pDCs act via a unique pathway to induce IFN-α. Positive controls for IFN-α induction in Flt3-derived dendritic cells were the TLR ligands RNA 40 and CpG 2216. The TLR7-specific control RNA 40 showed no IFN-α secretion in TLR7 $^{-/-}$ and MyD88 $^{-/-}$ cells. The TLR9-specific control CpG 2216 induced no IFN-α in MyD88 $^{-/-}$ cells, whereas for wild-type and TLR7 $^{-/-}$ cells IFN-α was detectable. The control RIG-I ligand 5`-3P RNA showed IFN-α secretion for wild-type, TLR7 $^{-/-}$ and MyD88 $^{-/-}$ cells. GM-CSF-derived dendritic cells can be regarded as analogs to human myeloid dendritic cells. In GM-CSF-derived dendritic cells, IFN-α production is mediated by cytosolic helicases and not as described for pDCs, via a unique pathway of TLR7 and TLR9. For this reason, upon stimulation with the TLR7-specific control RNA 40 and with the TLR9-specific control CpG 2216, there was no IFN-α secretion detectable in GM-CSF-derived DCs. But RNA 40 and CpG 2216 induced IL-6 in GM-CSF-derived DCs. The TLR9-specific control CpG 2216 showed no IL-6 secretion in MyD88 $^{-/-}$ cells, whereas for wild-type cells IL-6 was detectable. Upon transfection of equal concentrations of encapsulated A/PR/8/MDCK-RNA complexed to cationic transfection reagents or cathelicidins, a strong induction of IFN-α secretion was detected in wild-type and knockout dendritic cells from Flt3- and GM-CSF-derived dendritic cells, whereas for MDCK-RNA no IFN-α response was detectable. The results suggest that there is no TLR dependency for the recognition of A/PR/8/MDCK-RNA in murine immune cells (Figure 21).

A)

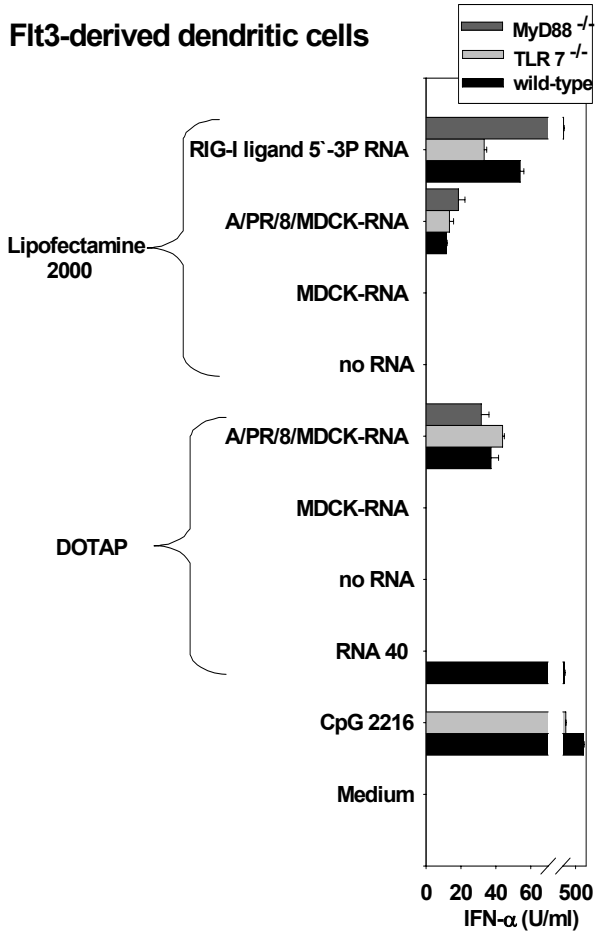

B)

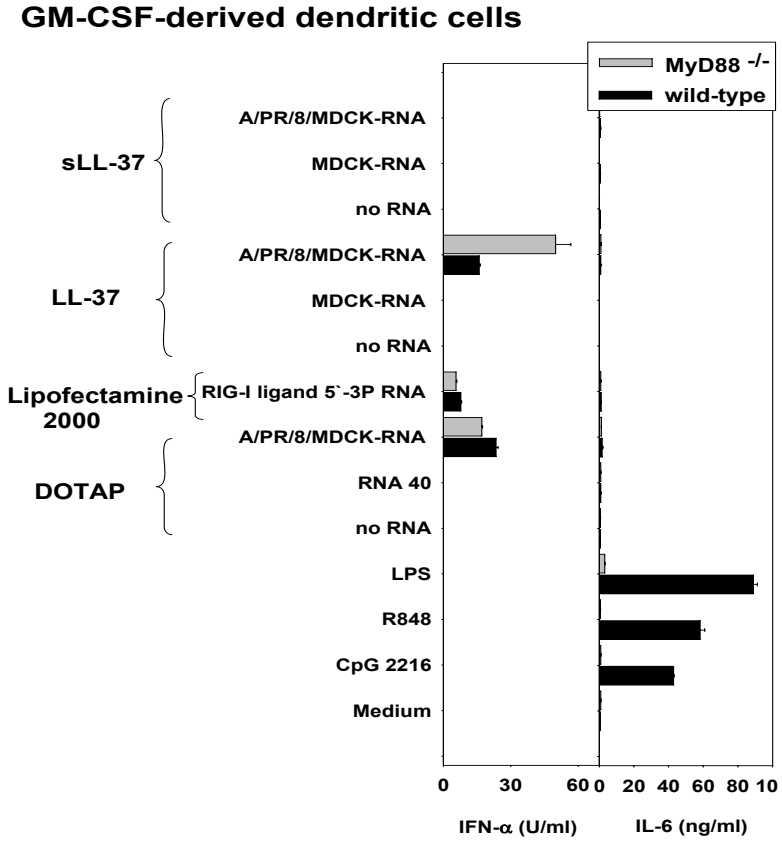

Figure 21: No influence of TLRs for the recognition of A/PR/8/MDCK-RNA. A) Uninfected and A/PR/8/MDCK-RNA (2 µg/ml) was complexed to DOTAP or Lipofectamine 2000 and used for stimulation of Flt3-derived dendritic cells generated from a wild-type, a TLR7- and a MyD88-deficient mouse, respectively. RNA 40, CpG 2216, and the RIG-I ligand 5`-3P RNA (0,2 µg/ml complexed to Lipofectamine 2000) served as specificity controls for the respective knockout cells. IFN-α secretion was measured 24 hours post stimulation by ELISA (for TLR7 n = 8, for MyD88 n = 4; one representative experiment is shown). B) 10 µg of total RNA from uninfected or A/PR/8-infected MDCK cells was complexed to 50 µg LL-37 and used for stimulation of GM-CSF- derived dendritic cells generated from a wild-type and a MyD88-deficient mouse at a final RNA concentration of 10 µg/ml. CpG 2216 and the RIG-I ligand 5`-3P RNA (0,2 µg/ml complexed to Lipofectamine 2000) served as specificity controls for the respective knockout cells. For comparison, A/PR/8/MDCK-RNA (2 µg/ml) was complexed to DOTAP. IFN-α and Il-6 secretion was measured 24 hours post stimulation by ELISA (for GM-CSF cultures n = 2, for macrophages n = 2; one representative experiment is shown).

To investigate whether TLR3, which utilizes the TRIF adaptor protein and not MyD88, is important for recognition of A/PR/8/MDCK-RNA, we generated macrophages from wild-type, TLR7- and TLR7&3 double-deficient mice (4.1.9.1). TLR3 is claimed to be important for Poly I:C detection (McCartney et al. 2009). Poly I:C is a synthetic dsRNA clinically applied as an immunomodulator (Verdijk et al. 1999). Because the specificity control Poly I:C did not work in our murine system, mice deficient for TLR3 were genotyped and confirmed for TLR3 deficiency (data not shown). Macrophages were stimulated as described in section 5.1, and the supernatants were used for detection of the cytokines IFN-ß, IFN-α, and IL-6 by ELISA as shown in Figure 22. In macrophages, IFN-α production is mediated by cytosolic helicases and not as described for pDCs via a unique pathway of TLR7 and TLR9. For this reason, upon stimulation with the TLR7-specific control RNA 40 and with the TLR9-specific control CpG 2216, there was no IFN-α secretion detectable in macrophages. But RNA 40 and CpG 2216 induced IL-6 in macrophages. LPS induced an IFN-ß response in a TRIF-dependent pathway in macrophages.

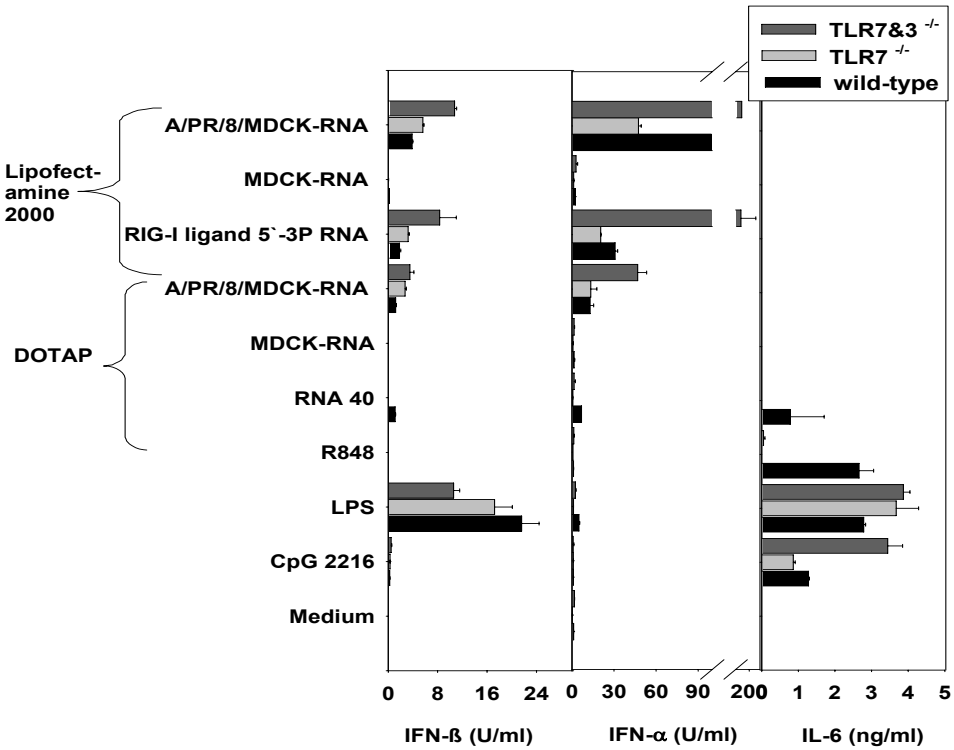

Figure 22: No influence of TLR3 for the recognition of A/PR/8/MDCK-RNA. Uninfected and A/PR/8/MDCK-RNA (2 µg/ml) was complexed to DOTAP or Lipofectamine 2000 and used for stimulation of macrophages generated from a wild-type, a TLR7- and a TLR7&3 double-deficient mouse, respectively. RNA 40, CpG 2216, R848, LPS, and the RIG-I ligand 5`-3P RNA (0,2 µg/ml complexed to Lipofectamine 2000) served as controls for cytokine secretion. Cytokines were measured 24 hours post stimulation by ELISA (for macrophages n = 2; for Flt3 cultures n = 4; one representative experiment is shown).

Upon transfection of equal concentrations of encapsulated A/PR/8/MDCK-RNA complexed to either DOTAP or Lipofectamine 2000, a strong induction of IFN-α and IFN-ß was detected in wild-type and in the TLR7- and TLR7&3 double-deficient macrophages, whereas for uninfected MDCK-RNA no type-I IFN response was detectable. These results further demonstrate that there is no TLR dependency for the recognition of A/PR/8/MDCK-RNA in murine immune cells.

Moreover, we used Flt3-derived dendritic cells from IPS-deficient mice, which is an important adaptor molecule for RIG-I or MDA-5 signaling, in order to investigate if RIG-I or MDA-5 are involved in the recognition of the A/PR/8/MDCK-RNA. Positive controls for IFN-α induction were the TLR ligands RNA 40 and CpG 2216. The ELISA data in Figure 23 show that the control RIG-I-ligand 5`-3P RNA failed to induce IFN-α in the respective knockout cells, whereas the TLR9-specific control CpG 2216 and the TLR7-specific control RNA 40 showed equal amounts of secreted IFN-α in wild-type compared to IPS $^{-/-}$ cells. In IPS $^{-/-}$ dendritic cells, IFN-α secretion upon transfection with A/PR/8/MDCK-RNA complexed to the cationic transfection reagents or to the cathelicidins was abrogated, indicating that either RIG-I or MDA-5 are responsible for recognizing the A/PR/8/MDCK-RNA.

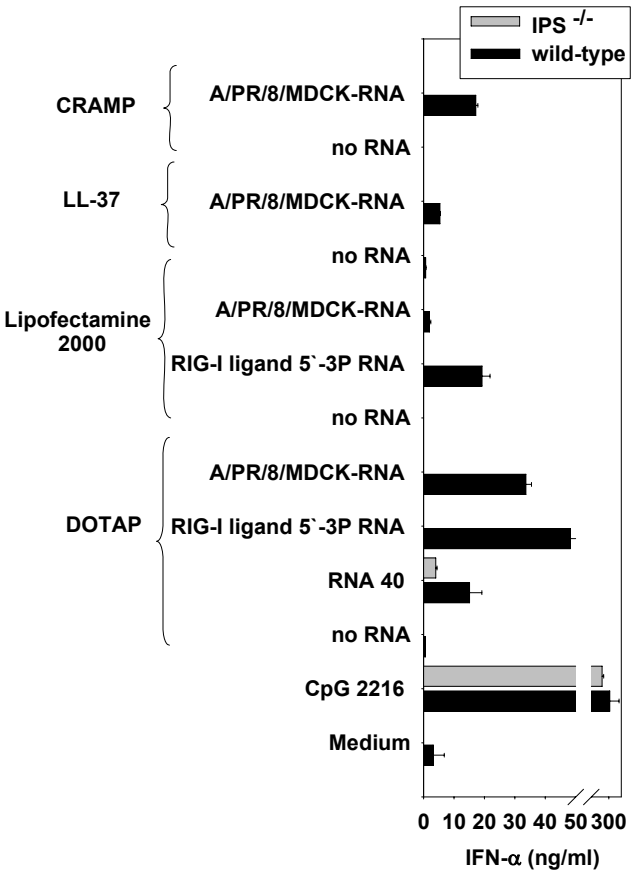

Figure 23: Relevance of IPS-dependent receptors for the recognition of A/PR/8/MDCK-RNA. RNA from A/PR/8-infected cells (2 µg/ml) was encapsulated with DOTAP or Lipofectamine 2000 and used for stimulation of Flt3-derived dendritic cells generated from a wild-type, a TLR7- and an IPS-deficient mouse, respectively. In addition, 10 µg of total RNA from uninfected or A/PR/8-infected MDCK cells was complexed to 50 µg LL-37 or CRAMP and used for stimulation of murine Flt3-derived dendritic cells at a final RNA concentration of 10 µg/ml. RNA 40, CpG 2216, and the RIG-I ligand 5`-3P RNA (2 µg/ml) served as specificity controls for the respective knockout cells. IFN-α secretion was measured 24 hours post stimulation by ELISA (A/PR/8/MDCK-RNA complexed to cationic transfection reagents for Flt3 cultures: n = 2 / A/PR/8/MDCK-RNA complexed to cathelicidins for Flt3 cultures n = 3, for GM-CSF cultures n = 1, for BM cultures n = 1; one representative experiment is shown).

To analyze whether MDA-5 is involved in the recognition of A/PR/8/MDCK-RNA, we used Flt3-derived dendritic cells and bone marrow-generated cells from MDA-5-deficient mice. MDA-5 is described to be important for Poly I:C detection (McCartney et al. 2009). Because the specificity control Poly I:C did not work in our murine system, mice deficient for MDA-5 were genotyped and confirmed for MDA-5 deficiency (data not shown). Positive controls for IFN-α induction were the TLR ligands RNA 40 and CpG 2216. IFN-α secretion upon transfection with A/PR/8/MDCK-RNA complexed to cationic transfection reagents or to cathelicidins was not abrogated in MDA-5-deficient mice (Figure 24), indicating that MDA-5 is not involved in the recognition of A/PR/8/MDCK-RNA. These results suggest that an IPS-dependent receptor is responsible for recognition of A/PR/8/MDCK-RNA with a strong evidence for RIG-I. Because a RIG-I-deficient mouse was not available, we could not prove an involvement of RIG-I in the murine system.

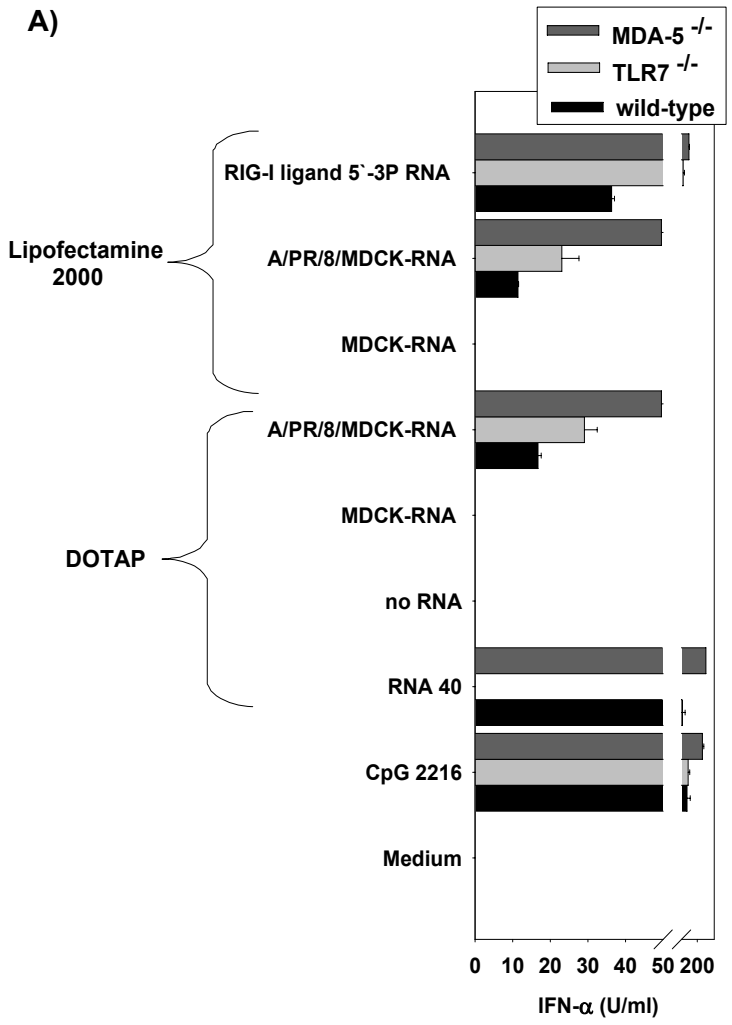

Figure 24: Relevance of IPS-dependent receptors and MDA-5 for the recognition of A/PR/8/MDCK-RNA. A) RNA from uninfected and A/PR/8-infected cells (2 µg/ml) was encapsulated with DOTAP or Lipofectamine 2000 and used for stimulation of Flt3-derived dendritic cells generated from a wild-type, a TLR7- and a MDA-5-deficient mouse, respectively. RNA 40, CpG 2216, and the RIG-I ligand 5`-3P RNA (0.2 µg/ml) served as controls for IFN-α secretion. IFN-α secretion was measured 24 hours post stimulation by ELISA (for TLR 7 n = 8, for MDA-5 n = 1; one representative experiment is shown).

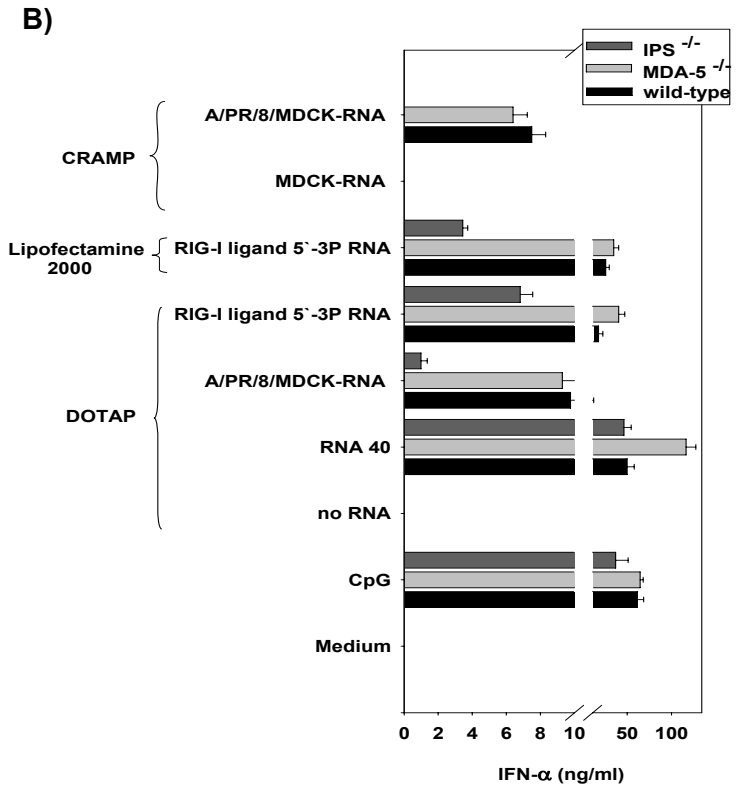

Figure 24: Relevance of IPS-dependent receptors and MDA-5 for the recognition of A/PR/8/MDCK-RNA. B) 10 µg of total RNA from uninfected or A/PR/8-infected MDCK cells was complexed to 50 µg LL-37 or CRAMP and used for stimulation of murine bone marrow cells generated from a wild-type, an IPS- and a MDA-5-deficient mouse at a final RNA concentration of 10 µg/ml. The RIG-I ligand 5`-3P RNA (2 µg/ml complexed to Lipofectamine 2000) served as specificity control for the respective knockout cells. IFN-α secretion was measured 24 hours post stimulation by ELISA (for Flt3 cultures n = 1, for BM cultures n = 1; one representative experiment is shown).

To confirm the RIG-I-dependent detection of A/PR/8/MDCK-RNA, human HEK293 cells, which lack functional TLRs (with the possible exception of TLR3), were transfected with plasmids encoding RIG-I and MDA-5 (4.12) (Yoneyama et al. 2004; Yoneyama et al. 2005). The normally MDA-5-specific ligand Poly I:C was found to show enhanced IFN-ß activation in RIG-I-transfected cells, but when complexed to Lipofectamine 2000 there was little detectable increase in IFN-ß reporter activity in MDA-5-transfected cells. The question arises as to whether or not our MDA-5 is functional. Cells were transfected with MDCK-RNA and A/PR/8/MDCK-RNA, and IFN-ß activation was determined by Dual Luciferase Assay. Surprisingly, strong IFN-ß activation for A/PR/8/MDCK-RNA complexed to DOTAP or Lipofectamine 2000 was observed in untransfected cells (Figure 25). This activation by A/PR/8/MDCK-RNA, possibly observed due to the basal expression of RIG-I in untransfected HEK293 cells, was significantly enhanced in RIG-I-transfected HEK293 cells. We performed a PCR to determine endogenous expression of RIG-I in HEK293 cells (4.4). Therefore, total HEK293-RNA was assigned in cDNA. We performed one reaction by using the enzyme reverse transcriptase and one without this enzyme. To prevent amplification of genomic DNA, which has a large number of introns, the primers were designed as exon-intron spanning primers. Figure 25 C shows that HEK293 cells expressed endogenous RIG-I having a length of 530 bp. As expected, for the negative sample in which we used no enzyme, there was no PCR product detectable.

MDA-5-transfected cells showed for A/PR/8/MDCK-RNA complexed to DOTAP or Lipofectamine 2000 only a comparable IFN-ß activation like untransfected cells. For the respective RIG-I-specific control RIG-I ligand 5`-3P RNA complexed to Lipofectamine 2000, there was no IFN-ß activation in untransfected HEK293 cells, whereas in RIG-I-transfected HEK293 cells, there was a strong IFN-ß activation. In untransfected HEK293 cells, the immune response to A/PR/8/MDCK-RNA was abrogated after dephosphorylation and RNase III treatment, whereas in RIG-I-transfected HEK293 cells, CIP treatment of A/PR/8/MDCK-RNA had no influence, but RNase III treatment again abolished the IFN-α response. For the RIG-I ligand 5`-3P RNA complexed to Lipofectamine 2000, the IFN-α response was diminished in RIG-I-transfected cells upon CIP treatment.

To further show that A/PR/8/MDCK-RNA complexed to LL-37 was recognized in an IPS-dependent way, HEK293 cells were transfected with plasmids encoding for RIG-I and MDA-5. RIG-I-expressing HEK293 cells gained responsiveness to the RIG-I-specific control RIG-I ligand 5`-3P RNA complexed to Lipofectamine 2000. The A/PR/8/MDCK-RNA complexed to DOTAP or Lipofectamine 2000 was also recognized in RIG-I-transfected HEK293 cells. However upon stimulation with A/PR/8/MDCK-RNA complexed to LL-37 or CRAMP, no enhanced IFN-ß activation was detectable.

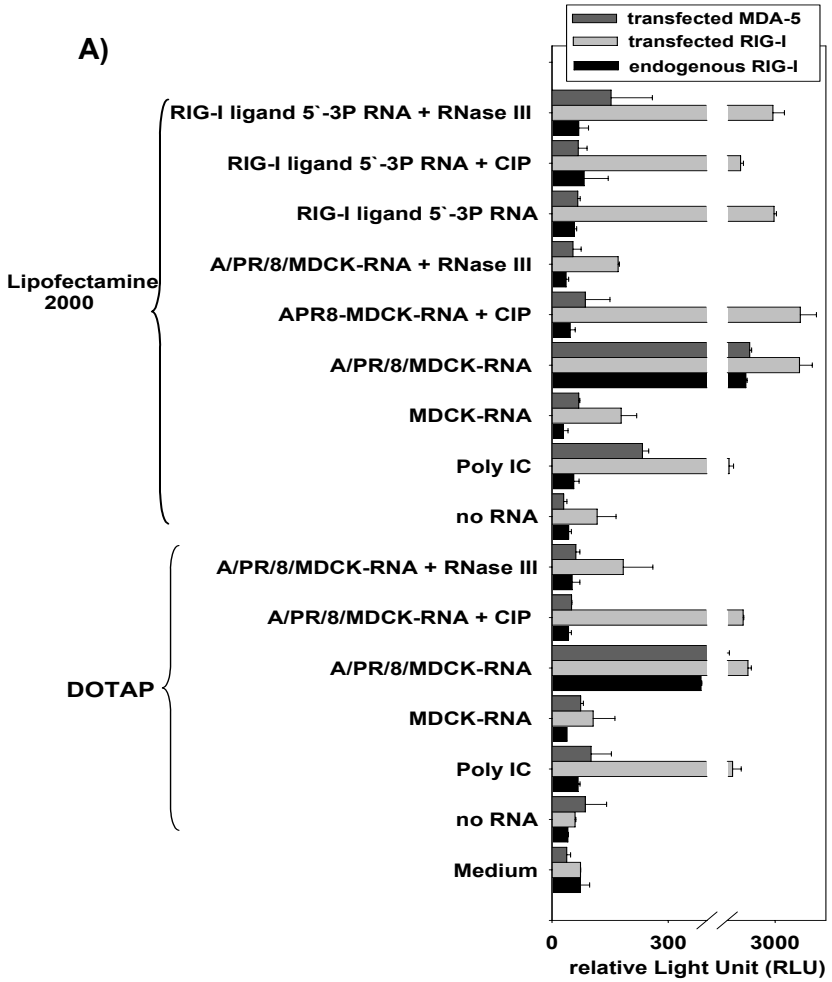

Figure 25: RIG-I-mediated recognition of RNA from A/PR/8-infected cells in non-immune cells. A) HEK293 cells were cotransfected with plasmids encoding the IFN-ß luciferase reporter construct (p125Luc), RIG-I and MDA-5 by electroporation. Transfected cells were treated with Poly IC (10 µg/ml), RNA from uninfected and A/PR/8-infected MDCK cells (2 µg/ml) and RIG-I ligand 5`-3P RNA (0.2 µg/ml) each complexed to DOTAP or Lipofectamine 2000 (either mock-, CIP- or RNase-III-treated). IFN-ß activation was determined by Dual Luciferase Assay (n = 10 for DOTAP and Lipofectamine 2000, one representative experiment is shown).

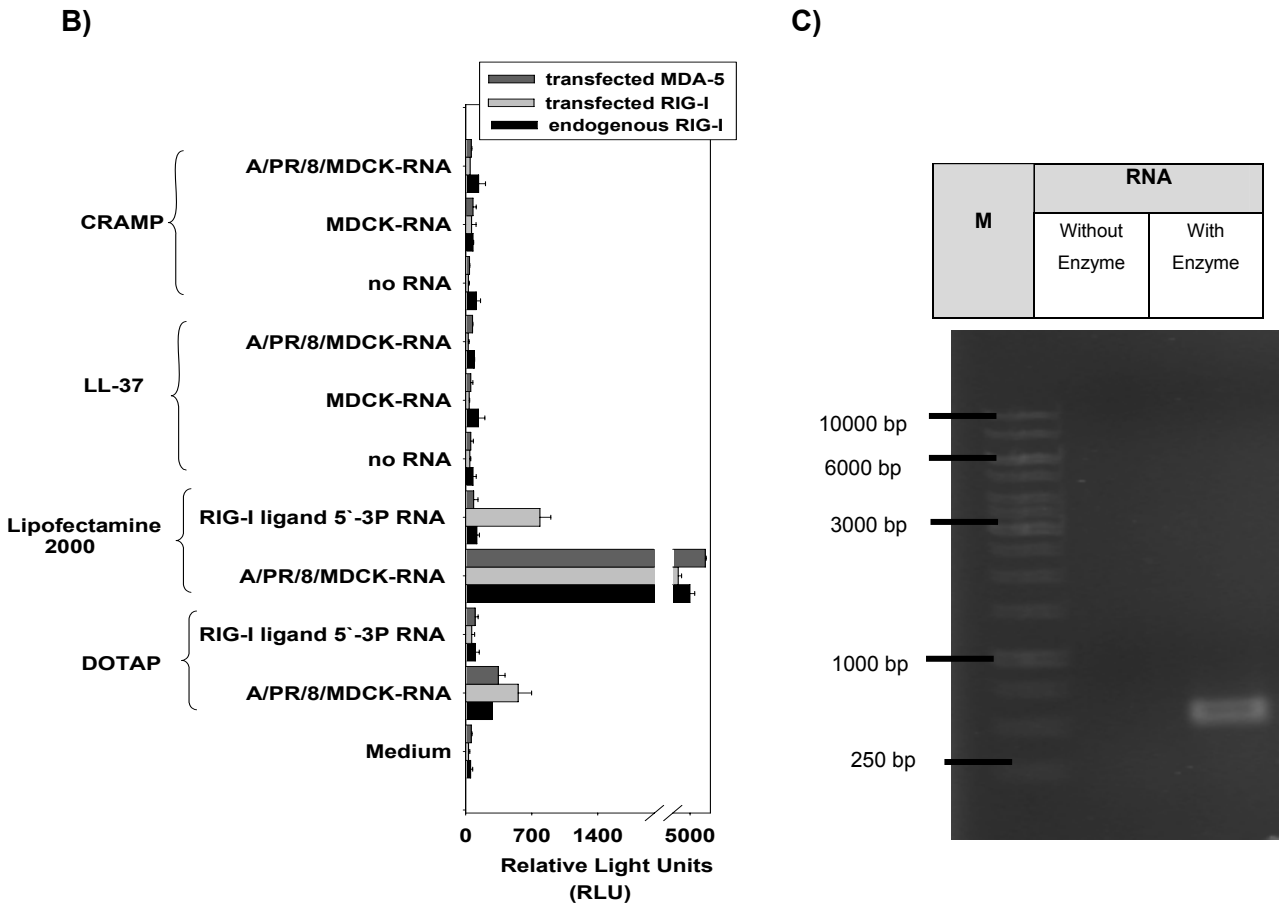

Figure 25: RIG-I-mediated recognition of RNA from A/PR/8-infected cells in non-immune cells. B) HEK293 cells were cotransfected with plasmids encoding the IFN-ß luciferase reporter construct (p125Luc), RIG-I and MDA-5 by electroporation. Transfected cells were treated with uninfected and A/PR/8/MDCK-RNA (2 µg/ml) each complexed to LL-37 and CRAMP. IFN-ß activation was determined by Dual Luciferase Assay (n = 3 for LL-37 and CRAMP, one representative experiment is shown).C) Ethidium bromide staining of a PCR of cDNA rewrited from HEK293-RNA to determine endogenous expression of RIG-I on an 1, 2 % agarose gel. Marker lane contains a 1 kbp DNA marker.

The results obtained by stimulating Flt3-derived dendritic cells from IPS-deficient mice and HEK293 cells overexpressing RIG-I with A/PR/8/MDCK-RNA complexed to cationic lipids or natural carriers and the phosphatase-dependent induction of IFN-α by A/PR/8/MDCK-RNA indicate that RIG-I or a yet unidentified IPS-dependent receptor is responsible for the recognition of A/PR/8/MDCK-RNA.

5.2.6. Influence of the length of antimicrobial peptides for the immunostimulatory ability

In comparison to the long CRAMP version, the shorter CRAMP version failed to induce IFN-α in complex with the A/PR/8/MDCK-RNA. We tested murine Flt3-derived dendritic cells with the different CRAMP versions (Figure 26) complexed to A/PR/8/MDCK-RNA and measured the IFN-α induction (Figure 27). This suggests that a certain length of the peptide is necessary for complexation of A/PR/8/MDCK-RNA in order to induce IFN-α in immune cells.

CRAMP1-39 **ISRLAGLLRKGGEKIGEKLKKIGQKIKNFFQKLVPQPEQ**

CRAMP **GLLRKGGEKIGEKLKKIGQKIKNFFQKLVPQPEQ**

Figure 26: Sequences of the different CRAMP versions. Shown are the sequences from the long CRAMP version (upper sequence) and the short CRAMP version (lower sequence).

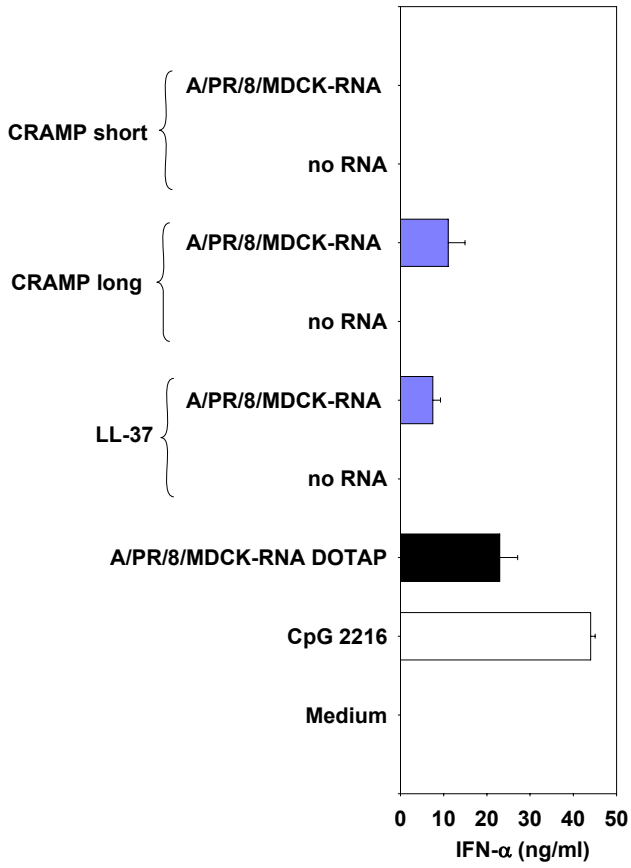

Figure 27: Influence of the length from CRAMP for complexation of A/PR/8/MDCK-RNA. 10 µg of total RNA from uninfected or A/PR/8-infected MDCK cells was complexed to 50 µg LL-37, CRAMP short or CRAMP long version and used for stimulation of murine Flt3-derived dendritic cells generated from a wild-type mouse at a final RNA concentration of 10 µg/ml. IFN-α secretion was measured 24 hours post stimulation by ELISA (n = 3, one representative experiment is shown).

5.2.7. Characterization of synthetic LL-37/CRAMP as carrier for immunostimulatory RNA

5.2.7.1. Localization studies of RNA/LL-37 complexes

We performed localization studies of RNA/LL-37 complexes in human monocytes using biotinylated LL-37 (4.8). These experiments demonstrate that LL-37 complexes localize to the endosome (EEA-1 positive) and to the lysosome (Lamp positive) (Figure 28). The use of Lamp showed a colocalization for the A/PR/8/MDCK-RNA complexed to biotinylated LL-37 to the lysosomes. A problem with the use of the lysotracker is that the lysotracker alone did not really stain lysosomes, but rather only in combination with A/PR/8/MDCK-RNA. For the use of EEA1, we first tested the secondary antibody rhodamine alone on the cells, in order to exclude an unspecific binding. The addition of biotinylated LL-37 with A/PR/8/MDCK-RNA seemed to show colocalization. One problem with this system is that the secondary antibody rhodamine also seemed to detect the biotinylated LL-37, or it bound unspecifically to the cells. Another marker for the early endosome was transferrin. But under the employed conditions, we were not able to detect a staining of the endosomes.

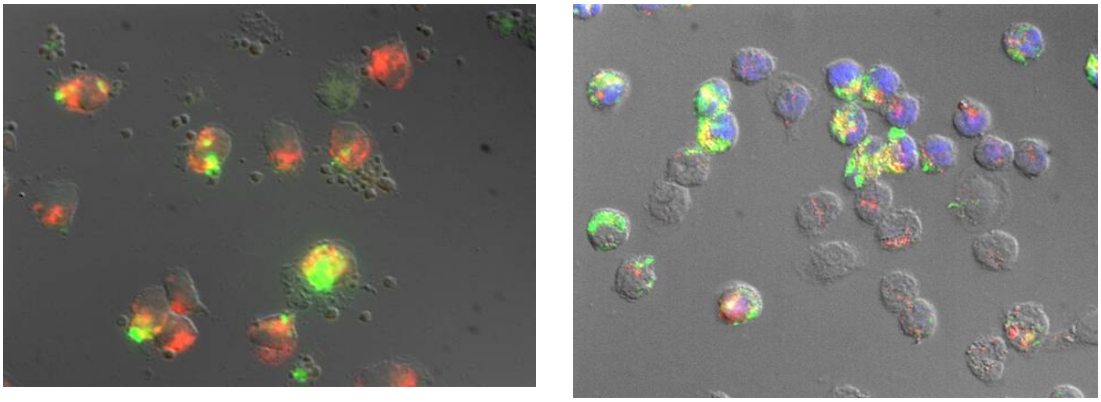

Figure 28: Fluorescence microscopy of human primary monocytes (enriched by counter flow centrifugation) and incubated with biotinylated LL-37 complexed to RNA isolated from A/PR/8-infected MDCK cells for 1h. (A) Cells were fixed and stained with DAPI and an antibody against EEA-1 followed by a secondary Rhodamine-labeled antibody and streptavidin-FITC. (B) Cells were fixed and stained with DAPI and an antibody against Lamp-1 followed by a secondary Rhodamine-labeled antibody and streptavidin-FITC.

5.2.8. Immunization of mice

Previous studies have shown the adjuvant function of RNA complexed to the cationic transfection reagent DOTAP. RNA induces the secretion of proinflammatory cytokines and type-I IFN and works as an adjuvant for the induction of cytotoxic T cells and antigen specific antibodies after subcutaneous immunization (Heil et al. 2004; Hamm et al. 2007). Others have used *in vitro* transcribed mRNAs coding for the antigen of choice complexed with protamine to induce cell-mediated and humoral immune responses (Scheel et al. 2006; Probst et al. 2007).

Because RNA is prone to hydrolysis, RNA molecules have to be protected from degradation through interaction with liposomes. Since DOTAP is toxic, we analyzed whether cathelicidins could function as a carrier in vaccine formulations. Cathelicidins have potent *in vivo* immunoenhancing effects that make them useful as vaccine adjuvants. They enhance antigen-specific humoral and cellular responses. CRAMP can enhance antigen-specific immune response to ovalbumin, a commonly used experimental model antigen (Kurosaka et al. 2005).

In the present study, we analyzed whether a mixture of RNA combined with ovalbumin complexed to CRAMP (4.11) might function as vaccine formulation in subcutaneous injections in the base of tails from mice (Figure 29). Mice were immunized with 100 µg ovalbumin, 100 µg RNA complexed to DOTAP or 40 µg RNA complexed to 200 µg CRAMP on day 1 and were boosted on day 21. Injections with DOTAP/Ovalbumin and CRAMP/Ovalbumin containing no RNA or solely buffer served as negative controls. In parallel, immunizations with CpG-DNA 1668 were performed to compare the adjuvant capacity of RNA.

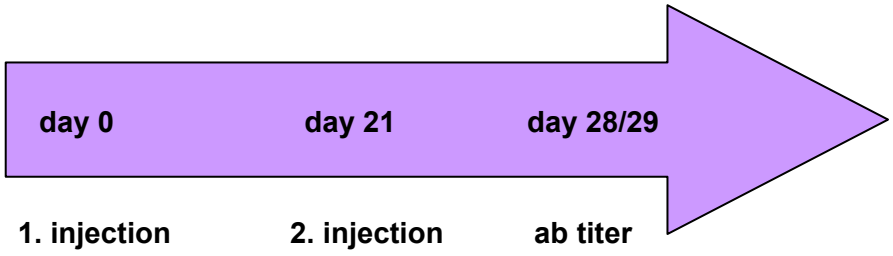

Figure 29: Injection scheme and anticipated analysis

The RNA-driven humoral response was analyzed by measuring the induction of ovalbumin-specific IgG antibodies (4.11.1.2) in the sera of immunized mice 1 week after the second injection.

As expected, CpG-DNA 1668 induced ovalbumin-specific IgG antibodies, although even injections of DOTAP/Ovalbumin induced ovalbumin-specific IgG antibodies. In combination with MDCK-RNA and A/PR/8/MDCK-RNA there was a little increase in the ovalbumin-specific IgG antibody response detectable for serum dilutions 1/3000 and 1/30000 (Figure 30).

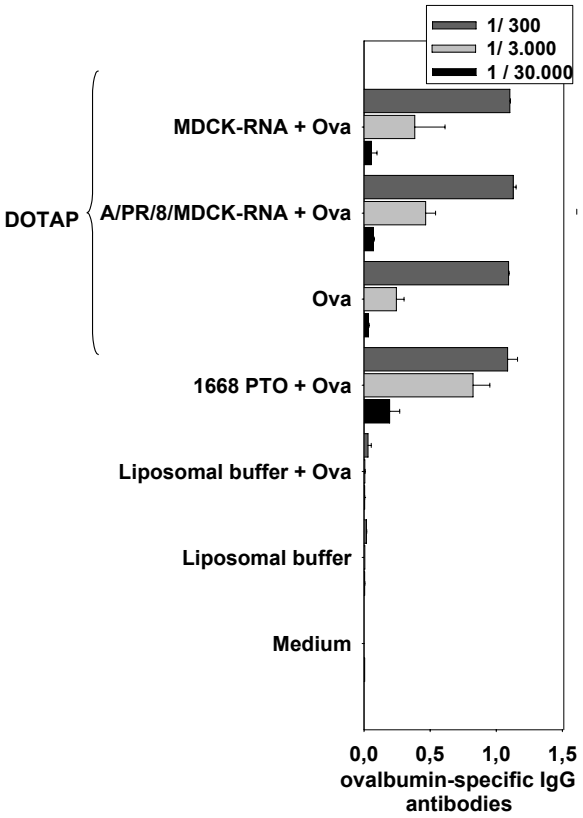

Figure 30: DOTAP enhancement of ovalbumin-specific humoral immune response. Serum samples were collected from mice after immunization. Total ovalbumin-specific IgG antibodies were measured by ELISA (n = 1, one representative experiment is shown). Depicted are the average ovalbumin-specific IgG antibody titers of each group (n = 2).

As expected, immunization of ovalbumin together with CRAMP enhanced ovalbumin-specific IgG antibody responses as compared to the immunization with ovalbumin alone. In combination with MDCK-RNA or A/PR/8/MDCK-RNA, there was an increase in the ovalbumin-specific IgG antibody response detectable for serum dilutions 1/3000 and 1/30000 (Figure 31). Regarding the high standard deviation for ovalbumin and CRAMP at

the dilution 1/300, the ovalbumin-specific IgG antibody response was difficult to compare with other stimuli. Future studies should analyze whether an increase in the IgG antibody response is measurable by varying the CRAMP concentration. For this experiment, we have chosen a similar CRAMP concentration (40 nmol = 176,77 µg) as proposed by Kurosaka et al. (Kurosaka et al. 2005).

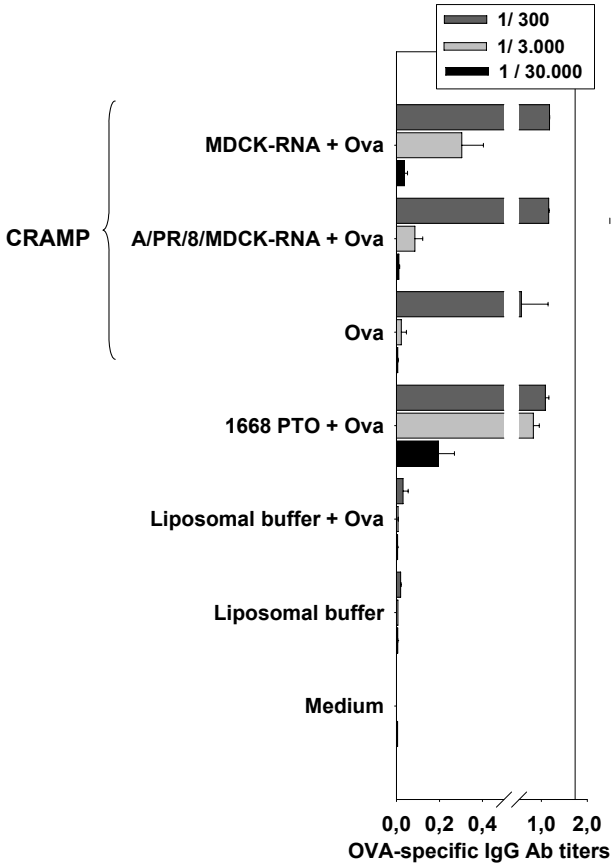

Figure 31: CRAMP enhancement of ovalbumin-specific humoral immune response. Serum samples were collected from mice after immunization. Total ovalbumin-specific IgG antibodies were measured by ELISA (n = 1, one representative experiment is shown). Shown are the average ovalbumin-specific IgG antibody titers of each group (n = 2).

5.2.9. Summary

Upon viral infection, LL-37 might form complexes with self-RNA and viral RNA. These complexes triggered a strong interferon production in human and murine immune cells. By using Flt3-derived dendritic cells from MyD88-deficient mice, TLRs were ruled out as being responsible for this reactivity. To further investigate the recognition mechanism, we generated Flt3-derived dendritic cells from IPS-deficient mice, which is an important adaptor molecule for RIG-I- and MDA-5-dependent signaling. We observed a strictly IPS-dependent IFN-α secretion upon transfection with A/PR/8/MDCK-RNA complexed to cationic lipids or cathelicidins. However, localization studies showed that LL-37 transfers nucleic acids to early endosomal/lysosomal compartments. The localization of LL-37 currently does not explain how endosomally delivered RNA triggers an IPS-1 dependent signaling pathway there. As found by Kurosaka et al., cathelicidins have potent *in vivo* immunoenhancing effects that make them useful as vaccine adjuvants (Kurosaka et al. 2005). Moreover, we analyzed whether CRAMP complexed to RNA functions as vaccine formulation in subcutaneous injections. In combination with differently tested RNAs, there was little detectable increase in the ovalbumin-specific IgG antibody response.

Our findings show that the 5`-triphosphate end of A/PR/8/MDCK-RNA is important for inducing IFN-α in murine immune cells and in human HEK293 cells. Dephosphorylation of the A/PR/8/MDCK-RNA reduced signaling, suggesting that RIG-I is responsible in Flt3-derived dendritic cells and in HEK293 cells for inducing IFN-α, and this was further demonstrated by using IPS-deficient mice. For human PBMC cells and HEK293 cells overexpressing RIG-I, we found only a small decrease in the IFN-α response after dephosphorylation. Here, the 5`-triphosphate end seems to play a minor role. Most important in this context is the observation that for A/PR/8/MDCK-RNA the ds character of RNA plays a major role for activation immune responses. For murine and human immune cells, we observed an abrogation for the IFN-α induction upon treatment with the ds-specific RNase III. Thus, for the ligand A/PR/8/MDCK-RNA, we see two important features for RIG-I signaling: the ds character and the 5`-triphosphate end.

5.3. Analysis of the immunostimulatory capacity of self-RNA

5.3.1. Comparing the immunostimulatory ability of RNA fragments generated by different techniques

5.3.1.1. Fragments generated by Ribonucleases

It has been suggested that small self-RNA fragments derived by RNase treatment be considered a non-self structure. In this study, we were interested in identifying the mechanism that explains how small self-RNA fragments are recognized by the innate immune system.

Recently, Malathi et al. have described a crucial role for 2`,5`-linked oligoadenylate (2-5A) activated RNase L in the degradation of self-RNA and the generation of stimulatory ligands of less than 200 nucleotides for MDA-5 and RIG-I (Malathi et al. 2007). We partly digested self-RNA with the ubiquitous RNase A (4.3.6) and generated fragments of 20 to 100 bp, which were visualized by ethidium bromide staining (Figure 32 B / Figure 34). These fragments were complexed to DOTAP or Lipofectamine 2000 and used for the stimulation of PBMC cells. The supernatants were used for detection of IFN-α by ELISA. The TLR ligands CpG 2216 and RNA 40 were taken as positive IFN-α inducers. Interestingly, the RNase A-treated self-RNAs complexed to the cationic transfection reagent DOTAP were able to mount a type-I interferon response in human PBMCs (Figure 32 A), whereas for untreated RNAs complexed to DOTAP there was no IFN-α response detectable.

A)

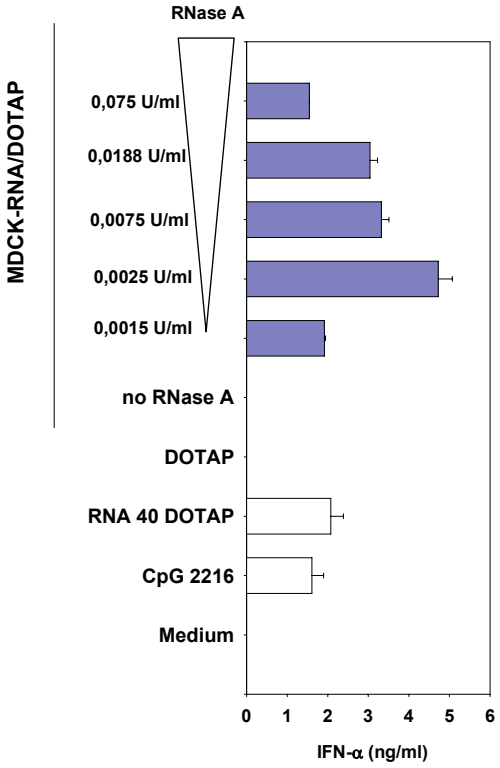

B)

RNA	M	MDCK-RNA				
RNase A [U/ml]	-	1,5 *10^{-3}	2,5 *10^{-3}	7,5 *10^{-3}	1,88* 10^{-2}	7,5* 10^{-2}

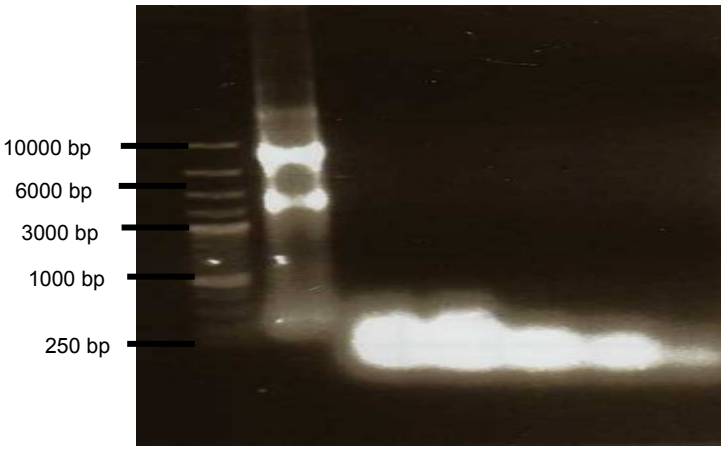

Figure 32: Effects of fragments generated by RNase treatment of self-RNA in human PBMCs. A) MDCK-RNA was treated with increasing amounts of RNase A complexed to DOTAP and used for stimulation of PBMC cells at a final concentration of 10 µg/ml. IFN-α production was measured 24 hours post stimulation by ELISA. CpG 2216 (1µM) and RNA 40 served as positive controls (n = > 10, one representative experiment is shown). B) Ethidium bromide staining of untreated total MDCK-RNA and partially RNase A-treated MDCK-RNA separated on an 1, 2 % agarose gel. Marker lane contains a 1 kbp DNA marker.

Influence of the transfection reagent for the immunostimulatory ability of RNA fragments

The RNase A-treated self-RNAs complexed to DOTAP induced IFN-α in human PBMCs, whereas for complexation to Lipofectamine 2000, no IFN-α response was detectable (Figure 33 A). RNase A-derived fragments complexed to DOTAP induced IFN-α in a concentration range of 5-10 µg/ml. For untreated RNAs complexed to DOTAP, there was also a background IFN-α response detectable in a concentration range of 1-2 µg/ml.

In addition, we tested whether RNase A-derived fragments complexed to cathelicidins like LL-37 (presented in section 5.2) induced an immune activation in human PBMC cells. As shown in Figure 33 B, there was no IFN-α response detectable.

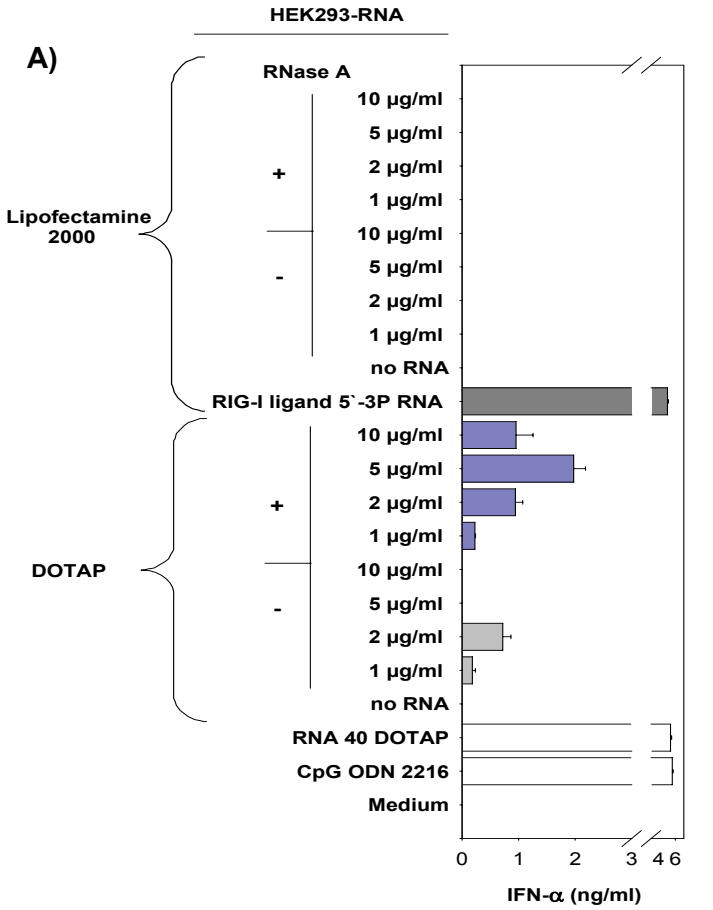

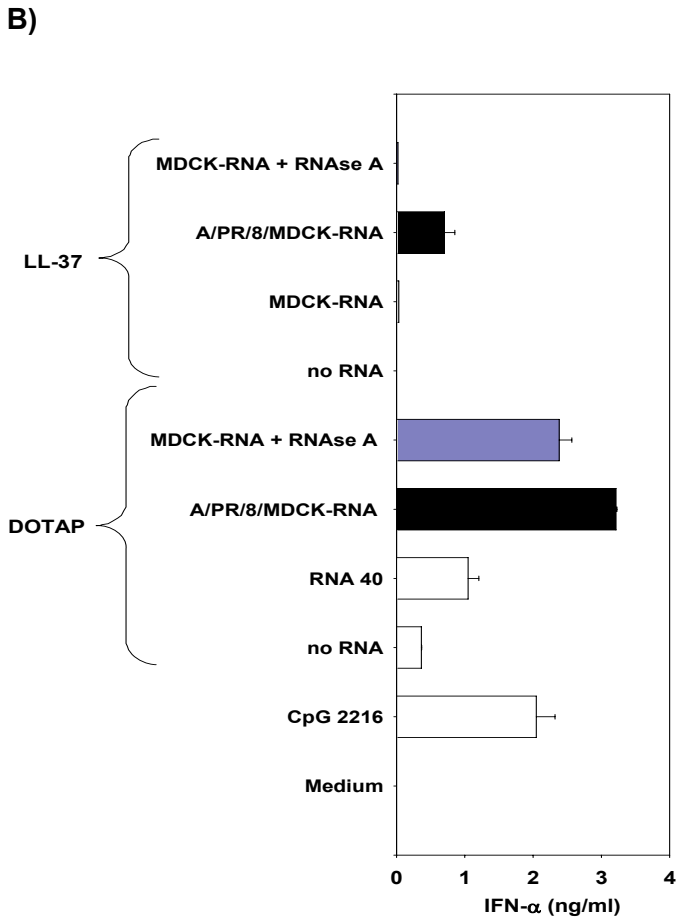

Figure 33: Influence of the transfection reagent for RNase A- derived fragments in human PBMC cells. A) HEK293-RNA was treated with RNase A and complexed to DOTAP or Lipofectamine 2000 and then used for stimulation of PBMC cells at different final RNA concentrations. RIG-I ligand 5`-3P RNA (0.2 µg/ml) complexed to Lipofectamine 2000 served as positive control for the transfection reagent Lipofectamine 2000 in human PBMC cells. IFN-α production was measured 24 hours post stimulation by ELISA. CpG 2216 (1µM) and RNA 40 served as positive controls for IFN-α secretion (n = 3, one representative experiment is shown). B) RNase A-derived fragments were complexed to LL-37 and used for stimulation of PBMC cells at 10 µg/ml final RNA concentration. IFN-α production was measured 24 hours post stimulation by ELISA. CpG 2216 (1µM) and RNA 40 served as positive controls (n = 4, one representative experiment is shown).

Size of RNase A generated fragments

With the help of a PAA gel (4.2.1), we further characterized the size of the fragments generated by RNase treatment of self-RNA. For this, we compared the size of the RNase-derived fragments with the size of RNA 40 (containg 20 bp) and RIG-I ligand 5`-3P RNA (containg 100 bp). In Figure 34, we see a smear of degradation fragments, showing a size in the range from < 20 bp to 100 bp.

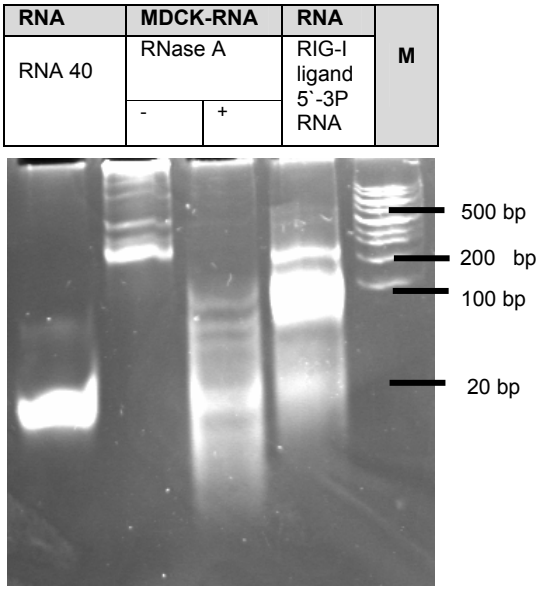

Figure 34: Analysis of degradation fragments by PAA gel electrophoresis. Marker lane contains a 100 bp marker.

Time dependence for generating immunostimulatory fragments by RNase A treatment

For a more detailed analysis of the fragments derived by RNase A treatment, we performed a kinetic analysis. Surprisingly, even after treatment of self-RNA with RNase A (4.3.6) for only one minute followed by phenol/chloroform extraction (4.2.5), there was a strong IFN-α-inducing activity when the fragments were complexed to DOTAP and used for stimulation of human PBMC cells (Figure 35 A). As a positive and negative IFN-α inducer, the same samples were chosen as described in section 5.3.1.1. The ethidium bromide staining shows that with the increase of time for incubation with RNase A the degradation of the self-RNA became more and more complete (Figure 35 B), whereas the

IFN-α induction is the same for the fragments generated by RNase A treatment at different times.

A)

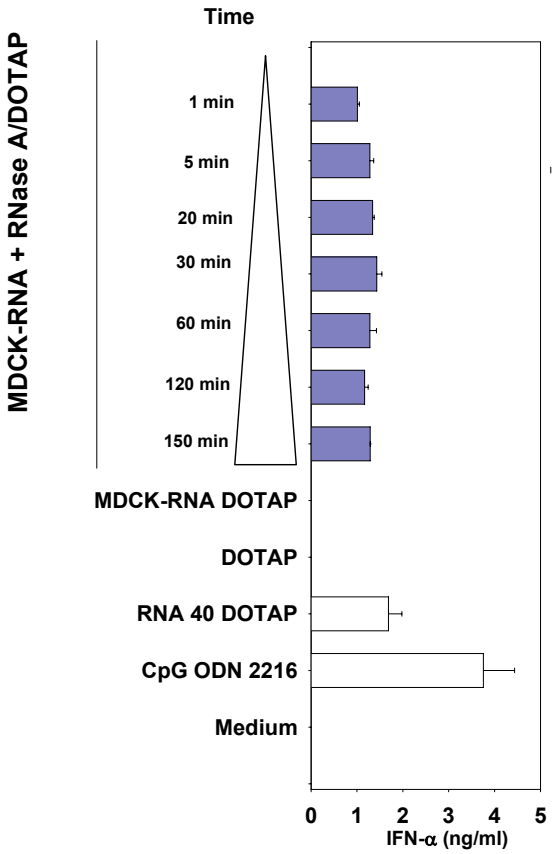

Figure 35: Influence of the time on the generation of immunostimulatory RNA fragments. A) Self-RNA was partially treated for different lengths of time with RNase A (0.0075 U/ml) complexed to DOTAP and used for stimulation of PBMC cells at a final RNA concentration of 10 µg/ml. IFN-α production was measured 24 hours post stimulation by ELISA (n = 4, one representative experiment is shown). CpG 2216 (1µM) and RNA 40 served as positive controls. B) At variable time intervals, RNase A-treated self-RNAs were analyzed by ethidium bromide staining. Treatment with RNase A is stopped by phenol/chloroform cleanup. RNAs are separated on an 1, 2 % agarose gel. Marker lane contains a 1 kbp DNA marker.

B)

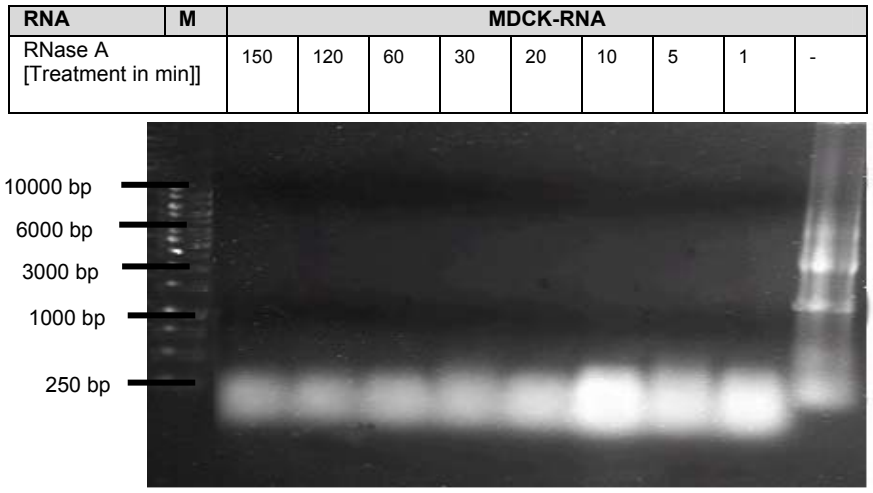

Different RNA types are cleaved to immunostimulatory fragments upon RNase A treatment

Next we wanted to examine whether self-RNAs from different sources become immunostimulatory upon incomplete RNase A treatment. Therefore, we isolated RNAs (4.3.1) from cancer cell lines like MDCK- and HEK293 cells, and, in order to exclude a cancer cell line phenomenon, we also tested RNAs from primary cells like murine liver or PBMCs (for PBMC-RNA: data not shown). For the stimulation of human PBMC cells we used different RNAs, either untreated or RNase A-treated. DOTAP was chosen as transfection reagent. CpG 2216 and RNA 40 were used as positive IFN-α inducers. Remarkably, the source of the non-immunostimulatory RNAs did not play a role in the IFN-α response induced after RNase A treatment in human PBMC cells (Figure 36). The fragments derived from RNase A treatment of all tested RNA types complexed to DOTAP induced IFN-α in human PBMC cells at different RNA concentrations.

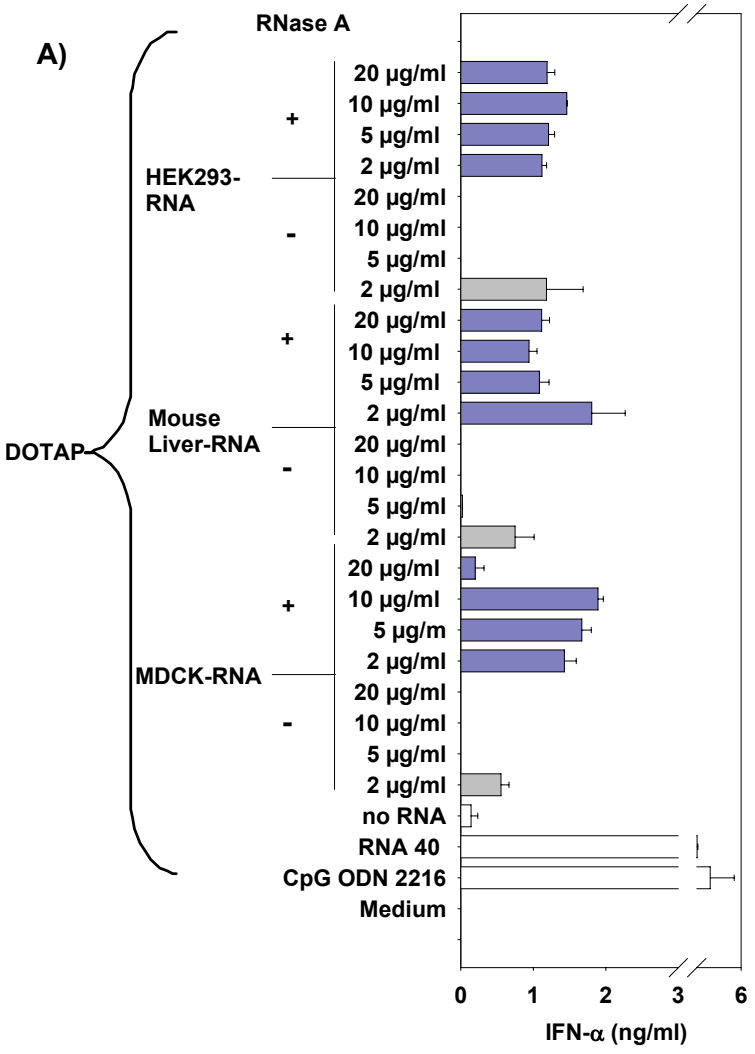

Figure 36: Influence of the RNA type on the generation of small immunostimulatory self-RNAs. A) Different RNA types, either mock or RNase A-treated (0.0075 U/ml), were complexed to DOTAP and used for stimulation of PBMC cells at different final RNA concentrations. IFN-α production was measured 24 hours post stimulation by ELISA. CpG 2216 (1µM) and RNA 40 served as positive controls (n = 6, one representative experiment is shown).

B)

RNA	M	RNA					
RNA type		MDCK	HEK 293	Liver	MDCK	HEK 293	Liver
RNase A (0,0075 U/ml)		-			+		

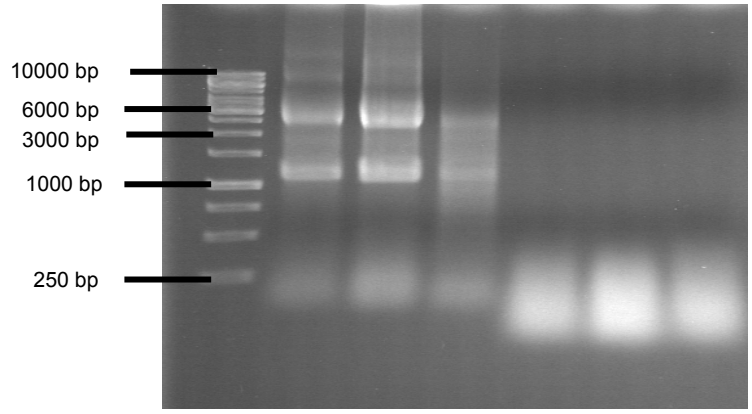

Figure 36: Influence of the RNA type on the generation of small immunostimulatory self-RNAs. B) Ethidium bromide staining of different RNA types, either mock or RNase A-treated, separated on an 1, 2 % agarose gel. Marker lane contains a 1 kbp DNA marker.

Different Ribonuclease-types generate immunostimulatory fragments

Our initial findings showed that fragments from self-RNAs generated by partial RNase A treatment induced an immune response when complexed to DOTAP in human PBMC cells. Next, we asked whether other RNase types also render self-RNAs immunostimulatory. Therefore, we generated fragments of self-RNA upon treatment with different RNase types (4.3.6), complexed them to DOTAP and tested their immunostimulatory potential in human PBMC cells. Different ends of the RNA fragments were generated, depending on the type of RNase used. Ribonucleases that hydrolyze RNA to 3`-phosphomonoester via 2`,3`-cyclic nucleosides are RNase A, RNase T1, and RNase T2 (Deshpande and Shankar 2002). Figure 37 B shows the ethidium bromide staining for the fragments generated by these ss-specific RNase types. As shown in Figure 37 A, the generated fragments with 3`-phosphoryl ends complexed to DOTAP all exhibited high immunostimulatory potential for human PBMC cells. Only treatment with the ds-specific RNase III did not lead to RNA degradation or generation of immunostimulatory self-RNA (Figure 37 A/B).

To determine if phosphate groups are important features of the RNA fragments, we treated the RNase-generated fragments with calf intestine phosphatase (CIP) (4.3.11). Dephosphorylation of the fragments showed no influence on the IFN-α response, suggesting that the recognition of the RNase cleavage products is not mediated through phosphate groups at least in human PBMC cells.

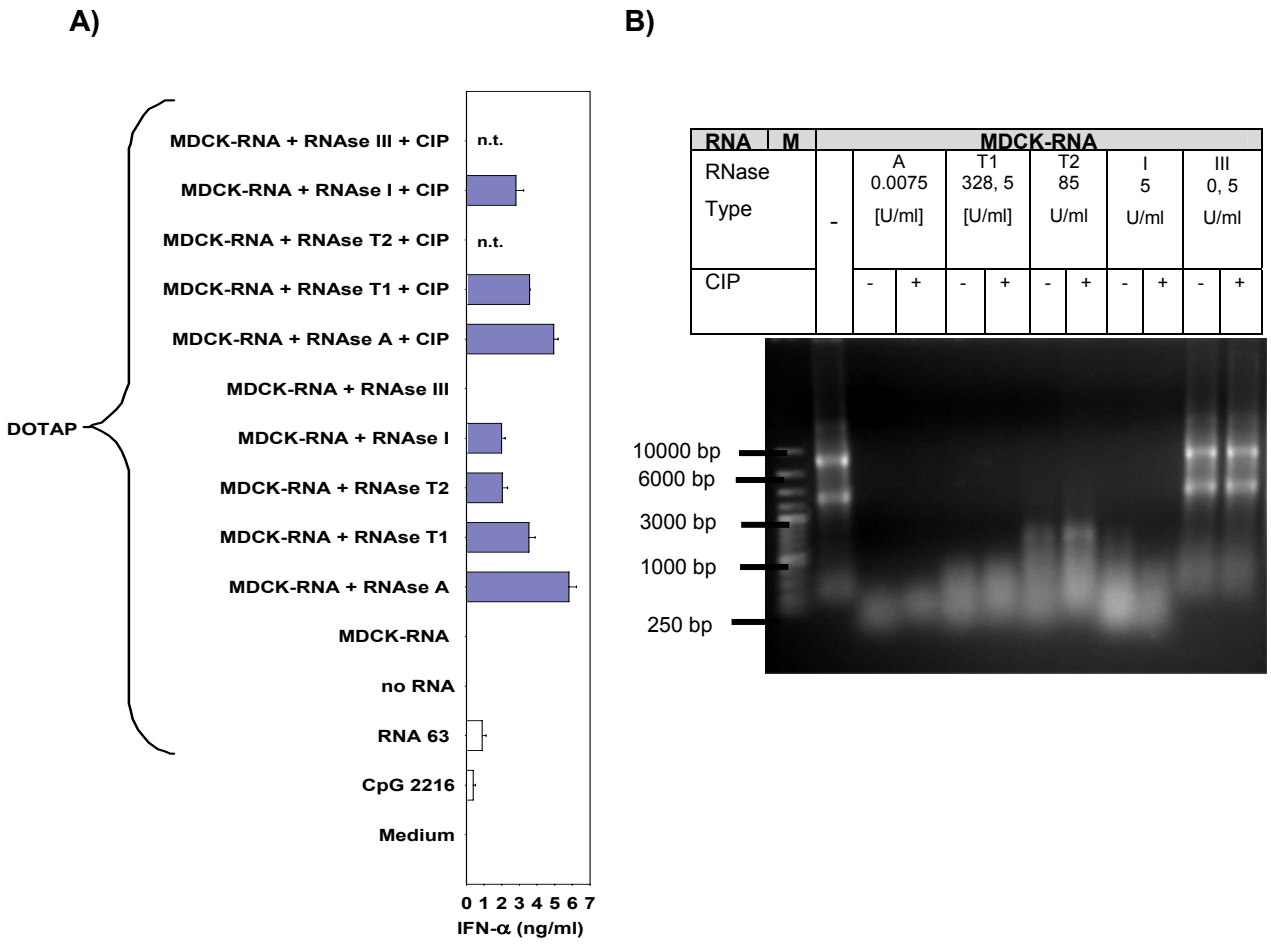

Figure 37: Comparing the ends generated by different RNase types. A) MDCK-RNA was partially treated with different RNase types (RNase A 0.0075 U/ml, RNase T1 328.5 U/ml, RNase T2 85 U/ml, RNase I 5 U/ml, RNase III 0.5 U/ml), either dephosphorylated or not, complexed to DOTAP and used for stimulation of PBMC cells at 10 µg/ml final RNA concentration. IFN-α production was measured 24 hours post stimulation by ELISA. CpG 2216 (1µM) and RNA 40 served as positive controls (n = 12, one representative experiment is shown). B) RNAs treated with different RNase types, either dephosphorylated or not, were analyzed on an 1, 2 % agarose gel by ethidium bromide staining. Marker lane contains a 1 kbp DNA marker (n.t.= not tested).

Besides these nucleases, there are ribonucleases like the S1 nuclease from Aspergillus oryzae (Desai and Shankar 2003) and the P1 nuclease from Penicillium citrinum (Desai and Shankar 2003) that hydrolyze RNA to 5`-phosphomonoester. These are zinc metalloproteins and contain three Zn^{2+} atoms per molecule of the enzyme (McCall et al. 2000) (1.4). We tested nucleases P and SvP for their ability to generate immunostimulatory RNA from self-RNA. Therefore, the fragments were complexed to DOTAP and used for stimulation of human PBMC cells. The ethidium bromide staining of the generated fragments is shown in Figure 38 B. The Nuclease P treatment was performed in a zinc buffer. Because of the metal-induced degradation of RNA, the untreated RNA was already degraded as shown in Figure 38 B lane 2. Figure 38 A shows

the IFN-α response from human PBMC cells to Nuclease P- and SvP-generated fragments complexed to DOTAP. The IFN-α response concerning the RNase types generating 5`-phosphate ends seemed to be lower and donor dependent. In conclusion, we observed an IFN-α induction with all the RNase types generating 3`-phosphate as well as 5`-phosphate RNA ends in human PBMC cells. The IFN-α response was independent from the phosphate end.

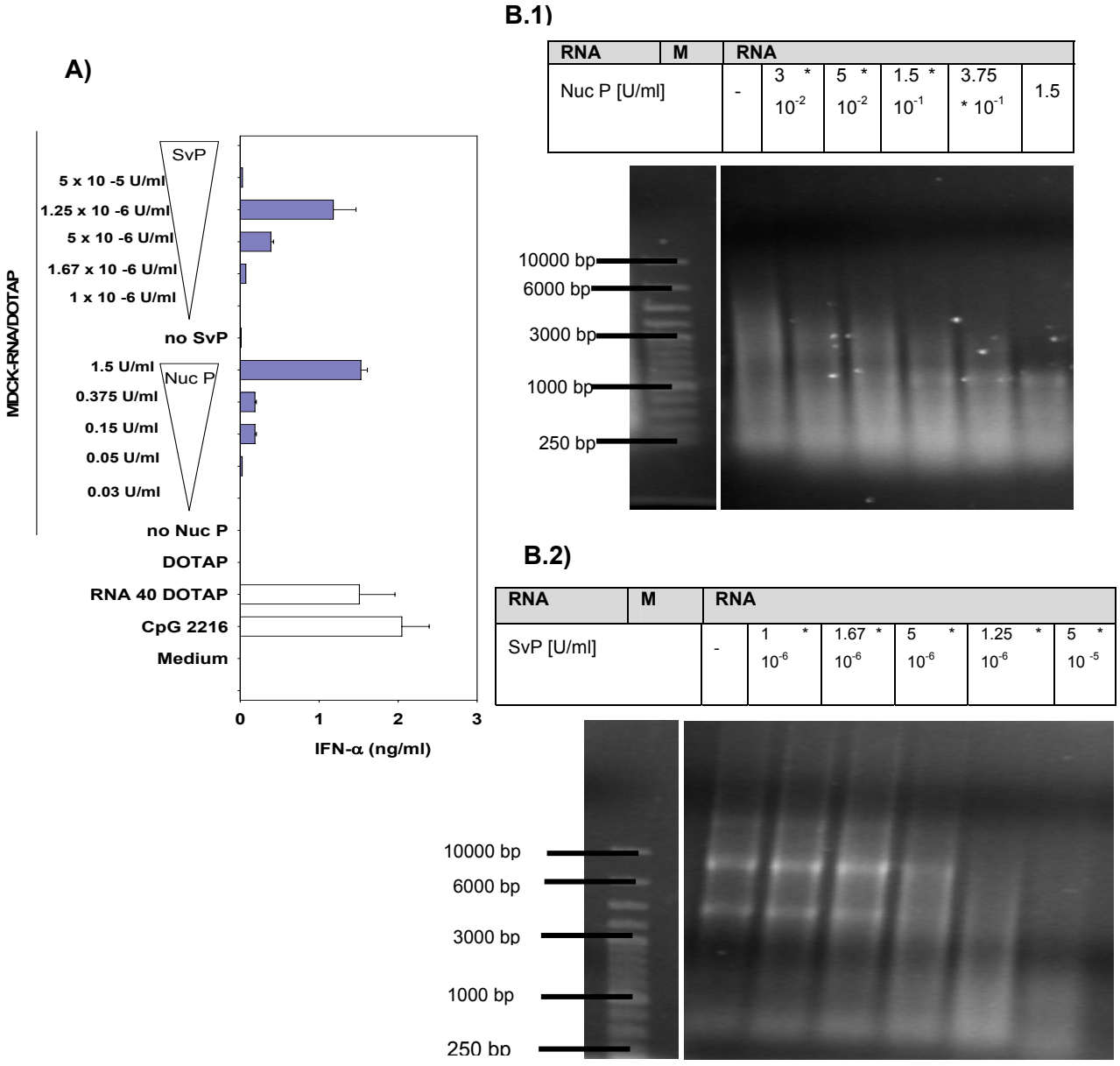

Figure 38: Comparing the ends generated by different RNase types. A) MDCK-RNA was partially treated with different RNase types complexed to DOTAP and used for stimulation of PBMC cells at 10 µg/ml final RNA concentration. IFN-α production was measured 24 hours post stimulation by ELISA. CpG 2216 (1µM) and RNA 40 served as positive controls (n = 8, one representative experiment is shown). B) Ethidium bromide staining of Nuclease P (B.1) and SvP treated RNAs (B.2) separated on an 1.2 % agarose gel. Marker lane contains a 1 kbp DNA marker. In lane 2 from picture B.1: untreated MDCK-RNA is degraded because of Zn^{2+}.

Another nuclease, called Benzonase, degrades both DNA and RNA, whether ss or ds, and shows no base preference (Kariko et al. 2004). It generates 5`-monophosphate-terminated products (Eaves and Jeffries 1963; Nestle and Roberts 1969). But upon stimulation of human PBMC cells with Benzonase generated fragments, there was almost no detectable IFN-α response (data not shown).

5.3.1.2. Further techniques for generating RNA fragments

Effect of ultrasound on RNA

The data presented above describe the ability of RNA fragments generated by RNase treatment to induce IFN-α in human PBMC cells. To analyze if fragment size is an important feature to induce IFN-α, we generated fragments by different techniques. Meidan et al. showed that ODNs clearly undergo chain shortening under the influence of ultrasound, suggesting that intramolecular cleavage at the phosphodiester internucleoside linkage is occurring. The mechanical (as opposed to the heating) effects of ultrasound are responsible for the observed ODN degradation (Meidan et al. 1997). For ultrasonic treatment, we exposed self-RNAs for different durations (0 s, 10 s, 30 s and 1 min) to ultrasound waves (4.3.9). The ethidium bromide staining in Figure 39 B shows that progressive fragmentation due to an increase in the duration of ultrasonic treatment resulted in a decrease in the size range of the fragments, reaching 100 - 500 bp in the last sample. But when we compared the size of fragments derived by ultrasonic treatment with the RNase A-generated fragments (which had a size in the range of 20 - 100 bp), we observed that the fragments produced by ultrasonic treatment were longer. The fragments derived by ultrasonic treatment were complexed to DOTAP and tested for their immunostimulatory potential in human PBMC cells. In contrast to the RNase A-generated fragments, the ultrasonic-derived fragments did not induce IFN-α (Figure 39 A). What is remarkable is that the background IFN-α response induced by self-RNA in a concentration range of 2 µg/ml (5.3.1.1) was reduced with the increase of ultrasonic treatment. This suggests that the feature responsible for inducing the background IFN-α response of self-RNA is destroyed with ultrasonic treatment. Upon treatment of self-RNA with the ds-specific RNase III, the background IFN-α response was also reduced, as discussed in section 5.2.4.

A)

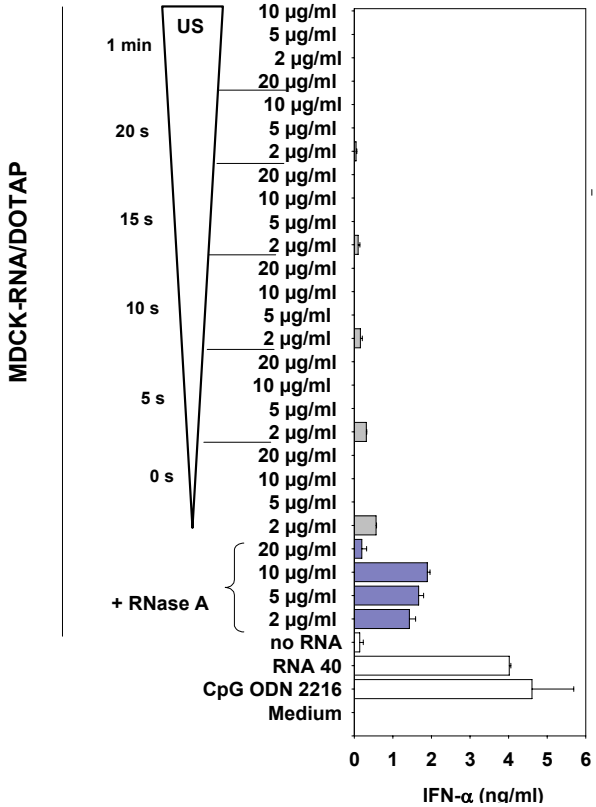

B)

RNA	M	MDCK-RNA					
Ultra sound waves [Treatment in s]		0	5	10	15	20	60

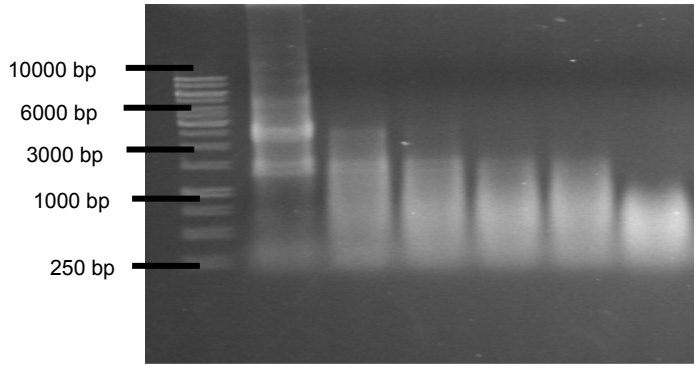

Figure 39: Effect of ultrasound waves on self-RNAs regarding immunostimulatory abilities. A) MDCK-RNA subjected to ultrasound waves was complexed to DOTAP and used for stimulation of PBMC cells at different final RNA concentrations. As a comparison, RNase A-treated (0.0075 U/ml) MDCK-RNA was additionally used at different RNA concentrations. IFN-α production was measured 24 hours post stimulation by ELISA. CpG 2216 (1µM) and RNA 40 served as positive controls (n = 10, one representative experiment is shown). B) Agarose gel electrophoresis patterns of RNAs subjected to ultrasound waves. Marker lane contains a 1 kbp DNA marker.

Metal ion-induced hydrolysis of RNA

Concerning the characterization of RNA fragments to induce IFN-α, we further evaluated RNA fragments generated by metal ion-induced hydrolysis. Self-RNA was treated with metal ions (4.3.8) followed by phenol/chloroform extraction (4.2.5), then complexed to DOTAP and used for the stimulation of human PBMC cells. The ethidium bromide staining in Figure 40 A and B shows that the fragments generated by Zn^{2+}- or Pb^{2+}-induced hydrolysis (4.3.8) were of similar size to the RNase A-derived fragments. The fragments produced by Zn^{2+}-induced hydrolysis complexed to DOTAP did not induce IFN-α, whereas the fragments produced by Pb^{2+}-induced hydrolysis complexed to DOTAP induced IFN-α in human PBMC cells (Figure 40).

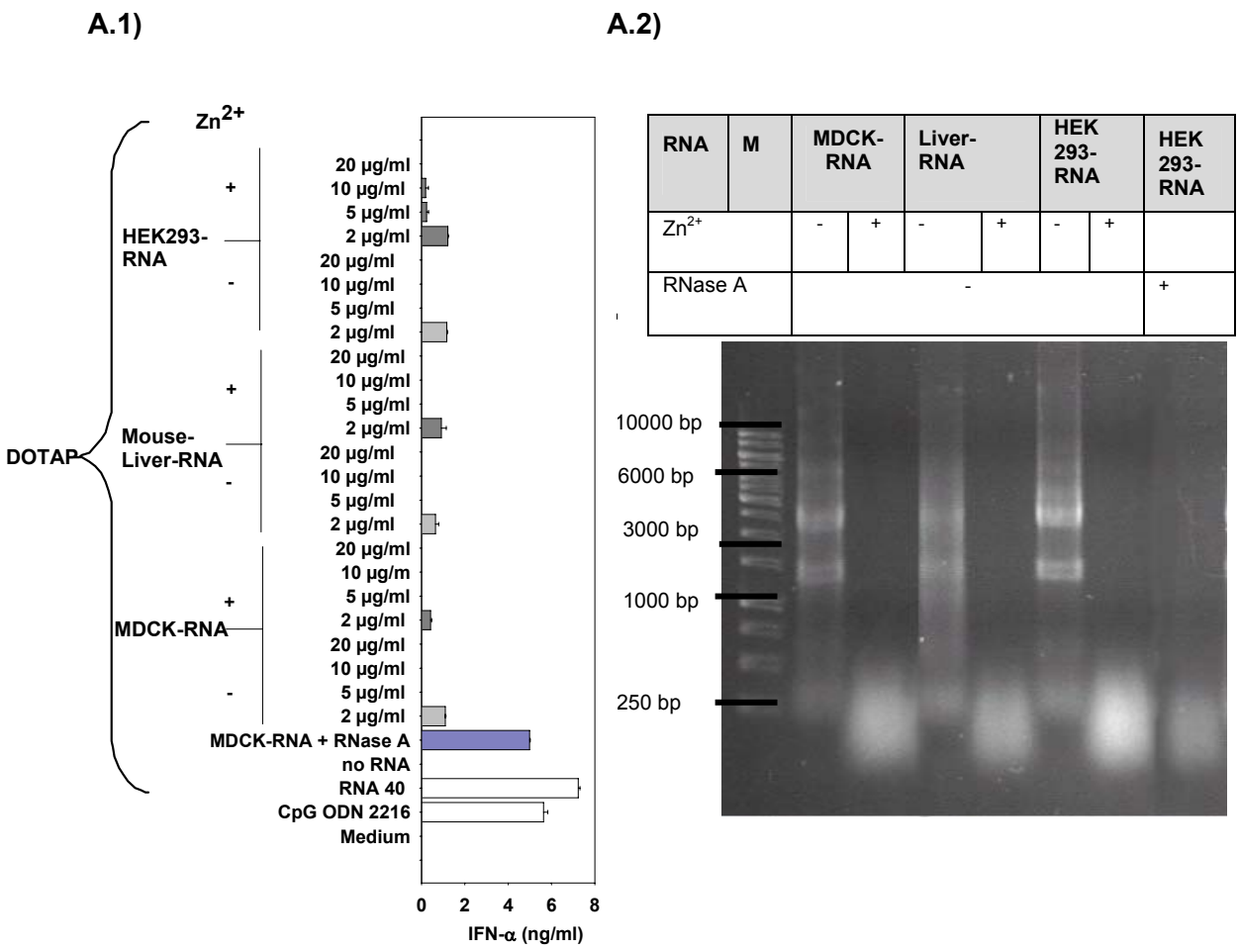

Figure 40: Effect of metal-ion induced hydrolysis of RNAs concerning immunostimulatory abilities. A.1) Fragments generated by Zn^{2+}-hydrolysis from different RNAs were complexed to DOTAP and used in the stimulation of PBMC cells at different final RNA concentrations. As a comparison, RNase A-treated (0.0075 U/ml) MDCK-RNA was also used. IFN-α production was measured 24 hours post stimulation by ELISA. CpG 2216 (1µM) and RNA 40 served as positive controls (n = 8, one representative experiment is shown). A.2) Agarose gel electrophoresis patterns of Zn^{2+}-induced cleavage of self-RNA. Marker lane contains a 1 kbp DNA marker.

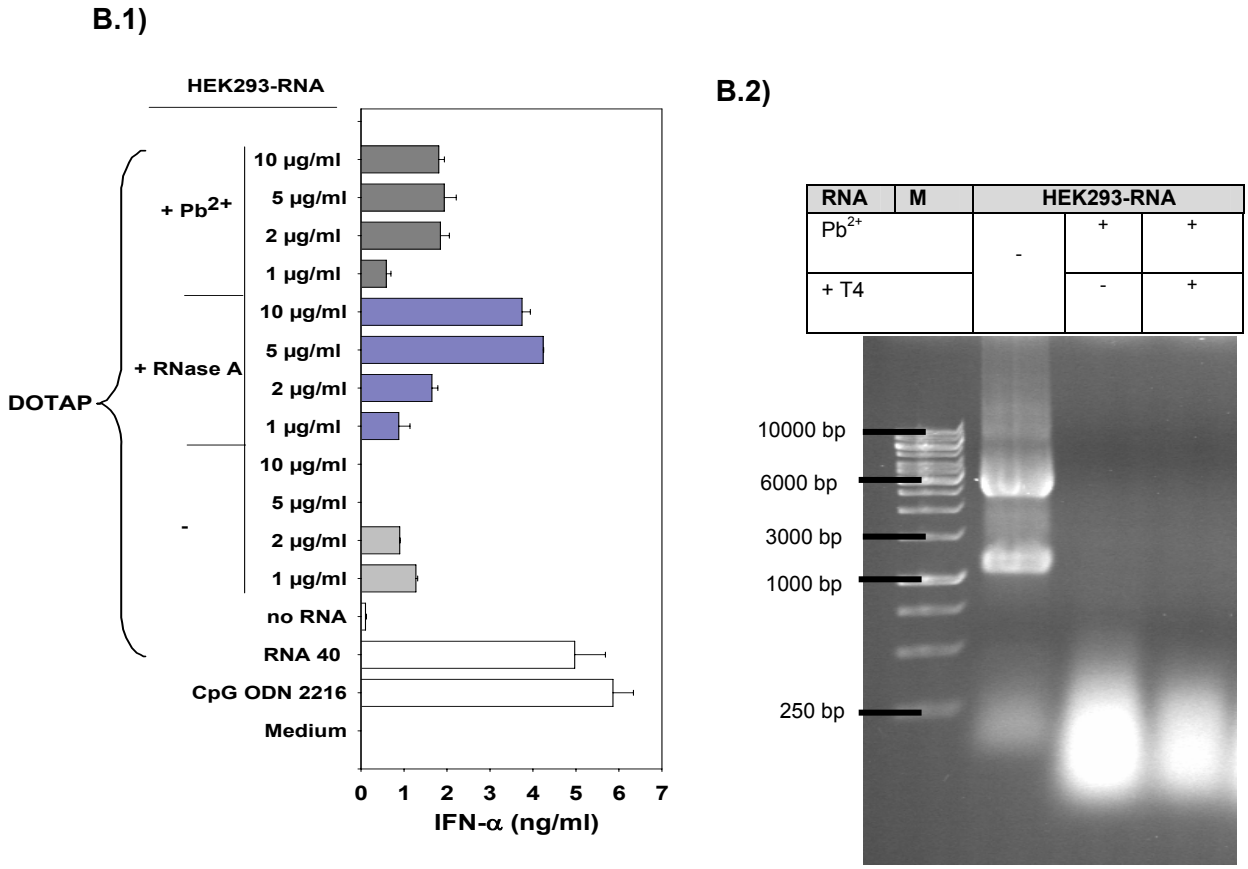

Figure 40 Effect of metal-ion induced hydrolysis of RNAs concerning immunostimulatory abilities. B.1) Fragments generated by Pb^{2+}-induced hydrolysis from different RNAs were complexed to DOTAP and used for stimulation of PBMC cells at different RNA concentrations. As a comparison, RNase A-treated (0.0075 U/ml) MDCK-RNA was also used. IFN-α production was measured 24 hours post stimulation by ELISA. CpG 2216 (1µM) and RNA 40 served as positive controls (n = 5, one representative experiment is shown). B.2) Agarose gel electrophoresis patterns of Pb^{2+}-induced cleavage of self-RNA. Marker lane contains a 1 kbp DNA marker.

For the fragments produced by Zn^{2+}-induced hydrolysis, there was only an IFN-α response detectable in the concentration range of 2 µg/ml RNA, which was also observed for untreated RNAs. The question arose as to whether different ends of the fragments were generated by different cleavage mechanisms.

5.3.1.3. Role of the 2`,3`-cyclic phosphate at the 3`-end of RNA

The enzyme T4 polynucleotide kinase (T4 PNK) catalyses the removal of a 2`,3`-cyclic phosphate. To analyze whether RNA fragments generated by different methods contain a

2`,3`-cyclic phosphate group, we treated the fragments with T4 PNK (4.3.7). The ethidium bromide staining shows that the removal of the phosphate group led to a reduced net charge of the transcripts, which can be monitored for lower electrophoretic mobility of the RNA in comparison to the untreated RNA (Figure 41 B).

First, we treated the fragments derived by RNase A treatment with T4 PNK, complexed them to DOTAP and stimulated human PBMC cells. An IFN-α response was detectable for either mock- or T4 PNK-treated RNase A-derived fragments (Figure 41 A).

Next, we treated fragments generated by metal hydrolysis with T4 PNK. But here, T4 PNK treatment showed only a variable IFN-α response when complexed to DOTAP and used in the stimulation of human PBMC cells (Figure 41 A).

This result suggests that the 2`,3`-cyclic phosphate group does not play a role for the immunostimulatory activity of the RNase A-generated fragments or the metal-induced fragments.

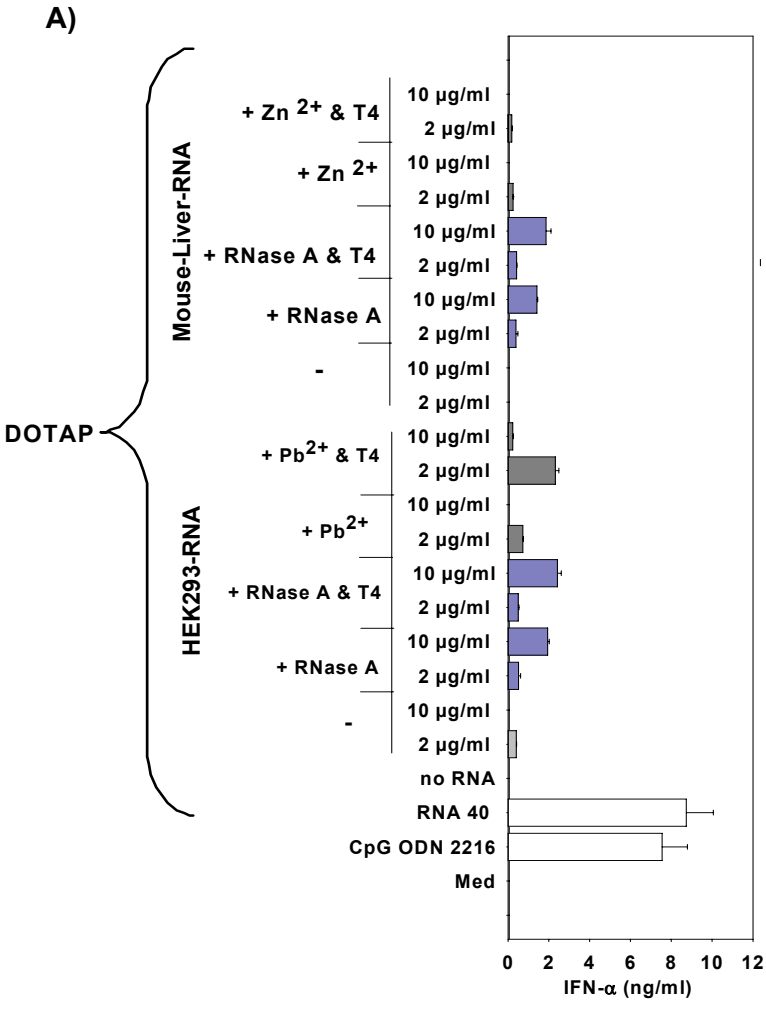

Figure 41: Comparison of fragments generated by RNase A treatment or by metal ion-induced hydrolysis, concerning the role of the 2`,3`- cyclic phosphate group at the 3` end. A) RNA fragments generated by RNase A treatment (0.0075 U/ml) or by metal ion–induced hydrolysis were either mock- or T4-treated, complexed to DOTAP and used for stimulation of PBMC cells at different final RNA concentrations. IFN-α production was measured 24 hours post stimulation by ELISA. CpG 2216 (1µM) and RNA 40 served as positive controls (for RNase A treatment n = 4, for metal ion-induced hydrolysis n = 2; one representative experiment is shown).

B)

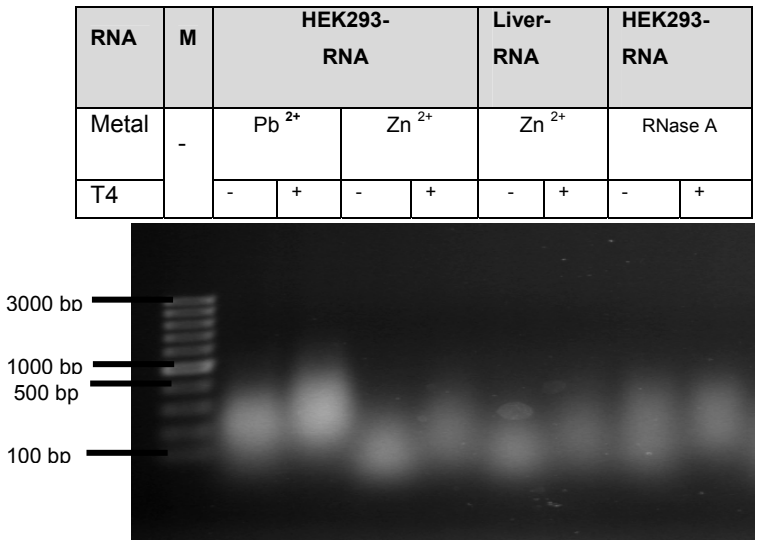

Figure 41: Comparison of fragments generated by RNase A treatment or by metal ion-induced hydrolysis, concerning the role of the 2`,3`-cyclic phosphate group at the 3` end. B) Fragments generated by metal ion-induced hydrolysis or by RNase A treatment were either mock- or T4-treated and analyzed by 1, 2 % agarose electrophoresis. Marker lane contains a 100 bp DNA marker.

5.3.2. Characterization of the immunostimulatory nature of self-RNA fragments

To gain further insight into the nature of those stimulatory RNA fragments of the ss or ds character, we incubated the RNase A-derived fragments with RNase III (4.3.10). Treatment of the stimulatory RNase A-derived fragments with RNase III, an enzyme that degrades long dsRNA into short dsRNA molecules, abolished the IFN-α response when complexed to DOTAP and used to stimulate PBMC cells (Figure 42 A). Ethidium bromide staining showed no difference for mock- or RNase III-treated fragments derived from RNase A treatment (Figure 42 B). Since RNase III is a ds-specific RNase, we can conclude that the stimulatory component of the RNase A-derived fragments is most likely double-stranded, whereas the components that are visualized by ethidium bromide staining upon RNase III treatment have ss character.

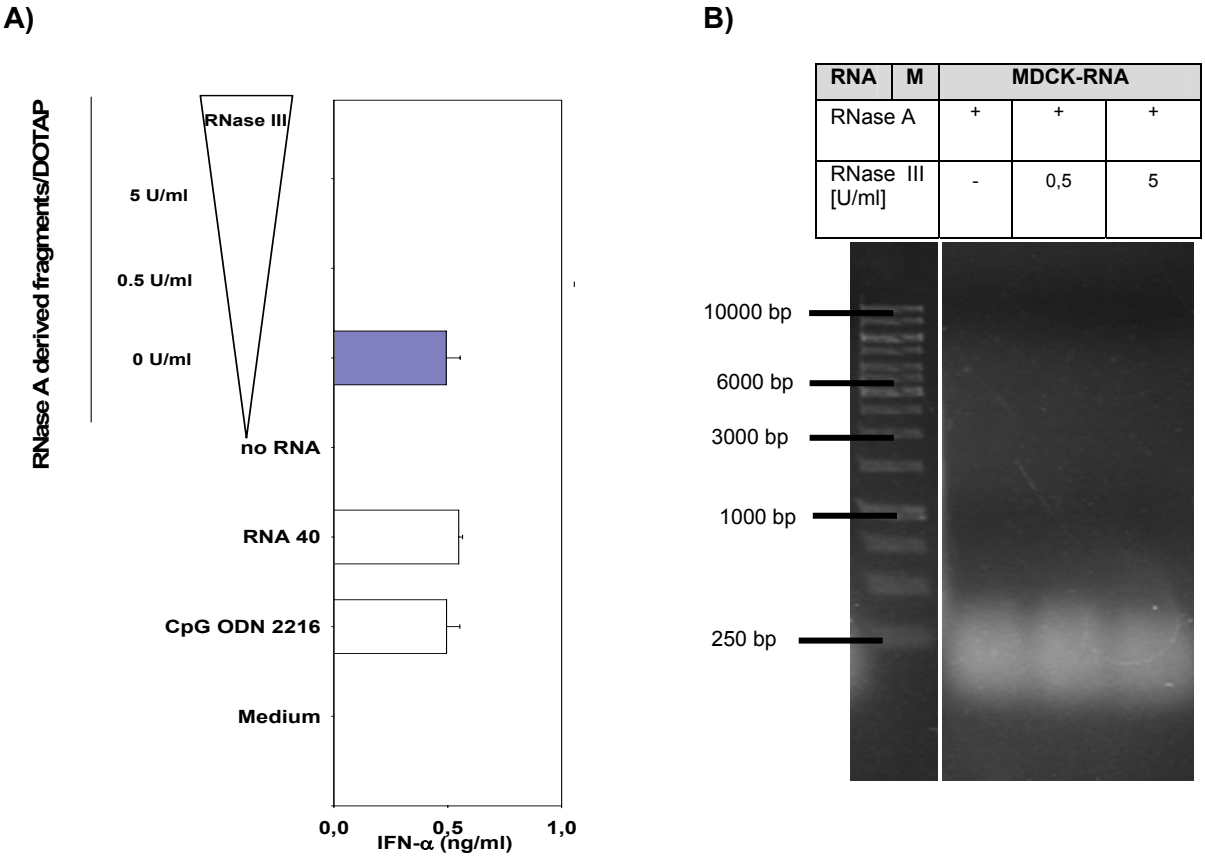

Figure 42: Influence of the ds character from fragments derived from partially-treated self-RNAs for inducing IFN-α. Fragments generated by RNase A treatment were additionally treated with RNase III, complexed to DOTAP and used for stimulation of PBMC cells at a final RNA concentration of 10 µg/ml. IFN-α production was measured 24 hours post stimulation by ELISA. CpG 2216 (1µM) and RNA 40 served as positive controls (n = 13, one representative experiment is shown). B) Ethidium bromide staining of fragments derived by RNase A that were additionally treated with RNase III and separated on an 1, 2 % agarose gel with a 1 kbp DNA marker.

5.3.3. Immunostimulatory RNA species

We sought to identify the immunostimulatory RNA species of the RNase A-derived fragments mixture and to examine if these species are modified.

5.3.3.1. Removal of single nucleosides

We tried to address the question of which fragments of the RNase A digest are responsible for the IFN-α inducing capacity. Upon treatment of self-RNA with RNase A, the digest contains single nucleosides and various longer RNA fragments. We used Micro Bio-Spin columns (4.2.6) in order to purify nucleic acids larger than 20 bases. Single

nucleosides were removed by this technique. Figure 43 shows that the first and second purified fractions of the RNase A-derived fragments were visible on an ethidium bromide stained gel. For the first fraction, we observed that it seemed more concentrated than the complete digest on an agarose gel. This could be explained by the fact that the first fraction contained larger fragments which could be better visualized by ethidium bromide staining, whereas single nucleosides were removed by Bio-Spin columns. As shown in Figure 43, the first fraction of the RNase A-treated self-RNA complexed to the cationic transfection reagent DOTAP stimulated human PBMC cells to produce IFN-α, whereas the following fractions containing single nucleosides showed no IFN-α secretion in human PBMC cells. This shows that fragments longer than 20 nucleotides and not single nucleosides are responsible for the immunostimulatory potential of the RNase A-derived fragments.

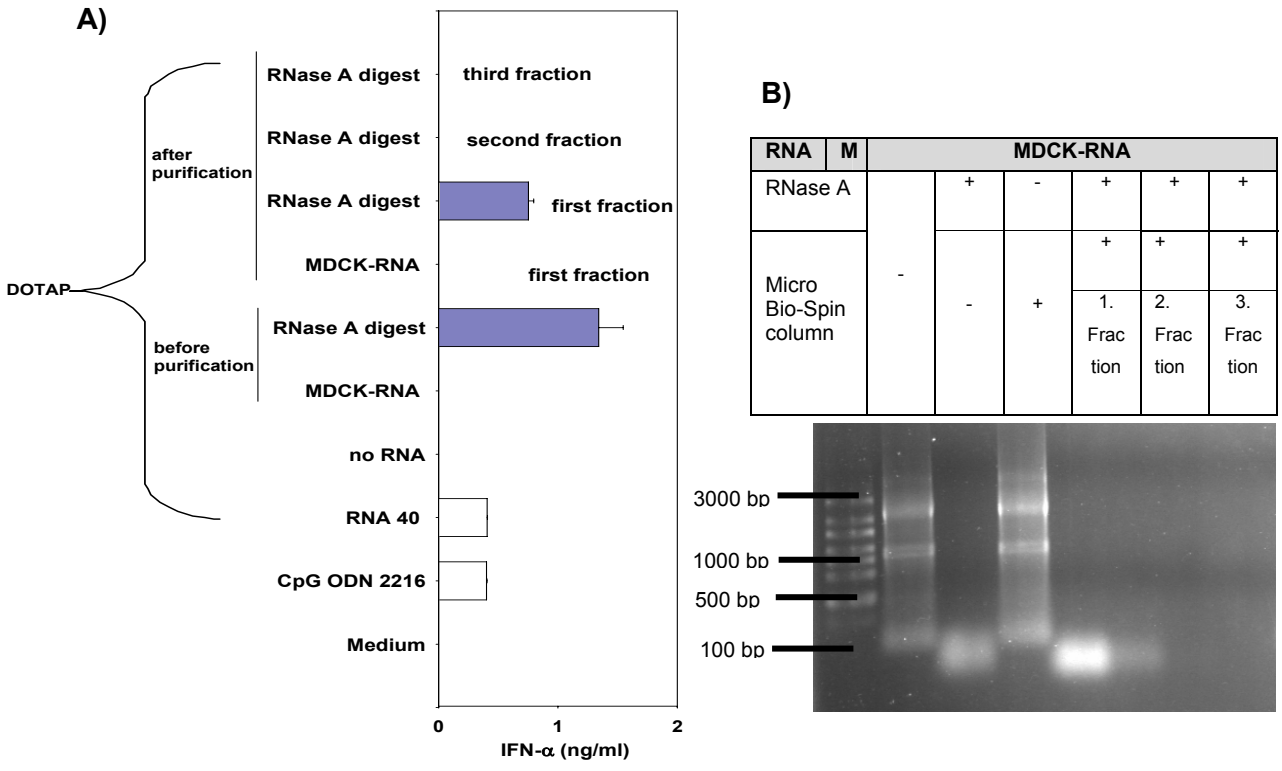

Figure 43: Fractionated RNAs derived by separating the RNase A digest with the help of Micro Bio-Spin columns were complexed to DOTAP and used for stimulation of PBMC cells at a final RNA concentration of 10 µg/ml. A) IFN-α production was measured 24 hours post stimulation by ELISA. CpG 2216 (1µM) and RNA 40 served as positive controls (n = 2, one representative experiment is shown). B) Fractionated RNase A-derived fragments were visualized by ethidium bromide staining on an 1, 2 % agarose gel with an RNA marker.

5.3.3.2. Oligonucleotide separation by HPLC

To identify the immunostimulatory RNA species of the RNase A-derived fragments, we fractionated the digest into different sizes by using XBRIDGE™ OST C_{18} columns (4.2.7) and high performance liquid chromatography (HPLC) (4.10). Figure 44 shows the HPLC patterns of fragments derived by RNase A treatment of self-RNA. The obtained fractions from the column showed longer RNA fragments as the time increases. The first fraction contained single nucleosides, whereas later fractions had longer RNA fragments.

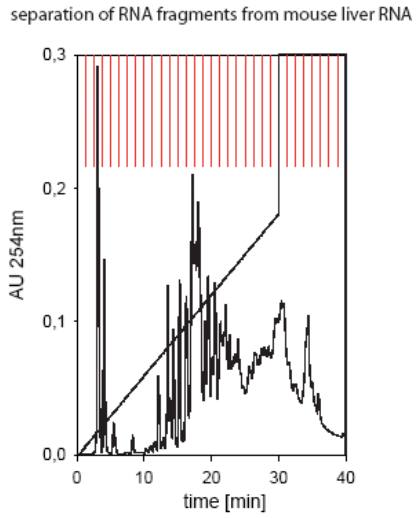

Figure 44: Characterization of RNA fragments obtained by RNase A treatment of self-RNA by HPLC analysis.

Before we tested which fraction contains the immunostimulatory RNA species, the obtained fractions were purified from remaining salts by using Waters C18 SepPak columns (4.2.7). Then the obtained fractions were complexed to DOTAP and used for stimulation of human PBMC cells. The first fractions (fractions 3-5) containing single nucleosides were not able to induce type-I interferon, whereas fractions obtained at a later date (fractions 16-19) contained the stimulatory RNA species (Figure 45). Surprisingly, these fractions could not be stained by ethidium bromide (Figure 46). Only larger fragments (fractions 21-29) could be visualized by ethidium bromide staining, but when complexed to DOTAP these fractions showed no ability to induce IFN-α in human PBMC cells.

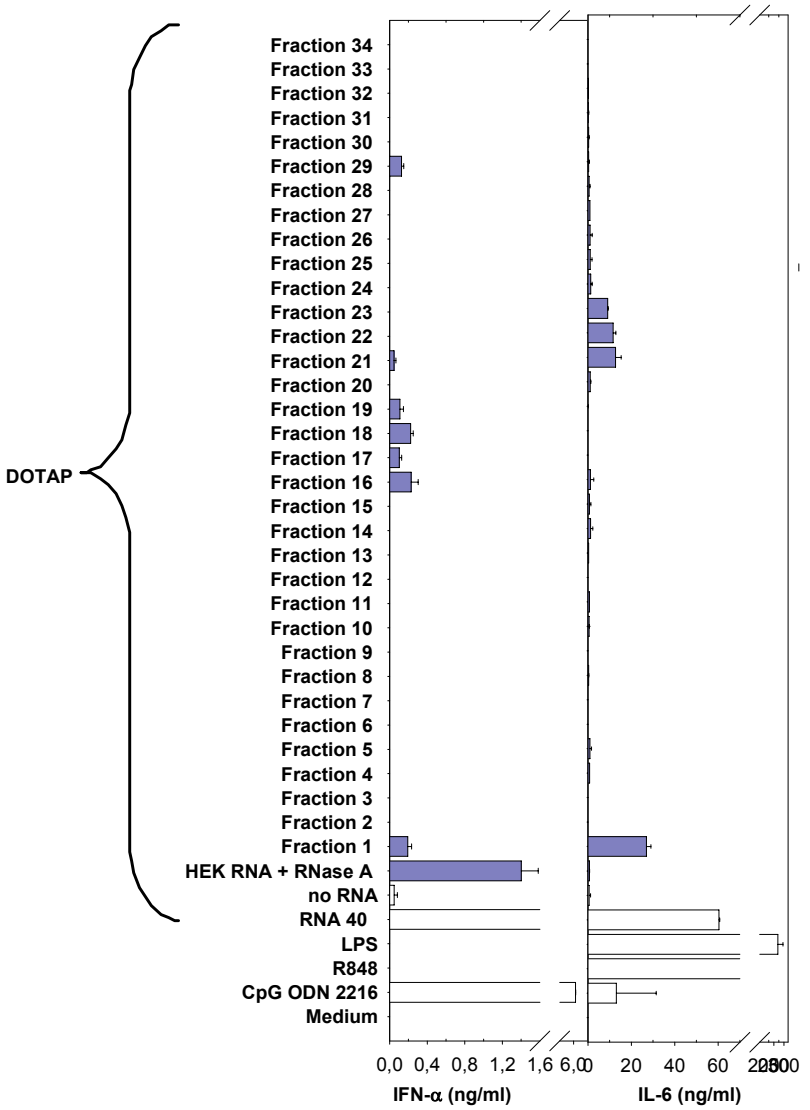

Figure 45: PBMC cells were stimulated with fractionated RNA fragments derived from RNase A treatment of self-RNA complexed to DOTAP. After 24 h, cytokines were quantified in the supernatant by ELISA (n = 2, one representative experiment is shown). For comparison RNase A treated (0.0075 U/ml) HEK293-RNA was additional used.

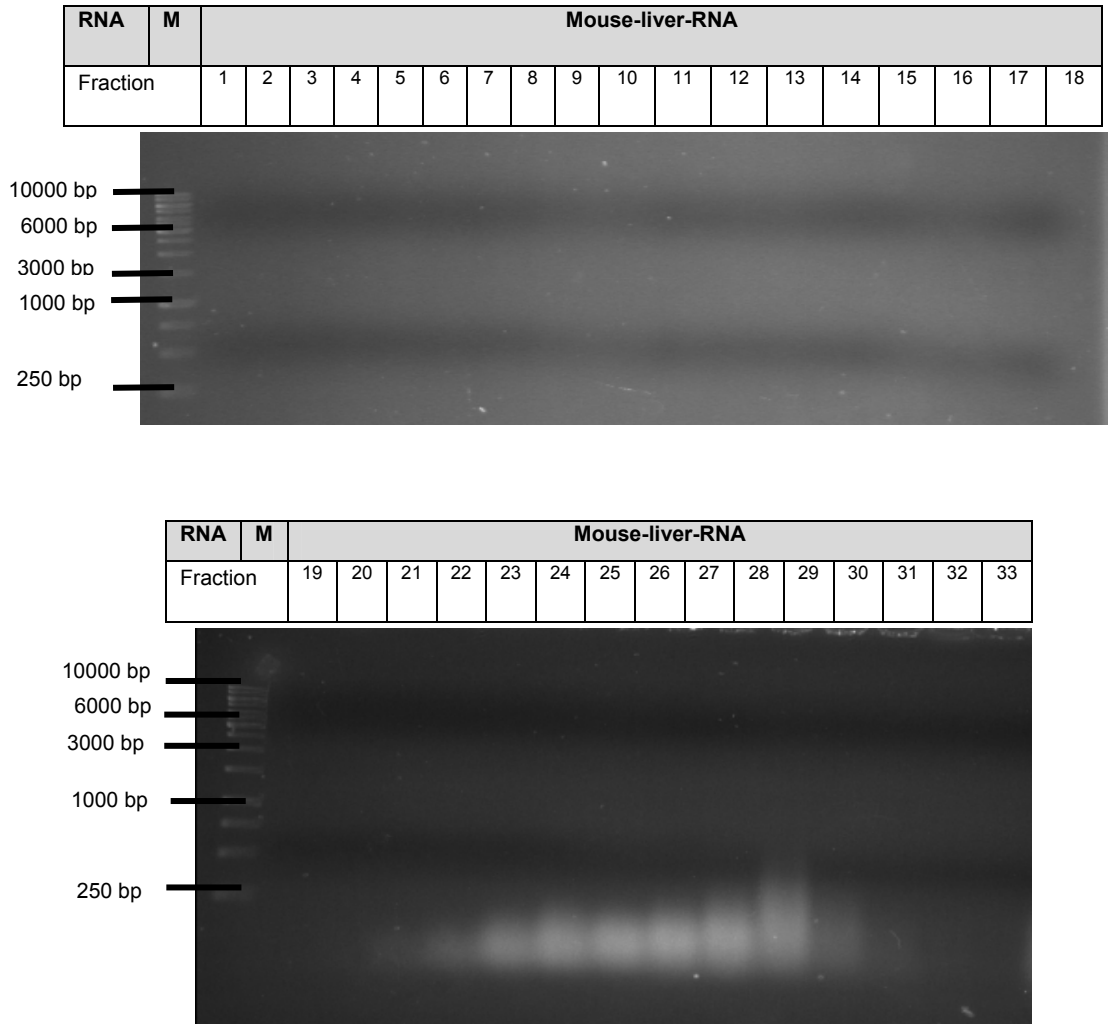

Figure 46: RNA fragments derived from RNase A treatment were fractionated with XBRIDGE^{TM} OST C_{18} columns and high performance liquid chromatography (HPLC) and visualized by ethidium bromide staining. Marker lane contains a 1 kbp DNA marker.

5.3.4. Identification of cell types recognizing RNase A-derived fragments

Monocytes are the main source of IFN-α upon recognition of RNase A-derived fragments

To address the question of which cell-types of the human PBMC cells are responsible for recognizing the RNase A-derived fragments and in order to induce IFN-α, we analyzed the

immune activation of monocytes (4.1.9.3) in comparison to PBMC (4.1.9.2) cells. The purity of the monocytes was controlled by FACS analysis (4.7). As shown in Figure 15, the isolated monocytes showed a purity of about 90%, whereas PBMCs contained only 28% monocytes. The monocytes were stimulated in the same way as described for PBMC cells. The supernatants were used for detection of IFN-α. Upon transfection of CpG 2216 and RNA 40, there was practically no IFN-α secretion detectable in human monocytes (we found only a weak secretion for RNA 40), whereas these ligands induced type-I interferon in human PBMC cells. Stimulation with fragments derived by RNase A treatment induced a strong type-I interferon response in human PBMC cells and monocytes (Figure 47).

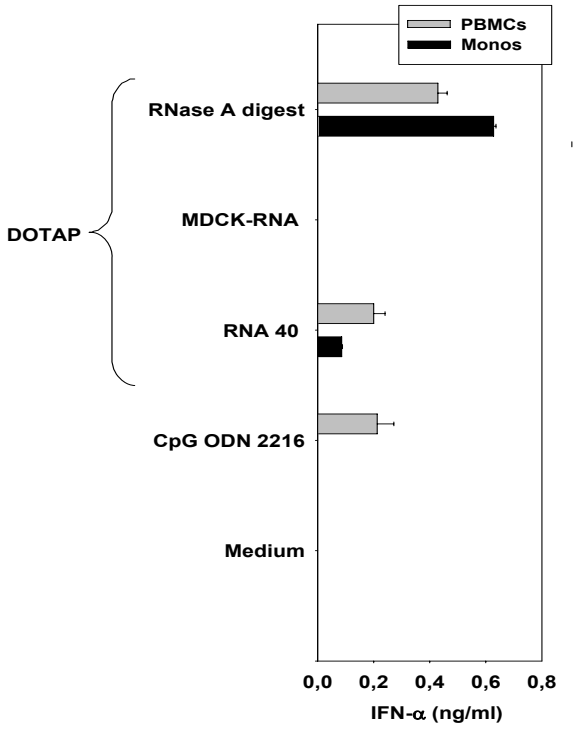

Figure 47: Analysis of the cell type of human PBMC cells responsible for recognizing RNase A-derived fragments. Fragments derived by RNase A treatment were complexed to DOTAP and used for stimulation of human PBMC cells and monocytes. IFN-α production was measured 24 hours post stimulation by ELISA. CpG 2216 (1 µM) and RNA 40 served as positive controls (for ca. 90 % purity monocytes n = 2, for ca. 70 % purity monocytes n = 1; one representative experiment is shown).

Influence of the serum concentration for the immunostimulatory ability of RNase A-derived fragments

Our initial findings showed that fragments derived by partially RNase treatment of self-RNA induced an immune response in human PBMC cells when complexed to DOTAP. We then wondered whether different serum concentrations might influence the immunostimulatory potential of RNase-derived fragments in human PBMC cells. Therefore, we used fragments generated by RNase treatment, complexed them to

DOTAP and tested their immunostimulatory potential in human PBMC cells exposed to different serum concentrations. As shown in Figure 48, the generated fragments complexed to DOTAP showed a serum-dependent IFN-α induction in human PBMC cells. The fragments induced the highest IFN-α response in human PBMC cells when using 1-2% serum, whereas for higher serum concentrations like 10% serum the immune response was decreased. With regard to other immune cells, like murine immune cells or human HEK293 cells which were maintained in 10% serum, this result is very important concerning the immunostimulatory ability of RNase-derived fragments.

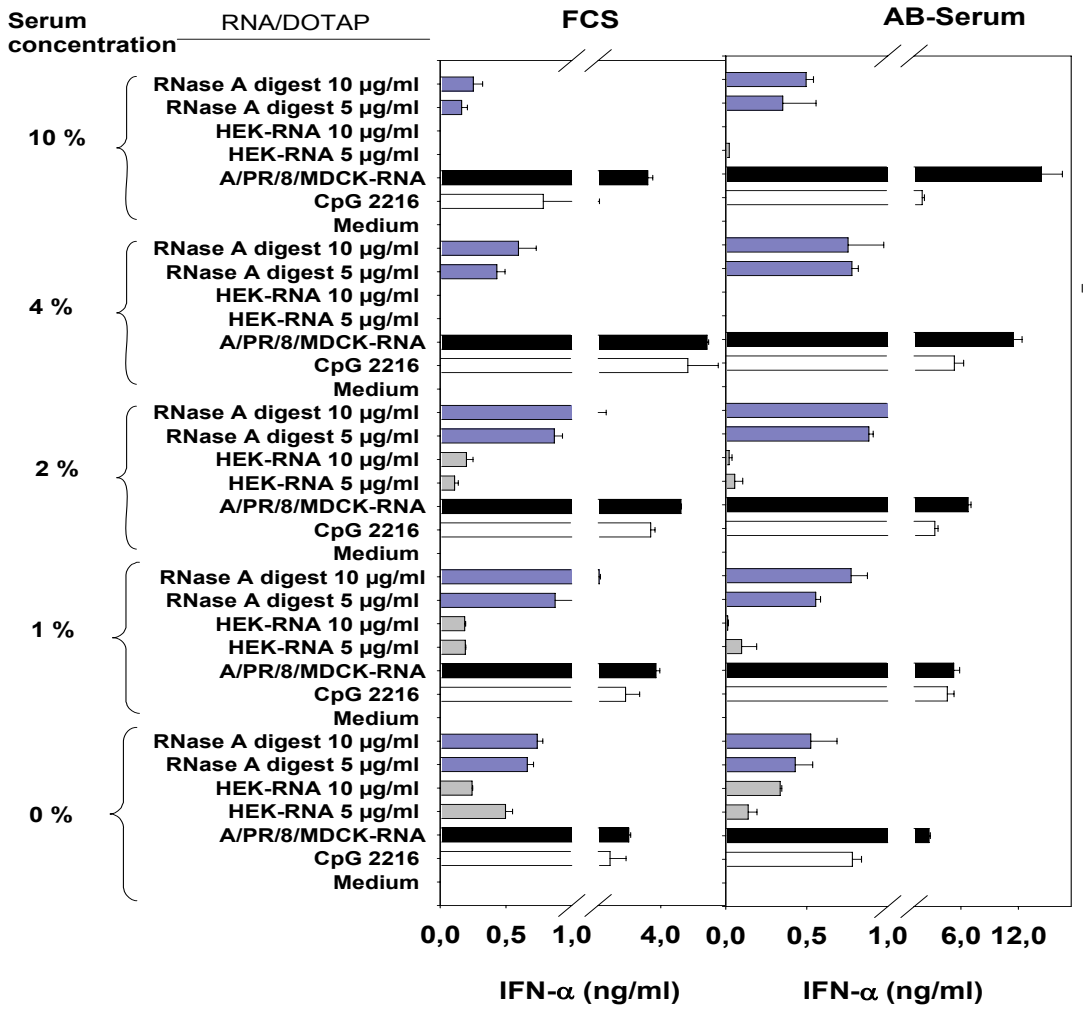

Figure 48: Influence of the serum concentration for stimulation of PBMC cells. PBMC cells were stimulated at different serum concentrations from 0 % to 10 % with different ligands. IFN-α production was measured 24 hours post stimulation by ELISA (n = 2, one representative experiment is shown). CpG 2216 (1µM) and RNA 40 served as positive controls.

Variable IFN-α responses for RNase A-derived fragments in murine immune cells

To investigate whether RIG-I or MDA-5 mediates the recognition of the fragments derived from RNase A treatment; we intended to use Flt3-derived dendritic cells lacking the downstream of RIG-I and MDA-5 working adaptor molecule IPS. The ability of the fragments to induce IFN-α in PBMC cells was additionally controlled (4.1.9.2).

First, we analyzed the immune activation of Flt3-derived dendritic cells (4.1.9.1) and measured IFN-α secretion by ELISA (4.9). Positive controls for IFN-α induction were the TLR ligands RNA 40 and CpG 2216. Upon transfection of RNase A-derived fragments complexed to DOTAP, there was always little-to-no IFN-α response detectable in Flt3-derived DCs. From n = 17 experiments performed in Flt3-derived dendritic cells and bone-marrow-derived dendritic cells, we observed in n = 5 experiments that the RNase A-derived fragments were not recognized by TLR7 (data not shown). For all the other experiments, there was no IFN-α secretion detectable upon stimulation with RNase A-generated fragments in wild-type Flt3-derived dendritic cells. The reason for the variable data might be a change in the FCS lot number. Regarding the result we found in human PBMC cells (namely, that the IFN-α inducing ability of the RNase A-derived fragments was dependent on the serum concentration), we tested different serum concentrations for Flt3-derived DCs. PBMC cells were normally stimulated in medium containing 2% AB serum, whereas Flt3-derived dendritic cells were cultivated in medium containing 10% FCS. For Flt3-derived dendritic cells, we found also a serum-dependent IFN-α induction for the fragments derived by RNase treatment (Figure 49). Whereas for serum concentrations below 5%, there was an IFN-α response detectable, for 10% serum concentration there was no IFN-α response. But this observation has to be reproduced.

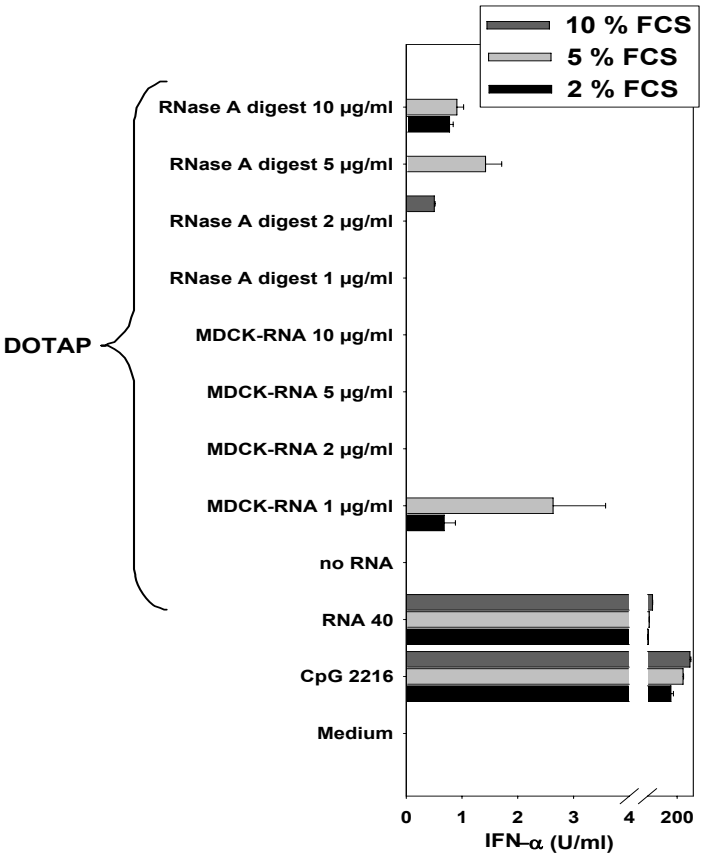

Figure 49: Analysis of the influence of serum for the recognition of fragments derived from RNase A treated self-RNAs. Either mock- or RNase A (0.0075 U/ml)-treated self-RNAs were complexed to DOTAP and used for stimulation of Flt3-derived dendritic cells generated from a wild-type mouse at a final RNA concentration of 10 µg/ml. RNA 40 and CpG 2216 served as positive controls. IFN-α secretion was measured 24 hours post stimulation by ELISA (for FCS Titration n = 1, one representative experiment is shown).

RIG-I dependent recognition of RNase A-derived fragments in HEK immune cells

To investigate whether RNase-derived fragments are recognized in an IPS-dependent way, HEK293 cells which lack functional TLRs (with the possible exception of TLR3) were transfected with plasmids encoding for RIG-I and MDA-5 (4.12) (Figure 50).

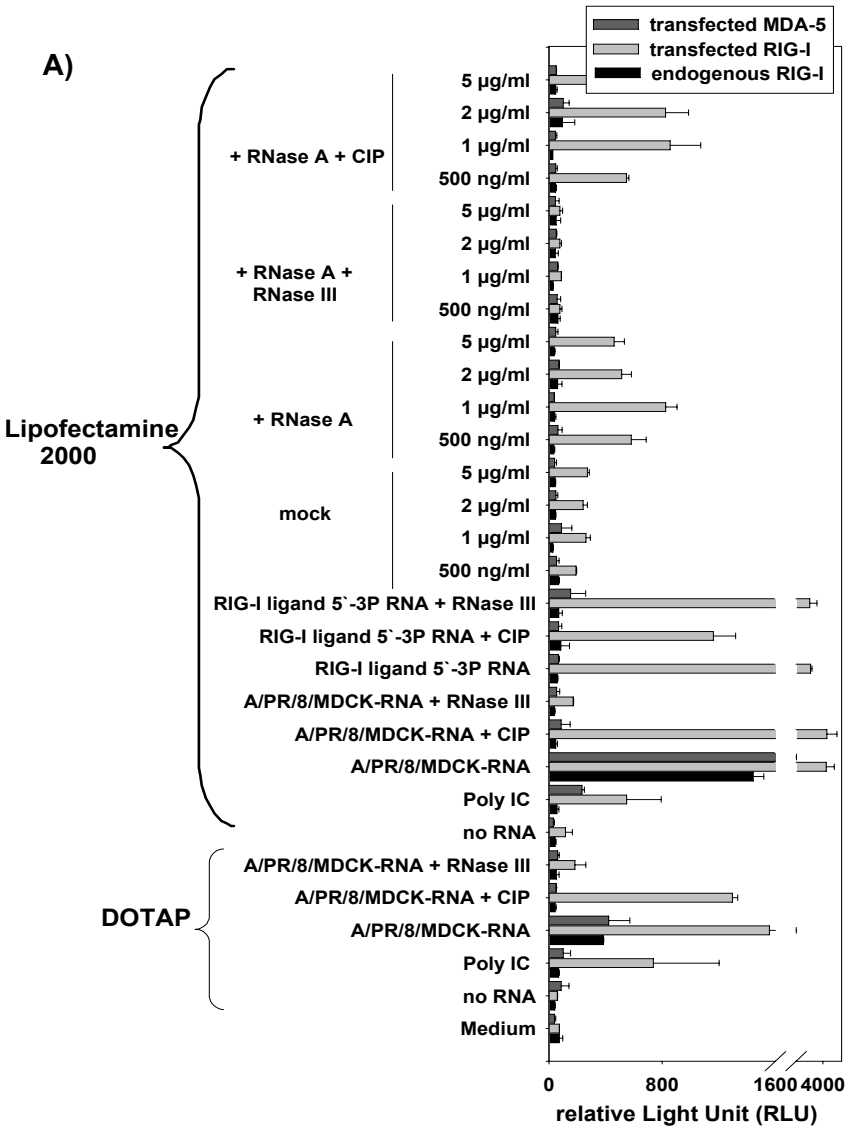

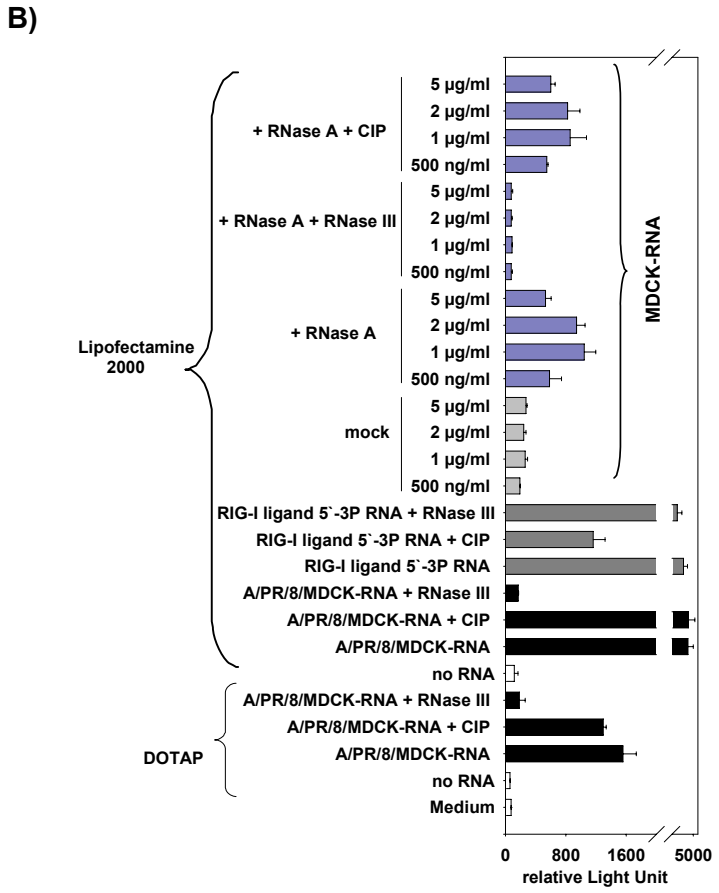

Figure 50: RIG-I-mediated recognition of RNA fragments in non-immune cells. A) HEK293 cells were cotransfected with plasmids encoding the IFN-ß luciferase reporter construct, RIG-I and MDA-5 by electroporation. B) summarizes the interesting part for RIG-I-transfected cells. Transfected cells were treated with Poly I:C (10 µg/ml), RIG-I ligand 5`-3P RNA (0.2 µg/ml), uninfected and A/PR/8/MDCK-RNA (2 µg/ml) each complexed to DOTAP or Lipofectamine 2000. In addition, the transfected cells were stimulated with RNase A (0.0075 U/ml)-derived fragments from self-RNA complexed to Lipofectamine 2000. These fragments were also RNase III- and CIP-treated. IFN-ß activation was determined by Dual Luciferase Assay (for RNAs in a concentration range between 200 ng/ml to 20 µg/ml complexed to Lipofectamine 2000 n = 6, one representative experiment is shown; for RNAs in a concentration range between 200 ng/ml to 50 µg/ml complexed to DOTAP n = 7, no experiment is shown).

The normally MDA-5-specific ligand Poly I:C was found to show enhanced IFN-ß activation in RIG-I-transfected cells, but when complexed to Lipofectamine 2000 there was little detectable IFN-ß increase in MDA-5-transfected cells. The question arose as to whether our MDA-5 was functional. RIG-I expressing HEK293 cells gained responsiveness to the RIG-I-specific control RIG-I ligand 5`-3P RNA complexed to Lipofectamine 2000. The A/PR/8/MDCK-RNA complexed to DOTAP or Lipofectamine 2000 was also recognized in RIG-I-transfected HEK293 cells in a CIP-independent but RNase III-dependent way, as described in section 5.2. Upon stimulation with the fragments derived from RNase A treatment complexed to Lipofectamine 2000 at a final RNA concentration of 1 µg/ml, IFN-ß activation was enhanced. As a control we also performed stimulation with untreated self-RNA, but there was no immune induction. The observed IFN-ß activation upon stimulation with RNase A-derived fragments was only detectable by using the transfection reagent Lipofectamine 2000, but not with DOTAP (data not shown). Upon RNase III treatment of the fragments derived from RNase A treatment, the immune response was abrogated showing the importance of the ds character of the fragments for the RIG-I-dependent immune response. The 5`-triphosphate has no influence on the recognition of the fragments, because dephosphorylation did not reduce IFN-ß activation. Thus, the RNase A-derived fragments are recognized in different ways by immune cells. Whereas in human PBMC cells IFN-α secretion was observed upon transfection with RNase A-derived fragments complexed to DOTAP at a final RNA concentration in the range of 5-50 µg/ml (further concentrations have not been tested; data only shown until 10 µg/ml), in human HEK293 cells IFN-ß activation was enhanced when the fragments were complexed to Lipofectamine 2000 at a final RNA concentration of 1 µg/ml. In conclusion, we could say that, depending on the immune cell type, different concentrations of the RNA fragments and different transfection reagents are necessary for inducing an immune activation. Regarding the results obtained by using HEK293 cells overexpressing RIG-I, we observed that RIG-I is the responsible receptor for recognizing RNase A-derived fragments. This result could not be confirmed by using respective knockout mice. Reasons for this variable immune response to the RNase A-derived fragments on murine immune cells might be that FCS is a problem or that the absence of a 5`-triphosphate end of the fragments might be essential for murine immune signaling.

5.3.5. Summary

In this study, we could show that small self-RNAs generated by RNase treatment represent an immunostimulatory pattern. These cleavage products complexed to DOTAP strongly triggered a type-I interferon response in human PBMC cells. Murine Flt3-derived dendritic cells showed a variable immune response to RNase-derived fragments. Considering the FCS dependency, optimal conditions for recognizing the RNase A-derived fragments in the murine system have to be found. However, non-professional immune cells were able to mount an IFN-ß response upon stimulation with the RNase-derived fragments complexed to Lipofectamine 2000. The viral RNA sensor protein RIG-I was shown to be responsible for the IFN-ß response in HEK23 cells. Nevertheless, the observed immunoactivation in both cells types, PBMCs and HEK293 cells, was not really comparable, because different transfection reagents were used. DOTAP facilitates endosomal delivery, whereas Lipofectamine 2000 ensures cytoplasmic translocation. At the moment, we can only understand the IFN-ß activation upon transfection of RNase-derived fragments complexed to Lipofectamine 2000 for HEK293 cells. We observed in the HEK system a RIG-I mediated immune recognition. The strong secretion of IFN-α upon stimulation of PBMCs with fragments complexed to DOTAP, is at the moment, difficult to explain. Since RIG-I is expressed in the cytoplasm, the involvement of RIG-I in RNase A-derived fragments recognition is in question for PBMC cells.

6. Discussion

The ability of the host to distinguish between self and foreign nucleic acids is important for the recognition of pathogens by pattern-recognition receptors. Viral RNA has been shown to represent an immunostimulatory pattern which induces a type-I interferon response in immune cells. Under certain circumstances, eukaryotic self-RNA may reach TLR-containing endosomes allowing for self-recognition. However, several mechanisms have evolved to avoid PRR-mediated activation by self-RNA that may result in inflammatory or autoimmune responses under other circumstances. Specific modifications are known to suppress immune activation when placed in an immunostimulatory RNA.

6.1. Recognition of 2`-O-ribose methylated RNA

6.1.1. RNA modifications

Mammalian RNA contains many modified nucleosides, making them significantly less stimulatory via TLR7 and -8 than bacterial RNA (Ishii and Akira 2005; Kariko et al. 2005). In eukaryotes, the synthesis and processing of rRNAs take place in the nucleolus (Kiss-Laszlo et al. 1998). Pre-rRNA molecules undergo a series of processing steps such as nucleoside modification in order to become mature rRNA molecules. The modifications are of three prevalent types: 2`-O-ribose methylation, pseudouridylation or base-methylation (Bachellerie et al. 2002). Ribose methylations are directed by snoRNAs (small nucleolar RNAs). These are found in the nucleolus and caja bodies (conserved subnuclear organelles present in the nucleoplasm), which specify the sites to be modified through the formation of a specific duplex at the rRNA modification site, while the catalytic function is provided by a common protein enzyme, methylase or pseudouridine synthase associated with the snoRNA (Bachellerie et al. 2002). The modifications are restricted to the functionally essential regions of mature RNA (Bachellerie et al. 2002). The human 18S, 5.8 S and 28S rRNAs together carry ~ 110 2`-O-methyl groups and almost 100 pseudouridines (Kiss 2001). Nucleoside modifications directed by snoRNA guides appear dispensable for cell viability or growth in most cases. However, they are likely to play an important biological role insofar as they fine-tune a wide range of RNA-RNA and RNA-protein interactions. Methylation of 2`-hydroxyl groups may protect RNA from hydrolytic degradation, enhance hydrophobic surfaces and stabilize helical stems. Due to their

flexible C-C glycosyl bonds and increased capacity to form H-bonds, pseudouridines may contribute to RNA tertiary structure (Bachellerie et al. 2002).

6.1.2. Analysis of the immunostimulatory potential of eukaryotic and *in vitro* transcribed 18S rRNA

First, the immunostimulatory effect of eukaryotic, especially purified 18S rRNA, was examined and compared to *in vitro* transcribed 18S rRNA. It was shown that only *in vitro* transcribed 18S rRNA, but not eukaryotic-purified 18S rRNA stimulated human PBMC cells to secrete type-I interferons. In the murine system comparable results were obtained. Transfection of 18S rRNA purified from cells was not immunostimulatory or induced only low amounts of proinflammatory cytokines in human PBMC cells, whereas *in vitro* transcribed 18S rRNA induced IFN-α and IL-6 when complexed to DOTAP in a TLR7 dependent manner. Since eukaryotic “natural” rRNA contains modifications in contrast to *in vitro* transcribed rRNA, we conclude that these modifications negatively influence the stimulatory potential of rRNA for IFN-α production (Maden 1990; Kariko et al. 2005). After *in vitro* transcription of eukaryotic 18S rRNA, the generated RNA type revealed immunostimulatory activity. These results suggest that TLR7 and -8 discriminate between "self" and "foreign" RNA-molecules and that this discrimination is due to structural modifications of rRNA rather than sequence differences. However, proinflammatory cytokines such as IL-6 and TNF-α were induced by *in vitro* synthesized as well as purified 18S rRNA. Thus, we can conclude that RNA modifications have a differential influence on modulation of cytokine production.

6.1.3. Effect of modifications at the 2`-position of ribose concerning the stimulatory potential of ssRNA

Within this work, it was shown that the introduction of modified nucleotides into RNA oligonucleotides derived from eukaryotic 18S rRNA resulted in an altered type-I interferon secretion. RNA oligonucleotides containing 2`-O-methoxy residues revealed that the 2`-position of the ribose is very important for immunorecognition. Ribose-methylation abolished or at least impaired the immunostimulatory effect of GU-rich ssRNA oligonucleotides.

Only 2`-O-methoxy-modified nucleosides (and none of the other modified nucleosides) were identified as significantly reducing IFN-α secretion in human and murine immune

cells. Immune cells responded to RNA 63-mediated stimulation with IFN-α and proinflammatory cytokine production (IL-6 and TNF-α) in a TLR7 dependent manner. IFN-α induction by RNA 63-2`-O-methyl was also significantly reduced, supporting the view that TLR7-mediated IFN-α production was abrogated by the 2`-O-ribose methylation of the guanosine at position 3. However, RNA 63-2`-O-methyl induced proinflammatory cytokines in human PBMC cells but not in murine immune cells. Since murine TLR8 *per se* is non-functional, the RNA 63-driven immunostimulatory activity in murine cells is strictly TLR7-dependent. It was shown that resiquimod (R-848) and GU-rich RNA activate immune cells via human and murine TLR7 as well as human TLR8 (Hemmi et al. 2002; Jurk et al. 2002; Heil et al. 2004). Stimulation of murine immune cells derived from a TLR7-deficient mouse and genetic complementation assays in HEK293 cells revealed that only human TLR8 conferred responsiveness to R-848, whereas murine TLR8 was not active (Hemmi et al. 2002; Bauer et al. 2008). Human TLR7 is expressed in pDCs, whereas TLR8 expression is found in monocytes. The cell type-specific expression usually results in specific cytokine profiles upon TLR7 (IFN-α production from pDCs) or TLR8 (TNF-α production from monocytes) activation (Bauer et al. 2008; Tluk et al. 2009). Since human TLR7 and TLR8 differ in their target cell selectivity and cytokine induction profile, we hypothesize that RNA 63-mediated IFN-α production is TLR7 dependent, whereas production of proinflammatory cytokines such as TNF-α is dependent on human TLR8. Indeed, genetic complementation experiments in HEK293 cells demonstrated that human TLR8 induces NF-κB upon stimulation with RNA 63 and RNA 63-2`-O-methyl (unpublished data). While RNA 63-2`-O-methyl induced proinflammatory cytokines in human PBMCs, for eukaryotic-purified 18S rRNA, there was only a weak proinflammatory cytokine secretion detectable. The reason for this might be that eukaryotic RNA contains further modifications like methylated bases and pseudouridines that inhibit the induction of proinflammatory cytokines.

Tluk et al. found that, by introducing a single 2`-O-methyl modification in self-RNA (U1 snRNA, which, in contrast to other eukaryotic RNAs, contains only few modifications), the immunostimulatory potential is decreased independent of the position of the modified nucleotide (Bauer et al. 2008; Tluk et al. 2009). Other studies have described the 2`-O-ribose methylation as useful RNA modification that destroys the immunostimulatory capacity of siRNA, which is widely used to modulate gene expression (Czauderna et al. 2003; Judge et al. 2006; Sioud 2006; Cekaite et al. 2007; Sioud et al. 2007; Eberle et al. 2008). It was shown that alternating 2`-O-ribose methylation of the sense strand within a siRNA duplex destroys its immunostimulatory function in immune cells, while reduction in

target gene expression is functional. Titration experiments with 2`-O-ribose methylated ssRNA added to immunostimulatory siRNA demonstrated that 2`-O-ribose methylation even acts as an inhibitor for RNA-driven immune stimulation via TLR7. This shows that 2`-O-ribose-methylated RNA bound stronger to TLR7 than unmodified RNA (Hamm et al. 2009).

6.2. Recognition of RNA from influenza-infected cells

6.2.1. Recognition of an influenza virus infection

Historical accounts of influenza infections date back centuries, and the ever-changing nature of the influenza genome has ensured that influenza infections remain a continuing major public health problem to this day. Influenza A viruses belong to the Orthomyxoviridae family and have a segmented ssRNA genome coding for different viral proteins (Lamb and Krug 1996). Influenza viruses are unusual among RNA viruses because all viral RNA synthesis – transcription and replication - occur in the nucleus of the infected cell (Flint et al. 2004). Virus infection elicts immune responses in all cells intended to contain the spread of the virus before intervention by the adaptive immune system (Pichlmair and Reis e Sousa 2007). The route of infection determines the cell types responsible for type-I IFN production (Takeuchi and Akira 2008). Macrophages and cDCs play critical roles in IFN-α production, particularly during the course of local RNA virus infection. pDCs function when the first line of defense is broken and play an important role in the production of IFN-α during systemic IFN-α infections (Takeuchi and Akira 2007). In the following, different receptors are discussed that recognize the RNA of influenza viruses infecting different cell types.

Viral RNA is sensed by receptors belonging to the TLR and RIG-like receptors (Diebold et al. 2004; Lund et al. 2004; Kato et al. 2006). These receptors target structures that are characteristic for viral RNA, such as ds conformation (Kato et al. 2008) or the presence of an accessible 5`-triphosphate (Hornung et al. 2006). Of course, it is possible that there are additional, as yet undefined, distinguishing features, which are recognized by the innate immune system. Recognition of endogenous RNA is limited by the restriction of TLRs to endosomal compartments, which only come into contact with RNA molecules that have been taken up via the endocytotic pathway. Besides this compartmentalization, it has been shown that nucleotide modifications as they occur in eukaryotic RNA are able to reduce immunostimulation (Kariko et al. 2005; Kato et al. 2006; Kariko and Weissman

2007). Besides the aforementioned receptors, the NLRP3 inflammasome mediates host defense against influenza infection through the sensing of viral RNA (Allen et al. 2009; Ichinohe et al. 2009; Owen and Gale 2009; Thomas et al. 2009). NALP3 has also been described as a cytosolic RNA sensor for bacterial RNA (Kanneganti et al. 2006; Eberle et al. 2009). NLRs represent the largest family of PRRs in humans (Ting and Davis 2005). They are further grouped into NODs and NALPs. NOD-like (nucleotide binding oligomerization domain) receptors are implicated in the recognition of bacterial components and activate the transcription factor NF-κB (Leber et al. 2008). NALPs reside in the cytosol in an inactive form. Upon activation, NALPs form multimeric protein complexes called inflammasomes. ACS (apoptosis-associated speck-like protein) represents an essential adaptor molecule for inflammasome signaling. It subsequently leads to the activation of pro-caspase-1, which leads to the processing of pro-IL-1ß and pro-Il-18 to produce mature cytokines (Tschopp et al. 2003; Martinon et al. 2007; Martinon 2008).

Moreover, the dsRNA-activated protein kinase (PKR) has been shown to have antiviral functions. PKR is a cytoplasmic serine-threonine kinase that is ubiquitously expressed and activated by binding dsRNA. Active PKR catalyzes phosphorylation of the eukaryotic initiation factor 2 (eIF-2), which inhibits translation initiation, thus preventing pathogen replication. Activation of PKR also induces type-I interferon induction (Balachandran et al. 2000; Bergmann et al. 2000; Barchet et al. 2005).

It is notable that monocytes required CD14 for influenza A virus-induced cytokine and chemokine production (Pauligk et al. 2004). CD14 might play an important role for the IPS-dependent recognition of A/PR/8/MDCK-RNA complexed to cationic lipids or to cathelicidins. It would be interesting to analyze the influence of CD14 on the recognition of A/PR/8/MDCK-RNA in CD14-deficient immune cells.

In addition to viral RNA recognized by the immune system, virion components are also pyrogenic as virosomes depleted of RNA but including viral lipid, haemagglutinin and neuraminidase induced fever (Brydon et al. 2005).

6.2.2. Role of cathelicidins in viral infections and autoimmune diseases

The role of LL-37/CRAMP in viral infections has not been thoroughly studied. LL-37 exhibits known selective antiviral activity against vaccinia virus (Howell et al. 2004) and may have potential antiviral properties against HSV-1 (Yasin et al. 2000) and HIV-1

(Bergman et al. 2007). But its role for the immune response against the influenza virus or other RNA viruses has not been analyzed. Previous studies have indicated that the release of antimicrobial proteins by neutrophils contribute to an early host defense against influenza virus infection. Treatment of mice infected with the influenza virus with LTB4, a lipid mediator of inflammation, led rapidly to the secretion of the human cathelicidin LL-37 and further antiviral peptides from neutrophils, reducing the viral load in their lungs (Flamand et al. 2007; Gaudreault and Gosselin 2008). In this study, it was investigated if LL-37 or its mouse homolog CRAMP could function as a carrier for RNA from A/PR/8-infected MDCK cells. We found that A/PR/8/MDCK-RNA complexed to LL-37 induced a type-I interferon response in human PBMC cells, whereas a scrambled form of LL-37 (sLL-37) conferred no immune activation. Upon transfection with self-RNA, there was no IFN-α response detectable when complexed to cathelicidins. In some rare cases the IFN-α response induced by A/PR/8/MDCK-RNA complexed to cathelicidins was variable in human PBMC cells. One possible explanation for the variable IFN-α response is that it was donor-dependent. Furthermore, as discussed in section 6.2.10, we have to consider that human plasma was found to completely block the antimicrobial activity of LL-37. It is possible that a formation of a complex between LL-37 and RNA was negatively influenced by human plasma, such that sometimes only variable IFN-α responses could be detected.
Recently, it was found that self-RNA-LL-37 complexes activate in human pDCs TLR7 and trigger the secretion of IFN-α (Ganguly et al. 2009). Furthermore, it was described that self-RNA complexed to LL-37 also trigger the activation of human classical myeloid dendritic cells (mDCs). This occurs through TLR8 and leads to the production of TNF-α and IL-6. We found that self-RNA complexed to LL-37 did not induce the secretion of IFN-α in human PBMC cells, but we observed an IL-6 and TNF-α secretion. Considering that we used another cell type than Ganguly et al., the induction of proinflammatory cytokines in PBMC cells by self-RNA complexed to cathelicidins is an interesting observation. In inflammatory or autoimmune situations, a variety of nucleotide-binding proteins such as autoantibodies, antimicrobial peptides and high mobility group box 1 (HMGB-1) are complexed with self-nucleic acids. The complex of self-nucleic acids and proteins may become resistant to degradation and reach the endolysosome, thereby inducing the secretion of cytokines.

6.2.3. Monocytes are responsible for recognition of RNA from A/PR/8-infected cells

To analyze the cell type within the PBMC cells responsible for recognizing A/PR/8/MDCK-RNA complexed to cationic lipids or cathelicidins, we isolated monocytes. Little is known about the contributon of pDC-independent IFN-α production capacity of human peripheral blood. So far, TLR-expressing DCs, primarily pDCs, are known as the principal IFN-α source in the immune system. Based on the discovery of cytoplasmatic helicases like RIG-I and MDA-5, the question arose as to how much IFN-α can be produced by non-DCs in peripheral blood. Stimulation of monocytes with A/PR/8/MDCK-RNA showed that monocytes represent the cell type responsible for recognizing the A/PR/8/MDCK-RNA complexed to cationic lipids or cathelicidins. The obtained monocytes had a purity of about 90%. Since monocytes do not express TLRs like TLR9 or TLR7 (Iwasaki and Medzhitov 2004; Barchet et al. 2008), but instead express cytosolic helicases, this result might give us a first indication of the responsible receptor. In order to exclude an involvement of pDCs, which are present in very low frequency in PBMC cells (0.2-0.5%), another approach might be to isolate pDCs by either magnetic or fluorescent cell sorting and to test their immunostimulatory ability upon stimulation with A/PR/8/MDCK-RNA complexed to cationic lipids or cathelicidins. Recent studies have already shown that human monocytes are highly susceptible to influenza A virus infection and release different cytokines like TNF-α, IL-6 and IFN-α (Nain et al. 1990; Kaufmann et al. 2001). Hansmann et al. were able to show that monocytes are the main IFN-α source after Poly (I:C)/DOTAP stimulation, suggesting that monocytes might represent an underestimated source of IFN-α in human peripheral blood (Hansmann et al. 2008).

6.2.4. Features of RNA from virus-infected cells which are important for induction of IFN-α

Contribution of the terminal 5`-triphosphate of RNA for RIG-I signaling

Previous studies have indicated that the 5`-triphosphate is a structural feature responsible for IFN-α-inducing activity of *in vitro* transcribed RNA and flu vRNA in monocytes, bone marrow-derived DCs and HEK293 cells transfected with IFN-ß reporter.

Dephosphorylation of the 5`-triphosphate end completely abrogated the IFN-α response in the aforementioned cells. However, pDCs showed no decrease in IFN-α secretion upon dephosphorylation of oligonucleotides. Triphosphate RNA-mediated IFN-α induction neither required endosomal maturation nor TLR7 (Hornung et al. 2006; Pichlmair et al. 2006).

Our findings showed that the 5`-triphosphate end of A/PR/8/MDCK-RNA complexed to DOTAP or Lipofectamine 2000 was important for inducing IFN-α in murine immune cells. Dephosphorylation of the A/PR/8/MDCK-RNA reduced signaling, suggesting that RIG-I senses the A/PR/8/MDCK-RNA in a 5`-triphosphate dependent manner in Flt3-derived dendritic cells. For the RIG-I ligand 5`-3P RNA complexed to Lipofectamine 2000, we observed the same behaviour as for A/PR/8/MDCK-RNA; the IFN-α induction was 5`-triphosphate dependent.

However, for human PBMC cells we observed only a minor decrease in the IFN-α response upon dephosphorylation of A/PR/8/MDCK-RNA complexed to DOTAP or Lipofectamine 2000. In contrast, for the RIG-I ligand 5`-3P RNA complexed to Lipofectamine 2000, the IFN-α response was abrogated upon dephosphorylation. We hypothesize that human immune cells express more RIG-I proteins than murine immune cells, so that in the human system a higher number of putative binding sites between RIG-I and the A/PR/8/MDCK-RNA are available, and the 5`-triphosphate end is no longer important for interaction. For the RIG-I ligand 5`-3P RNA, the nucleic acid length from 100 bp is not sufficient in order to have interactions with RIG-I proteins in a 5`-triphosphate independent way. Another possibility is that the murine RIG-I molecule and the human RIG-I molecule are different in the dependency of the 5`-triphosphate end. But the results obtained with the RIG-I ligand 5`-3P RNA complexed to Lipfectamine 2000 argue against the idea that the murine and the human RIG-I molecules behave differently as regards the 5`-triphosphate ends.

In untransfected HEK293 cells, the immune response to A/PR/8/MDCK-RNA complexed to DOTAP or Lipofectamine 2000 was abrogated after dephosphorylation, whereas in RIG-I-transfected HEK293 cells dephosphorylation of A/PR/8/MDCK-RNA had no influence. The RIG-I ligand 5`-3P RNA complexed to Lipofectamine 2000 induced IFN-ß activation only in RIG-I-transfected HEK293 cells, and the IFN-ß response was diminished after dephosphorylation. It seems that the A/PR/8-infected MDCK-RNA shows more putative binding sites even for only lowly expressed RIG-I proteins in untransfected HEK293 cells than the RIG-I ligand 5`-3P RNA. As discussed for PBMCs, we hypothesize that immune cells expressing more RIG-I proteins contain a higher number of putative

binding sites for the ligands and that, in this case, the 5`-triphosphate end is not important for recognition of the RNA through RIG-I. But further experiments are required, like radioactive labeling of the RNAs to prove that the phosphate group was efficiently removed.

Influence of the ds character of RNA for RIG-I signaling

The "panhandle" conformation of the A/PR/8/MDCK-RNA represents a second independent target structure for RIG-I signaling. Schmidt et al. have found that RIG-I ligands require base-paired structures in conjugation with a free 5`-triphosphate to trigger a type-I interferon response (Schmidt et al. 2009). We could show that immunostimulatory RNA from virus-infected cells was sensitive to ds- but not ss-specific RNases. The ds-specific RNase III abolished signaling of A/PR/8/MDCK-RNA complexed to DOTAP or Lipofectamine 2000 in human and murine immune cells, which indicates that the A/PR/8/MDCK-RNA contain base-paired regions.

In the past, most studies suggested that single-stranded 5`-triphosphate RNA is sufficient to bind to and activate RIG-I (Pichlmair et al. 2006). These studies used *in vitro* transcription for generation of 5`-triphosphate RNA without analyzing the purity of those RNA molecules. In fact, an unintended formation of dsRNA is the cause of RIG-I activity of the *in vitro* transcribed RNA (Schlee et al. 2009; Schmidt et al. 2009). Even for negative-strand RNA viruses known to activate RIG-I, it was shown by Schlee et al. that they contain 5` and 3` sequences that form a short ds with a perfect blunt end (panhandle) (Schlee et al. 2009). Interestingly, Myong et al. showed that RIG-I translocates on synthetic double-stranded RNA molecules and that this movement is enhanced in the presence of 5`-triphosphate (Myong et al. 2009). Some studies suggested that for ssRNA-viruses no dsRNA can be detected (Hornung et al. 2006; Pichlmair et al. 2006; Weber et al. 2006). However, the antibody used to demonstrate the absence of dsRNA (Weber et al. 2006) is limited to the detection of dsRNA longer than 40 bases (Bonin et al. 2000; Schlee et al. 2009). In contrast, other studies demonstrated that the most widely postulated triggers for cytokine induction on influenza virus infection are dsRNA intermediates produced during replication (Jacobs and Langland 1996; Majde 2000). Long dsRNA molecules are absent from uninfected cells. Madje et al. showed that dsRNA is released from dying influenza virus-infected cells (Majde et al. 1998).

Comparing the ligands A/PR/8/MDCK-RNA and the RIG-I ligand 5`-3P RNA in human PBMC cells with regard to the features important for recognition, we observed the

following: For A/PR/8/MDCK-RNA complexed to DOTAP or Lipofectamine 2000, phosphatase treatment had no influence on the IFN-α-inducing ability, but cleavage with the ds-specific RNase III abrogated IFN-α secretion in human PBMC cells. This shows that, for the recognition of RNA from virus-infected cells, the ds character or at least a "panhandle" conformation by pairing complementary 5` and 3` ends is important. In contrast, for the RIG-I ligand 5`-3P RNA complexed to DOTAP or Lipofectamine 2000, only the 5`-triphosphate seemd to be important, whereas treatment with the ds-specific RNase III had no influence for IFN-α secretion in human PBMC cells. A possible explanation is that for longer ligands the ds character is sufficient to induce IFN-α, and even after phosphatase treatment they remain immunostimulatory. In contrast, shorter ligands like the RIG-I ligand 5`-3P RNA need a 5`-triphosphate end for IFN-α secretion. At the moment, it is not clear whether dsRNA or hairpin dsRNA regions of the virus-infected RNA are responsible for inducing IFN-α. It is also possible that the RIG-I ligand 5`-3P RNA shows hairpin dsRNA regions, but that for inducing IFN-α a 5`-triphosphate end is necessary. Thus, we conclude that for the ligands A/PR/8/MDCK-RNA and RIG-I ligand 5`-3P RNA two important features for RIG-I signaling are necessary: the ds character and the 5`-triphosphate end. On the other hand, some studies indicate that RNase III cuts ssRNA specifically and seems to degrade dsRNA rather nonspecifically (Dunn 1976). In contrast, Sun et al. demonstrated that RNase III retains strict specificity for dsRNA (Sun et al. 2001). At the moment, it is not clear whether RNase III is a ds-specific RNase. Further analysis is required in order to prove that the ds character of the A/PR/8/MDCK-RNA is responsible for inducing IFN-α.

6.2.5. TLR-independent recognition of A/PR/8/MDCK-RNA

It is possible that ssRNA from viruses is recognized through the receptors TLR7 and/or TLR8 (Diebold et al. 2004; Heil et al. 2004). IFN-α production by pDCs from TLR7-deficient mice is impaired after infection with influenza virus or vesicular stomatitis virus (VSV) (Diebold et al. 2004; Lund et al. 2004). In this study, it was shown that A/PR/8/MDCK-RNA was recognized in a TLR7-independent way in Flt3-derived DCs, which consists of pDCs and cDCs. By using Flt3-derived DCs from TLR7- and MyD88-deficient mice and GM-CSF-derived DCs from MyD88-deficient mice, we showed that IFN-α secretion upon transfection of A/PR/8/MDCK-RNA complexed to cationic lipids or cathelicidins was not reduced in comparison to wild-type DCs. TLR7 does not seem to play an essential role in the innate immune response to RNA virus infection *in vivo.* There is not a significant difference between MyD88 $^{-/-}$ and wild-type mice in the susceptibility to

intranasal influenza virus infection and type-I IFN response (Barchet et al. 2005; Eisenacher et al. 2007).

The dsRNA-sensing TLR3 is localized in endosomes and is preferentially expressed in phagocytic cells. Thus, it is possible that after dendritic cells take up apoptotic bodies of virus-infected cells, dsRNAs are delivered into vesicles, where they are recognized by TLR3. Moreover, TLR3 is expressed on pulmonary epithelial cells and contributes to the immune response of respiratory epithelial cells (Guillot et al. 2005). Upon infection with influenza A virus in a TLR3-dependent manner, human lung epithelial cells express proinflammatory cytokines including IL-6 and IL-8 (Le Goffic et al. 2007). In this study, it was shown that A/PR/8/MDCK-RNA was recognized in a TLR3-independent way in murine immune cells. By using murine macrophages from TLR3-deficient mice, we demonstrated that IFN-α and IFN-ß secretion upon transfection of A/PR/8/MDCK-RNA complexed to DOTAP or Lipofectamine 2000 was not reduced in comparison to wild-type macrophages. Murine macrophages were chosen because murine pDCs do not express TLR3. The unaltered course and pathogenesis of influenza- and other negative-strand RNA virus infections in TLR3 $^{-/-}$ and MyD88 $^{-/-}$ mice (Edelmann et al. 2004; Lopez et al. 2004; Barchet et al. 2005) also argues against such a generalized role for TLRs as antiviral effectors. In addition, plasmacytoid dendritic cells (pDCs), which do not express TLR3, when isolated from the bone marrow of mice and infected *in vitro* with the influenza A virus, were found to secrete wild-type levels of IFN-α (Lund et al. 2004). The fact that GM-CSF-derived DCs and macrophages can be induced to produce IFN-α in response to RNA from virus-infected cells shows that this IFN-α response is mediated via TLR7 and TLR9 independent pathways (Fancke et al. 2008).

6.2.6. IPS-dependent recognition of A/PR/8/MDCK-RNA

It was found that the ubiquitously expressed RNA helicases play essential roles in the recognition of RNA viruses in various cell types, such as fibroblasts and conventional dendritic cells (cDCs) (Takeuchi and Akira 2008). The critical role of RIG-I in influenza A virus infection of epithelial cells was also shown (Siren et al. 2006; Le Goffic et al. 2007; Opitz et al. 2007). In this study, it could be shown that A/PR/8/MDCK-RNA was recognized in a RIG-I dependent way. The cytosolic helicase RIG-I is a key sensor of viral infections and is activated by RNA containing a triphosphate at the 5`-end (Hornung et al. 2006). However, the exact structure of RNA-activating RIG-I remains controversial (Schlee et al. 2009). By using Flt3-derived dendritic cells from IPS-deficient mice, which is an important adaptor molecule for RIG-I or MDA-5 signaling, we observed that IFN-α

secretion upon transfection of A/PR/8/MDCK-RNA complexed to cationic lipids or cathelicidins was significantly reduced in comparison to wild-type dendritic cells. We could rule out MDA-5 as a possible receptor for A/PR/8/MDCK-RNA complexed to cationic lipids or cathelicidins by using Flt3-derived DCs and bone-marrow derived DCs from MDA-5-deficient mice. Stimulation of HEK293 cells overexpressing RIG-I with A/PR/8/MDCK-RNA complexed to DOTAP or Lipofectamine 2000 resulted in a strongly enhanced IFN-ß response in comparison to untransfected HEK293 cells. In contrast, A/PR/8/MDCK-RNA complexed to LL-37 induced no detectable IFN-ß activation in RIG-I-transfected HEK293 cells, despite appropriate positive controls, which suggested either that the HEK293 cells lack some cofactor specifically required for A/PR/8/MDCK-RNA complexed to LL-37-induced activation of IFN-ß, or that the IFN-ß luciferase reporter used for these assay might be not sensitiv enough to detect the A/PR/8/MDCK-RNA complexed to LL-37.

In order to further prove the involvement of RIG-I for the recognition of A/PR/8/MDCK-RNA complexed to cationic lipids or cathelicidins, an analysis of immune activation of cells from RIG-I-deficient mice is necessary. But as mentioned earlier, RIG-I-deficient cells were not available at the time.

It is still not known which viral RNAs are sensed by RIG-I during influenza infection. Influenza virus RNA can trigger RIG-I activation *in vitro*, but it is difficult to explain how this happens during infection when the genome segments are coated by viral nucleoproteins and have the viral polymerase bound to their 5`-ends (Lamb and Krug 1996). For RIG-I to interact with the genome and the critical 5`-triphosphate moiety, these viral proteins need either to be displaced or to dissociate from the vRNA. The former process could be facilitated by the ATP-driven helicase activity of RIG-I, whereas the latter may occur naturally as part of an equilibrium reaction (Takahasi et al. 2008). A recent study observed that viral genomes are the major trigger for RIG-I in cells infected with negative-sense single-stranded RNA viruses (Rehwinkel et al. 2010).

6.2.7. Escape mechanism of viruses

Viruses have developed different strategies to evade or inhibit key elements of antiviral immunity. The nonstructural protein 1 (NS1) of some strains of the influenza virus possesses a dsRNA-binding site and sequesters dsRNA (Min and Krug 2006; Hale et al. 2008). However, this site also allows binding to ssRNA and the formation of a complex with RIG-I in the presence of 5`-triphosphate RNA (Pichlmair and Reis e Sousa 2007). This suggests that NS1 protein blocks type-I IFN induction by targeting RIG-I (Guo et al. 2007; Mibayashi et al. 2007; Opitz et al. 2007). Recently, it was shown that the influenza

A virus nonstructural protein 1 (NS1) specifically inhibits TRIM25-mediated RIG-I CARD ubiquitination, thereby suppressing RIG-I signal transduction (Gack et al. 2009).
For some negative-strand RNA viruses (e.g., Hantaan virus, Crimean-Congo hemorrhagic fever virus and Borna disease virus), it was shown that they process the 5`-termini to avoid RIG-I-dependent interferon induction (Habjan et al. 2008).

6.2.8. Localization studies of RNA/LL-37 complexes

We have performed localization studies of RNA/LL-37 complexes in human monocytes using biotinylated LL-37 (4.8). These experiments demonstrated that LL-37 complexes localized to the endosome (EEA-1 positive) and to the lysosome (Lamp positive). Of note is that we observed only the biotinylated LL-37 in the cells. We do not know if the complexes of LL-37 and the RNA could be detected in the endosome and the lysosome, or if the RNA was released earlier from the complex. This analysis has to be further extended to various human and murine immune cells, including tracking of fluorescence-labeled RNA.
A recent study showed that LL-37 retains DNA in the early endocytic compartments of pDCs (Lande et al. 2007). In contrast, another group showed that LL-37 transfers bacterial DNA to the nuclei of mammalian host cells (Sandgren et al. 2004). In this context, the influence of serum on the localization of LL-37 was discussed. It was shown that, in the absence of serum, LL-37 became localized to the nucleus in epithelial cells. When LL-37 was observed in the presence of human serum, it was only detected in cell-associated aggregates (Lau et al. 2006).
However, the localization of DOTAP and cathelicidins to early endosomal/lysosomal compartments does not currently explain how endosomally delivered RNA triggers an IPS-1 dependent signaling pathway there (Yasuda et al. 2005). Since RIG-I is expressed in the cytoplasm and has no access to the endosome, the involvement of RIG-I in RNA recognition is questionable. However, small amounts of RNA transported from the endosome in the cytoplasm might be sufficient for inducing an RIG-I dependent immune signaling. Moreover, it can be postulated that an unidentified IPS-dependent receptor may localize to the endosome and recognize immunostimulatory RNA. Alternatively, a previously unrecognized localization for RIG-I in the endosome is a possibility. The involvement of RIG-I has to be clarified through analysis of immune cells from RIG-I-deficient mice. Another possibility is that DOTAP transfers nucleic acids not only to the endosome, but also to the cytoplasm. For cationic liposomes, it was shown that the complex initiates a destabilization of the endosomal membrane that results in a flip-flop of

anionic lipids that are predominately located on the cytoplasmic face of the membrane. The anionic lipids laterally diffuse into the complex and form charge-neutralized ion pairs with cationic lipids. This displaces the ODN from the complex and the ODN can diffuse into the cytoplasm (Xu and Szoka 1996; Zelphati and Szoka 1996). For the transfection reagent Lipofectamine 2000, which delivers nucleic acids to the cytoplasm where RIG-I and MDA-5 reside, an IPS-dependent recognition of the A/PR/8/MDCK-RNA is comprehensible. Further localization studies with fluorescence-labeled RNA and biotinylated LL-37 will clarify where the cathelicidin/RNA complexes are transferred.

6.2.9. Immunization with natural carrier for RNA

Because RNA is prone to hydrolysis, RNA molecules have to be protected from degradation through interaction with liposomes. Since DOTAP is toxic, we analyzed if cathelicidins could function as a carrier in vaccine formulations. Previous studies have shown the adjuvant function of RNA complexed to the cationic transfection reagent DOTAP (Heil et al. 2004; Hamm et al. 2007). Cathelicidins have potent *in vivo* immunoenhancing effects that make them useful as vaccine adjuvants. CRAMP could enhance antigen-specific immune response to ovalbumin, a commonly used experimental model antigen (Kurosaka et al. 2005). In the present study, it was analyzed whether a mixture of RNA combined with ovalbumin complexed to CRAMP (4.11) can serve as a vaccine formulation in subcutaneous injections. Immunization of ovalbumin together with CRAMP enhanced ovalbumin-specific IgG antibody response compared to the immunization with ovalbumin alone. In the combination of the different RNAs, either uninfected self-MDCK-RNA or A/PR/8/MDCK-RNA, there was an increase in the ovalbumin-specific IgG antibody response detectable. Further studies should analyze if, by varying the CRAMP concentration, an increase in the IgG antibody response is measurable. Induction of cytotoxic T cells has to be analyzed by staining spleen cells with ovalbumin-peptide-specific tetramers. The antigenic ovalbumin-peptide is presented via MHC molecules and has the sequence SIINFEKL.
Since cathelicidins interact with the immune system receptors involved in chemotaxis and IL-1ß release (De et al. 2000; Elssner et al. 2004), it is important to study the contribution of cathelicidins to gene expression in a vaccine formulation. Its influence on gene expression (Affymetrix gene arrays) has to be analyzed and the cytokine production in primary immune cells or fibroblasts with cathelicidin/RNA complexes has to be compared to the induction patterns of DOTAP/RNA complexes.

6.2.10. Relevance of LL-37/RNA complexes and the influence of the microenvironment

In the experiments we performed, cathelicidin/RNA complexes are formed *in vitro* and then added to the cells. In order to assess the *in vivo* role of cathelicidin/RNA complexes, it is important to consider facts like the concentrations and the activity of the cathelicidins *in vivo.* Since LL-37 is cytotoxic at high concentrations, there is a need for tight control of the release of this peptide (Johansson et al. 1998). In plasma, the concentration of LL-37 is measured by ELISA to be 1.18 µg/ml (Sorensen et al. 1997). The microenvironment is critical for the activities of antimicrobial peptides (Gudmundsson and Agerberth 1999). Interestingly, human plasma is found to completely block the antimicrobial activity of LL-37, and apolipoprotein A-I is identified as the scavenger of LL-37 (Wang et al. 1998; Sorensen et al. 1999). The serum components provide a physiological mechanism to protect blood cells from potentially harmful effects of the peptide (Zanetti 2005).

In water, LL-37 exhibits a disordered structure. In physiological salt solutions, LL-37 forms a stable α-helical structure. The extent of helicity correlates with the antibacterial activity (Johansson et al. 1998). The ability of LL-37 to form α-helical aggregates can be rationalized by the Hofmeister effect. Here, the increasing ionic strength of the solvent makes it more and more unfavourable for the peptide to expose hydrophobic faces (Durr et al. 2006). The main determinants for the folding are certain anions as SO_4^-, HCO_3^-, and $CFOO^-$. In contrast, the Cl^- anion and cations have much less effect on the folding (Johansson et al. 1998). But it is observed that cathelicidins lose antimicrobial activity *in vitro* with the addition of physiological NaCl concentrations (Dorschner et al. 2006). In cystic fibrosis (CF), antimicrobial peptides are deactivated by increased salt concentrations because of a defective ion channel (Bals 2000; Bals and Hiemstra 2004). Gene transfer resulting in four-fold overexpression of LL-37 in a cystic fibrosis xenograft model succeeded in restoring bacterial killing to normal levels, suggesting that LL-37 may protect against bacterial lung infections and providing a possible therapeutic strategy for such infections (Bals et al. 1999). Ganguly et al. have found that RNA/LL-37 complexes are rapidly dissolved by the addition of sodium chloride (Ganguly et al. 2009). The influence of the microenvironment concerning the cathelicidin activity, make it difficult to judge the role of cathelidin/RNA complexes *in vivo,* for example in viral defense.

To further analyze the role of cathelicidins for the immune response against the influenza virus and other RNA viruses, wild-type and CRAMP-deficient mice should be intranasally infected with sublethal and lethal doses of A/PR/8, and survival, weight loss and influenza

titers in the lung should be analyzed. Since we hypothesize that cathelicidins are involved in RNA-mediated immune stimulation upon viral infection, this would demonstrate whether or not synthetic CRAMP reconstitutes an effective immune response in CRAMP-deficient mice and accelerates the anti-influenza immune response in wild-type mice.

6.3. Immunorecognition of self-RNA

6.3.1. Discrimination of self- versus non-self-nucleic acids

For DNA, CpG motifs in eukaryotic DNA have been identified (Bird 1986; Krieg et al. 1995). For rRNA, the major constituent of total cellular RNA, known modifications include modified nucleotides such as conversion of uridine to pseudouridine, methylation of 2`-hydroxyls (2`-O-methylation) and methylation of bases at different positions (Maden 1990; Decatur and Fournier 2003). However, the overall frequency of 2`-O-methylated bases is rather low and the distribution is not random (Maden 1990). These nucleic acid modifications of DNA and RNA represent a structural feature, which enables the immune system to distinguish self from non-self-nucleic acids (Krieg 2002; Diebold et al. 2004; Heil et al. 2004; Ganguly et al. 2009). However, it has recently become clear that this discrimination is primarily achieved by the intracellular localization of the TLRs, which allows the recognition of viral nucleic acids released into endosomal compartments (Barton et al. 2006). In contrast, self-nucleic acids are rapidly degraded in the extracellular environment and fail to access endosomal compartments (Barton et al. 2006). A possible exception to this situation may be the case of apoptotic cells, which might protect RNA from extracellular degradation and deliver it to the endosomes of phagocytes (Diebold et al. 2006).

Thus, responses to extracellular self-RNA are normally prevented by the endosomal seclusion of nucleic acid-recognizing Toll-like receptors (TLRs). The question arises as to whether self-nucleic acids can become a potent trigger of pDC activation when aberrantly transported into TLR-containing endosomes. Recently, it was found that self-RNA complexed to LL-37 activates TLR7 and triggers the secretion of IFN-α (Ganguly et al. 2009). Diebold et al. showed that both viral and self-RNA can trigger TLR7 activation equally efficiently, if delivered to endosomes. This suggests that TLR7 discriminates between viral and self-ligands on the basis of endosomal accessibility and uracil content

rather than sequence (Diebold et al. 2006). Also for DNA, the concept of self- versus non-self discrimination based on the presence of unmethylated CpG motifs was changed (Haas et al. 2008). Although synthetic phosphothioate DNA depends on unmethylated CpG motifs to induce TLR9 activation, phosphodiester DNA depends on the 2`-deoxyribose backbone. The ability for phosphodiester DNA to activate TLR9 depends on the formation of multimeric aggragates, indicated by the finding that eukaryotic DNA becomes immunostimulatory under certain circumstances that promote efficient DNA uptake such as DNA/antibody immune complexes, transfection or complexation to the antimicrobial peptide LL-37 (Boule et al. 2004; Lande et al. 2007). Recently, it was shown that a chimeric TLR9 that localized to the cell surface is able to recognize self-DNA which does not stimulate endosomal TLR9 (Barton et al. 2006).

We can conclude that both modification of the nucleic acid and compartimentalization of the receptor allow one to discriminate self versus non-self-nucleic acids in concert.

6.3.2. RNase treatment of self-RNAs

For the first time, we were able to show that immunologically inert self-RNA can be converted to immunostimulatory RNA by treatment with RNase A and that it is as immunostimulatory as RNA from virus-infected cells. It is already described how cellular RNA serves as a ligand that stimulates the RLR pathway during viral infection. Viral RNA stimulates 2`-5` oligoadenylate synthetase (2`-5` OAS) to promote activation of an endonuclease, RNase L, which subsequently cleaves self-RNA to make small RNA species. The cleaved RNA, which contains a 3`-monophosphate group, serves as the ligand for RIG-I and MDA-5 to initiate signaling leading to type-I IFN production (Malathi et al. 2007; Silverman 2007). These observations suggest that this RLR-mediated recognition may be a host defense mechanism to efficiently amplify type-I IFN responses (Kawai and Akira 2008).

Normally, it is found that RNase A, which cleaves both ssRNA and dsRNA at pyrimidine residues in low salt conditions, leads to the complete degradation and loss of activity of RNA (Libonati et al. 1980; Libonati and Sorrentino 1992; Aksoy et al. 2005).

In our current work, we tested self-RNAs of different species upon partial RNase A treatment for their immunostimulatory potential. The RNA preparations were formulated with DOTAP to increase endosomal delivery and Lipofectamine 2000 to ensure cytoplasmatic translocation and were tested for immune stimulation. Furthermore, phenol/chlororform purification of RNase-derived fragments showed no reduction of the immunostimulatory potential indicating that putative contaminations did not play a role for

recognition. We observed that RNA fragments of 20 to 100 bp derived by RNase A treatment of self-RNA complexed to DOTAP induced a type-I interferon response in human PBMCs, whereas the generated fragments complexed to Lipofectamine 2000 or alone induced no immune activation. Since DOTAP transfers the nucleic acids to the endosome, an endosomal receptor should be responsible for recognition of the RNase A-derived fragments. It seemed that the IFN-α response to the RNase A-derived fragments depends on the aberrant transport into endosomes, since the RNase A-derived fragments induced an immune activation only in combination with DOTAP but not alone or with Lipofectamine 2000. However, for different untreated RNA types complexed to DOTAP, there was an IFN-α response detectable when using them in a concentration range of 2 µg/ml. The reason for this phenomenon is unclear at the moment, especially as to why there was only an immune induction when using them in a concentration range of 2 µg/ml. This immune induction was only achieved in combination with DOTAP but not when given alone. Therefore, it must depend on an aberrant transport into the endosome. Ganguly et al. found that self-RNA-DOTAP and self-RNA-LL-37 complexes activate TLR8 by using HEK293 cells transfected with TLR8 (Ganguly et al. 2009). This finding might explain why self-RNA complexes only induce an immune activation in human PBMC cells and not in murine immune cells, which express only a non-functional TLR8. In addition, we observed that the RNase A-derived fragments complexed to cathelicidins induced no immune activation on PBMC cells. Since cathelicinds are already described for transferring nucleic acids to endosomal compartments, it is unknown why these RNA/cathelicitin complexes induce no IFN-α. It is possible that the size of the fragments generated by RNase treatment is too small for complexation to cathelicidins, since RNA 40 (20 bp) complexed to cathelicindis was also not able to induce IFN-α in human PBMC cells (data not shown).

Gel analysis revealed that the self-RNA was only partially digested. Upon complete digestion of self-RNA, there was no immune activation in human PBMC cells. A kinetic experiment showed that stimulatory fragments were even generated upon treatment with RNase A for only one minute. For complete degradation of the self-RNA, we had to add a higher amount of RNase A; a mere increase in time was not sufficient. The question arises as to whether the remained fragments are modified in such a manner that they become resistant for further cleavage by RNase A.

As the source of self-RNAs (either cancer cell lines or primary cells) did not play any role in the immunostimulatory potential of the RNase A-derived fragments, we concluded that the immunostimulatory capacity of the RNase A-derived fragments depends on the RNA itself and is not associated, for example, to the RNA of cancer cells.

In section 5.1, the impact of natural occurring modifications in ribosomal RNA on its TLR-dependent immune effects was investigated. Other studies might show that, for TLR7 signaling, 2`-modified RNA suppresses RNA immune activation even when co-incubated with a stimulatory unmodified RNA. Upon RNase A treatment of self-RNA, the digest contains a mixture of unmodified stimulatory self-RNAs and modified non-stimulatory self-RNAs. Since we think that the recognition of the generated self-RNA fragments depends on cytoplasmic receptors like RIG-I and MDA-5, the influence of RNA modifications on the activation of cytoplasmic receptors such as RIG-I and MDA-5 have to be further investigated. It is already discussed the fact that RNA modifications such as base-methylation, pseudouridine and 2´-O-methyl ribose as described in section 6.1.1 decrease RIG-I stimulatory activity when incorporated into 5`-triphosphate RNA oligonucleotides (Hornung et al. 2006).

The question arose regarding whether the IFN-α-inducing ability of RNase-derived fragments is due to the presence of foreign nucleic acids. A recent study showed a striking viral inhibition by heterologous RNA with a smaller inhibition than with homologous RNA, suggesting that the IFN-α production occurs as a reaction of cells to foreign nucleic acids (Rotem et al. 1963). In order to exclude the possibility of foreign nucleic acids for the IFN-α inducing ability of RNase A-derived fragments it should be analyzed whether or not RNA fragments from one PBMC donor also induce IFN-α on PBMC cells from the same donor.

6.3.3. Fragments generated by different techniques

The sites attacked in the RNA molecules by various treatments are expected to be different, corresponding to the different specifities of the enzymes and the basically different mode of action like ultrasonication or hydrolysis by metals. Although the degradation products were always heterodisperse, conditions could be controlled so as to yield breakdown within a given size range. This was checked in each experiment by agarose gel electrophoresis.

The various ss-specific ribonuclease types we tested generated different ends for the RNA fragments. Ribonucleases that hydrolyze RNA to 3`-phosphomonoester via 2`,3`-cyclic nucleosides are RNase A, RNase T1, and RNase T2 (Deshpande and Shankar 2002). Most ribonucleases cleave only after specific residues. Since RNase A specifically degrades RNA at C and U residues by cleaving the phosphodiester bond between the 5`-ribose of a nucleotide and the phosphate group attached to the 3`-ribose of an adjacent

pyrimidine nucleotide, certain RNA sequences should be enriched in the partial digest. But considering the ability of RNase I to degrade ssRNA to individual nucleoside 3`-monophosphates by cleaving every phosphodiester bond; it can be concluded that special sequences enriched in the partial digest are not responsible for the IFN-α inducing ability. Treatment with all the aforementioned ss-specific ribonuclease types resulted in the fragmentation of self-RNAs and the generation of immunostimulatory fragments when complexed to DOTAP on human PBMC cells. Only treatment with the ds-specific RNase III did not lead to RNA degradation and generation of immunostimulatory self-RNA.

Besides these nucleases, we tested the ribonucleases S1 from Aspergillus oryzae (Desai and Shankar 2003) and the P1 nuclease from Penicillium citrinum (Desai and Shankar 2003) that hydrolyze RNA to 5`-phosphomonoester. They generated fragments that induce a lower IFN-α response by PBMC cells. Furthermore, we have also to consider donor-dependent effects. For fragments generated by Benzonase, a nuclease which degrades both DNA and RNA, whether ss or ds, and shows no base preference, there was no IFN-α response detectable.

In conclusion, there was an IFN-α response detectable upon treatment with all the RNase types generating 3`-phosphate as well as 5`-phosphate ends on human PBMC cells. The IFN-α response seemed to be independent from the phosphate end. Dephosphorylation of the fragments showed no influence concerning the IFN-α response, suggesting that the recognition of the RNase-derived fragments was not mediated through phosphate ends at least in human PBMC cells. But consider the results for A/PR/8/MDCK-RNA from section 5.2, which showed no influence upon dephosphorylation for the immunostimulatory potential in human PBMC cells, whereas in murine cells and untransfected HEK293 cells the IFN-α response was abrogated upon dephosphorylation. This fact leaves it open as to whether RNase A-derived fragments would show a changed immunostimulatory potential in other immune cells upon dephosphorylation. In addition, we have to consider that we had no control for effective dephosphorylation. In the future, radioactive experiments will be necessary in order to show that the phosphate group is removed completely.

Fragments generated by ultrasonic treatment of self-RNA were not able to induce an IFN-α response when complexed to DOTAP in human PBMCs. Through intermolecular cleavage at the phosphodiester internucleoside linkage, the RNAs undergo chain shortening (Meidan et al. 1997). Ultrasonic degradation of DNA results in DNA fragments of 100-500 bp with a phosphorylated 5`-end and a free alcohol at the 3`-end (Elsner and Lindblad 1989). With increases in time for ultrasonic treatment of the self-RNAs, the generated fragments became smaller, reaching 100-500 bp. Although they were not in the

size range of the RNase A-derived fragments (20-100 bp), it seems that fragment size is not an important feature to induce IFN-α. It is remarkable that the IFN-α response induced by untreated self-RNAs in a concentration range of 2 µg/ml was reduced both with the increase of ultrasonic treatment and with RNase III treatment. It is possible that through the degradation of the self-RNA the structure responsible for inducing IFN-α is destroyed. We hypothezise that ultrasound treatment and incubation with the ds-specific RNase III destroyed the double-stranded structure of RNA. In the literature, self-RNA molecules, in particular those rich in uridine and guanosine and those in small nuclear ribonucleoprotein (snRNP), were shown to trigger pDCs to produce type I IFNs through TLR7 when delivered to endosomes by DOTAP at a concentration range of 3-10 µg/ml (Vollmer et al. 2005; Savarese et al. 2006). For mRNA complexed to PEI at a concentration range of 0.3-1 µg/ml an immune induction was also observed. Our experiments showed for the first time that a ds character of self-RNA or at least intermolecular secondary structures of self-RNA might be responsible for immune recognition. DsRNA is found only in minute amounts in normal cells and represents a danger signal when aberrantly transferred to the endosome (Majde et al. 1998; Weber et al. 2006). Edy et al. showed that fragmentation of double-stranded RNA either by RNase A, RNase III treatment or ultrasonic irradiation led to a significant fall in the capacity of RNA to induce the formation of circulatory interferon in the mice (Edy et al. 1974).

The IFN-α-inducing activity of self-RNA at a concentration of 2 µg/ml, which can not be observed for further higher or lower concentrations, can be described by a Heidelberger curve. Also for titration of A/PR/8/MDCK-RNA a Heidelberger curve could be observed (data not shown). Complexation of an increasing amount of nucleic acids led to a decrease in the initial zeta potential value of liposomes, and this influenced the transfection efficiency of the liposomes (Almofti et al. 2003). A change in the zeta potential upon forming different charge ratios of nucleic acids to liposomes might explain the Heidelberger curve. Moreover, a change in the zeta potential might also be a reason for self-RNA becoming immunostimulatory upon RNase A treatment.

Fragments generated by metal-induced hydrolysis of self-RNAs showed the same size as RNase A-derived fragments. For fragments derived by Zn^{2+}-induced hydrolysis, there was no IFN-α response detectable when complexed to DOTAP in human PBMCs. However, for fragments derived by Pb^{2+}-induced hydrolysis, there was an IFN-α response detectable when complexed to DOTAP in human PBMC cells. It is difficult to explain the different behaviour of the fragments generated by metal-ion induced hydrolysis. Pb^{2+}-induced cleavage occurs preferentially in bulges, loops and other ssRNA regions (Hartmann et al.

2005). Since Zn^{2+} is a component of the single-stranded specific enzymes S1 nuclease and P1 nuclease (McCall et al. 2000), we can conclude that Zn^{2+} like Pb^{2+}, preferentially cleaves ssRNA. Both metal ions might cleave the phosphodiester bond by generating a 2`,3`-cyclic phosphate and 5`-hydroxyl groups as cleavage products (Matsuo et al. 1995; Yashiro et al. 2002; Hartmann et al. 2005; Wang et al. 2007). Thus, Pb^{2+} and Zn^{2+} behave in a similar way concerning the cleavage of RNA.

A further question arises as to whether fragments derived by ultrasonic treatment or Zn^{2+}-induced hydrolysis really do not show any stimulatory potential in PBMC cells. Further concentrations of the fragments need to be tested. In addition, it should be controlled regarding whether or not they induce an immune response when complexed to Lipofectamine 2000. Moreover, a novel method has to be developed in order to analyze and compare the different ends of the fragments generated by the different techniques. It has to be analyzed what makes the difference between the fragments generated by Pb^{2+} and Zn^{2+}-induced hydrolysis.

The removal of the 2`,3`-cyclic phosphate of RNase A-derived fragments or metal-induced fragments also did not change the stimulatory properities. We checked if the 2`,3`-cyclic phosphate is either responsible for the IFN-α-inducing ablilities of RNase A-derived fragments or if the 2`,3`-cyclic phosphate might inhibit the stimulatory potential of fragments generated by Zn^{2+}-induced hydrolysis.

It is also interesting to note that proteasomes show endonuclease activity (Pouch et al. 1995; Petit et al. 1997). The best characterized properties of proteasomes are their multiple endopeptidase activities (Petit et al. 1997). Surprisingly, two distinct α-type subunits of 20S proteasomes (subunit zeta and iota) have been identified that are associated with RNase activity. Proteasome subunits zeta and iota hydrolyzed tobacco mosaic virus RNA, whereas none of the other subunits degraded the RNA under the same conditions (Petit et al. 1997). Furthermore, it was shown that proteasomal endonuclease activity is rather RNA specific, since 5S rRNA, 9S globin mRNA and lysyl-tRNA were not degraded by proteasomes (Pouch et al. 1995). It was claimed that proteasomes might be involved in the destabilisation of cytokines mRNAs containing AUUUA sequences as well as of viral mRNAs (Jarrousse et al. 1999; Gautier-Bert et al. 2003). It has also been observed that 18S rRNA fragments are degraded by proteasomes (Petit et al. 1997; Horikoshi et al. 1998). It would be very interesting to analyze whether self-RNA becomes immunostimulatory upon incubation with proteasomes. Since proteasomes are located in the cytoplasm (in addition to the nucleus), RNA fragments could be detected for example by the cytosolic helicases upon incubation with proteasomes.

6.3.4. Double-stranded character is important for IFN-α signaling

The conformation of the RNase A-derived fragments (either ss or ds) was analyzed by treatment with the ds-specific RNase III. The RNase A-derived fragments were treated in different ways, then complexed to DOTAP and used for the stimulation of PBMC cells. The effect of the treatment was controlled by agarose electrophoresis. We were able to show that immunostimulatory RNase A-derived fragments were sensitive to ds-specific RNase III. RNase III abolished signaling by RNase A-derived fragments complexed to DOTAP in human immune cells. Schmidt et al. have found that RIG-I ligands require base-paired structures in conjugation with a free 5`-triphosphate to trigger a type-I interferon response (Schmidt et al. 2009). The ds character gives the first indication of RIG-I-dependent immune signaling. Since ethidium bromide staining showed no difference for mock or RNase III-treated RNase A-derived fragments, we can conclude that only the stimulatory fraction of the digest shows ds character, whereas other components of the digest are of an ss nature. It can be hypothesized that some of the fragments derived by RNase A digest have the propensity to form ds structures that are recognized by immune cells, whereas most of them are of ss conformation.
In conclusion, the RNase III treatment of RNase A-derived fragments showed that the stimulatory principle of the digest might be ds. Regarding the observation that RNase III also cuts ssRNA (Dunn 1976), further analysis is required in order to analyze the conformation of RNase A-derived fragments.

6.3.5. Identification of the immunostimulatory RNA species

Self-RNA is highly methylated and contains numbers of pseudouridines, which have been shown to lack the ability to activate endosomal TLRs (Kariko et al. 2005; Robbins et al. 2007). Host-derived RNA contains many modifications, but nucleotide modifications are usually found in clusters, leaving a significant number of RNA nucleotides unmodified. In 18S rRNA approximately 40 positions are modified by 2`-O-methyl groups (4.3% modified nucleosides), and the occurrence is clustered (Maden 1990). Since the sequence of rRNA contains numerous stretches rich in guanosine and uridine, it is unclear why these non-modified sequences within rRNA do not activate immune cells. Our finding that fragments derived by RNase treatment of self-RNA can activate the immune system indicates that non-modified sequences in mammalian RNA are sufficient to induce immune activation if

RNA is protected from extracellular degradation and transported into endosomal compartments.

The ethidium bromide staining of the RNase A-derived fragments on a PAA gel shows a smear of degradation fragments, showing a size in the range from < 20 bp to 100 bp. However, below the marker size of 100 bp we were able to observe a pattern of ca. 3 distinct bands. The production of such specific fragments indicated that splitting of the RNA was not a random process. Concerning the conditions employed for the digest—either mild conditions (low concentration of the enzyme, short incubation time) or stronger conditions—the band pattern showed some variability from one experimental series to another. The long smear in the gel is a result of unspecific random degradation. The RNA bands might be responsible for the IFN-α inducing activity of the RNase A-derived fragments. To test this, the RNA bands should be eluted from the PAA gel and tested for their immunostimulatory ability as described by Edy et al. (Edy et al. 1976). The various data in the literature on partial or complete digestion of RNA by RNases are difficult to compare, as different conditions (time, enzyme:substrate ratio) of digestion and different assays have been used by different authors. Depending on the conditions for the RNase A digest, there was either a band pattern (Edy et al. 1976) or no specific cleavage products generated (Wreschner et al. 1981).

In order to address the question regarding which fragments of the RNase A digest are responsible for the IFN-α inducing capacity, we used Micro Bio-Spin columns which purify nucleic acids larger than 20 bases by removing single nucleosides. The first fraction, which contains larger fragments, when complexed to the cationic transfection reagent DOTAP, stimulated human PBMC cells to produce IFN-α, whereas the subsequent fractions containing single nucleosides showed no IFN-α secretion in human PBMC cells. This showed that fragments longer than 20 nucleotides and not single nucleosides are responsible for the immunostimulatory potential.

To identify the immunostimulatory RNA species of the RNase A-derived fragments, we fractionated the digest into different sizes by using XBRIDGE^{TM} OST C_{18} columns and high performance liquid chromatography (HPLC). The obtained fractions from the column showed longer RNA fragments with the increase in time. The first fractions (fractions 3-5) containing single nucleosides were not able to induce type-I interferon when complexed to DOTAP in human PBMC cells, whereas fractions obtained at a later time (fractions 16-19) contained the stimulatory RNA species. Surpisingly, these fractions could not be stained with ethidium bromide. These fractions might be of an ss character, since ssRNA fragments cannot be stained with ethidium bromide. Only larger fragments (fractions 21-

29) could be visualized by ethidium bromide staining, but these fractions showed no ability to induce IFN-α in human PBMC cells when complexed to DOTAP. The finding that the stimulatory fragments could not be stained with ethidium bromide could explain the behaviour of the RNase A-derived fragments upon RNase III treatment. Whether the sample was mock- or RNase III-treated could not be visualized by ethidium bromide staining. Another possibility might be to try the staining of the fragments with Syber Gold (Invitrogen), which shows a high sensitivity to nucleic acids.

The IFN-α response induced by the fractionated fragments was only low in comparison to the complete digest. It is possible that the stimulatory capacity of the fragments is lost after passing through several columns or that an interplay between different fractions is necessary for inducing a high IFN-α response. Remembering the FCS sensitivity of the RNase A-derived fragments, it becomes apparent that the immunostimulatory activity of the fragments is very subtle.

The identified fragments should be used to create a RNA (cDNA) sequence library, followed by T/A-cloning and sequencing. Identified sequences will be validated for their immunostimulatory potential after *in vitro* transcription or chemical synthesis and complexation to DOTAP in human PBMC cells.

So far, only the immunostimulatory capacity of a mixture containing ribosomal RNA, transfer RNA and mRNA has been demonstrated. It is currently unknown whether certain RNA species or RNA sequences mediate immune stimulation. For this reason, various RNA species from total RNA such as ribosomal RNA (rRNA), transfer RNA (tRNA) or messenger RNA (mRNA) have to be purified and analyzed for their immunostimulatory potential after partial RNase A treatment.

6.3.6. Monocytes are responsible for recognition of RNase A-derived fragments

Comparing the immunostimulatory ability of the fragments derived from RNase treatment in human monocytes and PBMC cells showed that monocytes represent the cell type responsible for recognizing the RNase-derived fragments. Thus, as shown by Hansmann et al. for stimulation with Poly (I:C)/DOTAP, we observed also that monocytes have the capacity to produce high amounts of IFN-α upon stimulation with RNase A-derived fragments complexed to DOTAP (Hansmann et al. 2008). The obtained monocytes had a purity of about 90%. Since monocytes do not express TLRs like TLR9 or TLR7, but instead express cytosolic helicases, this result might give us a first indication of the

responsible receptor. In order to exclude an involvement of DCs, another approach might be to analyze whether depletion of myeloid and plasmacytoid DC subsets via antibodies from PBMC cells actually reduce the IFN-α producing capacity of human PBMCs upon stimulation with RNase-derived fragments.

6.3.7. Receptor for recognition of fragments from self-RNA

Very little is known about small self-RNA recognition. TLRs could be involved due to (1) a possible decreased number of nucleotide modifications in the cleavage products compared to the full length eukaryotic RNA, or (2) the presence of particular sequence patterns of a certain length. Furthermore, the cytosolic RNA-helicases RIG-I and MDA-5 might detect the fragments generated by RNase digest due to the fact that (1) the cleavage products show the right ends like phosphates and thereby represent a possible target structure for RIG-I, or (2) the fragments form structures that display partial ds conformation. For small self-RNAs produced by the action of RNase L on cellular RNA it was shown that the signaling involves RIG-I, MDA-5 and IPS-1 (Malathi et al. 2007).
To investigate whether TLRs or cytosolic helicases mediate the recognition of the fragments derived from RNase A treatment; we planned to use Flt3-derived dendritic cells from respective knockout mice. But for Flt3-derived dendritic cells, it was observed that there was often only a very low or no IFN-α response to the RNase-derived fragments, although the fragments were controlled parallel on PBMC cells. It is possible that the IFN-α response induced by RNase A-derived fragments in Flt3-derived dendritic cells was below the threshold of the ELISA. For future experiments, it should be analyzed whether the RNase A-derived fragments induce an expression of the activation marker CD69 in Flt3-derived dendritic cells. Another important aspect may be that the RNase A-derived fragments do not contain a 5`-triphosphate end, which murine immune cells need more for RIG-I dependent signaling than do human immune cells (6.2.4). The possibility that the immune induction of RNase A-derived fragments is species-specific, which in our case would means that it only works for human PBMC cells and not for murine immune cells, is excluded by the observation that RNase L-derived fragments of self-RNA induced an IPS-dependent immune activation in murine MEF cells (Malathi et al. 2007). Since some experiments indicate that the recognition of partially digested self-RNA fragments is IPS-dependent (Malathi et al. 2007), the Flt3-derived dendritic cells expressing TLR 7 and 9 may represent the wrong cell type for recognizing the fragments derived by RNase A digest. But in GM-CSF and M-CSF derived cells, which are regarded as analogs to human

myeloid dendritic cells, there was also no IFN-α response detectable upon transfection of fragments derived from RNase treatment (data not shown).

Using HEK293 cells transfected with RIG-I expression vectors along with IFN-ß reporter plasmid, we observed that the fragments derived by RNase A treatment activated RIG-I when complexed to Lipofectamine 2000 but not when complexed to DOTAP or given alone. Upon RNase III treatment of RNase A-derived fragments complexed to Lipofectamine 2000, the immune response was abrogated, showing that the ds character of the fragments was important for the RIG-I dependent immune response. The phosphate end had no influence for the recognition of the fragments, because dephosphorylation did not reduce IFN-ß activation. But here again the question arose as to how efficient the dephosphorylation method was.

Regarding the FCS sensitivity of the RNase A-derived fragments, it becomes apparent that the immunostimulatory activity of the fragments is very subtle. The generated fragments complexed to DOTAP showed a serum dependent IFN-α induction in human PBMC cells. The fragments induced the highest IFN-α response in human PBMC cells when using 1-2% serum, whereas for higher serum concentrations like 10% serum the immune response was decreased. The exact composition of FCS (proteins, antibodies, growth factors) is generally less defined and can vary from batch to batch. For example, a higher titer of antibodies binding to the RNA fragments might attenuate the immunostimulatory potential of the RNase A-derived fragments. With regard to other immune cells, e.g., murine immune cells or human HEK293 cells maintained in 10% serum, this could explain the variable IFN-α response for RNase A-derived fragments on murine and human HEK293 cells. For Flt3-derived DCs, we did find that the IFN-α response to RNase A-generated fragments was increased by testing lower serum concentrations, but unfortunately this result was not reproducible. Further experiments with GM-CSF and M-CSF derived cells should show whether fragments generated by RNase treatment induced an immune response by using lower serum concentrations. If this were the case, the responsible receptor for recognizing the fragments derived by RNase treatment could be identified by using the respective knockout mice. Considering the serum sensitivity of the fragments, we also tested different serum concentrations in HEK293 cells and observed an increase in the IFN-ß response for fragments complexed to Lipofectamine 2000 but not for DOTAP by using lower serum concentrations (data not shown).

The data obtained by stimulating human monocytes already exclude an involvement of TLR9 or TLR7, so only the responsibility of the cytosolic helicases has to be tested.

6.3.8. Cell types and transfection reagents

The RNase A-derived fragments were recognized by immune cells in different ways as shown in Table 6. Whereas in human PBMC cells IFN-α secretion was observed upon transfection with RNase A-derived fragments complexed to DOTAP at a final RNA concentration in the range of 5-50 µg/ml (further concentrations were not tested), in human HEK293 cells, overexpressing RIG-I IFN-ß activation was enhanced when the fragments were complexed to Lipofectamine 2000 at a final RNA concentration of 1 µg/ml. For murine immune cells, we could only observe a variable IFN-α response. In conclusion, we can say that, depending on the immune cell type, different concentrations of the RNA fragments and different transfection reagents are necessary for inducing an immune activation.

Table 6: Influence of the cell type and the transfection reagent for the recognition of RNase A-derived fragments (LF 2000 = Lipofectamine 2000)

Cell type	**PBMC cells and monocytes**			**Flt3 cells**		**HEK293 cells**	
Transfection reagent	DOTAP	LF 2000	LL-37	DOTAP	LF 2000	DOTAP	LF 2000
RNA fragments [µg/ml]	5-50 µg/ml	5-50 µg/ml	10 µg/ml	5-50 µg/ml	5-50 µg/ml	0.2-50 µg/ml	1 µg/ml
Immune response	IFN-α	-	-	low IFN-α	-	-	IFN-ß

6.3.9. Relevance of the recognition of self-RNA fragments

Extracellular self-RNA normally does not lead to innate immune activation because it is rapidly degraded by RNases and fails to access endosomal compartments of dendritic cells. However, in some autoimmune diseases, self-nucleic acids gain access to endosomal compartments by the help of autoantibodies or antimicrobial peptides (Gilliet et al. 2008). For example, in systemic lupus erythematosus (SLE), self-RNA and self-DNA are complexed with autoantibodies, which deliver the nucleic acids into endosomal compartments of pDCs via FcγRII-mediated endocytosis (Ronnblom and Alm 2003; Barrat

et al. 2005; Means et al. 2005), leading to an aberrant IFN-α production (Theofilopoulos et al. 2005; Banchereau and Pascual 2006). DC activation by immune complexes formed by U1snRNP and SLE-IgG or isolated U1snRNA in complex with cationic liposomes is largely mediated by TLR7 (Vollmer et al. 2005; Savarese et al. 2006). In psoriasis, self-DNA forms complexes with the cationic antimicrobial peptide LL-37, which gain access to endosomal TLR9 (Lande et al. 2007). Recently, it was found that LL-37 also forms complexes with self-RNA (Ganguly et al. 2009). These complexes are highly protected from RNase degradation and gain access to endosomal compartments, where they trigger TLR7. Moreover, it should be noted that self-RNA could activate the RIG-I pathway under specific circumstances, for example, when excess RNA is not properly degraded by nucleases or mitochondrial RNA is released (Krug 2008). An important protective mechanism is the rapid clearance of apoptotic material and degradation of excess nucleic acids by nucleases. Severe autoimmune diseases develop in mice and humans with defects in these enzymes. For example, the Aicardi-Goutieres syndrome shows four mutations: one affects the DNAse III, and the other three were relocated to the RNAseH2 (Crow et al. 2006; Rigby et al. 2008). Furthermore, it is possible that RNA degraded during apoptosis and delivered to endosomes activated immune cells (Diebold et al. 2006).

The data obtained in this work regarding self-RNA fragments, which induced an IFN-α response in human PBMC cells upon complexation to DOTAP or an IFN-ß activation in HEK293 cells upon complexation to Lipofectamine 2000, clearly demonstrates the possible role of self-RNA fragments generated by incomplete RNase treatment in autoimmune diseases.

For future work, it would be interesting to use the ability of the self-RNA fragments complexed to cationic lipids to induce IFN-α. A pratical approach would be to analyze their role for vaccination studies.

To further gain insight into changes in immune cells induced by RNase-derived fragments, their global transcriptional profile could be analyzed with Microarray chips. This method allows the observation of the expression of thousands of genes and their coordinate change in a given condition. Therefore, RNA has to be isolated from immune cells after stimulation with RNase-derived fragments or medium alone, and hybridized to the Affymetrix chip. So, different expressed genes which are induced following stimulation with RNase A-derived fragments could be identified.

7. Summary

RNA provides a stimulus for innate immunity either by activating the endosomal TLRs (3, 7 and 8) or by triggering cytosolic RNA sensors (RIG-I and MDA-5). RNA recognition results in the secretion of type-I interferons and / or proinflammatory cytokines. Recognition of foreign RNA is thought to occur due to the presence of non-self strucures, such as abundance of nucleotide modifications, ds conformation or the presence of a terminal 5`-triphosphate. Discrimination between self and non-self-RNAs is very important to prevent constant induction of type-I IFNs which would lead to autoimmune responses. However, the exact structural requirements for RNA recognition are still mainly unidentified. Within this work, the influence of RNA modifications and the immunostimulatory potentials of RNA from influenza-infected cells, small self-RNAs and cathelicidin/RNA complexes were analyzed.

The first part of this thesis identified the 2`-position of the ribose as crucial for TLR7-mediated immunorecognition by introducing nucleotide modifications in RNA. We were able to show that a single 2`-O-ribose methylation within a natural fragment of 18S rRNA prevented IFN-α production, however secretion of proinflammatory cytokines was not impaired in human immune cells but in murine immune cells. Since murine TLR8 is non-functional, the RNA 63-induced immunostimulatory activity in murine cells was strictly TLR7-dependent.

In the second part of this thesis we introduced the human antimicrobial peptide LL-37 and its murine homolog cathelicidin-related antimicrobial peptide (CRAMP), which function as carriers for RNA from virus-infected cells and induce innate immune activation. In the past, it was shown that ss-synthetic oligonucleotides (ORN) complexed to the cationic transfection reagent DOTAP induce antigen-specific cytotoxic T cells and antibodies in a TLR7-dependent manner. Since DOTAP is toxic, we analyzed whether cathelicidin/RNA complexes could function as carriers in vaccine formulations. Moreover, we investigated the characterictics of RNA extracted from influenza-infected cells, which was recognized as having a non-self structure. Immune cells are potently activated by viral RNA but not by mammalian total RNA, which is abundant in modified nucleosides. It was demonstrated that the 5`-triphosphate moiety of RNA from influenza-infected cells is not the only target structure for RIG-I but that the ds character of RNA from influenza-infected cells represent a second structural feature that activate RIG-I.

The third part of this thesis concentrated on the interesting observation that RNase A treatment of non-immunostimulatory self-RNA rendered it immunostimulatory. First, we determined the size of the fragments and the responsible receptor for recognizing the cleavage products. In addition, we tested other RNase types, especially concerning their generated ends. In order to determine whether the conformation of the stimulatory RNA fragments were ss or ds, we treated the RNase digest with the ds-specifc RNAse III. Moreover, we generated RNA fragments of similar size by ultrasonic treatment and metal-induced hydrolysis and analyzed their ability to induce IFN-α. The immunostimulatory potential of self-RNA fragments may be useful as a possible vaccine formulation. Besides the possible advantages of RNA fragments, their possible role in autoimmune diseases have to be considered.

Finally, on the basis of the results obtained up to this point, we have generated convincing data concerning the immunostimulatory capacity of RNA and cathelicidin complexes. A key finding of this thesis was the observation that self-RNA became immunostimulatory upon RNase treatment. Further investigations will show whether, besides RIG-I, additional immune system receptors are involved in the recognition of fragments generated by RNase treatment of self-RNAs and whether cathelicidin/RNA complexes could function as vaccines.

8. Zusammenfassung

RNA stellt einen Stimulus für das angeborene Immunsystem durch die Aktivierung der endosomalen TLRs (3, 7 und 8) oder der zytosolischen RNA Sensoren (RIG-I und MDA-5) dar. Die Erkennung von RNA resultiert in der Sekretion von Typ-I Interferonen und / oder proinflammatorischen Zytokinen. Fremd-RNA wird über das Vorhandensein von "Nicht-Selbst" Strukturen, wie gehäufte Nukleotidmodifikationen, doppelsträngige Konformation oder eine terminale 5`- Triphosphategruppe, erkannt. Diese Unterscheidung zwischen Selbst- und Fremd-RNA verhindert eine permanente Typ-I Interferon Sekretion und somit Autoimmunerkrankungen. Jedoch ist nach wie vor wenig über die strukturellen Einzelheiten der RNA Erkennung bekannt. In dieser Arbeit wurde der Einfluss von RNA-Modifikationen und das immunstimulatorische Potential von RNA aus Influenza-infizierten Zellen, Selbst-RNA Fragmenten sowie von Cathelizidine/RNA Komplexen analysiert.

Der erste Teil der Arbeit identifizierte durch die Einführung entsprechender Modifikationen die 2`-Position der Ribose als entscheidende Struktur für die Erkennung durch TLR7. Es konnte gezeigt werden, dass die Methylierung der Ribose innerhalb eines natürlichen Fragmentes der 18S rRNA die Induktion von IFN-α in humanen und murinen Immunzellen sowie die Sekretion von proinflammatorischen Zytokinen in murinen Immunzellen, nicht jedoch in humanen Immunzellen, unterdrückte. Die RNA 63 induzierte immunstimulatorische Aktivität in murinen Immunzellen ist TLR7 abhängig, da der murine TLR8 nicht funktionell ist. In humanen Immunzellen verwandelte eine 2`-O-Methylierung einen TLR7/TLR8 Liganden zu einen TLR8-spezifischen Liganden und induzierte proinflammatorische Zytokine.

Im zweiten Teil dieser Arbeit führten wir das antimikrobielle Peptid LL-37 und sein murines Homolog CRAMP ein, welche als Träger für RNA aus virus-infizierten Zellen fungieren und eine Immunantwort auslösen. In der Vergangenheit wurde gezeigt, dass einzelsträngige synthetische Oligonukleotide (ORN) komplexiert mit dem kationischen Transfektionsreagenz DOTAP antigen-spezifische zytotoxische T-Zellen und Antikörper in einer TLR7 abhängigen Weise induzierten. Da DOTAP toxisch ist, analysierten wir, ob Cathelizidine/RNA Komplexe in Impfstoffen eingesetzt werden könnten. Außerdem untersuchten wir die Charakteristika von RNA, welche aus Influenza-infizierten Zellen isoliert und als "Nicht-Selbst" Struktur erkannt wurde. Immunzellen werden durch virale RNA aktiviert aber nicht durch eukaryotische RNA, welche gehäuft Nukleotidmodifikationen enthält. Es konnte gezeigt werden, dass eine terminale 5`-

Triphosphatgruppe nicht die einzige Erkennungsstruktur in RNA aus Influenza-infizierten Zellen darstellt, sondern auch die Doppelstrangkonformation von RNA als unabhängiger Stimulus für RIG-I fungiert.

Der dritte Teil dieser Arbeit konzentrierte sich auf die Beobachtung, dass eine RNase A Behandlung von nicht-immunstimulatorischer Selbst-RNA dieser immunstimulatorische Eigenschaften verleiht. Zuerst analysierten wir die Größe der RNA Fragmente und den verantwortlichen Rezeptor, der die RNA Spaltprodukte erkennt. Zusätzlich testeten wir andere RNase Typen hinsichtlich der generierten Enden und ihrer immunstimulatorischen Eigenschaften. Um die Konformation der stimulatorischen RNA Fragmente zu bestimmen, d.h. ob sie einzelsträngig oder doppelsträngig vorlagen, behandelten wir den Verdau mit der Doppelstrang-spezifischen RNase III. Zusätzlich generierten wir RNA Fragmente gleicher Größe durch Ultraschall-Behandlung und Metall-induzierter Hydrolyse und analyzierten ihre Fähigkeiten, IFN-α zu induzieren. Das immunstimulatorische Potential von Selbst-RNA Fragmenten könnte als mögliches Adjuvantium Verwendung finden. Allerdings müsste hierbei neben den möglichen Vorteilen von RNA Fragmenten, auch deren eventuelle Rolle in Autoimmunerkrankungen bedacht werden.

Auf der Basis der bisher erzielten Ergebnisse haben wir überzeugende Daten bezüglich der immunstimulatorischen Kapazität von RNA und Cathelizidine Komplexen gewonnen. Die Haupterkenntnis dieser Arbeit war, dass Selbst-RNA durch RNase Behandlung immunstimulatorisch wird. Weitere Untersuchungen werden zeigen, ob neben RIG-I weitere Rezeptoren des Immunsystems an der Erkennung von RNA Fragmenten beteiligt sind, und ob RNA/Cathelizidine Komplexe als Adjuvantien fungieren können.

9. Literature

9.1. Paper & Books

Abbas, A. K., Lichtman, A. H., Pallai, S. (2007). Cellular and Molecular Immunology, 6th edition.

Ablasser, A., F. Bauernfeind, et al. (2009). "RIG-I-dependent sensing of poly(dA:dT) through the induction of an RNA polymerase III-transcribed RNA intermediate." Nat Immunol.

Afonina, E., R. Stauber, et al. (1998). "The human poly(A)-binding protein 1 shuttles between the nucleus and the cytoplasm." J Biol Chem **273**(21): 13015-21.

Agerberth, B. O. L.-E., J. Charo, et al. (2000). "The human antimicrobial and chemotactic peptides LL-37 and alpha-defensins are expressed by specific lymphocyte and monocyte populations." Blood **96**(9): 3086-93.

Ahmad-Nejad, P., H. Hacker, et al. (2002). "Bacterial CpG-DNA and lipopolysaccharides activate Toll-like receptors at distinct cellular compartments." Eur J Immunol **32**(7): 1958-68.

Ahmad-Nejad, P. O. T., H. Hacker, et al. (2002). "Bacterial CpG-DNA and lipopolysaccharides activate Toll-like receptors at distinct cellular compartments." Eur J Immunol **32**(7): 1958-68.

Akira, S. O. T. and K. Takeda (2004). "Toll-like receptor signalling." Nat Rev Immunol **4**(7): 499-511.

Akira, S. O. T., S. Uematsu, et al. (2006). "Pathogen recognition and innate immunity." Cell **124**(4): 783-801.

Aksoy, E. O. R., C. S. Zouain, et al. (2005). "Double-stranded RNAs from the helminth parasite Schistosoma activate TLR3 in dendritic cells." J Biol Chem **280**(1): 277-83.

Alalwani, M. S., J. Sierigk, et al. (2010). "The antimicrobial peptide LL-37 modulates the inflammatory and host defense response of human neutrophils." Eur J Immunol.

Alexopoulou, L. O. T., A. C. Holt, et al. (2001). "Recognition of double-stranded RNA and activation of NF-kappaB by Toll-like receptor 3." Nature **413**(6857): 732-8.

Aliyari, R. and S. W. Ding (2009). "RNA-based viral immunity initiated by the Dicer family of host immune receptors." Immunol Rev **227**(1): 176-88.

Allen, I. C., M. A. Scull, et al. (2009). "The NLRP3 inflammasome mediates in vivo innate immunity to influenza A virus through recognition of viral RNA." Immunity **30**(4): 556-65.

Almofti, M. R., H. Harashima, et al. (2003). "Cationic liposome-mediated gene delivery: biophysical study and mechanism of internalization." Arch Biochem Biophys **410**(2): 246-53.

Arnold, U. and R. Ulbrich-Hofmann (2006). "Natural and engineered ribonucleases as potential cancer therapeutics." Biotechnol Lett **28**(20): 1615-22.

Astriab-Fisher, A., M. H. Fisher, et al. (2004). "Increased uptake of antisense oligonucleotides by delivery as double stranded complexes." Biochem Pharmacol **68**(3): 403-7.

Bachellerie, J. P. and J. Cavaille (1997). "Guiding ribose methylation of rRNA." Trends Biochem Sci **22**(7): 257-61.

Bachellerie, J. P., J. Cavaille, et al. (2002). "The expanding snoRNA world." Biochimie **84**(8): 775-90.

Balachandran, S., P. C. Roberts, et al. (2000). "Essential role for the dsRNA-dependent protein kinase PKR in innate immunity to viral infection." Immunity **13**(1): 129-41.

Bals, R. O. L.-B. (2000). "Epithelial antimicrobial peptides in host defense against infection." Respir Res **1**(3): 141-50.

Bals, R. O. L.-B. and P. S. Hiemstra (2004). "Innate immunity in the lung: how epithelial cells fight against respiratory pathogens." Eur Respir J **23**(2): 327-33.

Bals, R. O. L.-B., X. Wang, et al. (1998). "The peptide antibiotic LL-37/hCAP-18 is expressed in epithelia of the human lung where it has broad antimicrobial activity at the airway surface." Proc Natl Acad Sci U S A **95**(16): 9541-6.

Bals, R. O. L.-B., D. J. Weiner, et al. (1999). "Transfer of a cathelicidin peptide antibiotic gene restores bacterial killing in a cystic fibrosis xenograft model." J Clin Invest **103**(8): 1113-7.

Banchereau, J. O. I. and V. Pascual (2006). "Type I interferon in systemic lupus erythematosus and other autoimmune diseases." Immunity **25**(3): 383-92.

Barchet, W., A. Krug, et al. (2005). "Dendritic cells respond to influenza virus through TLR7- and PKR-independent pathways." Eur J Immunol **35**(1): 236-42.

Barchet, W. O. T., V. Wimmenauer, et al. (2008). "Accessing the therapeutic potential of immunostimulatory nucleic acids." Curr Opin Immunol **20**(4): 389-95.

Barral, P. M., D. Sarkar, et al. (2009). "RIG-I is cleaved during picornavirus infection." Virology **391**(2): 171-6.

Barral, P. M., D. Sarkar, et al. (2009). "Functions of the cytoplasmic RNA sensors RIG-I and MDA-5: Key regulators of innate immunity." Pharmacol Ther.

Barrat, F. J., T. Meeker, et al. (2005). "Nucleic acids of mammalian origin can act as endogenous ligands for Toll-like receptors and may promote systemic lupus erythematosus." J Exp Med **202**(8): 1131-9.

Barton, G. M. T., J. C. Kagan, et al. (2006). "Intracellular localization of Toll-like receptor 9 prevents recognition of self DNA but facilitates access to viral DNA." Nat Immunol **7**(1): 49-56.

Bauer, S., S. Pigisch, et al. (2008). "Recognition of nucleic acid and nucleic acid analogs by Toll-like receptors 7, 8 and 9." Immunobiology **213**(3-4): 315-28.

Bauer, S. O. T., C. J. Kirschning, et al. (2001). "Human TLR9 confers responsiveness to bacterial DNA via species-specific CpG motif recognition." Proc Natl Acad Sci U S A **98**(16): 9237-42.

Baumgarth, N. and C. L. Bevins (2007). "Autoimmune disease: skin deep but complex." Nature **449**(7162): 551-3.

Bergman, P. n. z. l., L. Walter-Jallow, et al. (2007). "The antimicrobial peptide LL-37 inhibits HIV-1 replication." Curr HIV Res **5**(4): 410-5.

Bergmann, M., A. Garcia-Sastre, et al. (2000). "Influenza virus NS1 protein counteracts PKR-mediated inhibition of replication." J Virol **74**(13): 6203-6.

Besch, R., H. Poeck, et al. (2009). "Proapoptotic signaling induced by RIG-I and MDA-5 results in type I interferon-independent apoptosis in human melanoma cells." J Clin Invest **119**(8): 2399-411.

Bird, A. P. (1986). "CpG-rich islands and the function of DNA methylation." Nature **321**(6067): 209-13.

Bisbal, C. and R. H. Silverman (2007). "Diverse functions of RNase L and implications in pathology." Biochimie **89**(6-7): 789-98.

Bonin, M., J. Oberstrass, et al. (2000). "Determination of preferential binding sites for anti-dsRNA antibodies on double-stranded RNA by scanning force microscopy." Rna **6**(4): 563-70.

Boule, M. W., C. Broughton, et al. (2004). "Toll-like receptor 9-dependent and -independent dendritic cell activation by chromatin-immunoglobulin G complexes." J Exp Med **199**(12): 1631-40.

Brogden, K. A. O. L.-A. P. (2005). "Antimicrobial peptides: pore formers or metabolic inhibitors in bacteria?" Nat Rev Microbiol **3**(3): 238-50.
Brydon, E. W. I. A., S. J. Morris, et al. (2005). "Role of apoptosis and cytokines in influenza virus morbidity." FEMS Microbiol Rev **29**(4): 837-50.
Cao, X. (2009). "New DNA-sensing pathway feeds RIG-I with RNA." Nat Immunol **10**(10): 1049-51.
Carmell, M. A. O. R. and G. J. Hannon (2004). "RNase III enzymes and the initiation of gene silencing." Nat Struct Mol Biol **11**(3): 214-8.
Cekaite, L., G. Furset, et al. (2007). "Gene expression analysis in blood cells in response to unmodified and 2'-modified siRNAs reveals TLR-dependent and independent effects." J Mol Biol **365**(1): 90-108.
Cereijido, M., E. S. Robbins, et al. (1978). "Polarized monolayers formed by epithelial cells on a permeable and translucent support." J Cell Biol **77**(3): 853-80.
Chiu, Y. H., J. B. Macmillan, et al. (2009). "RNA polymerase III detects cytosolic DNA and induces type I interferons through the RIG-I pathway." Cell **138**(3): 576-91.
Choi, M. K., Z. Wang, et al. (2009). "A selective contribution of the RIG-I-like receptor pathway to type I interferon responses activated by cytosolic DNA." Proc Natl Acad Sci U S A **106**(42): 17870-5.
Cirioni, O. O. L.-K., A. Giacometti, et al. (2006). "LL-37 protects rats against lethal sepsis caused by gram-negative bacteria." Antimicrob Agents Chemother **50**(5): 1672-9.
Conrad, C. and R. Rauhut (2002). "Ribonuclease III: new sense from nuisance." Int J Biochem Cell Biol **34**(2): 116-29.
Cordin, O., J. Banroques, et al. (2006). "The DEAD-box protein family of RNA helicases." Gene **367**: 17-37.
Crow, Y. J., A. Leitch, et al. (2006). "Mutations in genes encoding ribonuclease H2 subunits cause Aicardi-Goutieres syndrome and mimic congenital viral brain infection." Nat Genet **38**(8): 910-6.
Cuchillo, C. M., X. Pares, et al. (1993). "The role of 2',3'-cyclic phosphodiesters in the bovine pancreatic ribonuclease A catalysed cleavage of RNA: intermediates or products?" FEBS Lett **333**(3): 207-10.
Cui, S. O. R.-I., K. Eisenacher, et al. (2008). "The C-terminal regulatory domain is the RNA 5'-triphosphate sensor of RIG-I." Mol Cell **29**(2): 169-79.
Czaja, R., M. Struhalla, et al. (2004). "RNase T1 variant RV cleaves single-stranded RNA after purines due to specific recognition by the Asn46 side chain amide." Biochemistry **43**(10): 2854-62.
Czauderna, F., M. Fechtner, et al. (2003). "Structural variations and stabilising modifications of synthetic siRNAs in mammalian cells." Nucleic Acids Res **31**(11): 2705-16.
Dalby, B., S. Cates, et al. (2004). "Advanced transfection with Lipofectamine 2000 reagent: primary neurons, siRNA, and high-throughput applications." Methods **33**(2): 95-103.
Davidson, D. J. O. L.-K., A. J. Currie, et al. (2004). "The cationic antimicrobial peptide LL-37 modulates dendritic cell differentiation and dendritic cell-induced T cell polarization." J Immunol **172**(2): 1146-56.
De Jong, J. C. I. E. P., G. F. Rimmelzwaan, et al. (2000). "Influenza virus: a master of metamorphosis." J Infect **40**(3): 218-28.
De, Y. O. L.-O. F., Q. Chen, et al. (2000). "LL-37, the neutrophil granule- and epithelial cell-derived cathelicidin, utilizes formyl peptide receptor-like 1 (FPRL1) as a receptor to chemoattract human peripheral blood neutrophils, monocytes, and T cells." J Exp Med **192**(7): 1069-74.
Decatur, W. A. and M. J. Fournier (2003). "RNA-guided nucleotide modification of ribosomal and other RNAs." J Biol Chem **278**(2): 695-8.

Deddouche, S., N. Matt, et al. (2008). "The DExD/H-box helicase Dicer-2 mediates the induction of antiviral activity in drosophila." Nat Immunol **9**(12): 1425-32.
Desai, N. A. and V. Shankar (2003). "Single-strand-specific nucleases." FEMS Microbiol Rev **26**(5): 457-91.
Deshpande, R. A. and V. Shankar (2002). "Ribonucleases from T2 family." Crit Rev Microbiol **28**(2): 79-122.
Diebold, S. S. O. T., C. Massacrier, et al. (2006). "Nucleic acid agonists for Toll-like receptor 7 are defined by the presence of uridine ribonucleotides." Eur J Immunol **36**(12): 3256-67.
Diebold, S. S. T., T. Kaisho, et al. (2004). "Innate antiviral responses by means of TLR7-mediated recognition of single-stranded RNA." Science **303**(5663): 1529-31.
Dorschner, R. A., B. Lopez-Garcia, et al. (2004). "Innate immune defense of the nail unit by antimicrobial peptides." J Am Acad Dermatol **50**(3): 343-8.
Dorschner, R. A. L.-K., V. K. Pestonjamasp, et al. (2001). "Cutaneous injury induces the release of cathelicidin anti-microbial peptides active against group A Streptococcus." J Invest Dermatol **117**(1): 91-7.
Dorschner, R. A. O. L.-I. E., B. Lopez-Garcia, et al. (2006). "The mammalian ionic environment dictates microbial susceptibility to antimicrobial defense peptides." Faseb J **20**(1): 35-42.
Drider, D., J. M. Santos, et al. (1999). "The role of Escherichia coli RNase E and RNase III in the processing of the citQRP operon mRNA from Lactococcus lactis biovar diacetylactis." J Mol Microbiol Biotechnol **1**(2): 337-46.
Dunn, J. J. (1976). "RNase III cleavage of single-stranded RNA. Effect of ionic strength on the fideltiy of cleavage." J Biol Chem **251**(12): 3807-14.
Durr, U. H. O. L.-L. a., U. S. Sudheendra, et al. (2006). "LL-37, the only human member of the cathelicidin family of antimicrobial peptides." Biochim Biophys Acta **1758**(9): 1408-25.
Dyer, K. D. and H. F. Rosenberg (2006). "The RNase a superfamily: generation of diversity and innate host defense." Mol Divers **10**(4): 585-97.
Eaves, G. N. and C. D. Jeffries (1963). "Isolation and Properties of an Exocellular Nuclease of Serratia Marcescens." J Bacteriol **85**(2): 273-8.
Eberle, F., K. Giessler, et al. (2008). "Modifications in small interfering RNA that separate immunostimulation from RNA interference." J Immunol **180**(5): 3229-37.
Eberle, F., M. Sirin, et al. (2009). "Bacterial RNA is recognized by different sets of immunoreceptors." Eur J Immunol **39**(9): 2537-47.
Edelmann, K. H. O. I. R.-M. T., S. Richardson-Burns, et al. (2004). "Does Toll-like receptor 3 play a biological role in virus infections?" Virology **322**(2): 231-8.
Edy, V. G., M. Szekely, et al. (1974). "Effect of fragmentation on interferon induction by double-stranded virus RNA." J Gen Virol **23**(2): 191-5.
Edy, V. G., M. Szekely, et al. (1976). "Action of nucleases on double-stranded RNA." Eur J Biochem **61**(2): 563-72.
Eisenacher, K., C. Steinberg, et al. (2007). "The role of viral nucleic acid recognition in dendritic cells for innate and adaptive antiviral immunity." Immunobiology **212**(9-10): 701-14.
Elsner, H. I. and E. B. Lindblad (1989). "Ultrasonic degradation of DNA." DNA **8**(10): 697-701.
Elssner, A. O. L.-P. X., M. Duncan, et al. (2004). "A novel P2X7 receptor activator, the human cathelicidin-derived peptide LL37, induces IL-1 beta processing and release." J Immunol **172**(8): 4987-94.
Fancke, B., M. Suter, et al. (2008). "M-CSF: a novel plasmacytoid and conventional dendritic cell poietin." Blood **111**(1): 150-9.

Figdor, C. G., J. M. Leemans, et al. (1983). "Theory and practice of centrifugal elutriation (CE). Factors influencing the separation of human blood cells." Cell Biophys **5**(2): 105-18.

Fitzgerald-Bocarsly, P., J. Dai, et al. (2008). "Plasmacytoid dendritic cells and type I IFN: 50 years of convergent history." Cytokine Growth Factor Rev **19**(1): 3-19.

Flamand, L. O. L.-L. B., M. J. Tremblay, et al. (2007). "Leukotriene B4 triggers the in vitro and in vivo release of potent antimicrobial agents." J Immunol **178**(12): 8036-45.

Flint, S. J., L. W. Enquist, et al. (2004). "Princples of virology." American Society for Microbiology.

Frohm, M. O. L.-E., B. Agerberth, et al. (1997). "The expression of the gene coding for the antibacterial peptide LL-37 is induced in human keratinocytes during inflammatory disorders." J Biol Chem **272**(24): 15258-63.

Gack, M. U., R. A. Albrecht, et al. (2009). "Influenza A virus NS1 targets the ubiquitin ligase TRIM25 to evade recognition by the host viral RNA sensor RIG-I." Cell Host Microbe **5**(5): 439-49.

Gallo, R. L. O. L.-C., K. J. Kim, et al. (1997). "Identification of CRAMP, a cathelin-related antimicrobial peptide expressed in the embryonic and adult mouse." J Biol Chem **272**(20): 13088-93.

Gan, J., G. Shaw, et al. (2008). "A stepwise model for double-stranded RNA processing by ribonuclease III." Mol Microbiol **67**(1): 143-54.

Ganguly, D., G. Chamilos, et al. (2009). "Self-RNA-antimicrobial peptide complexes activate human dendritic cells through TLR7 and TLR8." J Exp Med **206**(9): 1983-94.

Garcia-Sastre, A. I. I., R. K. Durbin, et al. (1998). "The role of interferon in influenza virus tissue tropism." J Virol **72**(11): 8550-8.

Garcia, M., Z. Dogusan, et al. (2009). "Regulation and function of the cytosolic viral RNA sensor RIG-I in pancreatic beta cells." Biochim Biophys Acta.

Gaudreault, E. and J. Gosselin (2008). "Leukotriene B4 induces release of antimicrobial peptides in lungs of virally infected mice." J Immunol **180**(9): 6211-21.

Gaush, C. R., W. L. Hard, et al. (1966). "Characterization of an established line of canine kidney cells (MDCK)." Proc Soc Exp Biol Med **122**(3): 931-5.

Gautier-Bert, K., B. Murol, et al. (2003). "Substrate affinity and substrate specificity of proteasomes with RNase activity." Mol Biol Rep **30**(1): 1-7.

Gilliet, M. o. D., W. Cao, et al. (2008). "Plasmacytoid dendritic cells: sensing nucleic acids in viral infection and autoimmune diseases." Nat Rev Immunol **8**(8): 594-606.

Gilliet, M. O. L. and R. Lande (2008). "Antimicrobial peptides and self-DNA in autoimmune skin inflammation." Curr Opin Immunol **20**(4): 401-407.

Gitlin, L. O. R. M., W. Barchet, et al. (2006). "Essential role of mda-5 in type I IFN responses to polyriboinosinic:polyribocytidylic acid and encephalomyocarditis picornavirus." Proc Natl Acad Sci U S A **103**(22): 8459-64.

Gudmundsson, G. H., K. P. Magnusson, et al. (1995). "Structure of the gene for porcine peptide antibiotic PR-39, a cathelin gene family member: comparative mapping of the locus for the human peptide antibiotic FALL-39." Proc Natl Acad Sci U S A **92**(15): 7085-9.

Gudmundsson, G. H. O. L.-a. P. and B. Agerberth (1999). "Neutrophil antibacterial peptides, multifunctional effector molecules in the mammalian immune system." J Immunol Methods **232**(1-2): 45-54.

Gudmundsson, G. H. O. L.-L. a., B. Agerberth, et al. (1996). "The human gene FALL39 and processing of the cathelin precursor to the antibacterial peptide LL-37 in granulocytes." Eur J Biochem **238**(2): 325-32.

Guillot, L. I. T. M. R., R. Le Goffic, et al. (2005). "Involvement of toll-like receptor 3 in the immune response of lung epithelial cells to double-stranded RNA and influenza A virus." J Biol Chem **280**(7): 5571-80.

Guo, Z. I. N., L. M. Chen, et al. (2007). "NS1 protein of influenza A virus inhibits the function of intracytoplasmic pathogen sensor, RIG-I." Am J Respir Cell Mol Biol **36**(3): 263-9.

Haas, T. O. D., J. Metzger, et al. (2008). "The DNA sugar backbone 2' deoxyribose determines toll-like receptor 9 activation." Immunity **28**(3): 315-23.

Habjan, M. o. v. r., I. Andersson, et al. (2008). "Processing of genome 5' termini as a strategy of negative-strand RNA viruses to avoid RIG-I-dependent interferon induction." PLoS ONE **3**(4): e2032.

Hale, B. G., R. E. Randall, et al. (2008). "The multifunctional NS1 protein of influenza A viruses." J Gen Virol **89**(Pt 10): 2359-76.

Hamm, S., E. Latz, et al. (2009). "Alternating 2'-O-ribose methylation is a universal approach for generating non-stimulatory siRNA by acting as TLR7 antagonist." Immunobiology.

Hamm, S. O. I. V., A. Heit, et al. (2007). "Immunostimulatory RNA is a potent inducer of antigen-specific cytotoxic and humoral immune response in vivo." Int Immunol **19**(3): 297-304.

Hansmann, L., S. Groeger, et al. (2008). "Human monocytes represent a competitive source of interferon-alpha in peripheral blood." Clin Immunol **127**(2): 252-64.

Hartmann, R. K., A. Bindereif , et al. (2005). "Handbook of RNA Biochemistry." Wiley-VCH Verlag GmbH & Co. KGaA, Weinheim.

Hausmann, S., J. B. Marq, et al. (2008). "RIG-I and dsRNA-induced IFNbeta activation." PLoS One **3**(12): e3965.

Heil, F., H. Hemmi, et al. (2004). "Species-specific recognition of single-stranded RNA via toll-like receptor 7 and 8." Science **303**(5663): 1526-9.

Heil, F. O. T., P. Ahmad-Nejad, et al. (2003). "The Toll-like receptor 7 (TLR7)-specific stimulus loxoribine uncovers a strong relationship within the TLR7, 8 and 9 subfamily." Eur J Immunol **33**(11): 2987-97.

Heilborn, J. D. O. L.-W., M. F. Nilsson, et al. (2003). "The cathelicidin anti-microbial peptide LL-37 is involved in re-epithelialization of human skin wounds and is lacking in chronic ulcer epithelium." J Invest Dermatol **120**(3): 379-89.

Hemmi, H., T. Kaisho, et al. (2002). "Small anti-viral compounds activate immune cells via the TLR7 MyD88-dependent signaling pathway." Nat Immunol **3**(2): 196-200.

Hemmi, H. O. T., O. Takeuchi, et al. (2000). "A Toll-like receptor recognizes bacterial DNA." Nature **408**(6813): 740-5.

Hochrein, H. v. r. a. I. i., B. Schlatter, et al. (2004). "Herpes simplex virus type-1 induces IFN-alpha production via Toll-like receptor 9-dependent and -independent pathways." Proc Natl Acad Sci U S A **101**(31): 11416-21.

Hoerr, I., R. Obst, et al. (2000). "In vivo application of RNA leads to induction of specific cytotoxic T lymphocytes and antibodies." Eur J Immunol **30**(1): 1-7.

Horikoshi, T., J. Page, et al. (1998). "Proteasomal RNase activity in human epidermis." In Vivo **12**(2): 155-8.

Hornung, V., A. Ablasser, et al. (2009). "AIM2 recognizes cytosolic dsDNA and forms a caspase-1-activating inflammasome with ASC." Nature **458**(7237): 514-8.

Hornung, V. and E. Latz (2010). "Intracellular DNA recognition." Nat Rev Immunol **10**(2): 123-30.

Hornung, V. O. R.-I., J. Ellegast, et al. (2006). "5'-Triphosphate RNA is the ligand for RIG-I." Science **314**(5801): 994-7.

Hornung, V. o. s., M. Guenthner-Biller, et al. (2005). "Sequence-specific potent induction of IFN-alpha by short interfering RNA in plasmacytoid dendritic cells through TLR7." Nat Med **11**(3): 263-70.

Howell, M. D. o. L.-V., J. F. Jones, et al. (2004). "Selective killing of vaccinia virus by LL-37: implications for eczema vaccinatum." J Immunol **172**(3): 1763-7.

Ichinohe, T., H. K. Lee, et al. (2009). "Inflammasome recognition of influenza virus is essential for adaptive immune responses." J Exp Med **206**(1): 79-87.
Ikegame, S., M. Takeda, et al. (2010). "Both RIG-I and MDA5 RNA helicases contribute to the induction of alpha/beta interferon in measles virus-infected human cells." J Virol **84**(1): 372-9.
Ishii, K. J. O. D., C. Coban, et al. (2006). "A Toll-like receptor-independent antiviral response induced by double-stranded B-form DNA." Nat Immunol **7**(1): 40-8.
Ishii, K. J. s. R. and S. Akira (2005). "TLR ignores methylated RNA?" Immunity **23**(2): 111-3.
Ishikawa, H., Z. Ma, et al. (2009). "STING regulates intracellular DNA-mediated, type I interferon-dependent innate immunity." Nature.
Ishikawa, H. O. a. and G. N. Barber (2008). "STING is an endoplasmic reticulum adaptor that facilitates innate immune signalling." Nature **455**(7213): 674-8.
Iwasaki, A. and R. Medzhitov (2004). "Toll-like receptor control of the adaptive immune responses." Nat Immunol **5**(10): 987-95.
Jacobs, B. L. and J. O. Langland (1996). "When two strands are better than one: the mediators and modulators of the cellular responses to double-stranded RNA." Virology **219**(2): 339-49.
Janeway, C. A., Jr. ordner allgemein and R. Medzhitov (2002). "Innate immune recognition." Annu Rev Immunol **20**: 197-216.
Janeway, C. A., Travers, P., Walport, M. (2005). Immunobiology, the immune system in health and disease, 6th edition
Jarrousse, A. S., F. Petit, et al. (1999). "Possible involvement of proteasomes (prosomes) in AUUUA-mediated mRNA decay." J Biol Chem **274**(9): 5925-30.
Jenssen, H. O. L.-a. P., P. Hamill, et al. (2006). "Peptide antimicrobial agents." Clin Microbiol Rev **19**(3): 491-511.
Johansson, J. O. L.-I. i., G. H. Gudmundsson, et al. (1998). "Conformation-dependent antibacterial activity of the naturally occurring human peptide LL-37." J Biol Chem **273**(6): 3718-24.
Judge, A. D., G. Bola, et al. (2006). "Design of noninflammatory synthetic siRNA mediating potent gene silencing in vivo." Mol Ther **13**(3): 494-505.
Jurk, M. T., F. Heil, et al. (2002). "Human TLR7 or TLR8 independently confer responsiveness to the antiviral compound R-848." Nat Immunol **3**(6): 499.
Kandler, K. o. L.-B., R. Shaykhiev, et al. (2006). "The anti-microbial peptide LL-37 inhibits the activation of dendritic cells by TLR ligands." Int Immunol **18**(12): 1729-36.
Kanneganti, T. D., N. Ozoren, et al. (2006). "Bacterial RNA and small antiviral compounds activate caspase-1 through cryopyrin/Nalp3." Nature **440**(7081): 233-6.
Kariko, K. O. S. R., M. Buckstein, et al. (2005). "Suppression of RNA recognition by Toll-like receptors: the impact of nucleoside modification and the evolutionary origin of RNA." Immunity **23**(2): 165-75.
Kariko, K. O. s. R., H. Ni, et al. (2004). "mRNA is an endogenous ligand for Toll-like receptor 3." J Biol Chem **279**(13): 12542-50.
Kariko, K. r. and D. Weissman (2007). "Naturally occurring nucleoside modifications suppress the immunostimulatory activity of RNA: implication for therapeutic RNA development." Curr Opin Drug Discov Devel **10**(5): 523-32.
Kato, H. o. R.-I., S. Sato, et al. (2005). "Cell type-specific involvement of RIG-I in antiviral response." Immunity **23**(1): 19-28.
Kato, H. O. R.-I., O. Takeuchi, et al. (2008). "Length-dependent recognition of double-stranded ribonucleic acids by retinoic acid-inducible gene-I and melanoma differentiation-associated gene 5." J Exp Med **205**(7): 1601-10.
Kato, H. O. R.-I., O. Takeuchi, et al. (2006). "Differential roles of MDA5 and RIG-I helicases in the recognition of RNA viruses." Nature **441**(7089): 101-5.

Kaufmann, A., R. Salentin, et al. (2001). "Defense against influenza A virus infection: essential role of the chemokine system." Immunobiology **204**(5): 603-13.
Kawai, T. and S. Akira (2008). "Toll-like receptor and RIG-I-like receptor signaling." Ann N Y Acad Sci **1143**: 1-20.
Kawai, T. R. I. M. I., K. Takahashi, et al. (2005). "IPS-1, an adaptor triggering RIG-I- and Mda5-mediated type I interferon induction." Nat Immunol **6**(10): 981-8.
Kim, M. J., S. Y. Hwang, et al. (2008). "Negative feedback regulation of RIG-I-mediated antiviral signaling by interferon-induced ISG15 conjugation." J Virol **82**(3): 1474-83.
Kirikae, T., M. Hirata, et al. (1998). "Protective effects of a human 18-kilodalton cationic antimicrobial protein (CAP18)-derived peptide against murine endotoxemia." Infect Immun **66**(5): 1861-8.
Kiss-Laszlo, Z., Y. Henry, et al. (1998). "Sequence and structural elements of methylation guide snoRNAs essential for site-specific ribose methylation of pre-rRNA." Embo J **17**(3): 797-807.
Kiss, T. (2001). "Small nucleolar RNA-guided post-transcriptional modification of cellular RNAs." Embo J **20**(14): 3617-22.
Klenk, H. D. I. H., R. Rott, et al. (1975). "Activation of influenza A viruses by trypsin treatment." Virology **68**(2): 426-39.
Koczulla, R. O. L.-B., G. von Degenfeld, et al. (2003). "An angiogenic role for the human peptide antibiotic LL-37/hCAP-18." J Clin Invest **111**(11): 1665-72.
Koyama, S., K. J. Ishii, et al. (2007). "Differential role of TLR- and RLR-signaling in the immune responses to influenza A virus infection and vaccination." J Immunol **179**(7): 4711-20.
Krieg, A. M., A. K. Yi, et al. (1995). "CpG motifs in bacterial DNA trigger direct B-cell activation." Nature **374**(6522): 546-9.
Krieg, A. M. O. C. (2002). "CpG motifs in bacterial DNA and their immune effects." Annu Rev Immunol **20**: 709-60.
Krug, A., G. D. Luker, et al. (2004). "Herpes simplex virus type 1 activates murine natural interferon-producing cells through toll-like receptor 9." Blood **103**(4): 1433-7.
Krug, A. S. (2008). "Nucleic acid recognition receptors in autoimmunity." Handb Exp Pharmacol(183): 129-51.
Kumagai, Y., H. Kumar, et al. (2009). "Cutting Edge: TLR-Dependent viral recognition along with type I IFN positive feedback signaling masks the requirement of viral replication for IFN-{alpha} production in plasmacytoid dendritic cells." J Immunol **182**(7): 3960-4.
Kumagai, Y., O. Takeuchi, et al. (2007). "Alveolar macrophages are the primary interferon-alpha producer in pulmonary infection with RNA viruses." Immunity **27**(2): 240-52.
Kumar, H. O. R.-I., T. Kawai, et al. (2006). "Essential role of IPS-1 in innate immune responses against RNA viruses." J Exp Med **203**(7): 1795-803.
Kurosaka, K. O. L.-I., Q. Chen, et al. (2005). "Mouse cathelin-related antimicrobial peptide chemoattracts leukocytes using formyl peptide receptor-like 1/mouse formyl peptide receptor-like 2 as the receptor and acts as an immune adjuvant." J Immunol **174**(10): 6257-65.
Kurz, K. (1998). "Hydrolytische Spaltung von Nucleinsäuren- vom Enzymmechanismus zum Enzymmodell." Chemie in unserer Zeit, Wiley-VCH Verlag GmbH, 69469 Weinheim: 94-103.
Lamb, R. A. and R. M. Krug (1996). "Orthomyxoviridae: The viruses and their replication." Field, B. N., Knipe, D.N., et al. (eds), Virology. Lippincott-Raven Publishers, Philadelphia.
: 1353-1395.
Lande, R. O. L.-L., J. Gregorio, et al. (2007). "Plasmacytoid dendritic cells sense self-DNA coupled with antimicrobial peptide." Nature.

Langlois, M. A., C. Boniface, et al. (2005). "Cytoplasmic and nuclear retained DMPK mRNAs are targets for RNA interference in myotonic dystrophy cells." J Biol Chem **280**(17): 16949-54.

Larrick, J. W. O. L.-S., M. Hirata, et al. (1995). "Human CAP18: a novel antimicrobial lipopolysaccharide-binding protein." Infect Immun **63**(4): 1291-7.

Lau, Y. E. O. L.-A., D. M. Bowdish, et al. (2006). "Apoptosis of airway epithelial cells: human serum sensitive induction by the cathelicidin LL-37." Am J Respir Cell Mol Biol **34**(4): 399-409.

Le Goffic, R. O. T. T. R., J. Pothlichet, et al. (2007). "Cutting Edge: Influenza A virus activates TLR3-dependent inflammatory and RIG-I-dependent antiviral responses in human lung epithelial cells." J Immunol **178**(6): 3368-72.

Leber, J. H., G. T. Crimmins, et al. (2008). "Distinct TLR- and NLR-mediated transcriptional responses to an intracellular pathogen." PLoS Pathog **4**(1): e6.

Lee, J., T. H. Chuang, et al. (2003). "Molecular basis for the immunostimulatory activity of guanine nucleoside analogs: activation of Toll-like receptor 7." Proc Natl Acad Sci U S A **100**(11): 6646-51.

Lee, M. S. T. and Y. J. Kim (2007). "Signaling pathways downstream of pattern-recognition receptors and their cross talk." Annu Rev Biochem **76**: 447-80.

Lemaitre, B. D., E. Nicolas, et al. (1996). "The dorsoventral regulatory gene cassette spatzle/Toll/cactus controls the potent antifungal response in Drosophila adults." Cell **86**(6): 973-83.

Leung, D. W., K. C. Prins, et al. (2010). "Structural basis for dsRNA recognition and interferon antagonism by Ebola VP35." Nat Struct Mol Biol **17**(2): 165-72.

Libonati, M., A. Carsana, et al. (1980). "Double-stranded RNA." Mol Cell Biochem **31**(3): 147-64.

Libonati, M. and S. Sorrentino (1992). "Revisiting the action of bovine ribonuclease A and pancreatic-type ribonucleases on double-stranded RNA." Mol Cell Biochem **117**(2): 139-51.

Lipford, G. B., T. Sparwasser, et al. (2000). "CpG-DNA-mediated transient lymphadenopathy is associated with a state of Th1 predisposition to antigen-driven responses." J Immunol **165**(3): 1228-35.

Liu, Y. J. O. D. (2005). "IPC: professional type 1 interferon-producing cells and plasmacytoid dendritic cell precursors." Annu Rev Immunol **23**: 275-306.

Loo, Y. M. O. v. r. a. I., J. Fornek, et al. (2008). "Distinct RIG-I and MDA5 signaling by RNA viruses in innate immunity." J Virol **82**(1): 335-45.

Lopez, C. B., B. Moltedo, et al. (2004). "TLR-independent induction of dendritic cell maturation and adaptive immunity by negative-strand RNA viruses." J Immunol **173**(11): 6882-9.

Luhtala, N. and R. Parker (2010). "T2 Family ribonucleases: ancient enzymes with diverse roles." Trends Biochem Sci.

Lund, J. M. r. o. v. a. i., L. Alexopoulou, et al. (2004). "Recognition of single-stranded RNA viruses by Toll-like receptor 7." Proc Natl Acad Sci U S A **101**(15): 5598-603.

Maden, B. E. (1990). "The numerous modified nucleotides in eukaryotic ribosomal RNA." Prog Nucleic Acid Res Mol Biol **39**: 241-303.

Majde, J. A. (2000). "Viral double-stranded RNA, cytokines, and the flu." J Interferon Cytokine Res **20**(3): 259-72.

Majde, J. A., N. Guha-Thakurta, et al. (1998). "Spontaneous release of stable viral double-stranded RNA into the extracellular medium by influenza virus-infected MDCK epithelial cells: implications for the viral acute phase response." Arch Virol **143**(12): 2371-80.

Majde, J. A. I. d. R., N. Guha-Thakurta, et al. (1998). "Spontaneous release of stable viral double-stranded RNA into the extracellular medium by influenza virus-infected

MDCK epithelial cells: implications for the viral acute phase response." Arch Virol **143**(12): 2371-80.
Malathi, K., B. Dong, et al. (2007). "Small self-RNA generated by RNase L amplifies antiviral innate immunity." Nature **448**(7155): 816-9.
Martinon, F. (2008). "Detection of immune danger signals by NALP3." J Leukoc Biol **83**(3): 507-11.
Martinon, F., O. Gaide, et al. (2007). "NALP inflammasomes: a central role in innate immunity." Semin Immunopathol **29**(3): 213-29.
Matlin, K. S. and K. Simons (1984). "Sorting of an apical plasma membrane glycoprotein occurs before it reaches the cell surface in cultured epithelial cells." J Cell Biol **99**(6): 2131-9.
Matsumoto, M., K. Funami, et al. (2003). "Subcellular localization of Toll-like receptor 3 in human dendritic cells." J Immunol **171**(6): 3154-62.
Matsuo, M., T. Yokogawa, et al. (1995). "Highly specific and efficient cleavage of squid tRNA(Lys) catalyzed by magnesium ions." J Biol Chem **270**(17): 10097-104.
McCall, K. A., C. Huang, et al. (2000). "Function and mechanism of zinc metalloenzymes." J Nutr **130**(5S Suppl): 1437S-46S.
McCartney, S., W. Vermi, et al. (2009). "Distinct and complementary functions of MDA5 and TLR3 in poly(I:C)-mediated activation of mouse NK cells." J Exp Med **206**(13): 2967-76.
McCartney, S. A. and M. Colonna (2009). "Viral sensors: diversity in pathogen recognition." Immunol Rev **227**(1): 87-94.
Meador, J., 3rd, B. Cannon, et al. (1990). "Purification and characterization of Escherichia coli RNase I. Comparisons with RNase M." Eur J Biochem **187**(3): 549-53.
Means, T. K., E. Latz, et al. (2005). "Human lupus autoantibody-DNA complexes activate DCs through cooperation of CD32 and TLR9." J Clin Invest **115**(2): 407-17.
Meidan, V. M., D. Dunnion, et al. (1997). "Effect of ultrasound on the stability of oligonucleotides in vitro." International Journal of Pharmaceutics **152**: 121-125.
Meylan, E. R.-I. M. I., J. Curran, et al. (2005). "Cardif is an adaptor protein in the RIG-I antiviral pathway and is targeted by hepatitis C virus." Nature **437**(7062): 1167-72.
Mibayashi, M., L. Martinez-Sobrido, et al. (2007). "Inhibition of retinoic acid-inducible gene I-mediated induction of beta interferon by the NS1 protein of influenza A virus." J Virol **81**(2): 514-24.
Min, J. Y. and R. M. Krug (2006). "The primary function of RNA binding by the influenza A virus NS1 protein in infected cells: Inhibiting the 2'-5' oligo (A) synthetase/RNase L pathway." Proc Natl Acad Sci U S A **103**(18): 7100-5.
Molhoek, E. M., A. L. den Hertog, et al. (2009). "Structure-function relationship of the human antimicrobial peptide LL-37 and LL-37 fragments in the modulation of TLR responses." Biol Chem.
Mookherjee, N. O. L.-I. f. o. T., K. L. Brown, et al. (2006). "Modulation of the TLR-mediated inflammatory response by the endogenous human host defense peptide LL-37." J Immunol **176**(4): 2455-64.
Muruve, D. A. O. D., V. Petrilli, et al. (2008). "The inflammasome recognizes cytosolic microbial and host DNA and triggers an innate immune response." Nature **452**(7183): 103-7.
Myong, S., S. Cui, et al. (2009). "Cytosolic Viral Sensor RIG-I Is a 5'-Triphosphate-Dependent Translocase on Double-Stranded RNA." Science.
Nagaoka, I., S. Hirota, et al. (2001). "Cathelicidin family of antibacterial peptides CAP18 and CAP11 inhibit the expression of TNF-alpha by blocking the binding of LPS to CD14(+) cells." J Immunol **167**(6): 3329-38.
Nain, M., F. Hinder, et al. (1990). "Tumor necrosis factor-alpha production of influenza A virus-infected macrophages and potentiating effect of lipopolysaccharides." J Immunol **145**(6): 1921-8.

Nain, M. I. G., F. Hinder, et al. (1990). "Tumor necrosis factor-alpha production of influenza A virus-infected macrophages and potentiating effect of lipopolysaccharides." J Immunol **145**(6): 1921-8.
Nestle, M. and W. K. Roberts (1969). "An extracellular nuclease from Serratia marcescens. II. Specificity of the enzyme." J Biol Chem **244**(19): 5219-25.
Nicholson, A. W. (1999). "Function, mechanism and regulation of bacterial ribonucleases." FEMS Microbiol Rev **23**(3): 371-90.
O'Hagan, D. T., M. L. MacKichan, et al. (2001). "Recent developments in adjuvants for vaccines against infectious diseases." Biomol Eng **18**(3): 69-85.
Opitz, B. I. I., A. Rejaibi, et al. (2007). "IFNbeta induction by influenza A virus is mediated by RIG-I which is regulated by the viral NS1 protein." Cell Microbiol **9**(4): 930-8.
Opitz, B. I. R. T., A. Rejaibi, et al. (2007). "IFNbeta induction by influenza A virus is mediated by RIG-I which is regulated by the viral NS1 protein." Cell Microbiol **9**(4): 930-8.
Owen, D. M. and M. Gale, Jr. (2009). "Fighting the flu with inflammasome signaling." Immunity **30**(4): 476-8.
Papon, L., A. Oteiza, et al. (2009). "The viral RNA recognition sensor RIG-I is degraded during encephalomyocarditis virus (EMCV) infection." Virology.
Pauligk, C. I. G., M. Nain, et al. (2004). "CD14 is required for influenza A virus-induced cytokine and chemokine production." Immunobiology **209**(1-2): 3-10.
Pertzev, A. V. and A. W. Nicholson (2006). "Characterization of RNA sequence determinants and antideterminants of processing reactivity for a minimal substrate of Escherichia coli ribonuclease III." Nucleic Acids Res **34**(13): 3708-21.
Petit, F., A. S. Jarrousse, et al. (1997). "Proteasome (prosome) associated endonuclease activity." Mol Biol Rep **24**(1-2): 113-7.
Petit, F., A. S. Jarrousse, et al. (1997). "Involvement of proteasomal subunits zeta and iota in RNA degradation." Biochem J **326 (Pt 1)**: 93-8.
Pichlmair, A., O. Schulz, et al. (2009). "Activation of MDA5 requires higher order RNA structures generated during virus infection." J Virol.
Pichlmair, A. O. R.-I., O. Schulz, et al. (2006). "RIG-I-mediated antiviral responses to single-stranded RNA bearing 5'-phosphates." Science **314**(5801): 997-1001.
Pichlmair, A. V. r. and C. Reis e Sousa (2007). "Innate recognition of viruses." Immunity **27**(3): 370-83.
Pippig, D. A., J. C. Hellmuth, et al. (2009). "The regulatory domain of the RIG-I family ATPase LGP2 senses double-stranded RNA." Nucleic Acids Res.
Pouch, M. N., F. Petit, et al. (1995). "Identification and initial characterization of a specific proteasome (prosome) associated RNase activity." J Biol Chem **270**(37): 22023-8.
Probst, J., S. Brechtel, et al. (2006). "Characterization of the ribonuclease activity on the skin surface." Genet Vaccines Ther **4**: 4.
Probst, J. U. M., B. Weide, et al. (2007). "Spontaneous cellular uptake of exogenous messenger RNA in vivo is nucleic acid-specific, saturable and ion dependent." Gene Ther **14**(15): 1175-80.
Pulendran, B. and R. Ahmed (2006). "Translating innate immunity into immunological memory: implications for vaccine development." Cell **124**(4): 849-63.
Raines, R. T. (1998). "Ribonuclease A." Chem Rev **98**(3): 1045-1066.
Ramanathan, B. L.-A. P., E. G. Davis, et al. (2002). "Cathelicidins: microbicidal activity, mechanisms of action, and roles in innate immunity." Microbes Infect **4**(3): 361-72.
Rehwinkel, J. and C. Reis e Sousa (2010). "RIGorous detection: exposing virus through RNA sensing." Science **327**(5963): 284-6.
Rehwinkel, J., C. P. Tan, et al. (2010). "RIG-I Detects Viral Genomic RNA during Negative-Strand RNA Virus Infection." Cell **140**(3): 397-408.

Riedl, P., D. Stober, et al. (2002). "Priming Th1 immunity to viral core particles is facilitated by trace amounts of RNA bound to its arginine-rich domain." J Immunol **168**(10): 4951-9.
Rifkin, I. R. A., E. A. Leadbetter, et al. (2005). "Toll-like receptors, endogenous ligands, and systemic autoimmune disease." Immunol Rev **204**: 27-42.
Rigby, R. E., A. Leitch, et al. (2008). "Nucleic acid-mediated inflammatory diseases." Bioessays **30**(9): 833-42.
Robbins, M. s. R., A. Judge, et al. (2007). "2'-O-methyl-modified RNAs act as TLR7 antagonists." Mol Ther **15**(9): 1663-9.
Robertson, H. D., R. E. Webster, et al. (1968). "Purification and properties of ribonuclease III from Escherichia coli." J Biol Chem **243**(1): 82-91.
Romoren, K. D., B. J. Thu, et al. (2004). "Transfection efficiency and cytotoxicity of cationic liposomes in salmonid cell lines of hepatocyte and macrophage origin." Biochim Biophys Acta **1663**(1-2): 127-34.
Ronnblom, L. and G. V. Alm (2003). "Systemic lupus erythematosus and the type I interferon system." Arthritis Res Ther **5**(2): 68-75.
Rosenberg, H. F. (2008). "RNase A ribonucleases and host defense: an evolving story." J Leukoc Biol **83**(5): 1079-87.
Rotem, Z., R. A. Cox, et al. (1963). "Inhibition of virus multiplication by foreign nucleic acid." Nature **197**: 564-6.
Rothenfusser, S. O. R. I. L., N. Goutagny, et al. (2005). "The RNA helicase Lgp2 inhibits TLR-independent sensing of viral replication by retinoic acid-inducible gene-I." J Immunol **175**(8): 5260-8.
Saito, T., R. Hirai, et al. (2007). "Regulation of innate antiviral defenses through a shared repressor domain in RIG-I and LGP2." Proc Natl Acad Sci U S A **104**(2): 582-7.
Saito, T. O. R.-I. and M. Gale, Jr. (2008). "Differential recognition of double-stranded RNA by RIG-I-like receptors in antiviral immunity." J Exp Med **205**(7): 1523-7.
Saito, T. R. I. M. I., D. M. Owen, et al. (2008). "Innate immunity induced by composition-dependent RIG-I recognition of hepatitis C virus RNA." Nature **454**(7203): 523-7.
Sandgren, S. O. L., A. Wittrup, et al. (2004). "The human antimicrobial peptide LL-37 transfers extracellular DNA plasmid to the nuclear compartment of mammalian cells via lipid rafts and proteoglycan-dependent endocytosis." J Biol Chem **279**(17): 17951-6.
Satoh, T., H. Kato, et al. (2010). "LGP2 is a positive regulator of RIG-I- and MDA5-mediated antiviral responses." Proc Natl Acad Sci U S A **107**(4): 1512-7.
Savarese, E., O. W. Chae, et al. (2006). "U1 small nuclear ribonucleoprotein immune complexes induce type I interferon in plasmacytoid dendritic cells through TLR7." Blood **107**(8): 3229-34.
Scheel, B., S. Braedel, et al. (2004). "Immunostimulating capacities of stabilized RNA molecules." Eur J Immunol **34**(2): 537-47.
Scheel, B. V., S. Aulwurm, et al. (2006). "Therapeutic anti-tumor immunity triggered by injections of immunostimulating single-stranded RNA." Eur J Immunol **36**(10): 2807-16.
Scheel, B. v. t., S. Braedel, et al. (2004). "Immunostimulating capacities of stabilized RNA molecules." Eur J Immunol **34**(2): 537-47.
Schlee, M., E. Hartmann, et al. (2009). "Approaching the RNA ligand for RIG-I?" Immunol Rev **227**(1): 66-74.
Schlee, M., A. Roth, et al. (2009). "Recognition of 5' triphosphate by RIG-I helicase requires short blunt double-stranded RNA as contained in panhandle of negative-strand virus." Immunity **31**(1): 25-34.
Schmidt, A., T. Schwerd, et al. (2009). "5'-triphosphate RNA requires base-paired structures to activate antiviral signaling via RIG-I." Proc Natl Acad Sci U S A.

Scott, M. G. O. L.-L. a., D. J. Davidson, et al. (2002). "The human antimicrobial peptide LL-37 is a multifunctional modulator of innate immune responses." J Immunol **169**(7): 3883-91.

Seth, R. B. O. R.-I., L. Sun, et al. (2005). "Identification and characterization of MAVS, a mitochondrial antiviral signaling protein that activates NF-kappaB and IRF 3." Cell **122**(5): 669-82.

Seth, R. B. O. v. r., L. Sun, et al. (2006). "Antiviral innate immunity pathways." Cell Res **16**(2): 141-7.

Silverman, R. H. (2007). "A scientific journey through the 2-5A/RNase L system." Cytokine Growth Factor Rev **18**(5-6): 381-8.

Silverman, R. H. (2007). "Viral encounters with 2',5'-oligoadenylate synthetase and RNase L during the interferon antiviral response." J Virol **81**(23): 12720-9.

Sioud, M. (2006). "Single-stranded small interfering RNA are more immunostimulatory than their double-stranded counterparts: a central role for 2'-hydroxyl uridines in immune responses." Eur J Immunol **36**(5): 1222-30.

Sioud, M., G. Furset, et al. (2007). "Suppression of immunostimulatory siRNA-driven innate immune activation by 2'-modified RNAs." Biochem Biophys Res Commun **361**(1): 122-6.

Siren, J. o. v. r. a., T. Imaizumi, et al. (2006). "Retinoic acid inducible gene-I and mda-5 are involved in influenza A virus-induced expression of antiviral cytokines." Microbes Infect **8**(8): 2013-20.

Sorensen, O., J. B. Cowland, et al. (1997). "An ELISA for hCAP-18, the cathelicidin present in human neutrophils and plasma." J Immunol Methods **206**(1-2): 53-9.

Sorensen, O. E. L.-.-P., P. Follin, et al. (2001). "Human cathelicidin, hCAP-18, is processed to the antimicrobial peptide LL-37 by extracellular cleavage with proteinase 3." Blood **97**(12): 3951-9.

Sorensen, O. O. L.-L., T. Bratt, et al. (1999). "The human antibacterial cathelicidin, hCAP-18, is bound to lipoproteins in plasma." J Biol Chem **274**(32): 22445-51.

Stetson, D. B. O. D. and R. Medzhitov (2006). "Recognition of cytosolic DNA activates an IRF3-dependent innate immune response." Immunity **24**(1): 93-103.

Sun, Q. R. M. I., L. Sun, et al. (2006). "The specific and essential role of MAVS in antiviral innate immune responses." Immunity **24**(5): 633-42.

Sun, W., E. Jun, et al. (2001). "Intrinsic double-stranded-RNA processing activity of Escherichia coli ribonuclease III lacking the dsRNA-binding domain." Biochemistry **40**(49): 14976-84.

Takahasi, K., H. Kumeta, et al. (2009). "Solution structures of cytosolic RNA sensor MDA5 and LGP2 C-terminal domains: identification of the RNA recognition loop in RIG-I-like receptors." J Biol Chem **284**(26): 17465-74.

Takahasi, K. o. R. I., M. Yoneyama, et al. (2008). "Nonself RNA-sensing mechanism of RIG-I helicase and activation of antiviral immune responses." Mol Cell **29**(4): 428-40.

Takaoka, A. O. D., Z. Wang, et al. (2007). "DAI (DLM-1/ZBP1) is a cytosolic DNA sensor and an activator of innate immune response." Nature **448**(7152): 501-5.

Takeuchi, O. O. V. r. and S. Akira (2007). "Recognition of viruses by innate immunity." Immunol Rev **220**: 214-24.

Takeuchi, O. O. v. r. a. I. and S. Akira (2008). "MDA5/RIG-I and virus recognition." Curr Opin Immunol **20**(1): 17-22.

Termen, S., M. Tollin, et al. (2003). "Phylogeny, processing and expression of the rat cathelicidin rCRAMP: a model for innate antimicrobial peptides." Cell Mol Life Sci **60**(3): 536-49.

Theofilopoulos, A. N. O. A., R. Baccala, et al. (2005). "Type I interferons (alpha/beta) in immunity and autoimmunity." Annu Rev Immunol **23**: 307-36.

Thomas, P. G., P. Dash, et al. (2009). "The intracellular sensor NLRP3 mediates key innate and healing responses to influenza A virus via the regulation of caspase-1." Immunity **30**(4): 566-75.

Thompson, J. E., F. D. Venegas, et al. (1994). "Energetics of catalysis by ribonucleases: fate of the 2',3'-cyclic phosphodiester intermediate." Biochemistry **33**(23): 7408-14.

Ting, J. P. and B. K. Davis (2005). "CATERPILLER: a novel gene family important in immunity, cell death, and diseases." Annu Rev Immunol **23**: 387-414.

Tluk, S., M. Jurk, et al. (2009). "Sequences derived from self-RNA containing certain natural modifications act as suppressors of RNA-mediated inflammatory immune responses." Int Immunol **21**(5): 607-19.

Tschopp, J., F. Martinon, et al. (2003). "NALPs: a novel protein family involved in inflammation." Nat Rev Mol Cell Biol **4**(2): 95-104.

Tsurui, H., Y. Kumazawa, et al. (1994). "Batchwise purification of specific tRNAs by a solid-phase DNA probe." Anal Biochem **221**(1): 166-72.

Turner, J. O. L.-L. a., Y. Cho, et al. (1998). "Activities of LL-37, a cathelin-associated antimicrobial peptide of human neutrophils." Antimicrob Agents Chemother **42**(9): 2206-14.

Uematsu, S. B. and S. Akira (2008). "Toll-Like receptors (TLRs) and their ligands." Handb Exp Pharmacol(183): 1-20.

Uzri, D. and L. Gehrke (2009). "Nucleotide sequences and modifications that determine RIG-I/RNA binding and signaling activities." J Virol.

Verdijk, R. M., T. Mutis, et al. (1999). "Polyriboinosinic polyribocytidylic acid (poly(I:C)) induces stable maturation of functionally active human dendritic cells." J Immunol **163**(1): 57-61.

Volbeda, A., A. Lahm, et al. (1991). "Crystal structure of Penicillium citrinum P1 nuclease at 2.8 A resolution." Embo J **10**(7): 1607-18.

Vollmer, J., S. Tluk, et al. (2005). "Immune stimulation mediated by autoantigen binding sites within small nuclear RNAs involves Toll-like receptors 7 and 8." J Exp Med **202**(11): 1575-85.

Wang, Q., T. Niittymaki, et al. (2007). "Metal ion promoted cleavage of RNA phosphodiester bonds: from Zn(II) aqua ion to artificial ribonucleases." Nucleic Acids Symp Ser (Oxf)(51): 65-6.

Wang, Y. O. L.-L., B. Agerberth, et al. (1998). "Apolipoprotein A-I binds and inhibits the human antibacterial/cytotoxic peptide LL-37." J Biol Chem **273**(50): 33115-8.

Weber, F. d. s. R., V. Wagner, et al. (2006). "Double-stranded RNA is produced by positive-strand RNA viruses and DNA viruses but not in detectable amounts by negative-strand RNA viruses." J Virol **80**(10): 5059-64.

Westwood, A., S. J. Elvin, et al. (2006). "Immunological responses after immunisation of mice with microparticles containing antigen and single stranded RNA (polyuridylic acid)." Vaccine **24**(11): 1736-43.

Wreschner, D. H., T. C. James, et al. (1981). "Ribosomal RNA cleavage, nuclease activation and 2-5A(ppp(A2'p)nA) in interferon-treated cells." Nucleic Acids Res **9**(7): 1571-81.

Xu, L. G. R.-I. M. I., Y. Y. Wang, et al. (2005). "VISA is an adapter protein required for virus-triggered IFN-beta signaling." Mol Cell **19**(6): 727-40.

Xu, Y. O. D. and F. C. Szoka, Jr. (1996). "Mechanism of DNA release from cationic liposome/DNA complexes used in cell transfection." Biochemistry **35**(18): 5616-23.

Yang, D. O. L.-A. P., A. Biragyn, et al. (2004). "Multiple roles of antimicrobial defensins, cathelicidins, and eosinophil-derived neurotoxin in host defense." Annu Rev Immunol **22**: 181-215.

Yashiro, M., M. Higuchi, et al. (2002). "Effect of Alkaline Earth Metal Ions on the Phisphodiester Hydrolysis of RNA." Bull. Chem. Soc. Jpn. **75**: 1843-1844.

Yasin, B. s. s., M. Pang, et al. (2000). "Evaluation of the inactivation of infectious Herpes simplex virus by host-defense peptides." Eur J Clin Microbiol Infect Dis **19**(3): 187-94.

Yasuda, K., M. Rutz, et al. (2006). "CpG motif-independent activation of TLR9 upon endosomal translocation of "natural" phosphodiester DNA." Eur J Immunol **36**(2): 431-6.

Yasuda, K. O. D., P. Yu, et al. (2005). "Endosomal translocation of vertebrate DNA activates dendritic cells via TLR9-dependent and -independent pathways." J Immunol **174**(10): 6129-36.

Yoneyama, M. and T. Fujita (2010). "Recognition of viral nucleic acids in innate immunity." Rev Med Virol **20**(1): 4-22.

Yoneyama, M. o. R., M. Kikuchi, et al. (2004). "The RNA helicase RIG-I has an essential function in double-stranded RNA-induced innate antiviral responses." Nat Immunol **5**(7): 730-7.

Yoneyama, M. O. R. I. a., M. Kikuchi, et al. (2005). "Shared and unique functions of the DExD/H-box helicases RIG-I, MDA5, and LGP2 in antiviral innate immunity." J Immunol **175**(5): 2851-8.

Yusupov, M. M., G. Z. Yusupova, et al. (2001). "Crystal structure of the ribosome at 5.5 A resolution." Science **292**(5518): 883-96.

Zaiou, M. O. L.-C. P., V. Nizet, et al. (2003). "Antimicrobial and protease inhibitory functions of the human cathelicidin (hCAP18/LL-37) prosequence." J Invest Dermatol **120**(5): 810-6.

Zaiou, M. O. L.-L. a. and R. L. Gallo (2002). "Cathelicidins, essential gene-encoded mammalian antibiotics." J Mol Med **80**(9): 549-61.

Zanetti, M., R. Gennaro, et al. (1995). "Cathelicidins: a novel protein family with a common proregion and a variable C-terminal antimicrobial domain." FEBS Lett **374**(1): 1-5.

Zanetti, M. O. L.-a. P. (2005). "The role of cathelicidins in the innate host defenses of mammals." Curr Issues Mol Biol **7**(2): 179-96.

Zanetti, M. O. L.-L. a. (2004). "Cathelicidins, multifunctional peptides of the innate immunity." J Leukoc Biol **75**(1): 39-48.

Zasloff, M. o. L.-a. P. (2002). "Antimicrobial peptides of multicellular organisms." Nature **415**(6870): 389-95.

Zelphati, O. O. D. and F. C. Szoka, Jr. (1996). "Mechanism of oligonucleotide release from cationic liposomes." Proc Natl Acad Sci U S A **93**(21): 11493-8.

Zhong, B. a., Y. Yang, et al. (2008). "The adaptor protein MITA links virus-sensing receptors to IRF3 transcription factor activation." Immunity **29**(4): 538-50.

9.2. Doctoral thesis

Cuzic-Feltens, S., 2006. Investigation of the catalytic mechanism of RNase P: the role of divalent metal ions and functional groups important for catalysis.

Eberle, F., 2009. Activation of Innate Immunity by Ribonucleic Acids.

Hamm S., 2006. Immunstimulatorische Eigenschaften von RNA.

Pauglik, C., 2002. Molekulare Wechselwirkungen zwischen Infleunza A-Viren und humanen Monozyten: Genregulation und Signalübertragung.

Wegscheid B., 2006. *In vitro* and *in vivo* investigations on the interaction of bacterial RNase P with tRNA 3`-CCA.

9.3. Diploma thesis and Master thesis

Gürtler, C., 2008. Charakterisierung der immunologischen Funktion der adenosine deaminase acting on RNA 1 (ADAR1).

Pigisch S., 2005. Immunstimulatorische und modulierende Eigenschaften von RNA.

10. Abbreviations and Units

°C	celsius
µ	micro (10^{-6})
A	adenosine
A_{260}	absorption at 260 nm
AA	amino acids
APC	allophycocyanine
APS	ammonium persulfate, $(NH_4)_2S_2O_8$
Bp	base pair(s)
BPB	bromphenol blue
BSA	bovine serum albumin
C	cytosine
Cardif	Caspase activation recruitment domain inducing IFN-ß
CD	cluster of differentiation
cDNA	complementary desoxyribonucleic acid
c_{End}	end concentration
c_{Stock}	stock concentration
DAPI	4,6 Diamin-2-phenylindoldihydrochlorid
DC	dendritic cell
DEPC	diethylpyrocarbonat
DMEM	Dulbecco's Modified Eagles Medium
DNA	deoxyribonucleic acid
DNase	deoxyribonuclease
DOTAP	N-[1-(2,3-Dioleoyloxy)propyl]-N,N,N-trimethyl-ammoniummethylsulfate
dNTP	deoxynucleoside triphosphates
ds	double-strand
DTT	dithiothreitol
EDTA	ethylenediamine tetraacedic acid
ELISA	enzyme-linked Immunosorbent Assay
FACS	fluorescence-activated cell sorting
FCS	fetal calf serum
FITC	fluoresceinisothiocyanat

Flt3	Fms-like tyrosine kinase 3-ligand
FSC	forward scatter
g	gram
G	guanosine
GM-CSF	granulocyte macrophage-colony stimulating factor
h	hour(s)
HEK293	human embryonic kidney cells
HEPES	N-2-Hydroxyethylpiperazin-N`-2-ethane sulfonic acid
HPLC	high performance liquid chromatography
HRP	horseraddish peroxidase
IFN	interferon
IKB	inhibitor KB
IKK	IKB kinase
IL	interleukin
IPS-1	interferon-ß promoter stimulator 1
IRAK	IL-1-receptor-associated kinase
IRF	interferon regulatory factor
kb	kilo bases
l	liter
LB	Luria-Bertani
LBP	LPS-binding-protein
LPS	Lipopolysaccharide
LGP2	Laboratory of genetics and physiology 2
LRR	leucine-rich-repeats
LTA	Lipoteichoic acid
m	milli (10^{-3})
M	molar [mol/l]
mA	millampere
MAVS	mitochondrial differentiation-associated gene 5
MDA-5	melanoma differentiation-associated gene 5
MDCK	Madin Darby canine kidney
mDC	myeloid dendritic cell
MHC	major histocompatibility complex

min	minute
mM	millimolar
mRNA	messenger RNA
MOPS	3-(N-morpholino)-Propansulfonsäure
MW	molecular weight
MyD88	myeloid differentiation primary response protein 88
n	nano (10^{-9})
n.t.	not tested
NF-κB	nuclear factor κB
NLR	NOD (nucleotide-binding and oligomerization domain)-like receptor
nt(s)	nucleotide(s)
NTP	ribonucleosidtriphosphate
OD	optical density
ODN	oligodeoxyribonucleoside
OPD	o-Phenylendiamin Dihydrochloride
p.a.	pro analysis
PAA	polyacrylamide
PAGE	polyacrylamide gel electrophoresis
PAMP	pathogen-associated molecular pattern
PBS^{def}	phosphate buffered saline -deficient of calcium and magnesium
PBS^{++}	phosphate buffered saline with calcium and magnesium
PBMC	peripheral blood mononuclear cell
PCR	polymerase chain reaction
pDC	plasmacytoid dendritic cell
PE	phycoerythrin
Poly (I:C)	polyinosine-deoxycytidylic acid
PRR	pattern recognition receptor
PTO	phosphothioate
R-848	resiquimod
RIG-I	retinoic acid inducible gene I
RLR	RIG-I-like receptors
RNA	ribonucleic acid
rRNA	ribosomal RNA

RNase	ribonuclease
RP-HPLC	reverse phase high performance liquid chromatography
rpm	rounds per minute
RPMI 1640	Roswell Park Memorial Institute
RT	reverse transcriptase
RT	room temperature
s	second
SDS	natriumdodecylsulfate
ss	single-strand
SSC	side scatter
T	thymine
TAE	Tris/Acetate/EDTA
TBE	Tris-Borate-EDTA Buffer
TEACL	tetraethylammoniumchloride
TEMED	tetramethylethylendiamin
TIR	Toll/Il-1-receptor
TLR	toll like receptor
Tm	melting temperature
TNF	Tumor-Necrosis-Factor
tRNA	transfer RNA
Tris	tris-hydroxymethylaminomethan
U	Unit(s) (unit for enzyme activity)
VISA	virus induced signaling adaptor
WT	wild-type
XCB	xylene cyanol blue

Acknowledgements

I would like to thank…

… Prof. Dr. Bauer for the excellent scientific supervision of my work, for always showing an interest in the progress of the project and supporting with his insightful discussions and helpful advices. I also want to mention that he also helps with lab works and with planning the experiments.

… Prof. Dr. Hartmann for also helping in the work with his knowledge in working with RNA and in suggesting proper RNA experiments.

… Prof. Dr. Maike Petersen and Prof. Dr. Udo Bakowsky for participation in the examination commission.

… Dr. Marianne Nain for introducing me into the basics of immunology at the beginning of my work and for fruitful office-discussions. She always takes time for personal matters and supports me in finding a proper way between research and personal time.

… Dr. Philipp Yu for his helpful discussions and intellectual wisdom. He introduced me into the basics of molecular biology and has always an open ear for some questions.

… Dr. Andreas Kaufmann for helping to improve myself by challenging me with questions, ideas, or problems I have overlooked. He was always there, when I needed him.

… Elfriede Klein for always being available as an additional hand if necessary and enlivening the lab routine. She has a big heart and has been like a mother to me-I will miss her.

… all members of the Bauer group for always being open for discussions, cooperativeness and helpful in problem-solving strategies and especially for the friendly atmosphere in- and outside the lab. Especially, I want to thank the students Claudia Gürtler, Iris Eberhardt, Katharina Jeltsch, Heike Schreiner, Yang Zaou, Judith Bauer, Antje Kessler, Gernold Nees, Edgar Djoko Kamdem, Markus Dudek, Jenny Großmann, Cornelius Menze, Wolger Lübben and Joschka Willemsen for spending a nice time in the lab.

… and finally my family and my friends for their love and support during my entire PhD, especially my sister Amke for always being interested in my life.

Publications arising from this work

Articles

TLR8-mediated recognition of 2`-O-ribose methylated RNA

Posters

4 th Spring School on Immunology of the Deutsche Gesellschaft für Immunologie (DGfi), Ettal, 2-7 March 2008 "RNA recognition in immune cells"

Oral presentations

Joint Annual Meeting of Immunology of the ÖGAI & DGfI, Vienna, Septembre 3-6, 2008 "RNA recognition in immune cells"

Lebenslauf

Tina von Thülen

	Geburtsdatum	23.06.1980
	Geburtsort	Wilhelmshaven
	Familienstand	ledig
	Nationalität	deutsch

10/1993 – 05/2000 Mariengymnasium, Jever (Abitur)

10/2000-10/2004 **Studium der Pharmazie**, Philipps-Universität Marburg

08/2002	1. Staatsexamen
10/2004	2. Staatsexamen
11/2005	3. Staatsexamen

11/2004 – 04/2005 **Diplomarbeit** in der Arbeitsgruppe von Herrn Prof. Dr. Hartmann, Institut für Pharmazeutische Chemie, Marburg
Thema: Charakterisierung von 2`-Fluor-Pyrimidin-modifizierten RNA-Aptameren gegen das murine Lipopolysaccharid-bindende Protein
Verteidigung im Juli 2006

05/2005 – 10/2005 Praktikum im Rahmen des **Praktischen Jahres** für Pharmazeuten in der Stern-Apotheke, Gießen

12/2005 **Approbation als Apothekerin**

seit 06/2006 03/2010 **Doktorarbeit** in der Arbeitsgruppe von Herrn Prof. Dr. Stefan Bauer, Institut für Immunologie, BMFZ, Marburg

Selbstständigkeitserklärung

Ich versichere, dass ich meine Dissertation

"Immunstimulation with RNA"

selbständig, ohne unerlaubte Hilfe angefertigt und mich dabei keiner anderen als der von mir ausdrücklichbezeichneten Quellen und Hilfen bedient habe.

Die Dissertation wurde in der jetzigen oder einer ähnlichen Form noch an keiner anderen Hochschule eingereicht und hat noch keinen sonstigen Prüfungszwecken gedient.

Marburg, den 20.04.2010

_____ _____

(Ort/Datum) Unterschrift mit Vor- und Zuname